Technische Universität Chemnitz

Sonderforschungsbereich 393

Numerische Simulation auf massiv parallelen Rechnern

Thomas Apel

Anisotropic Finite Elements: Local Estimates and Applications

Preprint SFB393/99-03

Habilitationsschrift

zur Erlangung des akademischen Grades
doctor rerum naturalium habilitatus
(Dr. rer. nat. habil.)

Preprint-Reihe des Chemnitzer SFB 393

SFB393/99-03 **January 1999**

Author's address:

Thomas Apel
TU Chemnitz
Fakultät für Mathematik
D-09107 Chemnitz

apel@mathematik.tu-chemnitz.de
http://www.tu-chemnitz.de/~tap/

Preface

The solution of elliptic boundary value problems may have *anisotropic behaviour* in parts of the domain. That means that the solution varies significantly only in certain directions. Examples include diffusion problems in domains with edges and singularly perturbed convection-diffusion-reaction problems where boundary or interior layers appear. In such cases it is an obvious idea to reflect this anisotropy in the discretization by using *anisotropic meshes* with a small mesh size in the direction of the rapid variation of the solution and a larger mesh size in the perpendicular direction. Anisotropic meshes can also be advantageous if surfaces with strongly anisotropic curvature (the front side of a wing of an airplane) or thin layers of different material are to be discretized.

In order to describe anisotropic elements mathematically we introduce the term *aspect ratio*. The aspect ratio is the ratio of the diameter of the element e and the supremum of the diameters of all balls contained in e. A finite element is called anisotropic if the aspect ratio tends to infinity when the mesh size or some (small perturbation) parameter tends to zero. Contrary, elements are called *isotropic* if the aspect ratio is bounded by a moderate constant. Triangular elements are isotropic if they satisfy Zlámal's *minimal* angle condition.

Already in the fifties and seventies it was shown that certain local interpolation error estimates can be proved for some classes of anisotropic finite elements. The minimal angle condition is replaced by the weaker *maximal* angle condition. Nevertheless, the majority of papers and books on the finite element method excludes anisotropic finite elements.

Since the end of the eighties anisotropic elements are considered in the international literature more intensively. Examples of using anisotropic elements include interpolation tasks, singular perturbation and flow problems, the treatment of edge singularities, and adaptive procedures. The corresponding papers lead to two conclusions. First, anisotropic mesh refinement offers a great potential for the construction of efficient numerical procedures (interpolation, finite element method, boundary element method, finite volume method), more efficient than it is possible with the restriction to a bounded aspect ratio. So one can expect a broad utilization of such meshes. Second, there are still challenges to set all the ingredients of such methods on a solid mathematical basis. These ingredients include a-priori and a-posteriori error estimates and the solution of the arising system of algebraic equations.

The aim of this monograph is to establish interpolation and approximation properties of finite element spaces on anisotropic meshes. In particular, such topics are chosen where the author himself contributed to the development: anisotropic local interpolation error estimates for several types of two- and three-dimensional finite elements and a-priori estimates of the discretization error for model problems with edge singularities or boundary layers. Several results have not been presented before.

We are restricted here to model problems since detailed knowledge of properties of the solution is necessary. However, much effort is spent to treat arbitrary polygonal/polyhedral domains and finite elements of any approximation order. It is a future task to apply these results to more

complex problems and to complement them with mathematically founded adaptive strategies and optimal preconditioning techniques for solving the arising systems of linear equations.

The monograph is organized into 30 sections which form six chapters:

1. Preliminaries,
2. Lagrange interpolation,
3. Scott-Zhang interpolation,
4. Anisotropic finite element approximations near edges,
5. Anisotropic finite element approximations in boundary layers,
6. Open problems.

A detailed outline is given in Section 2.

This work was possible only with the help, stimulation, and encouragement of many people. Bernd Heinrich (Chemnitz) directed my attention to anisotropic finite elements about ten years ago, and since then he has given many valuable comments. Together with Manfred Dobrowolski (Würzburg) we set the basis for deriving anisotropic interpolation error estimates. Anna-Margarete Sändig (Stuttgart) and Serge Nicaise (Valenciennes, France) answered with patience many questions about singularities. Gert Lube (Göttingen) introduced me to the world of singularly perturbed problems. From all them and also from the other co-authors John R. Whiteman (Uxbridge, United Kingdom), Roland Mücke (Baden, Switzerland), and Frank Milde (Chemnitz) I profited in joint work into mesh refinement techniques. The author had also valuable discussions with many colleagues at the *Fakultät für Mathematik* of the *Technische Universtät Chemnitz*, among them in particular Michael Jung, Gerd Kunert, Michael Lorenz, Arnd Meyer, and Reinhold Schneider. The computations were carried out with the help of Michael Jung, Frank Milde, and Uwe Reichel. The work was supported by *Deutsche Forschungsgemeinschaft* and *Deutscher Akademischer Austauschdienst*. Finally, I want to thank my wife for her encouragement and patience over the years. All this help and support is gratefully acknowledged.

Contents

Chapter I

Preliminaries

1 Introduction to anisotropic finite elements

Many physical phenomena and engineering problems can be formulated mathematically by boundary value problems for linear, elliptic partial differential equations. Examples include diffusion and heat conduction problems (sometimes involving convection), the calculation of electrostatic potential distributions, and the calculation of displacement fields in linear elasticity. The task of solving linear elliptic boundary value problems can also be encountered as a repeated ingredient in the solution of nonlinear (after linearization), time-dependent (after semi-discretization), or inverse problems. The investigation of particular aspects of the numerical solution of such problems has motivated the research which is documented in this report.

To develop the main ideas we introduce some basic notation. Assume that the boundary value problem is given in weak form:

$$Find\ u \in V_0 : a(u,v) = \langle f, v\rangle \quad \forall v \in V_0. \tag{1.1}$$

Here we denote by V_0 a subspace of $V := W^{1,2}(\Omega)$ where $\Omega \subset \mathbb{R}^d$ $(d = 2,3)$ is a bounded polygonal/polyhedral domain. The duality pair $\langle .,. \rangle : V' \times V \to \mathbb{R}$ characterizes a linear functional $\langle f, . \rangle$ on V_0. Without going into too much detail here, we demand that the bilinear form $a(.,.) : V \times V \to \mathbb{R}$ has properties such that (1.1) has a unique solution $u \in V_0$. This framework is general enough to cover symmetric and non-symmetric bilinear forms, as well as scalar and vector-valued functions u. In the latter case the definition of V has to be modified to $V := [W^{1,2}(\Omega)]^n$.

The basic principle of the numerical solution of problem (1.1) via the Galerkin finite element method is to replace V_0 by a family of finite-dimensional spaces V_{0h}. The finite element solution is then defined by:

$$Find\ u_h \in V_{0h} : a(u_h, v_h) = \langle f, v_h\rangle \quad \forall v_h \in V_{0h}. \tag{1.2}$$

We remark that also the bilinear and linear forms could be modified to depend upon the parameter h, but we will keep the explanation as simple as possible here. In the h-version of the finite element method, the spaces $V_h \subset V$ and $V_{0h} \subset V_0$ are defined relative to a family $\mathcal{F} = \{\mathcal{T}_h\}$ of meshes $\mathcal{T}_h := \{e\}$,

$$V_h := \{v_h \in V : v_h|_e \in \mathcal{P}_{k,e} \quad \forall e \in \mathcal{T}_h\}, \quad V_{0h} := V_0 \cap V_h. \tag{1.3}$$

The element type determines the space $\mathcal{P}_{k,e}$ of shape functions. The meshes are assumed to satisfy the usual admissibility conditions [63, pages 38, 51]:

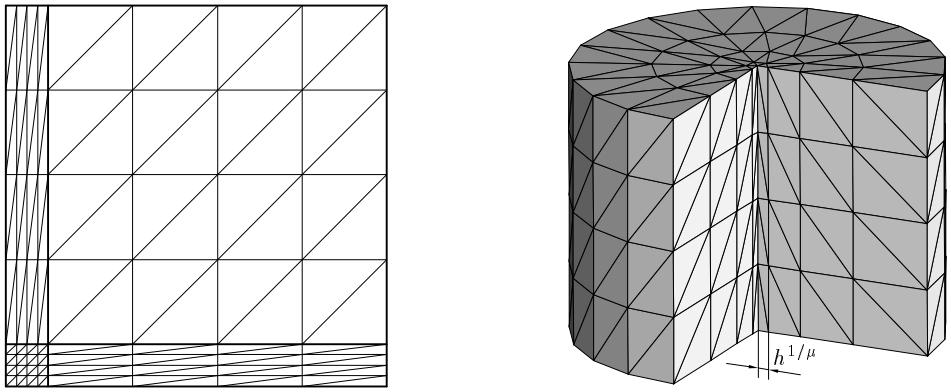

Figure 1.1: Examples of anisotropic meshes. Left: in a boundary layer. Right: near an edge.

1. The domain is covered by the closure of the finite elements e, $\overline{\Omega} = \bigcup_{e \in \mathcal{T}_h} \overline{e}$.
2. The finite elements are disjoint, $e \cap e' = \emptyset \quad \forall e, e' \in \mathcal{T}_h$, $e \neq e'$.
3. Any edge ($d = 2$) or face ($d = 3$) of any element $e \in \mathcal{T}_h$ is either a subset of the boundary $\partial\Omega$ or edge/face of another element $e' \in \mathcal{T}_h$.

Denote by $\operatorname{diam}(e)$ the diameter of the finite element e, and by ϱ_e the supremum of the diameters of all balls contained in e. Then it is assumed in the classical finite element theory that

$$\operatorname{diam}(e) \lesssim \varrho_e . \tag{1.4}$$

(The notation $\lesssim$ means *smaller than up to a constant.*) The ratio of $\operatorname{diam}(e)$ and ϱ_e is called *aspect ratio* of the element e. In this sense, (1.4) is equivalent to the assumption of a bounded aspect ratio. Elements which satisfy (1.4) are called *isotropic elements*, see, for example, [175]. Triangular elements are isotropic if they satisfy Zlámal's *minimal* angle condition [208].

Consider now boundary value problems with a solution which has *anisotropic behaviour* near certain manifolds $M \subset \overline{\Omega}$. That means that the solution varies significantly only perpendicularly to M. Examples include diffusion problems in domains with edges M, see Chapter IV, and singularly perturbed convection-diffusion-reaction problems where M is part of the boundary or an interior manifold, see Chapter V. In such cases it is an obvious idea to reflect this anisotropy in the discretization by using meshes with *anisotropic elements* [9, 175] (sometimes also called elongated elements [205]). These elements have a small mesh size in the direction of the rapid variation of the solution and a larger mesh size in the perpendicular direction. Examples are given in Figure 1.1. Anisotropic meshes can also be advantageous if surfaces with strongly anisotropic curvature (the front side of a wing of an airplane, for example [175, Figure 6]) or thin layers of different material are to be discretized.

Anisotropic elements do not satisfy condition (1.4). Conversely, they are characterized by

$$\frac{\operatorname{diam}(e)}{\varrho_e} \to \infty \tag{1.5}$$

where the limit can be considered as $h \to 0$ (near edges) or $\varepsilon \to 0$ (in layers) where ε is some (small perturbation) parameter of the problem. We note that the investigation of anisotropic elements also forms a basis for using highly distorted elements in the meshing of thin slots or

layers of different materials, for example in an electronic motor. Here, the elements are not anisotropic in the sense of (1.5) but the constant in (1.4) is very large.

First mathematical considerations of anisotropic elements go back to the fifties [187] and seventies [27, 84, 108] Nevertheless, the majority of papers and books on the finite element method excludes such elements. Some commercial finite element codes even prohibit elements with large aspect ratio, for example an aspect ratio greater than 5.

Since the end of the eighties anisotropic elements are considered more intensively, for example for interpolation tasks [9, 12, 21, 35, 69, 119, 120, 160, 202], in singular perturbation and flow problems [2, 13, 41, 73, 114, 152, 173, 186, 204, 205], for the treatment of edge singularities [9, 19, 21, 153], and in adaptive procedures [58, 62, 117, 152, 155, 174, 205]. This list is certainly incomplete, but from the papers we can draw two conclusions. First, anisotropic mesh refinement offers a great potential for the construction of efficient numerical procedures (interpolation; h-, r-, and hp-version of the finite element method; boundary element method, finite volume method), more efficient than it is possible with the restriction to a bounded aspect ratio. So one can expect a broad utilization of such meshes. Second, there are still challenges to set all the ingredients of such methods (including a-priori and a-posteriori error estimates and the solution of the arising system of algebraic equations) on a solid mathematical basis.

2 Outline

This monograph is an attempt to present a survey of interpolation results and applications in connection with anisotropic finite element meshes. The aim is to understand the approximation properties of finite element spaces on anisotropic meshes. In particular, such topics are chosen where the author himself contributed to the development:

- anisotropic local interpolation error estimates for several types of two- and three-dimensional finite elements and
- a-priori estimates of the discretization error for model problems with edge singularities or boundary layers.

So the reader will find several new results as well.

Thirty sections form six chapters: *Preliminaries*, *Lagrangian interpolation*, *Scott-Zhang interpolation*, *Anisotropic discretizations near edges*, *Anisotropic discretizations in boundary layers*, and *Open problems*. We will now motivate and describe the contents.

A primary task is to investigate the interpolation error since local interpolation error estimates are basic ingredients for deriving a-priori estimates of the finite element error, for proving the equivalence of error estimators and the exact error, and for investigating multi-level algorithms. For Lagrangian finite elements, the *Lagrangian interpolant*, also called *nodal interpolant*, is the simplest one. It is defined by

$$\mathrm{I}_h u := \sum_{i \in I} u(X^{(i)}) \varphi_i(x), \tag{2.1}$$

where $X^{(i)}$ are the nodes and $\varphi_i(x)$ are the *nodal basis functions*:

$$\varphi_i(X^{(j)}) = \delta_{i,j}, \quad i, j \in I. \tag{2.2}$$

Since I_h is defined locally on every element the interpolation error $u - \mathrm{I}_h u$ can be estimated elementwise.

Let us start with a result of the classical interpolation theory, see, for example, [63]. For functions $u \in W^{\ell,p}(e)$ the interpolation error can be estimated in the form

$$|u - \mathrm{I}_h u; W^{m,q}(e)| \lesssim (\mathrm{meas}_d e)^{1/q-1/p} (\mathrm{diam}\, e)^{\ell} \varrho_e^{-m} |u; W^{\ell,p}(e)|, \tag{2.3}$$

where $\mathrm{meas}_d e$ is the area/volume of the element e and $|\,.\,; W^{\ell,p}(e)|$ means a seminorm in the Sobolev space $W^{\ell,p}(e)$. The admissible ranges of the parameters ℓ, m, p, and q depend on the space dimension d and the polynomial degree k of the shape functions.

For isotropic elements we can rewrite estimate (2.3) and get

$$|u - \mathrm{I}_h u; W^{m,q}(e)| \lesssim (\mathrm{meas}_d e)^{1/q-1/p} (\mathrm{diam}\, e)^{\ell-m} |u; W^{\ell,p}(e)|. \tag{2.4}$$

For several special cases it was proved that this estimates holds true for certain classes of anisotropic elements as well. Triangular and tetrahedral elements were investigated in [27, 108, 119, 120] and, as the oldest reference, [187, pages 209–213]. In all of these papers it is shown that anisotropic elements can be applied when a *maximal angle condition* is satisfied. Quadrilateral elements were investigated similarly in [108, 202]. We summarize these contributions in more detail in Section 10.

These results were rarely exploited for finite element error estimates because the possible advantage of using elements with independent length scales in different directions was not extracted; only the diameter appeared in the local interpolation error estimates. If we use anisotropic elements in order to compensate a large directional derivative of the solution by a small element size in this direction, then we need a sharper interpolation error estimate. We investigate in this monograph estimates of the type

$$|u - \mathrm{I}_h u; W^{m,q}(e)| \lesssim (\mathrm{meas}_d e)^{1/q-1/p} \sum_{\substack{\alpha_1+\cdots+\alpha_d=\ell-m \\ \alpha_1,\ldots,\alpha_d \geq 0}} h_{1,e}^{\alpha_1} \cdots h_{d,e}^{\alpha_d} \left| \frac{\partial^{\ell-m} u}{\partial x_1^{\alpha_1} \cdots \partial x_d^{\alpha_d}}; W^{m,p}(e) \right|, \tag{2.5}$$

where $h_{1,e}, \ldots, h_{d,e}$ are suitably defined element sizes. We will call estimates of this type *anisotropic*, in contrary to the *isotropic* estimate in (2.4) where the different element scales $h_{1,e}, \ldots, h_{d,e}$ are not exploited.

Special cases of estimate (2.5) were proved for triangular and rectangular elements in [37, 84, 153, 155] and [150, pages 82–84 and page 90], see Section 10 for the individual contributions. An intensive study for all types of elements including tetrahedra and bricks and also for higher order shape functions started with the paper [9] and continued in various directions in [5, 12, 14, 19, 20, 21]. Based on [9], some of the results were obtained independently also in [35].

In Chapter II (Sections 4–10) of this report we present the whole interpolation theory for anisotropic elements in a systematic way. The main strategy is fairly standard, namely, to derive first the estimate on a reference element $\hat{e}$ and to apply a coordinate transformation $x = F_e(\hat{x})$ with $e = F_e(\hat{e})$. Nevertheless, there are mainly two obstructions which prevent an obvious solution. We have first to recognize that sharper estimates on the reference element have to be shown for proving estimates of type (2.4) or (2.5) for *anisotropic* elements, sharper than it is necessary for isotropic elements, see Section 4.2. We will see in Chapter II that these estimates can be derived for all element types on the basis of an abstract result given in Subsection 4.3.

A second peculiarity of the proof of anisotropic interpolation error estimates is that the transformation F_e has to be investigated very carefully. We obtain essential assumptions on the geometry of the elements (like the maximal angle condition) and on the location of the elements in the coordinate system (a coordinate system condition). These conditions are formulated in Sections 5–9 for each element type separately.

Triangular elements are considered in Section 5. We prove the estimate on the reference element (Lemma 5.1), formulate the maximal angle condition and the coordinate system condition,

prove estimate (2.5) under the assumptions

$$1 \le \ell \le k+1, \quad p \in [1,\infty], \quad 0 \le m \le \ell - 1,$$
$$q \in [1,\infty] \quad \text{such that } W^{\ell-m,p} \hookrightarrow L^q(e),$$
$$p > 2 \quad \text{if } \ell = 1$$

(Theorem 5.5, k is the polynomial degree), and derive the corresponding estimate of type (2.4) (Corollary 5.6). In the discussion, we give examples that the assumptions $m \le \ell - 1$ (up to exceptional cases like $m = \ell = 0$, $p = \infty$), and $p > 2$ if $\ell = 1$, as well as the maximal angle condition are necessary.

Tetrahedral elements can be considered in the same way but they need special care, as investigated in Section 6. First, we need at least two reference elements, one for elements with three long edges, the other for elements with four long edges. Second, Lemma 6.1 (the counterpart of Lemma 5.1, the estimate on the reference element) does not hold for $p \le 2$ if $m = \ell - 1$ (Example 6.2). This includes in particular the case $m = k$, $p = 2$, which is often used when $k = 1$. Third, the proof of the properties of the transformation $x = F_e(\hat{x})$ is more challenging due to the greater variability (Lemma 6.3). Additionally to the estimates which are analogous to Section 5, we prove two more types of anisotropic interpolation error estimates. At the end of Subsection 6.1, we consider functions with additional smoothness, $u \in W^{k+2,p}(e)$, as a remedy to treat the case $m = k$, $p \le 2$ (Theorem 6.5). Furthermore, we derive in Subsection 6.2 local interpolation error estimates for functions from weighted Sobolev spaces (Theorems 6.9 and 6.11). Special cases of these theorems were proved in [19, 21] to be able to treat edge singularities.

The estimates for triangles extend to *affine quadrilateral elements*, that are parallelograms. There is only one small difference in the proof of Lemma 7.1 (estimate on the reference element) where attention is needed. But there are two more reasons why a whole section is devoted to quadrilateral elements. First, for *rectangular elements* we can prove for $k \ge 2$ a slightly sharper estimate, with less terms on the right hand side (Theorem 7.11 and Remark 7.12). Second, for *more general elements* than parallelograms, for example trapezes, the transformation $x = F_e(\hat{x})$ is non-linear. This leads not only to a technically more complex transformation of the estimate, but also to a non-optimal result with lower order terms on the right hand side (Lemma 7.16) [5]. Nevertheless, we were finally able to reproduce the estimates of the affine elements (Theorem 7.17, Corollary 7.18). The section ends with an example showing the necessity of an assumption on the geometry of the non-affine elements.

In Section 8 we formulate all statements for (first affine, then non-affine) *hexahedral elements*. It turns out that all ideas for the proofs are already contained in Sections 5–7. For the same reason we shortened also the discussion of *pentahedral elements* (triangular prisms) in Section 9.

The last section of Chapter II is devoted to historical remarks and alternative approaches. We discuss related interpolation results of other authors and ideas of their proof. These are sometimes really fascinating though they were not sufficient for our purposes.

For several investigations, the Lagrangian interpolant turns out to be not appropriate. One drawback is that nodal values of u have to be well defined for the definition of $\mathrm{I}_h u$. Even more, it is not sufficient for the proof of local interpolation error estimates to consider functions $u \in W^{\ell,p}(e) \cap \mathcal{C}(\overline{e})$. We need assumptions on ℓ and p which imply the Sobolev embedding $W^{\ell,p}(e) \hookrightarrow \mathcal{C}(\overline{e})$ (though this embedding is explicitly used only in the case $m = 0$). Consequently, the Lagrange interpolation is not suited for functions $u \in W^{\ell,p}(\Omega)$ when $p\ell \le d$ (besides the exceptional case $p = 1$, $\ell = d$), for example for $u \in W^{1,2}(\Omega)$.

A second drawback is that the anisotropic elements imply further restrictions on the range of the parameters. In particular, the estimate

$$|u - \mathrm{I}_h u; W^{1,p}(e)| \lesssim \sum_{i=1}^{3} h_{i,e} \left| \frac{\partial u}{\partial x_i}; W^{1,p}(e) \right|$$

and even the simplified version

$$|u - \mathrm{I}_h u; W^{1,p}(e)| \lesssim \operatorname{diam} e \; |u; W^{2,p}(e)|$$

hold only for $p > 2$ in three dimensions. This restriction leads to a non-optimal approximation result in our investigation of the anisotropically refined meshes near edges [19, 20], see Remark 19.3 on page 102.

A remedy (at least for the first drawback) is to mollify u in some neighbourhood σ_i of $X^{(i)}$ and to use values of the mollified function for the definition of the interpolant. Such approaches have been investigated for isotropic meshes by several authors, see, for example, [64, 171], [150, pages 92–102], [151, pages 15–19]. In Chapter III we investigate first the *Scott-Zhang operator* [171]. It turns out that estimates of type (2.5) can be proved in the $L^q(e)$-norm ($m = 0$, Theorem 12.1). But Example 12.2 shows that this approach cannot be applied for $m > 0$.

Therefore we suggest in Sections 13–15 three alternative operators. They can be viewed as *modifications/adaptions* of the Scott-Zhang operator. These operators allow to prove local stability and approximation estimates with different generality, see Theorems 13.3, 14.2, and 15.1 for functions from classical Sobolev spaces, and Lemmata 13.5 and 15.3 for functions from weighted Sobolev spaces. But for all three operators the ranges of the parameters ℓ, m, p, and q contain those of the Lagrange interpolation. We compare the operators in detail in Section 17.

The stability and approximation properties are investigated for *five types of two- and three-dimensional finite elements* with *shape functions of arbitrary order*. However, we restrict ourselves to *elements of tensor product type*. Such elements contain certain orthogonal edges/faces, see Section 3 for the exact definition.

As it was the case with the Lagrange interpolation, the proof of the properties of the Scott-Zhang operator for isotropic elements cannot be applied directly for anisotropic elements. Some new ideas were necessary. Unfortunately, these ideas depend on the geometrical conditions on the mesh mentioned above. That means that the generalization to a broader class of elements will contain not only a more general coordinate transformation. It is a task for the future to develop some new ideas.

Chapters IV and V (Sections 18–26) contain anisotropic discretization strategies and global error estimates for model problems, for example the Poisson problem and the convection-diffusion-reaction problem. The differential operators in these problems are simple, the solution is always only a scalar function. Our main interest is to treat typical peculiarities (typical also for more complex problems) like boundary layers or edge and corner singularities. We focus on the applicability of the techniques to *general polygonal/polyhedral domains* and to piecewise polynomial trial functions of *arbitrary* (but fixed) *degree* k.

For about ten years the author has been interested in elliptic problems, posed over domains with corners and *edges*. The latest results are contained in Chapter IV.

The solution of such problems has both singular and anisotropic behaviour. The singularity leads to a reduced convergence order of the finite element method on quasi-uniform meshes. A remedy is local mesh refinement, and it turns out that the adequate refinement is anisotropic [9, 19, 21]. Note that isotropic refinement can be applied as well [11, 23], but only for a moderate singularity exponent $\lambda > 1/3$, and computations show that the additional refinement *along* the edge is not necessary. Section 19 may serve as a more detailed introduction.

In Section 20, we consider the Poisson problem,

$$-\Delta u = f \quad \text{in } \Omega, \qquad u = 0 \quad \text{on } \Gamma_1, \qquad \frac{\partial u}{\partial n} = 0 \quad \text{on } \Gamma_2 := \partial\Omega \setminus \Gamma_1,$$

for simplicity over a three-dimensional tensor product domain $\Omega = G \times (0, z_0)$. We prove for model cases and piecewise linear trial functions the approximation estimate

$$\|u - u_h; W^{m,2}(\Omega)\| \lesssim h^{2-m} \|f; L^2(\Omega)\|, \qquad m = 0, 1,$$

by using the Scott-Zhang interpolation results (Theorem 20.2 and Corollary 20.3). Using the Lagrange interpolant we needed in former papers more smoothness of the data ($f \in W^{4,2}(\Omega)$ in [9]) or a stronger refinement condition [19].

By using trial functions of higher degree k and a corresponding stronger anisotropic mesh grading one can prove for model cases (Examples 20.9 and 20.10) that edge singularities can be approximated according to

$$\|u - u_h; W^{1,2}(\Omega)\| \lesssim h^k.$$

The basis for this estimate is set by the global interpolation error estimates in Theorems 20.7 and 20.8. Of course, the right hand side f has to be sufficiently smooth.

Note that we present asymptotic estimates always in terms of $h := \max_{e \in \mathcal{T}_h} \operatorname{diam} e$. Since we advocate only strategies where the number of elements is $N_{\text{el}} \sim h^{-d}$, the error can easily be expressed in terms of N_{el} or the number N of unknowns (degrees of freedom).

For general polyhedral domains or more general differential operators one has to combine the anisotropic refinement near singular edges with an isotropic refinement for treating the additional corner singularities. One of the challenges has been to describe a family of meshes which is both suited for proving approximation error estimates and for a simple realization in a computer program. With our proposal [21], see also the summary in Section 21, the construction of such meshes is principally known. The analysis is done, however only in the case of piecewise linear trial functions, $k = 1$ (Theorem 21.4 and Corollary 21.5). The difficulty for $k \geq 2$ consists in a sufficiently fine description of the properties of the solution u. The section is completed with a computation of the Poisson equation in the Fichera domain.

One of the surprising results is that the anisotropic mesh grading does not disturb the asymptotics of the condition number κ of the stiffness matrix. We show in Subsection 20.3 that $\kappa \lesssim h^{-2}$ as in the case of a family of quasi-uniform meshes and a smooth solution.

In Chapter V we consider singularly perturbed problems. The solution of the model problem

$$-\varepsilon^2 \Delta u + cu = f \quad \text{in } \Omega \subset \mathbb{R}^d \quad (d = 2, 3), \qquad u = 0 \quad \text{auf } \partial\Omega,$$

is characterized for $0 < \varepsilon \ll 1$ by a boundary layer of width $\mathcal{O}(\varepsilon |\ln \varepsilon|)$. The derivatives normal to the boundary layer include negative powers of ε and are therefore large in comparison with derivatives in tangential direction. Therefore, as in the case of edge singularities, the natural way to resolve the boundary layer is to use anisotropic finite elements. As shown in Section 24, isotropic local mesh refinement leads only to an approximation result which is not uniformly valid with respect to the perturbation parameter ε.

Error estimates for the anisotropic discretizations were derived in the energy norm

$$|||\,.\,|||_\Omega \sim \varepsilon |\,.\,; W^{1,2}(\Omega)| + \|\,.\,; L^2(\Omega)\|$$

in [6, 14] for a class of simplicial meshes ($d = 2, 3$) and in [5] for meshes with quadrilateral elements. In all these papers the width a of the refinement zone is $\mathcal{O}(\varepsilon |\ln \varepsilon|)$ and corner/edge singularities were excluded by demanding certain compatibility conditions on the data.

In Section 25 we summarize and extend this analysis (Lemmata 25.4–25.6, Theorems 25.8 and 25.9). On the one hand we incorporate an additional mesh refinement to treat also *corner singularities*. This is restricted to two dimensions but the techniques should work also in three dimensions. The critical point is to obtain a detailed description of the properties of the solution. On the other hand, results in related literature led to the assumption that for $h \geq \varepsilon$ (which is the interesting case in practice) a numerical layer of width $a = \mathcal{O}(\varepsilon |\ln h|)$ is more appropriate. Therefore we investigate also this case in Section 25. The final result is

$$|||\, u - u_h \,|||_\Omega \lesssim h^k \varepsilon^{1/2} \min\{|\ln h|^{k+1/2};\ |\ln \varepsilon|^{k+1}\} + h^{k+1},$$

if $a = a_* \varepsilon \min\{|\ln h|;\ |\ln \varepsilon|\}$ with a suitable constant a_* is chosen (Corollary 25.11). The section ends with a discussion of insufficient refinement near the corners (Lemmata 25.14 and 25.16).

A more difficult singularly perturbed problem is obtained by including a convection term,

$$-\varepsilon \Delta u + b \cdot \nabla u + cu = f \quad \text{in } \Omega \subset \mathbb{R}^d \quad (d = 2, 3), \qquad u = 0 \quad \text{auf } \partial\Omega.$$

In Section 26 we present in a uniform notation some approximation results for a *pure* (Theorem 26.5) and a *stabilized* Galerkin finite element method on anisotropic meshes (Theorem 26.6). These results were mainly derived in [13, 73, 186]. An approximation error estimate with optimal convergence order which is also uniformly valid with respect to the perturbation parameter ε is derived for the stabilized method only in the case of rather small stabilization parameters (Remark 26.7). It needs further investigation whether the method is stable enough or whether the proof can be extended to a stronger stabilization.

Chapter VI (Sections 27–29) is devoted to some topics which are treated unsatisfactorily up to now. Section 27 serves as an introduction. We comment on some problems which were left open in Chapters III–V, and also on a more complex application.

A-priori estimates of the finite element error form only one of the two legs of the finite element analysis. The other leg consists in *a-posteriori error estimates*. They are the basis for assessing the quality of a particular finite element solution and for the creation of *automatic mesh adapting finite element strategies*. However, the majority of papers on this topic assume a family of isotropic meshes. In Section 28 we review results for anisotropic meshes.

The calculation of a finite element solution u_h includes the solution of an algebraic system of equations for the coefficients of the representation of u_h in a certain basis. Most often the nodal basis, see (2.2), is used but then the system matrix is ill-conditioned. Therefore a preconditioned system of equations is solved. Modern *preconditioners* are optimal in the sense that the condition number of the preconditioned matrix is independent of the number of unknowns. But, as with the case of error estimators, most of the theory is restricted to families of isotropic meshes. In Section 29, we summarize some preliminary results of our ongoing research into preconditioning techniques for anisotropic finite element discretizations.

Finally, with Section 30, a short description of software is appended. The three software packages were used for the numerical examples throughout the whole monograph.

3 Notation and analytical background

The main intention of this section is to introduce and to collect notation which is used uniformly throughout the report. Other notation may have different meaning in different sections.

General notation

Let us define the following:

d	the space dimension, $d = 2, 3$,
$\|.\|$	the Euclidean norm in $\mathbb{R}^d$,
$(x_1, \ldots, x_d)$	a global Cartesian coordinate system,
dist (G_1, G_2)	the distance of two points or domains $G_1, G_2 \subset \mathbb{R}^d$, dist $(G_1, G_2) := \inf_{x \in G_1, y \in G_2} \|x - y\|$.

We identify a point $x \in \mathbb{R}^d$ with its vector of coordinates $(x_1, \ldots, x_d)^T$.

We denote by $\mathbb{N}$ the set of non-negative integers and use a multi-index notation with $\alpha := (\alpha_1, \ldots, \alpha_d)$, $\alpha_i \in \mathbb{N}$,

$$|\alpha| := \sum_{i=1}^{d} \alpha_i, \quad \alpha! := \alpha_1! \cdots \alpha_d!, \quad x^\alpha := x_1^{\alpha_1} \cdots x_d^{\alpha_d}, \quad \text{and } D^\alpha := \frac{\partial^{\alpha_1}}{\partial x_1^{\alpha_1}} \cdots \frac{\partial^{\alpha_d}}{\partial x_d^{\alpha_d}}.$$

The notation $a \lesssim b$ and $a \sim b$ means the existence of positive constants C_1 and C_2 (which are independent of $\mathcal{T}_h$ and of the function under consideration) such that $a \le C_2 b$ and $C_1 b \le a \le C_2 b$, respectively. When problems with a perturbation parameter ε are considered then C_1 and C_2 are also independent of ε.

Reference elements

Finite elements $e \subset \mathbb{R}^d$ are defined via a (finite number of) reference element(s) $\hat{e} \subset \mathbb{R}^d$,

$\hat{e} := \{(\hat{x}_1, \hat{x}_2)^T \in \mathbb{R}^2 : 0 < \hat{x}_1 < 1,\ 0 < \hat{x}_2 < 1 - \hat{x}_1\}$	for triangles,
$\hat{e} := \{(\hat{x}_1, \hat{x}_2)^T \in \mathbb{R}^2 : 0 < \hat{x}_1, \hat{x}_2 < 1\}$	for rectangles,
$\hat{e} := \{(\hat{x}_1, \hat{x}_2, \hat{x}_3)^T \in \mathbb{R}^3 : 0 < \hat{x}_1, \hat{x}_3 < 1,\ 0 < \hat{x}_2 < 1 - \hat{x}_1\}$	for pentahedra,
$\hat{e} := \{(\hat{x}_1, \hat{x}_2, \hat{x}_3)^T \in \mathbb{R}^3 : 0 < \hat{x}_1, \hat{x}_2, \hat{x}_3 < 1\}$	for hexahedra.

For tetrahedra we consider two reference elements. The first is

$$\hat{e} := \{(\hat{x}_1, \hat{x}_2, \hat{x}_3)^T \in \mathbb{R}^3 : 0 < \hat{x}_1 < 1,\ 0 < \hat{x}_2 < 1 - \hat{x}_1,\ 0 < \hat{x}_3 < 1 - \hat{x}_1 - \hat{x}_2\} \tag{3.1}$$

for tetrahedra that have three edges E with $\text{meas}_1 E \sim \text{diam}(e)$. The second is

$$\hat{e} := \{(\hat{x}_1, \hat{x}_2, \hat{x}_3)^T \in \mathbb{R}^3 : 0 < \hat{x}_1 < 1,\ 0 < \hat{x}_2 < 1 - \hat{x}_1,\ 0 < \hat{x}_3 < \hat{x}_1\} \tag{3.2}$$

$$\text{or } \hat{e} := \{(\hat{x}_1, \hat{x}_2, \hat{x}_3)^T \in \mathbb{R}^3 : 0 < \hat{x}_1 < 1,\ 0 < \hat{x}_2 < 1 - \hat{x}_1,\ \hat{x}_1 < \hat{x}_3 < 1 - \hat{x}_2\} \tag{3.3}$$

for tetrahedra with four edges E with $\text{meas}_1 E \sim \text{diam}(e)$. The reason for having two choices for the second reference element is that the first one is considered if $h_3 = o(h_1)$ and the second one if $h_1 = o(h_3)$. Depending on the application it may be more natural to use $h_1 \gtrsim h_2 \gtrsim h_3$ or $h_1 \lesssim h_2 \lesssim h_3$. The use of these two variants for a second reference element prevents us from using a permutation of the axes of the coordinate system. (In the case of five edges E with $\text{meas}_1 E \sim \text{diam}(e)$ we can use either of the reference elements.)

Polynomial spaces

With respect to the type of the reference element $\hat{e}$ we define polynomial spaces $\mathcal{P}_{k,\hat{e}}$,

$$\mathcal{P}_{k,\hat{e}} \supset \mathcal{P}_k^d := \left\{ \sum_{|\alpha| \le k} a_\alpha x^\alpha, \;\; a_\alpha \in \mathbb{R}, \;\; \alpha = (\alpha_1, \ldots, \alpha_d) \right\}, \tag{3.4}$$

namely

$$\mathcal{P}_{k,\hat{e}} := \mathcal{P}_k^d \qquad \text{for triangular/tetrahedral elements,}$$

$$\mathcal{P}_{k,\hat{e}} := \mathcal{Q}_k^d := \left\{ \sum_{0 \le \alpha_{1,} \alpha_{2,} \alpha_3 \le k} a_\alpha x^\alpha, \;\; a_\alpha \in \mathbb{R} \right\} \qquad \text{for quadrilateral/hexahedral elements,}$$

$$\mathcal{P}_{k,\hat{e}} := \left\{ \sum_{\substack{0 \le \alpha_1 + \alpha_2 \le k \\ 0 \le \alpha_3 \le k}} a_\alpha x^\alpha, \;\; a_\alpha \in \mathbb{R} \right\} \qquad \text{for pentahedral elements.}$$

For simplicity of notation later on, we define

$$\mathcal{P}_{-1}^d := \{0\}.$$

The mapping to the element e

Let n_e be the number of *vertices* of $\hat{e}$. The nodal shape functions $\{\hat{\psi}_i\}_{i=1}^{n_e}$ in the case $k = 1$ are also used for the mapping $x = F_e(\hat{x})$ of $\hat{e}$ onto e. Let the vertices of e be locally enumerated as $i = 1, \ldots, n_e$ and denoted by $X_e^{(i)} := (X_{1,e}^{(i)}, X_{2,e}^{(i)})^T$. Then the subparametric mapping

$$x = F_e(\hat{x}) := \sum_{i=1}^{n_e} X_e^{(i)} \hat{\psi}_i(\hat{x}) \in (P_{1,\hat{e}})^d \tag{3.5}$$

defines e via $e = F_e(\hat{e})$. If this transformation is affine then the element is called *affine*. According to [182, Section 3.3] the element is *isoparametric* when the shape functions are used for the polynomial transformation F from the reference element $\hat{e}$ to the element e. The term *subparametric* indicates that only a subset of the shape functions is used.

Note that only the vertices of e enter into the transformation (3.5), hence the shape of e is defined by its vertices. In particular, all edges of e are straight. More general elements are not considered here. Therefore all triangular and tetrahedral elements are affine. Other affine elements are parallelograms, parallelepipeds, and prismatic pentahedra.

As an alternative to (3.5), an affine mapping can be written as

$$x = B_e \hat{x} + b_e, \quad B_e := (b_{i,j,e})_{i,j=1}^d \in \mathbb{R}^{d \times d}, \quad b_e := (b_{i,e})_{i=1}^d \in \mathbb{R}^d. \tag{3.6}$$

In particular, we say that e is a *tensor product element* if B_e is a diagonal matrix,

$$b_{i,j,e} = 0 \quad \text{for } i \ne j. \tag{3.7}$$

In three dimensions, we also define *elements of tensor product type* by demanding

$$b_{1,3,e} = b_{2,3,e} = b_{3,1,e} = b_{3,2,e} = 0, \quad \left| \begin{matrix} b_{1,1,e} & b_{1,2,e} \\ b_{2,1,e} & b_{2,2,e} \end{matrix} \right| \sim b_{1,1,e}^2 \sim b_{2,2,e}^2. \tag{3.8}$$

In three dimensions, tensor product elements are of tensor product type if $b_{1,1,e} \sim b_{2,2,e}$. Since we do not need this distinction in the two-dimensional case we will say that tensor product elements are also of tensor product type there. We introduce these special types of elements here in order to simplify the mapping for the use in Chapter III.

The elements e

Let us consider Lagrangian finite elements and define the following:

N_e	the number of nodes of e,
$\{\hat{X}^{(i)}\}_{i=1}^{N_e}$	the set of *nodes* of $\hat{e}$, $\{\hat{X}^{(i)}\}_{i=1}^{N_e} := \{0, \frac{1}{k}, \frac{2}{k}, \ldots, 1\}^d \cap \overline{\hat{e}}$,
$\{\hat{\varphi}_i(\hat{x})\}_{i=1}^{N_e}$	the shape functions on the reference element,
	$\operatorname{span}\{\hat{\varphi}_i(\hat{x})\}_{i=1}^{N_e} = \mathcal{P}_{k,\hat{e}}$, $\hat{\varphi}_i(\hat{X}^{(j)}) = \delta_{i,j}$ $(i,j = 1, \ldots, N_e)$,
$\{\varphi_{i,e}(x)\}_{i=1}^{N_e}$	the shape functions on the element e in local enumeration,
	$\varphi_{i,e}(x) := \hat{\varphi}_i(F_e^{-1}(x))$ $(i = 1, \ldots, N_e)$,
$\mathcal{P}_{k,e}$	the linear space of shape functions on the element e,
	$\mathcal{P}_{k,e} := \operatorname{span}\{\varphi_{i,e}(x)\}_{i=1}^{N_e}$,
$\operatorname{diam}(e)$	the diameter of e, $\operatorname{diam}(e) := \sup_{x,y \in e} \lvert x - y \rvert$,
ϱ_e	the supremum of the diameters of all balls contained in e,
$h_{1,e}, \ldots, h_{d,e}$	element sizes, see Sections 5–9 and 11,
S_e	the patch of elements around e, $S_e := \operatorname{int} \bigcup \{\overline{e'} : e' \in \mathcal{T}_h, \overline{e'} \cap \overline{e} \neq \emptyset\}$,
I_e	the index set for the nodes $X^{(i)} \in \overline{e}$, $i \in I_e$, in *global* enumeration.

Note that the functions $\varphi_{i,e}(x)$ are polynomial only in the case of affine elements e. Since the considerations in Chapters II and III are local we will often omit the subscript e in the notation.

We point out that the term *finite element* means, according to [63, page 78], the triple $(e, \mathcal{P}_{k,e}, \Sigma_{k,e})$. Here, e is a non-empty subdomain of Ω with a Lipschitz boundary, $\mathcal{P}_{k,e}$ is the space of shape functions, and $\Sigma_{k,e}$ is a basis in $\mathcal{P}'_{k,e}$. However, sometimes we simply call e a finite element. In *Lagrangian finite elements* the functionals of $\Sigma_{k,e}$ result in the values at the nodes.

The family of meshes

For a mesh $\mathcal{T}_h$, we assume the usual admissibility conditions, see Section 1, and define the following:

h	the maximal element diameter, $h := \max_{e \in \mathcal{T}_h} \operatorname{diam}(e)$,
I	the index set for the nodes,
$\{X^{(i)}\}_{i \in I}$	the set of nodes of the mesh,
$\{\varphi_i\}_{i \in I}$	the set of trial functions in global enumeration,
V_h, V_{0h}	the spaces of trial functions, see (1.3), $V_h := \operatorname{span}\{\varphi_i\}_{i \in I}$,
N_{el}	the number of elements.

A mesh $\mathcal{T}_h$ is called *isotropic* iff all elements are isotropic, see (1.4). A family $\mathcal{F} = \{\mathcal{T}_h\}$ of isotropic meshes is called *quasi-uniform* iff $h \sim \operatorname{diam}(e)$ for all $e \in \mathcal{T}_h$, that means that the length scales of the elements are translation-invariant.

Approximation operators

We employ the following approximation operators:

Π_{σ_i}	the projection operator $L^2(\sigma_i) \to \mathcal{P}_{k,\sigma_i}$, see Sections 12, 16,
I_h	the nodal interpolation operator, see Sections 2, 4, and 17,
I	the nodal interpolation operator when applied on the reference element,
C_h	the Clement operator, see Sections 16 and 17,
O_h	the quasi-interpolation operator introduced by Oswald, see Sections 16, 17,
Z_h	the original Scott-Zhang operator, see Sections 12 and 16,
S_h	the modified Scott-Zhang operator using small edges(2D)/faces(3D), see Section 13 and 16,
L_h	the modified Scott-Zhang operator using large edges(2D)/faces(3D), see Section 14 and 16,
E_h	the modified Scott-Zhang operator using long edges (3D), see Section 15 and 16.

Function spaces

For a bounded domain $G \subset \mathbb{R}^d$ with Lipschitz boundary (the results may hold true for more general classes of domains such as domains satisfying a strong cone condition but we will not discuss this here) we denote by $\mathcal{C}(\overline{G})$ the space of functions which are continuous on $\overline{G}$. $\mathcal{C}^\infty(G)$ means the space of functions that have continuous derivatives of any order and $\mathcal{D}'(G)$ the space of distributions. Moreover, we introduce $\mathcal{C}_0^\infty(G) := \{v \in \mathcal{C}^\infty(G) : \operatorname{supp} v \subset G\}$.

Let $W^{\ell,p}(G)$, $\ell \in \mathbb{N}$, $p \in [1,\infty]$, be the Sobolev spaces with the norm

$$\|v; W^{\ell,p}(G)\|^p := \sum_{|\alpha|\le\ell} \int_G |D^\alpha v|^p$$

and the seminorms

$$|v; W^{\ell,p}(G)|^p := \sum_{|\alpha|=\ell} \int_G |D^\alpha v|^p, \qquad [v; W^{\ell,p}(G)]^p := \sum_{|\alpha|=1} \int_G |D^{\ell\alpha} v|^p$$

for $p < \infty$ and the usual modification for $p = \infty$. Note that the seminorm $|v; W^{\ell,p}(G)|$ contains all derivatives of order ℓ but $[v; W^{\ell,p}(G)]$ only the pure ("non-mixed") ones. The special case $W^{0,p}(G)$ is denoted by $L^p(G)$.

By introducing polar/cylindrical coordinates $x_1 = r\cos\phi$, $x_2 = r\sin\phi$, we define for $\ell \in \mathbb{N}$, $p \in [1,\infty]$, $\beta \in \mathbb{R}$, the weighted Sobolev spaces

$$V_\beta^{\ell,p}(G) := \{v \in \mathcal{D}'(G) : \|v; V_\beta^{\ell,p}(G)\| < \infty\}, \tag{3.9}$$

$$W_\beta^{\ell,p}(G) := \{v \in \mathcal{D}'(G) : \|v; W_\beta^{\ell,p}(G)\| < \infty\}, \tag{3.10}$$

where

$$\|v; V_\beta^{\ell,p}(G)\|^p := \sum_{|\alpha|\le\ell} \int_G |r^{\beta-\ell+|\alpha|} D^\alpha v|^p, \qquad |v; V_\beta^{\ell,p}(G)|^p := \sum_{|\alpha|=\ell} \int_G |r^\beta D^\alpha v|^p, \tag{3.11}$$

$$\|v; W_\beta^{\ell,p}(G)\|^p := \sum_{|\alpha|\le\ell} \int_G |r^\beta D^\alpha v|^p, \qquad |v; W_\beta^{\ell,p}(G)|^p := \sum_{|\alpha|=\ell} \int_G |r^\beta D^\alpha v|^p. \tag{3.12}$$

Moreover, let $R = R(x) := (x_1^2 + x_2^2 + x_3^2)^{1/2}$ and $\theta := r/R$ be the distance to the origin and the "angular distance" to the x_3-axis, respectively. We define for $\ell \in \mathbb{N}$, $p \in [1, \infty]$, $\beta, \delta \in \mathbb{R}$, weighted Sobolev spaces with two weights by

$$V^{\ell,p}_{\beta,\delta}(G) := \{v \in \mathcal{D}'(G) : \|v; V^{\ell,p}_{\beta,\delta}(G)\| < \infty\}$$

where

$$\|v; V^{\ell,p}_{\beta,\delta}(G)\|^p := \sum_{|\alpha| \le \ell} \int_G |R^{\beta-\ell+|\alpha|} \theta^{\delta-\ell+|\alpha|} D^\alpha v|^p, \tag{3.13}$$

$$|v; V^{\ell,p}_{\beta,\delta}(G)|^p := \sum_{|\alpha| = \ell} \int_G |R^{\beta} \theta^{\delta} D^\alpha v|^p. \tag{3.14}$$

Note that by this definition

$$V^{\ell,p}_{\beta}(G) = V^{\ell,p}_{\beta,\beta}(G). \tag{3.15}$$

Embedding and trace theorems

For two Banach spaces X and Y we denote by $X \hookrightarrow Y$ the continuous embedding of X into Y; this means $X \subset Y$ and

$$\exists C = C(G): \quad \|u; Y\| \le C \|u; X\| \quad \forall u \in X.$$

If the spaces are defined on a finite element e one has to separate out the dependence of C on h by making a transformation to a reference element.

Well known embedding theorems are

$$W^{\ell,p}(G) \hookrightarrow \mathcal{C}(\overline{G}) \quad \text{if} \begin{cases} \ell p > d, & p > 1, \\ \ell \ge d, & p = 1, \end{cases} \tag{3.16}$$

$$W^{\ell,p}(G) \hookrightarrow W^{m,p}(G) \quad \text{if } \ell \ge m, \tag{3.17}$$

$$W^{\ell,p}(G) \hookrightarrow W^{\ell,q}(G) \quad \text{if } p \ge q, \tag{3.18}$$

$$W^{\ell,p}(G) \hookrightarrow L^q(G) \quad \text{if} \begin{cases} \ell p < d, & \frac{1}{q} = \frac{1}{p} - \frac{\ell}{d}, \\ \ell p = d, & 1 \le q < \infty. \end{cases} \tag{3.19}$$

Let $M \subset \overline{G}$ be a manifold of dimension $\dim(M)$. If there exists a unique, continuous, linear trace operator $X(G) \to Y(M)$ then we will also write $X \hookrightarrow Y$. By analogy with the above, this means that

$$\exists C = C(G, M): \quad \|u; Y(M)\| \le C \|u; X(G)\| \quad \forall u \in X(G).$$

Here we have identified $u \in X(G)$ with its trace on M to keep the notation succinct. An important trace theorem is

$$W^{\ell,p}(G) \hookrightarrow L^p(M) \quad \text{if} \begin{cases} \ell p > d - \dim(M), & p > 1, \\ \ell \ge d - \dim(M), & p = 1. \end{cases} \tag{3.20}$$

For an introduction and overview about the theory of function spaces see, for example, [1, 87, 115, 116, 128, 146] or the summaries in finite element monographes as [57, 63].

Chapter II

Lagrange interpolation on anisotropic elements

This chapter is devoted to anisotropic local interpolation error estimates for anisotropic Lagrangian finite elements. In Section 4, two basic tasks are elaborated for proving such estimates. Moreover, an abstract error estimate is established which is used in Sections 5–9 to derive the estimates for all element types. Section 10 contains results and approaches of other authors which are related to the topic of this chapter.

Triangles, tetrahedra and quadrilateral elements are considered in separate sections in order to focus on special difficulties of these element classes.

4 General considerations

4.1 The aim of this chapter

The aim of this chapter is to prove anisotropic interpolation error estimates for anisotropic Lagrangian finite elements. The *Lagrangian interpolant*, also called *nodal interpolant*, is defined by

$$\mathrm{I}_h u := \sum_{i \in I} u(X^{(i)}) \varphi_i(x), \tag{4.1}$$

where $X^{(i)}$ are the nodes and $\varphi_i(x)$ are the nodal basis functions. Since I_h is defined locally on every element the interpolation error $u - \mathrm{I}_h u$ can be estimated elementwise. In Section 1, we motivated already that we are interested in error estimates of the form

$$|u - \mathrm{I}_h u; W^{m,q}(e)| \lesssim (\mathrm{meas}_d e)^{1/q - 1/p} \sum_{|\alpha| = \ell - m} h^\alpha |D^\alpha u; W^{m,p}(e)|. \tag{4.2}$$

The main result of this chapter is that this estimate holds for $u \in W^{\ell,p}(e)$, $1 \le \ell \le k+1$, $p \in [1,\infty]$, if $m \in \{0, \dots, \ell - 1\}$, $q \in [1,\infty]$ are such that $W^{\ell - m, p}(e) \hookrightarrow L^q(e)$ and if the conditions

$$p > d/\ell \qquad \text{if } m = 0 \text{ and } \ell = 1, \dots, d-1, \tag{4.3}$$

$$p > 2 \qquad \text{if } d = 3 \text{ and } m = \ell - 1 > 0, \tag{4.4}$$

are fulfilled. Additionally the element e has to satisfy assumptions on the geometry (like the maximal angle condition) and on the location in the coordinate system (coordinate system condition). We show also that all these conditions are necessary.

In this chapter we discuss also restrictions of the Lagrange interpolation. These include the following.

1. The operator I_h cannot be applied to discontinuous functions. Even more, it is not sufficient for the proof of local interpolation error estimates to consider functions $u \in W^{\ell,p}(e) \cap \mathcal{C}(\overline{e})$. We need assumptions on ℓ and p which imply the embedding

$$W^{\ell,p}(e) \hookrightarrow \mathcal{C}(\overline{e})$$

(We remark that this Sobolev embedding theorem is explicitly used only in the case $m = 0$, therefore (4.3) is formulated only for $m = 0$. But for $\ell \geq d$ the embedding theorem is valid for all $p \in [1, \infty]$ and in the remaining case $d = 3$, $m = 1$, $\ell = 2$ condition (4.4) implies this embedding.) Consequently, the Lagrange interpolation is not suited for some classes of functions, for example for $u \in W^{1,2}(\Omega)$.

2. The condition (4.4) implies that the estimate

$$|u - \mathrm{I}_h u; W^{1,p}(e)| \lesssim \sum_{|\alpha|=1} h^\alpha \left| D^\alpha u; W^{1,p}(e) \right|$$

is valid only for $p > 2$ in three dimensions. This restriction leads to a non-optimal approximation result in our investigation of the anisotropically refined meshes near edges [19, 20], see Remark 19.3 on page 102.

3. The case $m = \ell$ is not allowed. This means for example that the estimate

$$|u - \mathrm{I}_h u; W^{1,p}(e)| \lesssim |u; W^{1,p}(e)|$$

is not valid even when the Sobolev embedding theorem is fulfilled ($p > d$). Such estimates are of interest when finite element functions are to be interpolated on a coarser mesh.

We note however that the points 1 and 3 are general properties of the Lagrangian interpolation operator and not introduced by the anisotropic meshes. One remedy is to consider alternative interpolation operators. We will treat this in Chapter III.

For the investigation of the approximation error near edges we have used in [19, 21] another approach to cope with functions which are not contained in $W^{2,p}(e)$, $p > 2$. It turns out that the solution of the Poisson problem in domains with edges and corners can be described favourably in weighted Sobolev spaces $V^{\ell,p}_\beta(\Omega)$ or $V^{\ell,p}_{\beta,\delta}(\Omega)$, see Section 3 for the definition of these spaces. Therefore we derive in Subsection 6.2 estimates of $|u - \mathrm{I}_h u; W^{m,p}(e)|$ for functions u from such spaces.

The outline of the chapter is as follows. In the next subsection we elaborate two basic tasks to be solved in order to prove anisotropic interpolation error estimates. Then we prove in Subsection 4.3 an abstract error estimate for an approximation operator (Lemma 4.5). By verifying the assumptions of this lemma we derive in the following sections the estimates on the reference elements for all the element types. Moreover, we investigate in these sections which elements are admissible for the validity of anisotropic interpolation error estimates. For such elements we prove properties of the transformation $x = F(\hat{x})$ and conclude the error estimates.

We separate triangles, tetrahedra and quadrilateral elements in order to focus on special difficulties. We motivate this also in Subsection 4.2 and at the beginning of each section. The final section of this chapter, Section 10, contains results and approaches of other authors which are related to anisotropic elements.

4.2 Basic tasks for proving anisotropic interpolation error estimates

The main strategy to prove anisotropic interpolation error estimates is old, namely, to derive first the estimate on a reference element $\hat{e}$ and to apply a coordinate transformation $x = F_e(\hat{x})$ with $e = F_e(\hat{e})$. This procedure ensures that the constant in the transformed estimate depends only on $\hat{e}$, and not on (the size of) e.

For proving estimates of type (4.2) for anisotropic elements we have to recognize first that sharper estimates on the reference element have to be shown, sharper than it is necessary for isotropic elements. We give an example to elucidate this.

Example 4.1 Consider a triangular element e with linear interpolation. An estimate on the reference element $\hat{e} := \{(\hat{x}_1, \hat{x}_2)^T \in \mathbb{R}^2 : 0 < \hat{x}_1 < 1, 0 < \hat{x}_2 < 1 - \hat{x}_1\}$ is in this case

$$|\hat{v} - \mathrm{I}\hat{v}; W^{1,p}(\hat{e})| \lesssim |\hat{v}; W^{2,p}(\hat{e})|, \quad p \in [1, \infty]. \tag{4.5}$$

This means in particular

$$\|\hat{D}^{(0,1)}(\hat{v} - \mathrm{I}\hat{v}); L^p(\hat{e})\| \lesssim |\hat{v}; W^{2,p}(\hat{e})|, \quad p \in [1, \infty]. \tag{4.6}$$

Note that we omit the index h when the operator is applied on the reference element.

For the special element $e := \{x = (x_1, x_2)^T \in \mathbb{R}^2 : 0 < x_1 < h_1, 0 < x_2 < h_2(1 - x_1/h_1)\}$ we can directly calculate $\hat{D}^\alpha \hat{v} = h^\alpha D^\alpha v$ and

$$|\hat{v}; W^{\ell,p}(\hat{e})|^p = h_1 h_2 \sum_{|\alpha|=\ell} h^{\alpha p} \|D^\alpha v; L^p(e)\|^p .$$

In this way we conclude the estimate

$$\|D^{(0,1)}(v - \mathrm{I}_h v); L^p(e)\|^p \lesssim h_1^{2p} h_2^{-p} \|D^{(2,0)} v; L^p(e)\|^p + \sum_{|\alpha|=1} h^{\alpha p} \|D^{\alpha+(0,1)} v; L^p(e)\|^p .$$

If $h_2 = o(h_1)$ we have a term with the bad asymptotics $h_1^2 h_2^{-1} \sim [\mathrm{diam}\,(e)]^2 \varrho_e^{-1}$.

By tracing back the origin of this term we see that we have to prove

$$\|\hat{D}^{(0,1)}(\hat{v} - \mathrm{I}\hat{v}); L^p(\hat{e})\| \lesssim |\hat{D}^{(0,1)}\hat{v}; W^{1,p}(\hat{e})| \tag{4.7}$$

when we want to show an estimate of the quality (4.2). □

In conclusion of this example we can formulate a first basic task.

Basic task 1: Consider elements $\hat{e}$ with the polynomial space $\mathcal{P}_{k,\hat{e}}$ (see Section 3 for the definition). Let $\hat{u} \in W^{\ell,p}(\hat{e})$ with some $\ell \le k + 1$. Derive an estimate analogous to (4.7) for the interpolation error $\hat{u} - \mathrm{I}\hat{u}$ in the norm of $W^{m,q}$:

$$\|\hat{D}^\gamma(\hat{v} - \mathrm{I}\hat{v}); L^q(\hat{e})\| \lesssim |\hat{D}^\gamma \hat{v}; W^{\ell-m,p}(\hat{e})| \quad \forall \gamma : |\gamma| = m. \tag{4.8}$$

In particular, derive the ranges of k, ℓ, p, m, and q for which (4.8) is true.

We will see in this chapter that such estimates can be derived for all element types on the basis of the general Lemma 4.5 in Subsection 4.3. But the conditions for (4.8) must be elaborated with care. For example, (4.7) holds for $p \in [1, \infty]$ in the two-dimensional case, but only for $p \in (2, \infty]$ in three dimensions, see Sections 5 and 6. (Note that estimate (4.5) holds for $p \in (3/2, \infty]$ for $d = 3$.) This is one reason why we treat two- and three-dimensional elements in separate sections.

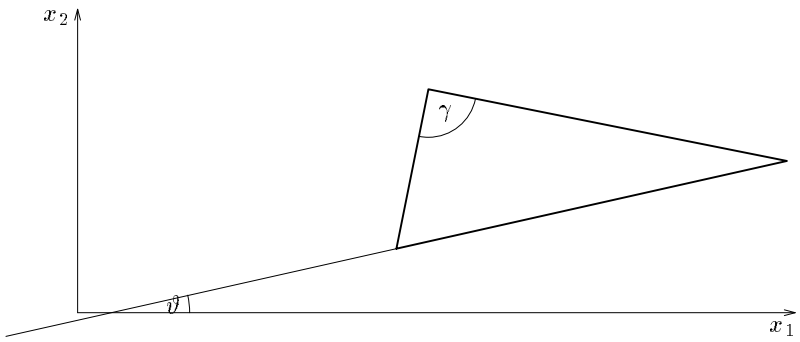

Figure 4.1: Illustration of the maximal angle condition and the coordinate system condition (triangle).

A second peculiarity of the proof of anisotropic interpolation error estimates is that the transformation F_e has to be investigated very carefully. For example, for the proof of estimate (4.2) in the case of triangular elements it is necessary to formulate conditions on the maximal interior angle γ (maximal angle condition: $\gamma \leq \gamma_* < \pi$) and the angle ϑ between the longest side and the x_1-axis (coordinate system condition: $|\sin\vartheta| \lesssim h_2/h_1$), see Figure 4.1 for an illustration. These conditions become more complicated in three dimensions. So one can formulate a second basic task.

Basic task 2: Describe classes of finite elements e for which (4.8) can be transformed (and summed up) to the desired estimate (4.2). In particular, define the element sizes $h_1, \ldots, h_d$ for such elements.

At this point we mention that this task involves more than the discussion of the transformation $x = F_e(\hat{e})$ when the element e is non-affine (for instance isoparametric). Consider the following example.

Example 4.2 Let us study the simplest isoparametric element, namely a quadrilateral element e with what are usually called bilinear basis functions. The reference element is defined by $\hat{e} := \{\hat{x} = (\hat{x}_1, \hat{x}_2)^T \in \mathbb{R}^2 : 0 < \hat{x}_1, \hat{x}_2 < 1\}$. Furthermore, denote by $\hat{\psi}_i(\hat{x}_1, \hat{x}_2)$, $i = 1, \ldots, 4$, the bilinear nodal shape functions. The transformation $F : \hat{e} \to e$ is given by

$$x = \sum_{i=1}^{4} X_e^{(i)} \hat{\psi}_i(\hat{x}) \tag{4.9}$$

which is affine only in the case where e is a parallelogram. (Recall from Section 3 that $X_e^{(i)} = (X_{1,e}^{(i)}, X_{2,e}^{(i)})^T$, $i = 1, \ldots, 4$, are the coordinates of the vertices of e.) The consequence is that

$$\hat{D}^{(1,1)} x_j \neq 0, \quad j = 1, 2,$$

in the non-affine case, which yields

$$\hat{D}^{(1,1)} \hat{u} = \sum_{|\alpha|=1} \sum_{|\beta|=1} D^{\alpha+\beta} u \, \hat{D}^{(1,0)} x^\alpha \hat{D}^{(0,1)} x^\beta + \sum_{|\alpha|=1} D^\alpha u \, \hat{D}^{(1,1)} x^\alpha .$$

Even in the case of isotropic elements, this is deficient because the second sum is only of order h due to $|\hat{D}^{(1,1)} x^\alpha| \lesssim h$ (usually), while the first term is of the desired order, h^2, due to $|\hat{D}^{(1,0)} x^\alpha| \lesssim h$ and $|\hat{D}^{(0,1)} x^\beta| \lesssim h$.

This peculiarity can be circumvented in the case of isotropic elements by showing an estimate without mixed derivatives,

$$|\hat{v} - \mathrm{I}\hat{v}; W^{m,p}(\hat{e})| \lesssim \|\hat{D}^{(2,0)}\hat{v}; L^p(\hat{e})\| + \|\hat{D}^{(0,2)}\hat{v}; L^p(\hat{e})\|, \quad m = 0, 1, \quad p \in [1, \infty).$$

But, for estimating $\|\hat{D}^{(0,1)}(\hat{v} - \mathrm{I}\hat{v}); L^p(\hat{e})\|$ in the anisotropic case, we have seen in Example 4.1 that the term $\|\hat{D}^{(2,0)}\hat{v}; L^p(\hat{e})\|$ must also be avoided on the right hand side. The consequence of the dilemma, that there cannot be avoided both $\|\hat{D}^{(1,1)}\hat{v}; L^p(\hat{e})\|$ and $\|\hat{D}^{(2,0)}\hat{v}; L^p(\hat{e})\|$, is that the transformation from $\hat{e}$ to e leads to a non-optimal estimate for non-affine elements. For example for the trapeze $e = \{(x_1, x_2) \in \mathbb{R}^2 : 0 < x_1 < h_1, 0 < x_2 < h_2(2 - x_1/h_1)\}$ we obtain by transforming (4.8) with $p = q = 2$, $\ell = 2$, $m = 1$, $\gamma = (0, 1)$ the estimate

$$\|D^{(0,1)}(v - \mathrm{I}_h v); L^2(e)\| \lesssim \sum_{|\alpha|=1} h^\alpha \|D^{\alpha+(0,1)}v; L^2(e)\| + \|D^{(0,1)}v; L^2(e)\| \tag{4.10}$$

which has no convergence order. If this estimate were sharp then anisotropic triangles would be preferable to anisotropic quadrilateral elements.

Fortunately, it turns out that this estimate is not sharp. In Theorem 7.17 we show that an estimate of type (4.1) can be proved for certain classes of non-affine elements. This is also a reason why we treat simplicial and non-simplicial elements in separate sections. □

4.3 Basic lemmata

One of the key ideas for deriving *convergence orders* in local interpolation error estimates is the observation that the seminorm $|\,.\,; W^{\ell,p}(\hat{e})|$ is a norm in the quotient space $W^{\ell,p}(\hat{e})/\mathcal{P}^d_{\ell-1}$,

$$\inf_{\hat{w} \in \mathcal{P}^d_{\ell-1}} \|\hat{u} - \hat{w}; W^{\ell,p}(\hat{e})\| \sim |\hat{u}; W^{\ell,p}(\hat{e})|.$$

This is already elaborated in the classical theory, see, for example, [63, Section 3.1]. For anisotropic error estimates we need a generalization of this relation. Since we use the lemma in the next chapter as well we must formulate it with quite general assumption on the domain.

Lemma 4.3 *Let $G = \bigcup_{j=1}^J G_j \subset \mathbb{R}^d$ be a connected open set that is the union of a finite collection of domains $G_j \subset \mathbb{R}^d$ that are star-shaped with respect to balls B_j. Let γ be a multi-index with $m := |\gamma|$ and $u \in L^1(G)$ be a function with $D^\gamma u \in W^{\ell-m,p}(G)$, where $\ell, m \in \mathbb{N}$, $0 \le m \le \ell$, $p \in [1, \infty]$. Then there exists a polynomial $w \in \mathcal{P}^d_{\ell-1}$ such that*

$$\|D^\gamma(u - w); W^{\ell-m,p}(G)\| \lesssim |D^\gamma u; W^{\ell-m,p}(G)|. \tag{4.11}$$

The constant depends only on d, ℓ, $\operatorname{diam} G_j$ and $\operatorname{diam} B_j$ $(j = 1, \ldots, J)$. The polynomial w depends only on ℓ, u, B_j $(j = 1, \ldots, J)$, but not on γ.

Proof The lemma was proved in more general form by Dupont and Scott [76]. By setting $A = \{\alpha : |\alpha| = \ell\}$ in [76, Theorem 4.2] we obtain the assertion for domains that are star-shaped with respect to a balls. The generalization of the class of domains is discussed in Remark 7.3 of that paper. ■

Since this short citation of the proof may not be satisfactory let us explain the main ideas for the proof. Let $G \subset \mathbb{R}^d$ be a bounded domain that is star-shaped with respect to a ball B.

Let a function $\phi \in \mathcal{C}_0^\infty(B)$ be given with $\int_B \phi = 1$, and a function (in the distribution sense) $u \in \mathcal{D}'(G)$. Then the Sobolev representation of u is defined by [76]

$$\begin{aligned} u &= Q^{(\ell)}u + R^{(\ell)}u, \quad \ell \geq 1, \\ (Q^{(\ell)}u)(x) &:= \sum_{|\alpha|\leq \ell-1} \int_B \phi(y)\,(D^\alpha u)(y)\,\frac{(x-y)^\alpha}{\alpha!}\,\mathrm{d}y \;\in\; \mathcal{P}^d_{\ell-1}, \\ (R^{(\ell)}u)(x) &:= \ell \sum_{|\alpha|=\ell} \int_G k(x,y)\,(D^\alpha u)(y)\,\frac{(x-y)^\alpha}{\alpha!}\,\mathrm{d}y, \\ k(x,y) &:= \int_0^1 s^{-d-1}\phi(x+s^{-1}(y-x))\,\mathrm{d}s. \end{aligned}$$

$Q^{(\ell)}u$ is an approximation of u with some nice properties including [76, Theorem 3.1, Remark 3.2, Theorem 3.2]

$$D^\alpha Q^{(\ell)}u = Q^{(\ell-|\alpha|)}D^\alpha u, \quad |\alpha| \leq \ell, \tag{4.12}$$

$$\|Q^{(\ell)}u; W^{\ell-1,\infty}(G)\| \leq C\,\|u; L^1(B)\|, \tag{4.13}$$

$$\|u - Q^{(\ell)}u; W^{\ell-1,p}(G)\| \leq C\,|u; W^{\ell,p}(G)|, \tag{4.14}$$

where the constant C depends only on d, ℓ, $\mathrm{diam}G$ and ϕ. Further results include more general classes of polynomials, estimates in fractional order Sobolev spaces, and the relaxation of domain constraints.

With (4.12) and (4.14) we can prove Lemma 4.3: If $D^\gamma u \in W^{\ell-m,p}(G)$ then

$$\|D^\gamma(u - Q^{(\ell)}u); W^{\ell-m,p}(G)\| = \|D^\gamma u - Q^{(\ell-m)}D^\gamma u; W^{\ell-m,p}(G)\| \lesssim |D^\gamma u; W^{\ell-m,p}(G)|.$$

Remark 4.4 We remark that an assertion similar to (4.11) was proved in [9, Lemmata 1 and 2] by a generalization of the Bramble-Hilbert theory [53]. In this paper we considered more general Sobolev spaces $H(\mathcal{P})^p$ which are defined via a set of multi-indices $\mathcal{P} \subset \mathbb{N}^d$, a parameter $p \in [1,\infty]$, and the seminorm

$$\|v; H(\mathcal{P})^p\|^p := \sum_{\alpha\in\mathcal{P}} \|D^\alpha v; L^p(\Omega)\|^p.$$

(Note that $H(\mathcal{P}^d_\ell)^p = W^{\ell,p}(\Omega)$, $d = \dim\Omega$.) However, the class domains is in that paper not as general as in Lemma 4.3 and the polynomial w depends on γ.

Second, the reader who is interested in the dependence of the constant in estimates like (4.11) on the diameters of G_j and B_j is referred to [104].

We give now a general error estimate for any finite element $(\hat{e}, \mathcal{P}_{k,\hat{e}}, \Sigma_{k,\hat{e}})$ considered in Sections 5–9. The following lemma and its proof can be found in a more general setting (non-standard Sobolev spaces, see Remark 4.4), but restricted to $q = p$, in [9, Lemma 3].

Lemma 4.5 *Let $\mathrm{I} : \mathcal{C}(\overline{\hat{e}}) \to \mathcal{P}_{k,\hat{e}}$ be a linear operator. Fix $m, \ell \in \mathbb{N}$ and $p, q \in [1,\infty]$ such that $0 \leq m \leq \ell \leq k+1$ and*

$$W^{\ell-m,p}(\hat{e}) \hookrightarrow L^q(\hat{e}). \tag{4.15}$$

Consider a multi-index γ with $|\gamma| = m$ and define $j := \dim \hat{D}^\gamma \mathcal{P}_{k,\hat{e}}$. Assume that there are linear functionals F_i, $i = 1,\ldots,j$, such that

$$F_i \in \big(W^{\ell-m,p}(\hat{e})\big)' \quad \forall i = 1,\ldots,j, \tag{4.16}$$

$$F_i(\hat{D}^\gamma(\hat{u} - \mathrm{I}\hat{u})) = 0 \quad \forall i = 1,\ldots,j, \quad \forall \hat{u} \in \mathcal{C}(\overline{\hat{e}}) : \hat{D}^\gamma \hat{u} \in W^{\ell-m,p}(\hat{e}), \tag{4.17}$$

$$\hat{w} \in \mathcal{P}_{k,\hat{e}} \quad \text{and} \quad F_i(\hat{D}^\gamma \hat{w}) = 0 \quad \forall i = 1,\ldots,j, \quad \Longrightarrow \quad \hat{D}^\gamma \hat{w} = 0. \tag{4.18}$$

Then the error can be estimated for all $\hat{u} \in \mathcal{C}(\overline{\hat{e}})$ *with* $\hat{D}^\gamma \hat{u} \in W^{\ell-m,p}(\hat{e})$ *by*

$$\|\hat{D}^\gamma(\hat{u} - \mathrm{I}\hat{u}); L^q(\hat{e})\| \lesssim |\hat{D}^\gamma \hat{u}; W^{\ell-m,p}(\hat{e})|. \tag{4.19}$$

Proof For all $\hat{v} \in \mathcal{P}^d_{\ell-1}$ we have by the triangle inequality

$$\|\hat{D}^\gamma(\hat{u} - \mathrm{I}\hat{u}); L^q(\hat{e})\| \le \|\hat{D}^\gamma(\hat{u} - \hat{v}); L^q(\hat{e})\| + \|\hat{D}^\gamma(\hat{v} - \mathrm{I}\hat{u}); L^q(\hat{e})\|. \tag{4.20}$$

We note that $\hat{v} - \mathrm{I}\hat{u} \in \mathcal{P}_{k,\hat{e}}$ because $\ell \le k+1$ and $\mathcal{P}_{k,\hat{e}} \supset \mathcal{P}^d_k$. That means $D^\gamma(\hat{v} - \mathrm{I}\hat{u}) \in D^\gamma \mathcal{P}_{k,\hat{e}}$. Since the polynomial spaces are finite-dimensional all norms are equivalent. Together with (4.18), (4.17), and (4.16) we derive for any $\hat{v} \in \mathcal{P}^d_{\ell-1}$

$$\|\hat{D}^\gamma(\hat{v} - \mathrm{I}\hat{u}); L^q(\hat{e})\| \sim \sum_{i=1}^{j} |F_i(\hat{D}^\gamma(\hat{v} - \mathrm{I}\hat{u}))| = \sum_{i=1}^{j} |F_i(\hat{D}^\gamma(\hat{v} - \hat{u}))| \lesssim \|\hat{D}^\gamma(\hat{v} - \hat{u}); W^{\ell-m,p}(\hat{e})\|.$$

Using (4.20) and (4.15) we obtain for any $\hat{v} \in \mathcal{P}^d_{\ell-1}$

$$\|\hat{D}^\gamma(\hat{u} - \mathrm{I}\hat{u}); L^q(\hat{e})\| \lesssim \|\hat{D}^\gamma(\hat{u} - \hat{v}); W^{\ell-m,p}(\hat{e})\|.$$

By Lemma 4.3 we get the desired result. ∎

It remains to find for any γ and for any element $(\hat{e}, \mathcal{P}_{k,\hat{e}}, \Sigma_{k,\hat{e}})$ the functionals F_i, $i = 1, \ldots, j$, that satisfy (4.16)–(4.18). This is done in Sections 5–9 separately for each element type. It turns out that for the Lagrangian finite elements considered in this monograph, functionals can be defined for all γ with $|\gamma| \le k$, such that (4.17) and (4.18) are satisfied. The critical point is that they are not necessarily continuous for all combinations of k, ℓ, p, m, q, and d.

For other finite elements it is not clear whether such functionals exist. The following lemma provides a criterion for the existence of linear functionals satisfying the conditions (4.17) and (4.18). It was proved in [9], see [108] for similar considerations.

Lemma 4.6 *Let* $\mathcal{P}$ *be an arbitrary polynomial space, and* γ *be a multi-index. Define* $j := \dim D^\gamma \mathcal{P}$. *Assume that* $\mathrm{I} : \mathcal{C}^\mu(\overline{\hat{e}}) \to \mathcal{P}$ *is a linear operator with* $\mathrm{I}\hat{w} = \hat{w}$ $\forall \hat{w} \in \mathcal{P}$. *Then there exist linear functionals* $F_i : \mathcal{C}^\infty(\overline{\hat{e}}) \to \mathbb{R}$, $i = 1, \ldots, j$, *such that*

$$F_i(\hat{D}^\gamma(\hat{u} - \mathrm{I}\hat{u})) = 0 \quad \forall i = 1, \ldots, j, \quad \forall \hat{u} \in \mathcal{C}^\infty(\overline{\hat{e}}), \tag{4.21}$$

$$\hat{w} \in \mathcal{P} \quad \text{and} \quad F_i(\hat{D}^\gamma \hat{w}) = 0 \quad \forall i = 1, \ldots, j, \quad \Longrightarrow \quad \hat{D}^\gamma \hat{w} = 0 \tag{4.22}$$

if and only if the condition

$$\hat{u} \in \mathcal{C}^\infty(\overline{\hat{e}}) \quad \text{and} \quad \hat{D}^\gamma \hat{u} = 0 \quad \Longrightarrow \quad \hat{D}^\gamma \mathrm{I}\hat{u} = 0 \tag{4.23}$$

holds.

The application of this lemma is twofold. First, if condition (4.23) is violated, then an anisotropic interpolation error estimate of type (4.19) does not hold. This is the case, for example, for elements containing bubble functions [9, Table 2] or certain triangular serendipity elements [108, page 59f.]. (Nevertheless, such elements may be useful for other types of anisotropic approximation.) Second, if condition (4.23) is satisfied, one can find functionals $F_i : \mathcal{C}^\infty(\overline{\hat{e}}) \to \mathbb{R}$ satisfying (4.21), (4.22). For the application of Lemma 4.5 it remains to show that the F_i are also continuous with respect to $W^{\ell-m,p}(\hat{e})$.

Remark 4.7 It has been shown in [19, 20, 21] that Lemma 4.3 remains true when $W^{\ell-m,p}(G)$ is replaced by weighted Sobolev spaces $V^{\ell-m,p}_\beta(\hat{e})$ or $V^{\ell-m,p}_{\beta,\delta}(\hat{e})$, for the definition of these spaces see Section 3. The domain is restricted to $\hat{e}$ there; the generality as for G in Lemma 4.3 is not elaborated. Also, the polynomial w depends on γ there. But on this basis one can prove a version of Lemma 4.5 with $W^{\ell-m,p}(\hat{e})$ replaced by $V^{\ell-m,p}_\beta(\hat{e})$ or $V^{\ell-m,p}_{\beta,\delta}(\hat{e})$. We will use this in Subsection 6.2.

5 Triangular elements

In Subsection 4.2 we formulated two basic tasks in order to derive anisotropic interpolation error estimates. The first task, namely to derive a sharpened interpolation error estimate on the reference element was partially solved by Lemma 4.5. It remains to find functionals with certain properties. We will discuss this comprehensively in the first part of this section. In Lemma 5.1 we formulate the assertion. Prior the proof we show that the assumptions are sharp (Examples 5.2 and 5.3) and we give examples of the functionals in several cases of γ. Then the proof for the general γ should be understandable. We will see in the next sections that other element types can be treated with similar ideas.

In the second part of the section we discuss the affine transformation $x = F(\hat{x})$ and prove the anisotropic interpolation error estimate for the general element e (Theorem 5.5) and conclude the corresponding isotropic estimate (Corollary 5.6). In the remaining part of the section, we discuss the maximal angle condition and the coordinate system condition.

Let us consider the simplest Lagrangian finite elements, namely triangles. They are formally described by $(\hat{e}, \mathcal{P}_{k,\hat{e}}, \Sigma_{k,\hat{e}})$ with

$$\begin{aligned} \hat{e} &:= \{(\hat{x}_1, \hat{x}_2) \in \mathbb{R}^2 : 0 < \hat{x}_1 < 1, 0 < \hat{x}_2 < 1 - \hat{x}_1\}, \\ \mathcal{P}_{k,\hat{e}} &:= \mathcal{P}_k^2, \\ \Sigma_{k,\hat{e}} &:= \{f_i : \mathcal{C}(\overline{\hat{e}}) \to \mathbb{R} \text{ such that } f_i(\hat{u}) := \hat{u}(\hat{X}^{(i)})\}_{i=1}^{N_e}, \end{aligned}$$

where $N_e = \binom{k+2}{2}$ is the number of nodes and

$$\mathcal{X} := \{\hat{X}^{(i)}\}_{i=1}^{N_e} := \{(\tfrac{i}{k}, \tfrac{j}{k})^T \in \mathbb{R}^2\}_{0 \le i+j \le k} = \{\tfrac{1}{k}\alpha \in \mathbb{R}^2\}_{|\alpha| \le k}$$

is the set of nodes. Here, we identified a multi-index with a vector.

Lemma 5.1 *Let γ be a multi-index with $m := |\gamma|$ and $\hat{u} \in \mathcal{C}(\overline{\hat{e}})$ be a function with $\hat{D}^\gamma \hat{u} \in W^{\ell-m,p}(\hat{e})$, where $\ell, m \in \mathbb{N}$, $p \in [1, \infty]$ shall be such that $0 \le m \le \ell \le k+1$ and*

$$\begin{array}{ll} p = \infty & \text{if } m = 0 \text{ and } \ell = 0, \\ p > 2 & \text{if } m = 0 \text{ and } \ell = 1, \\ m < \ell & \text{if } \gamma_1 = 0 \text{ or } \gamma_2 = 0, \text{ and } m > 0. \end{array} \tag{5.1}$$

Fix $q \in [1, \infty]$ such that $W^{\ell-m,p}(\hat{e}) \hookrightarrow L^q(\hat{e})$. Then the estimate

$$\|\hat{D}^\gamma(\hat{u} - \mathrm{I}\hat{u}); L^q(\hat{e})\| \lesssim |\hat{D}^\gamma \hat{u}; W^{\ell-m,p}(\hat{e})| \tag{5.2}$$

holds.

Prior to the proof of the lemma we want to discuss the assumptions in (5.1).

- Example 5.2 shows for $p < \infty$ that the case $m = \ell$ must be excluded for pure derivatives ($\gamma_1 = 0$ or $\gamma_2 = 0$). (Note, however, that $\|\hat{D}^\gamma(\hat{u} - \mathrm{I}\hat{u}); L^q(\hat{e})\| \lesssim |\hat{u}; W^{\ell,p}(\hat{e})|$ can be shown for $m = \ell > 2/p$.) Observe that this example works both for $m > 0$ and $m = 0$. The instance $p = \infty$ is not covered by this example. For $m = \ell = 0$ one can even show that estimate (5.2) holds for all $q \in [1, \infty]$ because $\|\mathrm{I}\hat{u}; L^\infty(\hat{e})\| \le \|\hat{u}; L^\infty(\hat{e})\|$. The case $m = \ell > 0$, $p = \infty$, is not elaborated.

- Example 5.3 shows that $p > 2$ is necessary in the case $m = 0$, $\ell = 1$.

- If $\ell > k+1$ then (5.2) has to be modified to become

$$\|\hat{D}^\gamma(\hat{u} - \mathrm{I}\hat{u}); L^q(\hat{e})\| \lesssim \sum_{i=k+1}^{\ell} |\hat{D}^\gamma \hat{u}; W^{i-m,p}(\hat{e})|.$$

  This is useful only, when $u \in W^{k+1,p}(e)$ is not sufficient. For tetrahedral elements we use such arguments, see Theorem 6.5 on page 35. One can find estimates of this type also in [108], see Comments 10.4 and 10.10.

Example 5.2 Let $\gamma = (0, m)$, $m \geq 0$, $k \geq 1$ arbitrary,

$$\hat{u}_\varepsilon := \hat{x}_2^m \hat{w}_\varepsilon, \quad \hat{w}_\varepsilon(\hat{x}) := \min\{1; \varepsilon|\ln \hat{x}_1|\}.$$

Then one can calculate that

$$\hat{u}_0 := \lim_{\varepsilon\to 0} \hat{u}_\varepsilon = \begin{cases} \hat{x}_2^m & \text{if } \hat{x}_1 = 0, \\ 0 & \text{if } \hat{x}_1 > 0, \end{cases} \qquad \lim_{\varepsilon\to 0} \hat{D}^\gamma \hat{u}_\varepsilon = \begin{cases} m! & \text{if } \hat{x}_1 = 0, \\ 0 & \text{if } \hat{x}_1 > 0, \end{cases}$$

and [1, page 17]

$$\lim_{\varepsilon\to 0} \|\hat{D}^\gamma \hat{u}_\varepsilon; L^p(\hat{e})\| = \|\lim_{\varepsilon\to 0} \hat{D}^\gamma \hat{u}_\varepsilon; L^p(\hat{e})\| = 0 \quad \text{for } p < \infty, \tag{5.3}$$

but

$$\lim_{\varepsilon\to 0} \|\hat{D}^\gamma \hat{u}_\varepsilon - \hat{D}^\gamma \mathrm{I}\hat{u}_\varepsilon; L^q(\hat{e})\| = \|\hat{D}^\gamma \mathrm{I}\hat{u}_0; L^q(\hat{e})\| = C(k,m) \neq 0. \tag{5.4}$$

(The function u_0 is not continuous but it is defined pointwise. So the interpolation operator can be applied formally. In particular there holds $\mathrm{I}\hat{u}_0 = \lim_{\varepsilon\to 0} \mathrm{I}\hat{u}_\varepsilon$.) The last conclusion can be proved indirectly. Assume $\|\hat{D}^\gamma \mathrm{I}\hat{u}_0; L^q(\hat{e})\| = 0$ then $\hat{D}^\gamma \mathrm{I}\hat{u}_0 \equiv 0$. Consequently, we have

$$\begin{aligned} \mathrm{I}\hat{u}_0 &= \sum_{j=0}^{m-1} \hat{x}_2^j \hat{v}_{k-j}(\hat{x}_1) \quad \text{with } \hat{v}_{k-j} \in \mathcal{P}^1_{k-j}, \\ (\hat{u}_0 - \mathrm{I}\hat{u}_0)(0, x_2) &= x_2^m - \sum_{j=0}^{m-1} \hat{x}_2^j \hat{v}_{k-j}(0) \quad =: \quad \hat{V}_m(\hat{x}_2) \not\equiv 0, \quad \hat{V}_m \in \mathcal{P}^1_m. \end{aligned}$$

However, $\hat{V}_m(i/k) = 0$ for $i = 0, \ldots, k$ (interpolation property) leads to $\hat{V}_m \equiv 0$ which is a contradiction. In view of (5.3) and (5.4), the estimate (5.2) does not hold for $\gamma = (0, m)$, $m = \ell$, $p < \infty$. □

Example 5.3 Let be $k \geq 1$ arbitrary, $\ell = 1$, $p \leq 2$,

$$\hat{u}_\varepsilon := \min\{1; \varepsilon \ln|\ln(\hat{r}/\mathrm{e})|\}, \quad \hat{r} := (\hat{x}_1^2 + \hat{x}_2^2)^{1/2}.$$

We can calculate that

$$\hat{u}_0 := \lim_{\varepsilon\to 0} \hat{u}_\varepsilon = \begin{cases} 1 & \text{if } \hat{r} = 0, \\ 0 & \text{if } \hat{r} > 0, \end{cases}$$

and

$$\lim_{\varepsilon\to 0} |\hat{u}_\varepsilon; W^{1,p}(\hat{e})| \lesssim \lim_{\varepsilon\to 0} |\hat{u}_\varepsilon; W^{1,2}(\hat{e})| = 0$$

(in detail in [3, page 61]) but

$$\lim_{\varepsilon\to 0} \|\hat{u}_\varepsilon - \mathrm{I}\hat{u}_\varepsilon; L^q(\hat{e})\| = \|\mathrm{I}\hat{u}_0; L^q(\hat{e})\| \neq 0.$$

The last conclusion can be proved with similar arguments as in Example 5.2. Consequently, the estimate (5.2) does not hold for $\gamma = (0,0)$, $\ell = 1$, $p \leq 2$. Note that the example does not work for $p > 2$ because $\lim_{\varepsilon\to 0} |\hat{u}_\varepsilon; W^{1,p}(\hat{e})| = \infty$ then. □

Let us now turn to the proof of Lemma 5.1. In view of Lemma 4.5 we have to show that linear functionals with the desired properties exist. Before we do that in the general case we will illustrate the ideas by discussing some particular cases.

- For $k = 1$, $\gamma = (0,0)$, we have $j = \dim \mathcal{P}_{1,\hat{e}} = 3$. We can use $F_i(\hat{w}) = \hat{w}(\hat{X}^{(i)})$. Property (4.16) is shown via the Sobolev embedding theorem $W^{\ell,p}(\hat{e}) \hookrightarrow \mathcal{C}(\overline{\hat{e}})$ (see Section 3)

$$|F_i(\hat{w})| \le \|\hat{w}; \mathcal{C}(\overline{\hat{e}})\| \lesssim \|\hat{w}; W^{\ell,p}(\hat{e})\|$$

  which is valid if $\ell \ge 2$ or $p > 2$, $\ell = 1$. The proof of the properties (4.17) and (4.18) is trivial.

- For $k = 1$, $\gamma = (1,0)$, we have $\hat{D}^\gamma \mathcal{P}_{1,\hat{e}} = \mathcal{P}_0^2$ and thus $j = 1$. As the functional we consider

$$F_1(\hat{w}) = \int_0^1 \hat{w}(\hat{x}_1, 0)\, \mathrm{d}\hat{x}_1.$$

  Denote by $E := \{\hat{x} \in \overline{\hat{e}} : \hat{x}_2 = 0\}$ the edge of $\hat{e}$ which is integrated over. Then the continuity can be proved by a trace theorem (see Section 3):

$$|F_1(\hat{w})| \le \|\hat{w}; L^1(E)\| \lesssim \|\hat{w}; W^{\ell-1,p}(\hat{e})\|, \tag{5.5}$$

  where we need the condition $1 = m < \ell$. Property (4.17) is valid due to

$$F_1(\hat{D}^{(1,0)}(\hat{u} - \mathrm{I}\hat{u})) = (\hat{u} - \mathrm{I}\hat{u})\big|_{(0,0)}^{(1,0)} = 0.$$

  For showing (4.18) let $\hat{w} = a_0 + a_1\hat{x}_1 + a_2\hat{x}_2$, then $F_1(\hat{D}^\gamma \hat{w}) = \hat{D}^\gamma \hat{w} = a_1$.

  The case $\gamma = (0,1)$ is treated by analogy.

- For $k = 2$, $\gamma = (0,0)$, we have $j = 6$. Since also $N_e = 6$ we can proceed as in the case $k = 1$, $\gamma = (0,0)$.

- In the case $k = 2$, $\gamma = (1,0)$, we need three functionals. For

$$F_1(\hat{w}) = \int_0^{1/2} \hat{w}(\hat{x}_1, 0)\, \mathrm{d}\hat{x}_1, \quad F_2(\hat{w}) = \int_{1/2}^1 \hat{w}(\hat{x}_1, 0)\, \mathrm{d}\hat{x}_1, \quad F_3(\hat{w}) = \int_0^{1/2} \hat{w}(\hat{x}_1, \tfrac{1}{2})\, \mathrm{d}\hat{x}_1,$$

  we can show (4.16) and (4.17) as above. To illustrate the general proof below let us prove (4.18) in this special case in the same way: Let $\hat{w} \in \mathcal{P}_2^2$ be such that

$$F_i(\hat{D}^\gamma \hat{w}) = 0, \quad i = 1,2,3. \tag{5.6}$$

  Consider now the polynomial

$$\hat{W} := \hat{w} - \hat{w}(1,0)\cdot 2(\hat{x}_2 - \tfrac{1}{2})(\hat{x}_2 - 1) - \hat{w}(\tfrac{1}{2}, \tfrac{1}{2})\cdot[-4\hat{x}_2(\hat{x}_2 - 1)] - \hat{w}(0,1)\cdot 2\hat{x}_2(\hat{x}_2 - \tfrac{1}{2}) \in \mathcal{P}_2^2 \tag{5.7}$$

  which has the properties

$$\hat{D}^\gamma \hat{w} = \hat{D}^\gamma \hat{W} \quad \text{and} \quad \hat{W}(1,0) = \hat{W}(\tfrac{1}{2}, \tfrac{1}{2}) = \hat{W}(0,1) = 0. \tag{5.8}$$

  Consequently, we obtain from (5.6) and (5.8)

$$\begin{array}{rcccccccccc} 0 &=& F_3(D^\gamma \hat{w}) &=& F_3(D^\gamma \hat{W}) &=& W(\frac{1}{2}, \frac{1}{2}) - W(0, \frac{1}{2}) &\Longrightarrow& W(0, \frac{1}{2}) &=& 0, \\ 0 &=& F_2(D^\gamma \hat{w}) &=& F_2(D^\gamma \hat{W}) &=& W(1,0) - W(\frac{1}{2}, 0) &\Longrightarrow& W(\frac{1}{2}, 0) &=& 0, \\ 0 &=& F_1(D^\gamma \hat{w}) &=& F_1(D^\gamma \hat{W}) &=& W(\frac{1}{2}, 0) - W(0,0) &\Longrightarrow& W(0,0) &=& 0. \end{array}$$

  Therefore $\hat{W} \equiv 0$ and with (5.7) we get $\hat{w} = \hat{w}(\hat{x}_2)$, $\hat{D}^\gamma \hat{w} = 0$.

- For $k=2$, $\gamma=(1,1)$, we have $\hat{D}^\gamma \mathcal{P}_{k,\hat{e}} = \mathcal{P}_0^2$ and thus $j=1$. Let

$$F_1(\hat{w}) = \int_0^{1/2} \int_0^{1/2} \hat{w}(\hat{x}_1, \hat{x}_2)\, \mathrm{d}\hat{x}_1 \mathrm{d}\hat{x}_2,$$

  which satisfies conditions (4.16)–(4.18). In particular, F_1 is continuous for all $\ell = 2, 3$ and $p \in [1, \infty]$.

- For $k=2$, $\gamma=(2,0)$, we let

$$F_1(\hat{w}) = \int_0^{1/2} \int_\xi^{1/2+\xi} \hat{w}(\hat{x}_1, 0)\, \mathrm{d}\hat{x}_1 \mathrm{d}\xi,$$

  which also satisfies all conditions. Note that we need the condition $m < \ell$ to prove the continuity of F_1.

Proof (Lemma 5.1) Define $\mathcal{X}_\gamma := \{\hat{X}^{(i)} \in \mathcal{X} : \hat{X}^{(i)} + \frac{1}{k}\gamma \in \mathcal{X}\}$. By consideration of the Pascal triangle one realizes that the number of elements in $\mathcal{X}_\gamma$ is $|\mathcal{X}_\gamma| = \binom{k-m+2}{2} = j$ with j from Lemma 4.5. Let $\gamma =: \sum_{i=1}^m \gamma^{(i)}$, $|\gamma^{(i)}| = 1$, and define the operator Φ_α for $|\alpha| = 1$ by

$$(\Phi_\alpha \hat{w})(\hat{x}) := \int_{\hat{x}}^{\hat{x}+\frac{1}{k}\alpha} \hat{w}(\xi)\, \mathrm{d}\xi,$$

where the integral is to be understood as a line integral on the straight line connecting the points $\hat{x}, \hat{x} + \frac{1}{k}\alpha \in \mathbb{R}^2$. We can now set functionals F_i by

$$F_i(\hat{w}) := (\Phi_{\gamma^{(1)}} \circ \ldots \circ \Phi_{\gamma^{(m)}} \hat{w})(\hat{X}^{(i)}), \quad \text{for } \hat{X}^{(i)} \in \mathcal{X}_\gamma.$$

We see that $F_i(\hat{D}^\gamma \hat{w})$ is a linear combination of the values of $\hat{w}$ at the nodes $\hat{X} \in \mathcal{X} \cap \overline{G_i}$, where $G_i \subset \hat{e}$ is the domain of integration in the definition of F_i. Since $\hat{u} - \mathrm{I}\hat{u} = 0$ in these nodes, (4.17) is shown.

Assume there is a polynomial $\hat{w} \in \mathcal{P}_{k,\hat{e}}$ with $F_i(\hat{D}^\gamma \hat{w}) = 0$ for all $i = 1, \ldots, j$. Then there exists a polynomial $\hat{W} \in \mathcal{P}_{k,\hat{e}}$ with the properties $\hat{D}^\gamma \hat{W} = \hat{D}^\gamma \hat{w}$ and $\hat{W}(\hat{X}) = 0$ for all $\hat{X} \in \mathcal{X} \setminus \mathcal{X}_\gamma$. We show now recursively that $\hat{W}(\hat{X}) = 0$ for all $\hat{X} \in \mathcal{X}$. Indeed, start with an $\hat{X}^{(n)} \in \mathcal{X}_\gamma$ for which $\overline{G_n} \cap \mathcal{X}_\gamma = \hat{X}^{(n)}$, then $0 = F_n(\hat{D}^\gamma \hat{W}) = (-1)^m \hat{W}(\hat{X}^{(n)})$, $\hat{W}(\hat{X}^{(n)}) = 0$. Set $\mathcal{X}_\gamma := \mathcal{X}_\gamma \setminus \hat{X}^{(n)}$ and continue with the next node. Finally we get $\hat{W}(\hat{X}) = 0$ for all $\hat{X} \in \mathcal{X}$, $\hat{W} \equiv 0$. Thus $D^\gamma \hat{w} = 0$ and (4.18) is proved.

The boundedness of the functionals is shown for $\ell > m$ via $W^{\ell-m,p}(\hat{e}) \hookrightarrow W^{1,p}(\hat{e}) \hookrightarrow L^1(G_i)$, $|F_i(\hat{w})| \le \|\hat{w}; L^1(G_i)\| \lesssim \|\hat{w}; W^{1,p}(\hat{e})\|$. This embedding holds both for one- and two-dimensional G_i. For $\ell = m$ we need for $W^{\ell-m,p}(\hat{e}) = L^p(\hat{e}) \hookrightarrow L^1(G_i)$ that G_i is two-dimensional, that means $\gamma_1 \neq 0$ and $\gamma_2 \neq 0$. ∎

We note that partial cases of this lemma were proved in a slightly different way in [35], see Comment 10.8 on page 59.

The transformation of estimate (5.2) from the reference element $\hat{e}$ to the element $e = F(\hat{e})$ can be carried out by

$$x = F(\hat{x}) = B\hat{x} + b, \quad B = (b_{i,j})_{i,j=1}^2 \in \mathbb{R}^{2\times 2}, \quad b = (b_i)_{i=1}^2 \in \mathbb{R}^2, \tag{5.9}$$

see also (3.6). Since all considerations are local in one element e we omit the index e here and further on. We will now investigate the sizes of the entries $b_{i,j}$ and $b_{i,j}^{(-1)}$, $i, j = 1, 2$, of B and B^{-1}, respectively.

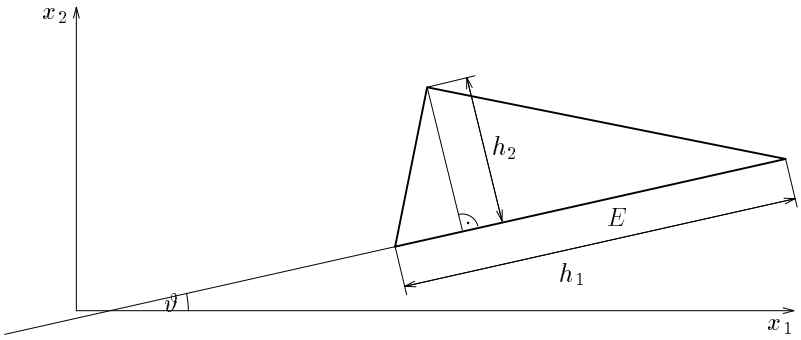

Figure 5.1: Illustration of the definition of the mesh sizes h_1, h_2 (triangle).

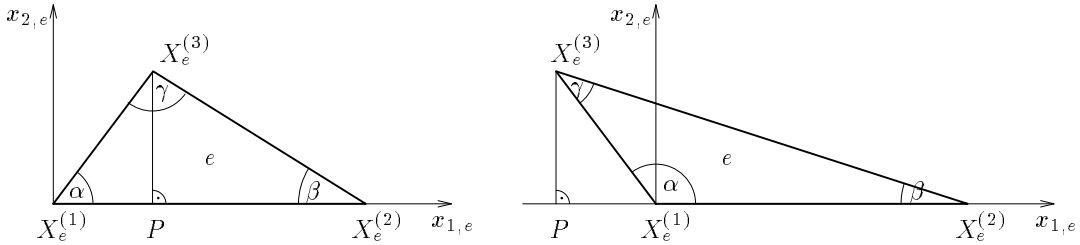

Figure 5.2: Notation and illustration of e in the coordinate system x_e.

Let E be the longest edge of e. Then we denote by $h_1 = h_{1,e} := \mathrm{meas}_1 E$ its length and by $h_2 = h_{2,e} := 2\mathrm{meas}_2 e / h_{1,e}$ the thickness of e perpendicularly to E, see Figure 5.1. We assume that the element satisfies a *maximal angle condition* and a *coordinate system condition*.

Maximal angle condition: There is a constant $\gamma_* < \pi$ (independent of h and $e \in \mathcal{T}_h$) such that the maximal interior angle γ of any element e is bounded by γ_*, $\gamma \le \gamma_*$.

Coordinate system condition: The angle ϑ between the longest side E and the x_1-axis is bounded by $|\sin\vartheta| \lesssim h_2/h_1$.

Other formulations of the maximal angle condition are discussed in Comment 10.1 on page 56.

Lemma 5.4 *Assume that a triangular element e satisfies the maximal angle condition and the coordinate system condition. Then the entries of the matrix B of (5.9) and of its inverse B^{-1} satisfy the following conditions:*

$$|b_{i,j}| \lesssim \min\{h_i; h_j\}, \qquad i,j = 1,2, \tag{5.10}$$

$$|b_{i,j}^{(-1)}| \lesssim \min\{h_i^{-1}; h_j^{-1}\}, \qquad i,j = 1,2. \tag{5.11}$$

Proof Enumerate the vertices of e counterclockwise such that $X_e^{(1)}$ and $X_e^{(3)}$ are the vertices of the shortest edge of e. Introduce an element related Cartesian coordinate system $x_e = (x_{1,e}, x_{2,e})$ such that $X_e^{(1)}$ lies at the origin and $X_e^{(2)}$ is also located at the $x_{1,e}$-axis. Furthermore, denote by P the foot of the perpendicular from $X_e^{(3)}$ to the $x_{1,e}$-axis. Note that P may lay outside of $\overline{e}$, see Figure 5.2 for an illustration. Split the transformation (5.9) into two parts,

$$x = B^{(1)} x_e + b, \qquad x_e = B^{(2)} \hat{x},$$

such that the columns of $B^{(2)}$ are the x_e-coordinates of $X_e^{(2)}$ and $X_e^{(3)}$, respectively. $B^{(1)}$ describes a rotation, and b contains the x-coordinates of $X_e^{(1)}$. Note that $B = B^{(1)}B^{(2)}$.

One of the edges $X_e^{(1)}X_e^{(2)}$ and $X_e^{(2)}X_e^{(3)}$ has length h_1 per definition. The other edge has a length of order h_1 by using the triangle inequality. Consequently, $|b_{1,1}^{(2)}| \sim h_1$, $b_{2,1}^{(2)} = 0$. Moreover, we can conclude that $|X_e^{(3)} - P| \sim h_2$ because $\mathrm{meas}_2 e = \frac{1}{2}h_1h_2$. The interior angle α at $X_e^{(1)}$ is not the smallest interior angle of e. Therefore, $|\sin\alpha| \sim 1$ by the maximal angle condition, and $|X_e^{(3)} - X_e^{(1)}| = |X_e^{(3)} - P|/|\sin\alpha| \sim h_2$. That means $|b_{1,2}^{(2)}| \lesssim h_2$, $|b_{2,2}^{(2)}| \lesssim h_2$.

Since $|X_e^{(1)} - X_e^{(2)}| \sim |X_e^{(3)} - X_e^{(2)}| \sim h_1$ we have

$$B^{(1)} = \begin{pmatrix} \cos\tilde{\vartheta} & \sin\tilde{\vartheta} \\ -\sin\tilde{\vartheta} & \cos\tilde{\vartheta} \end{pmatrix}$$

with $\tilde{\vartheta} \in \{\pm\vartheta;\ \pm\vartheta \pm \beta;\ \pi \pm \vartheta;\ \pi \pm \vartheta \pm \beta\}$, where β is the interior angle at $X_e^{(2)}$. From $\sin\beta \sim h_2/h_1$ we conclude $|\sin\tilde{\vartheta}| \lesssim h_2/h_1$ by using the coordinate system condition, that means (for $h_2 = o(h_1)$, otherwise there is nothing to prove) $|b_{1,1}^{(1)}| \sim |b_{2,2}^{(1)}| \sim 1$ and $|b_{1,2}^{(1)}| \sim |b_{2,1}^{(1)}| \lesssim h_2/h_1$.

The matrix multiplication results in $|b_{1,1}| \sim h_1$, $|b_{2,1}| \lesssim h_2^2/h_1 \le h_2$, $|b_{1,2}| \lesssim h_2$, $|b_{2,2}| \lesssim h_2$. The entries of the inverse matrix can be estimated by using the explicit formula of B^{-1} and $|\det B| = 2\,\mathrm{meas}_2 e = h_1h_2$. ∎

We note that Lemma 5.4 is implicitly contained in the proofs of Theorem 2 in [9] and Theorem 6 and Corollary 7 in [35]. We chose this kind of proof for a better understanding of the proof of the related Lemma 6.3.

Theorem 5.5 *Assume that the element e satisfies the maximal angle condition and the coordinate system condition. Let be $u \in W^{\ell,p}(e) \cap \mathcal{C}(\overline{e})$ where $\ell \in \mathbb{N}$, $1 \le \ell \le k+1$, $p \in [1,\infty]$. Fix $m \in \{0,\dots,\ell-1\}$ and $q \in [1,\infty]$ such that $W^{\ell-m,p}(e) \hookrightarrow L^q(e)$. Then the anisotropic interpolation error estimate*

$$|u - \mathrm{I}_h u; W^{m,q}(e)| \lesssim (\mathrm{meas}_2 e)^{1/q-1/p} \sum_{|\alpha|=\ell-m} h^\alpha |D^\alpha u; W^{m,p}(e)|$$

holds provided that $p > 2$ if $\ell = 1$. The result is also valid for $m = \ell = 0$, $p = \infty$, $q \in [1,\infty]$.

Note that $W^{\ell,p}(e) \hookrightarrow \mathcal{C}(\overline{e})$ for all admissible parameter sets except for $\ell = 0$, $p = \infty$.

Proof From Lemma 5.4 we obtain the relations

$$\left|\frac{\partial\hat{v}}{\partial\hat{x}_i}\right| \lesssim \sum_{j=1}^{2} \min\{h_i;\ h_j\} \left|\frac{\partial v}{\partial x_j}\right|, \quad \left|\frac{\partial v}{\partial x_i}\right| \lesssim \sum_{j=1}^{2} \min\{h_i^{-1};\ h_j^{-1}\} \left|\frac{\partial\hat{v}}{\partial\hat{x}_j}\right|,$$

and conclude (in multi-index notation)

$$|\hat{D}^\alpha\hat{v}| \lesssim \sum_{|s|=|\alpha|} h^s |D^s v|, \quad |\hat{D}^\beta\hat{v}| \lesssim h^\beta \sum_{|t|=|\beta|} |D^t v|, \quad |D^\gamma v| \lesssim \sum_{|\beta|=|\gamma|} h^{-\beta} |\hat{D}^\beta\hat{v}|. \tag{5.12}$$

These estimates and Lemma 5.1 imply for any γ with $|\gamma| = m$

$$\begin{aligned} \|D^\gamma(u - \mathrm{I}_h u); L^q(e)\| &\lesssim (\mathrm{meas}_2 e)^{1/q} \sum_{|\beta|=m} h^{-\beta} \|\hat{D}^\beta(\hat{u} - \mathrm{I}\hat{u}); L^q(\hat{e})\| \\ &\lesssim (\mathrm{meas}_2 e)^{1/q} \sum_{|\alpha|=\ell-m} \sum_{|\beta|=m} h^{-\beta} \|\hat{D}^{\alpha+\beta}\hat{u}; L^p(\hat{e})\| \end{aligned}$$

$$\begin{aligned} &\lesssim (\mathrm{meas}_2 e)^{1/q-1/p} \sum_{|\alpha|=\ell-m} \sum_{|\beta|=m} h^{-\beta} \sum_{|t|=m} \sum_{|s|=\ell-m} h^{\beta} h^{s} \|D^{s+t} u; L^p(e)\| \\ &\sim (\mathrm{meas}_2 e)^{1/q-1/p} \sum_{|s|=\ell-m} h^{s} |D^{s} u; W^{m,p}(e)|, \end{aligned}$$

and the theorem can be concluded by a summation over all γ with $|\gamma| = m$. ∎

This form of the proof was used first in [12] where the case $\ell = k+1$, $q = p$, was treated. Special cases were proved with other geometrical arguments in [9, 35, 84, 150], see also Comments 10.6–10.8 on pages 58–59.

Corollary 5.6 *Assume that the element e satisfies the maximal angle condition. Let be $u \in W^{\ell,p}(e) \cap \mathcal{C}(\overline{e})$ where $\ell \in \mathbb{N}$, $1 \le \ell \le k+1$, $p \in [1,\infty]$. Fix $m \in \{0,\dots,\ell-1\}$ and $q \in [1,\infty]$ such that $W^{\ell-m,p}(e) \hookrightarrow L^q(e)$. Then the isotropic interpolation error estimate (sometimes called estimate of Jamet type or of Synge type)*

$$|u - \mathrm{I}_h u; W^{m,q}(e)| \lesssim (\mathrm{meas}_2 e)^{1/q-1/p} (\mathrm{diam}\, e)^{\ell-m} |u; W^{\ell,p}(e)|$$

holds provided that $p > 2$ if $\ell = 1$. The result is also valid for $m = \ell = 0$, $p = \infty$, $q \in [1,\infty]$.

Proof If we assume the coordinate system condition the assertion follows immediately from Theorem 5.5. Since the seminorms remain equivalent during a rotation of the coordinate system, the coordinate system condition can be omitted. ∎

We remark that partial cases of this corollary were derived in [27, 108, 119, 187] without knowing anisotropic estimates, see Comments 10.2–10.5 on pages 56–57. We point out in particular that the assumptions made here are weaker than those in [108].

Let us now discuss the maximal angle condition and the coordinate system condition. We start with an example that shows the necessity of the maximal angle condition for the validity of the anisotropic error estimate of Theorem 5.5. We note, however, that the maximal angle condition is not necessary in the case $m = 0$.

Example 5.7 Consider $m = 1$, $\ell = 2$, the triangle e with the vertices $(0,0)$, $(h_1,0)$, $(\frac{1}{2}h_1, h_2)$, and the function $u = x_1^2$. One can directly calculate that $\mathrm{I}_h u = h_1 x_1 - \frac{1}{4} h_1^2 h_2^{-1} x_2$ and

$$\frac{\left\| D^{(0,1)}(u - \mathrm{I}_h u); L^q(e) \right\|}{(\mathrm{meas}_2 e)^{1/q-1/p} \sum\limits_{|\alpha|=1} h^{\alpha} |D^{\alpha} u; W^{1,p}(e)|} \sim \frac{h_1^2 h_2^{-1} (\mathrm{meas}_2 e)^{1/q}}{(\mathrm{meas}_2 e)^{1/q-1/p} h_1 (\mathrm{meas}_2 e)^{1/p}} = \frac{h_1}{h_2}$$

which is divergent for $h_2 = o(h_1)$. Thus the maximal angle condition is necessary. □

Remark 5.8 An uncontrollable growth of the interpolation error for elements with large angles gives no information about the approximation error of the corresponding finite element method. In the literature we can find two examples where triangles with large angles are considered and the interpolation error in the $W^{1,2}$-norm grows to infinity. But while in the paper of Babuška and Aziz [27] (see Figure 5.3, left-hand side) the finite element error grows to infinity as well, there is an example given by Dobrowolski in [9] where a modified interpolant and thus the finite element solution converges.

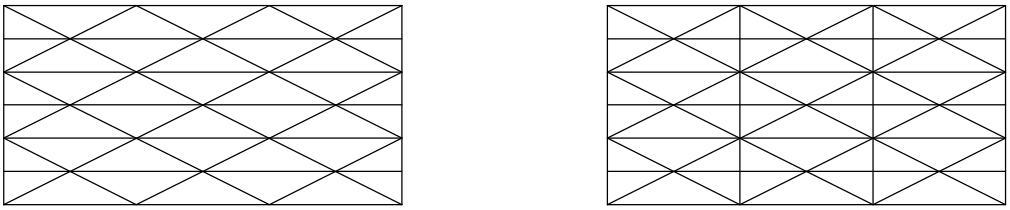

(a) Babuška's and Aziz' example. (b) Dobrowolski's example.

Figure 5.3: Example meshes containing elements with large angles.

Remark 5.9 Anisotropic triangular elements were also extensively investigated in [68, 69, 160]. In these papers, even a maximal angle condition was not demanded. This is possible only due to assumptions on the function to be interpolated, for example

$$\|D^{(2,0)}u; L^2(e)\| \le C_0 \|D^{(1,1)}u; L^2(e)\| \le C_0^2 \|D^{(0,2)}u; L^2(e)\|, \quad C_0 < 1,$$

The results are applied in an a-posteriori context for pure interpolation tasks [68, 69, 160] and in the finite element method/finite volume method [58, 62].

Example 5.7 shows a dilemma with the maximal angle condition: The element is strongly refined in a direction where no large derivatives appear. One might find the example not convincing. But, first, for proving a-priori finite element error estimates for a class of problems, this situation should be covered by the theory. Second, the components of vector functions can have different behaviour, for example a layer in one component while another component has uniformly bounded derivatives. So it must be possible to approximate a function on a mesh which was adapted for another function. Therefore we consider the maximal angle condition as necessary.

Remark 5.10 The coordinate system condition means a suitable alignment of the mesh with respect to a coordinate system (x_1, x_2) where the function u can be described favourably. Though we have seen in Remark 5.8 that a condition which is necessary for a successful interpolation may not be necessary for a good finite element approximation, we find in computations that the Galerkin/Least-squares method looses stability if the mesh is not aligned sufficiently well. For an illustration consider a convection-diffusion problem in the unit square,

$$\begin{aligned} -\varepsilon\Delta u + \begin{pmatrix} 1 \\ 0.5 \end{pmatrix} \cdot \nabla u &= 0 \quad \text{in } \Omega, \\ u &= 1 \quad \text{on } \{x \in \partial\Omega : x_1 = 0,\ 0.25 \le x_2 \le 1\}, \\ u &= 0 \quad \text{elsewhere on } \partial\Omega. \end{aligned}$$

An interior layer emanates from the discontinuity at $(0, 0.25)$ along the manifold $M_1 = \{x \in \Omega : x_2 = 0.5x_1 + 0.25\}$ and intersects at $(1, 0.75)$ with a boundary layer along $M_2 = \big[(0,1) \times \{1\}\big] \cup \big[\{1\} \times (0.75, 1)\big]$. An anisotropic mesh is constructed in the neighbourhood of M_1 and M_2 similarly to the one in Section 24. The maximal aspect ratio is about $h_1/h_2 = 240$. The layers are well resolved for $\varepsilon = 10^{-4}$ if the coordinate system condition is satisfied with respect to an orthogonal coordinate system with the x_1-axis at M_1, see Figure 5.4(a). On the other hand, wiggles occur at M_1 if the angle between M_1 and the x_1-axis is $2°$, see Figure 5.4(b). Thus the coordinate system condition should be treated carefully.

Remark 5.11 We note that the maximal angle condition and the coordinate system condition give us some freedom in the definition of the element parameters h_1 and h_2, and in the definition

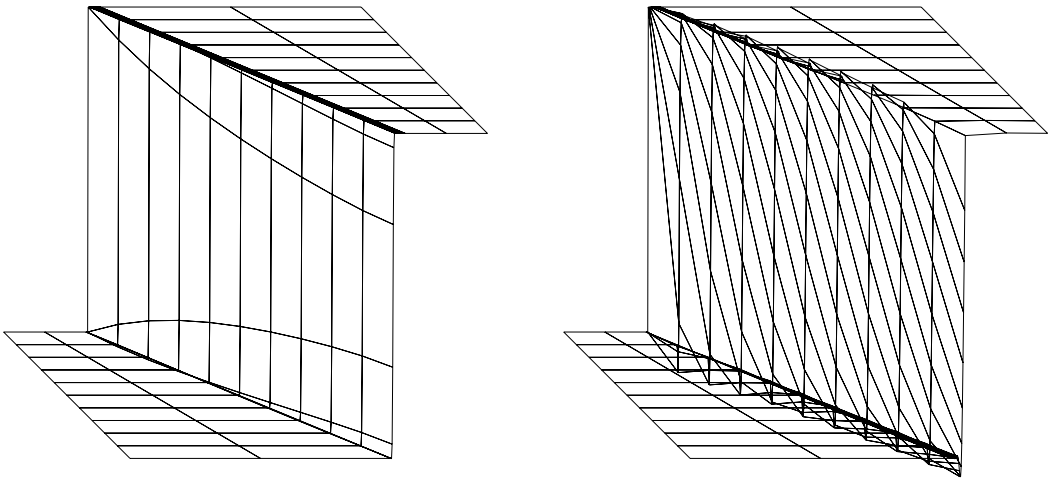

(a) (b)

Figure 5.4: Dependence of the resolution of an internal layer on the satisfaction of the coordinate system condition.

of the "stretching direction of the element". If $h_2 = o(h_1)$ then there are two edges of e which have a length of order h_1. For example, for triangles with a right angle it can be considered as more natural to use the lengths of the two perpendicular sides as h_1 and h_2, rather than the third (longest) one and the length of the height, see Figure 11.2 on page 67.

The maximal angle condition ensures that the diameter of the circle which contains all vertices of e, is also of order h_1. Moreover, we can consider the directions of both long sides as a stretching direction. The angle ϑ between any of those sides and the x_1-axis is bounded by $|\sin\vartheta| \lesssim h_2/h_1$.

6 Tetrahedral elements

6.1 Error estimates in classical Sobolev spaces

In this section we investigate tetrahedral elements. We use the same approach as for triangular elements but we have to be carefully at several places.

- The embedding theorems depend on the space dimension which leads to a restriction on the range of the parameter p, see Lemma 6.1 and Example 6.2.

- If the transformation $x = B\hat{x} + b$ from the reference element $\hat{e}$ to the element e shall satisfy conditions as in Lemma 5.4 then two reference elements have to be considered, one for elements with three long edges, the other for elements with four long edges, see (6.1) and (6.2).

Additionally to the estimates which are analogous to Section 5, we prove two more types of anisotropic interpolation error estimates. In Theorem 6.5, we consider functions with additional smoothness, $u \in W^{k+2,p}(e)$, as a remedy to treat the case $m = k$, $p \leq 2$, which had to be excluded in Theorem 6.4. Furthermore, we derive in Subsection 6.2 local interpolation error estimates for functions from weighted Sobolev spaces (Theorems 6.9 and 6.11).

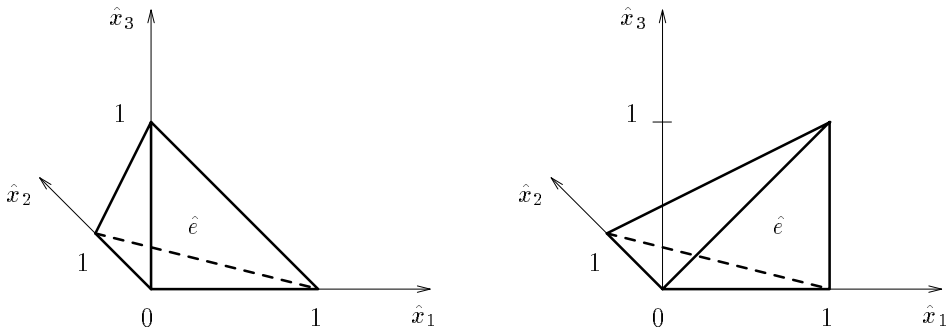

Figure 6.1: Reference elements for tetrahedral elements and $h_1 \gtrsim h_2 \gtrsim h_3$.

Consider two reference elements $\hat{e}$, compare Figure 6.1. We use

$$\hat{e} := \{(\hat{x}_1, \hat{x}_2, \hat{x}_3)^T \in \mathbb{R}^3 : 0 < \hat{x}_1 < 1,\ 0 < \hat{x}_2 < 1 - \hat{x}_1,\ 0 < \hat{x}_3 < 1 - \hat{x}_1 - \hat{x}_2\} \tag{6.1}$$

when the tetrahedron has three edges E with $\mathrm{meas}_1 E \sim \mathrm{diam}\,(e)$, and

$$\hat{e} := \{(\hat{x}_1, \hat{x}_2, \hat{x}_3)^T \in \mathbb{R}^3 : 0 < \hat{x}_1 < 1,\ 0 < \hat{x}_2 < 1 - \hat{x}_1,\ 0 < \hat{x}_3 < \hat{x}_1\} \tag{6.2}$$

when the tetrahedron has four edges E with $\mathrm{meas}_1 E \sim \mathrm{diam}\,(e)$. In the case of five edges E with $\mathrm{meas}_1 E \sim \mathrm{diam}\,(e)$ we can use either of the reference elements. Both reference elements satisfy the following Property (P) which is sufficient in the proof of Lemma 6.1. Later on, we will occasionally utilize further reference elements which all satisfy Property (P).

Property (P) For each axis of the coordinate system $(\hat{x}_1, \hat{x}_2, \hat{x}_3)$ there is one edge of $\hat{e}$ which has length one and is parallel to this axis.

The finite elements $(\hat{e}, \mathcal{P}_{k,\hat{e}}, \Sigma_{k,\hat{e}})$ are completed by setting

$$\begin{aligned} \mathcal{P}_{k,\hat{e}} &:= \mathcal{P}_k^3 \\ \Sigma_{k,\hat{e}} &:= \{f_i : \mathcal{C}(\overline{\hat{e}}) \to \mathbb{R} \text{ such that } f_i(\hat{u}) := \hat{u}(\hat{X}^{(i)})\}_{i=1}^{N_e} \end{aligned}$$

where $N_e = \binom{k+3}{3}$ is the number of nodes and

$$\mathcal{X} := \{\hat{X}^{(i)}\}_{i=1}^{N_e} := \overline{\hat{e}} \cap \{(\tfrac{i}{k}, \tfrac{j}{k}, \tfrac{n}{k})^T \in \mathbb{R}^3\}_{0 \le i,j,n \le k}$$

is the set of nodes.

Lemma 6.1 *Let $\hat{e}$ be a reference element satisfying Property (P). Consider a multi-index γ with $m := |\gamma|$ and a function $\hat{u} \in \mathcal{C}(\overline{\hat{e}})$ with $D^\gamma u \in W^{\ell-m,p}(\hat{e})$, where $\ell \in \mathbb{N}$, $p \in [1,\infty]$, shall be such that $0 \le m \le \ell \le k+1$ and*

$$\begin{aligned} &p = \infty && \text{if } m = 0 \text{ and } \ell = 0, \\ &p > 3/\ell && \text{if } m = 0 \text{ and } \ell = 1, 2, \\ &\ell > m && \text{if } \gamma_1 = 0 \text{ or } \gamma_2 = 0 \text{ or } \gamma_3 = 0, \\ &p > 2 && \text{if } \gamma \in \{(\ell-1,0,0);\ (0,\ell-1,0);\ (0,0,\ell-1)\}. \end{aligned} \tag{6.3}$$

Fix $q \in [1,\infty]$ such that $W^{\ell-m,p}(\hat{e}) \hookrightarrow L^q(\hat{e})$. Then the estimate

$$\|\hat{D}^\gamma(\hat{u} - \mathrm{I}\hat{u}); L^q(\hat{e})\| \lesssim |\hat{D}^\gamma \hat{u}; W^{\ell-m,p}(\hat{e})| \tag{6.4}$$

holds.

Proof The proof follows the lines of the proof of Lemma 5.1. Due to Property (P) the functionals can be chosen in the analogous way. The difference is that for a pure derivative the domains G_j are one-dimensional, that means, two dimensions less than the dimension of $\hat{e}$. In that case the embedding $W^{\ell-m,p}(\hat{e}) \hookrightarrow L^1(G_i)$ holds only if $\ell - m \geq 2$ or $\ell - m = 1$, $p > 2$. ■

Note that the case $m = \ell$ is only admitted if $\gamma_1 \neq 0$, $\gamma_2 \neq 0$, and $\gamma_3 \neq 0$. Example 5.2, page 23, can easily be modified to show the necessity of the condition $m < \ell$, at least for $p < \infty$: consider $\hat{u}_\varepsilon := \hat{x}_2^{\gamma_2}\hat{x}_3^{\gamma_3}\hat{w}_\varepsilon(\hat{x}_1)$ and proceed as on page 23. Example 5.3, page 23, can be used by defining $\hat{r} := (\hat{x}_1^2 + \hat{x}_2^2 + \hat{x}_3^2)^{1/2}$ to show that $p > 3$ is necessary for $m = 0$, $\ell = 1$. Let us finally present an example to show that $p > 2$ is necessary when $\gamma \in \{(\ell-1,0,0),(0,\ell-1,0),(0,0,\ell-1)\}$. Such an example was given in [9, page 283] for $m = k = 1$, $\ell = 2$, and is now modified for general $m = \ell - 1 \leq k$.

Example 6.2 Without loss of generality consider $\gamma = (0,0,\ell-1)$ and denote by E that edge of $\hat{e}$ which is parallel to the $\hat{x}_3$-axis. Let $p \leq 2$ and

$$\hat{u}_\varepsilon = \hat{x}_3^{\ell-1}\hat{w}_\varepsilon, \quad \hat{w}_\varepsilon(\hat{x}) := \min\{1; \varepsilon \ln|\ln(\hat{r}/\mathrm{e})|\}, \quad \hat{r} = \hat{r}(\hat{x}_1,\hat{x}_2) := \operatorname{dist}(\hat{x},E).$$

We can calculate that

$$\hat{u}_0 := \lim_{\varepsilon\to 0}\hat{u}_\varepsilon = \begin{cases} \hat{x}_3^{\ell-1} & \text{if } \hat{r}=0,\\ 0 & \text{if } \hat{r}>0,\end{cases} \qquad \lim_{\varepsilon\to 0}\hat{D}^\gamma\hat{u}_\varepsilon = \begin{cases} 1 & \text{if } \hat{r}=0,\\ 0 & \text{if } \hat{r}>0,\end{cases}$$

and

$$\lim_{\varepsilon\to 0}|\hat{D}^\gamma\hat{u}_\varepsilon; W^{1,p}(\hat{e})| \lesssim \lim_{\varepsilon\to 0}|\hat{D}^\gamma\hat{u}_\varepsilon; W^{1,2}(\hat{e})| = 0,$$

(in detail in [3, page 61]) but

$$\lim_{\varepsilon\to 0}\|\hat{D}^\gamma\hat{u}_\varepsilon - \hat{D}^\gamma\mathrm{I}\hat{u}_\varepsilon; L^q(\hat{e})\| = \|\hat{D}^\gamma\mathrm{I}\hat{u}_0; L^q(\hat{e})\| = C(k,\ell) \neq 0.$$

The last conclusion can be proved indirectly as in Example 5.2, page 23. Consequently, the estimate (6.4) does not hold for $\gamma = (0,0,\ell-1)$, $p \leq 2$. The example does not work for $p > 2$ because $\lim_{\varepsilon\to 0}|\hat{D}^\gamma\hat{u}_\varepsilon; W^{1,p}(\hat{e})| = \infty$ then. □

Our next aim is to investigate the transformation

$$x = F(\hat{x}) = B\hat{x} + b, \quad B = (b_{i,j})_{i,j=1}^3 \in \mathbb{R}^{3\times 3}, \quad b = (b_i)_{i=1}^3 \in \mathbb{R}^3, \tag{6.5}$$

compare (3.6). Again, we omit the index e here because the considerations apply to one (arbitrary) element e only.

Let E be the longest edge of e, and let Γ_E be the larger of the two faces of e with $E \subset \overline{\Gamma_E}$. Then we denote the element sizes h_1, h_2, h_3, according to

$$h_1 := \operatorname{meas}_1 E, \quad h_2 := 2\operatorname{meas}_2\Gamma_E/h_1, \quad h_3 := 6\operatorname{meas}_3\hat{e}/(h_1h_2),$$

compare Figure 6.2. Note that we have $h_1 \geq h_2 \geq h_3$ and $\operatorname{meas}_3 e = \frac{1}{6}h_1h_2h_3$ by this definition.

Enumerate the vertices of e such that $X_e^{(1)}$, $X_e^{(2)}$, and $X_e^{(3)}$ are the vertices of Γ_E, and $X_e^{(1)}$ and $X_e^{(3)}$ are the vertices of the shortest edge of Γ_E. To be unique we demand that the shortest of the three edges $X_e^{(1)}X_e^{(4)}$, $X_e^{(2)}X_e^{(4)}$, and $X_e^{(3)}X_e^{(4)}$ is either $X_e^{(1)}X_e^{(4)}$ (Case 1, Figure 6.3) or $X_e^{(2)}X_e^{(4)}$ (Case 2, Figure 6.4).

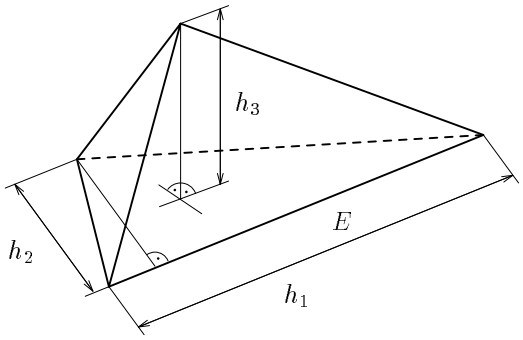

Figure 6.2: Illustration of the definition of the mesh sizes h_1, h_2, h_3 (tetrahedron).

Introduce an element related Cartesian coordinate system $x_e = (x_{1,e}, x_{2,e}, x_{3,e})$ such that $X_e^{(1)}$ lies at the origin, $X_e^{(2)}$ is located at the $x_{1,e}$-axis, and $X_e^{(3)}$ is contained in the $x_{1,e}, x_{2,e}$-plane. Note that the remaining vertex $X_e^{(4)}$ needs not to lay in the half space with $x_{3,e} > 0$ as in the figures, but it may also lay in the half space with $x_{3,e} < 0$.

The three-dimensional counterparts of the maximal angle condition and the coordinate system condition formulated in Section 5 read as follows:

Maximal angle condition: There is a constant $\gamma_* < \pi$ (independent of h and $e \in \mathcal{T}_h$) such that the maximal interior angle γ_F of the four faces as well as the maximal angle γ_E between two faces of any element e are bounded by γ_*, $\gamma_F \le \gamma_*$, $\gamma_E \le \gamma_*$.

Coordinate system condition: The transformation of the element related coordinate system $(x_{1,e}, x_{2,e}, x_{3,e})$ to the discretization independent system (x_1, x_2, x_3) can be determined as a translation and three rotations around the $x_{j,e}$-axes by angles ϑ_j $(j = 1, 2, 3)$, where

$$|\sin\vartheta_1| \lesssim h_3/h_2, \quad |\sin\vartheta_2| \lesssim h_3/h_1, \quad |\sin\vartheta_3| \lesssim h_2/h_1. \tag{6.6}$$

We remark first that alternative formulations of the maximal angle condition can be found in the literature, see Comment 10.9 on page 59. Moreover, if mesh refinement near edges (parallel to the x_3-axis) is considered it may be reasonable to demand $h_1 \sim h_2 \lesssim h_3$ and that one edge of e shall be parallel to the x_3-axis. In that case the coordinate system condition is satisfied, that means that it needs not to be postulated [21].

The two conditions yield properties of the transformation matrix B from (6.5) which are sufficient for our anisotropic interpolation error estimates.

Lemma 6.3 *Assume that the tetrahedron e satisfies the maximal angle condition and the coordinate system condition. Then the entries of the matrix B of (6.5) and of its inverse B^{-1} satisfy the following conditions:*

$$|b_{i,j}| \lesssim \min\{h_i;\ h_j\}, \quad i,j = 1,2,3, \tag{6.7}$$

$$|b_{i,j}^{(-1)}| \lesssim \min\{h_i^{-1};\ h_j^{-1}\}, \quad i,j = 1,2,3. \tag{6.8}$$

Proof As in the proof of Lemma 5.4 we split the transformation (6.5) into two parts

$$x = B^{(1)}x_e + b, \qquad x_e = B^{(2)}\hat{x},$$

with $B = B^{(1)}B^{(2)}$. The intermediate coordinate system was introduced above.

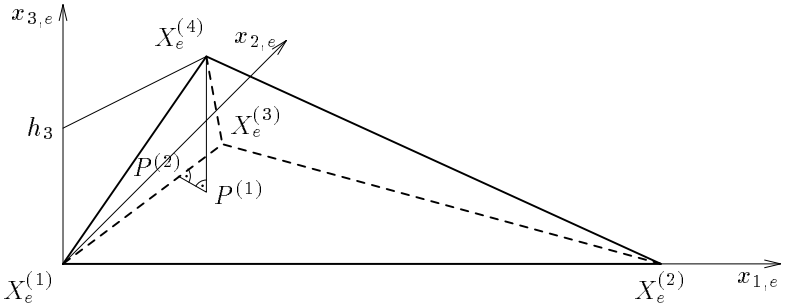

Figure 6.3: Notation and illustration of Case 1: tetrahedron with 3 long edges.

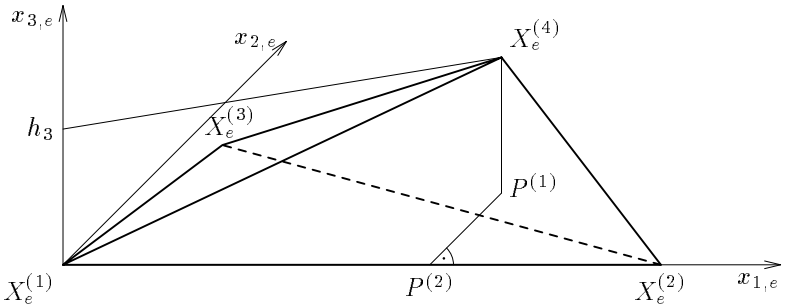

Figure 6.4: Notation and illustration of Case 2: tetrahedron with 4 long edges.

The matrix $B^{(1)}$ can be written as a product of three matrices $B^{(1,1)}$, $B^{(1,2)}$, and $B^{(1,3)}$, describing rotations:

$$B^{(1,1)} = \begin{pmatrix} 1 & 0 & 0 \\ 0 & \cos\vartheta_1 & \sin\vartheta_1 \\ 0 & -\sin\vartheta_1 & \cos\vartheta_1 \end{pmatrix}, \quad B^{(1,2)} = \begin{pmatrix} \cos\vartheta_2 & 0 & \sin\vartheta_2 \\ 0 & 1 & 0 \\ -\sin\vartheta_2 & 0 & \cos\vartheta_2 \end{pmatrix},$$

$$B^{(1,3)} = \begin{pmatrix} \cos\vartheta_3 & \sin\vartheta_3 & 0 \\ -\sin\vartheta_3 & \cos\vartheta_3 & 0 \\ 0 & 0 & 1 \end{pmatrix}.$$

Using (6.6) and $|\cos\vartheta_i| \sim 1$, $i = 1, 2, 3$, one can compute

$$|b_{i,j}^{(1)}| \lesssim \frac{\min\{h_i;\ h_j\}}{\max\{h_i;\ h_j\}}, \quad i, j = 1, 2, 3. \tag{6.9}$$

The first two columns of $B^{(2)}$ are the x_e-coordinates of $X_e^{(2)}$ and $X_e^{(3)}$, respectively. In the same way as in the proof of Lemma 5.4 we obtain

$$|b_{1,1}^{(2)}| \sim h_1, \quad b_{2,1}^{(2)} = b_{3,1}^{(2)} = 0, \tag{6.10}$$

$$|b_{1,2}^{(2)}| \lesssim h_2, \quad |b_{2,2}^{(2)}| \lesssim h_2, \quad b_{3,2}^{(2)} = 0. \tag{6.11}$$

The third column of $B^{(2)}$ is either $X_e^{(4)} - X_e^{(1)}$ (Case 1, see Figure 6.3) or $X_e^{(4)} - X_e^{(2)}$ (Case 2, see Figure 6.4) if the reference elements (6.1) or (6.2) are used, respectively. We show now for Case 1 (Case 2 can be treated by analogy) that $|X_e^{(4)} - X_e^{(1)}| \sim h_3$, which is the desired result,

namely

$$|b_{1,3}^{(2)}| \lesssim h_3, \quad |b_{2,3}^{(2)}| \lesssim h_3, \quad |b_{3,3}^{(2)}| \lesssim h_3. \tag{6.12}$$

Consider the angles $\gamma_{1,2}$, $\gamma_{1,3}$, and $\gamma_{1,4}$ between the faces intersecting at the edges $X_e^{(1)}X_e^{(2)}$, $X_e^{(1)}X_e^{(3)}$, $X_e^{(1)}X_e^{(4)}$, respectively. From spherical (Riemannian) geometry we know that $\gamma_{1,2} + \gamma_{1,3} + \gamma_{1,4} > \pi$. Using the maximal angle condition we conclude that for at least one of the two angles $\gamma_{1,n}$, $n = 2$ or $n = 3$, the relation $|\sin\gamma_{1,n}| \sim 1$ holds. (This idea was obtained from [120, Lemma 6].) Denote by $P^{(1)}$ the foot of the perpendicular from $X_e^{(4)}$ to the $x_{1,e}, x_{2,e}$-plane, by $P^{(2)}$ the foot of the perpendicular from $P^{(1)}$ to the edge $X_e^{(1)}X_e^{(n)}$, and by α the angle between $X_e^{(1)}X_e^{(4)}$ and $X_e^{(1)}X_e^{(n)}$. We obtain (6.12) via

$$|X_e^{(4)} - X_e^{(1)}| = \frac{|X_e^{(4)} - P^{(2)}|}{|\sin\alpha|} = \frac{|X_e^{(4)} - P^{(1)}|}{|\sin\alpha \sin\gamma_{1,n}|} = \frac{h_3}{|\sin\alpha \sin\gamma_{1,n}|} \sim h_3 \tag{6.13}$$

by using the maximal angle condition. (In Case 1, α is not the smallest angle of the triangle $X_e^{(1)}X_e^{(n)}X_e^{(4)}$ since $|X_e^{(1)} - X_e^{(4)}| \le |X_e^{(n)} - X_e^{(4)}|$ by definition.)

From (6.9)–(6.12) we conclude (6.7). Using $|\det B| = 6\,\mathrm{meas}_3 e = h_1h_2h_3$ and the explicit formula of B^{-1} we obtain (6.8). ∎

Theorem 6.4 *Assume that the element e satisfies the maximal angle condition and the coordinate system condition. Let be $u \in W^{\ell,p}(e) \cap \mathcal{C}(\overline{e})$ where $\ell \in \mathbb{N}$, $1 \le \ell \le k+1$, $p \in [1,\infty]$. Fix $m \in \{0,\dots,\ell-1\}$ and $q \in [1,\infty]$ such that $W^{\ell-m,p}(e) \hookrightarrow L^q(e)$. Then the anisotropic interpolation error estimate*

$$|u - \mathrm{I}_h u; W^{m,q}(e)| \lesssim (\mathrm{meas}_3 e)^{1/q-1/p} \sum_{|\alpha|=\ell-m} h^\alpha |D^\alpha u; W^{m,p}(e)|$$

holds provided that

$$\begin{aligned} &p > 3/\ell \quad \text{if } m = 0 \text{ and } \ell = 1,2, \\ &p > 2 \quad\;\; \text{if } m = \ell - 1 > 0. \end{aligned}$$

The result is also valid for $m = \ell = 0$, $p = \infty$, $q \in [1,\infty]$.

The proof is the same as for Theorem 5.5. Special cases were proved also in [35], see Comment 10.12 on page 60.

Theorem 6.5 *Assume that the element e satisfies the maximal angle condition and the coordinate system condition. Let be $u \in W^{k+2,p}(e) \cap \mathcal{C}(\overline{e})$, $p \in [1,\infty]$, $m \in \{0,\dots,k\}$, and $q \in [1,\infty]$. Then the anisotropic interpolation error estimate*

$$|u - \mathrm{I}_h u; W^{m,q}(e)| \lesssim (\mathrm{meas}_3 e)^{1/q-1/p} \sum_{k+1-m \le |\alpha| \le k+2-m} h^\alpha\, |D^\alpha u; W^{m,p}(e)|$$

holds provided that $W^{k+2-m,p}(e) \hookrightarrow L^q(e)$.

Proof The theorem can be proved as Theorem 6.4 by using Lemma 6.3 and analoga to Lemmata 4.5 and 6.1. Let us discuss the differences.

- Since $u \in W^{k+2,p}(e)$ the assumption $W^{k+2-m,p}(e) \hookrightarrow L^q(e)$ replaces now $W^{\ell-m,p}(e) \hookrightarrow L^q(e)$ from Theorem 6.4.

- The assumption $p > 2/\ell$ if $\ell = 1, 2$ is now reduced to $p > 2/(k+2)$ which can be neglected since $k + 2 \geq 3$.

- The assumption $p > 2$ if $m = \ell - 1$ was necessary to ensure the embedding $W^{\ell-m,p}(\hat{e}) \hookrightarrow L^1(G_i)$ in the proof of Lemma 6.1. Because of the additional smoothness $u \in W^{k+2,p}(e)$ this embedding is now $W^{k+2-m,p}(\hat{e}) \hookrightarrow L^1(G_i)$ which is satisfied for all $p \in [1, \infty]$ and all $m \in \{0, \ldots, k\}$.

- The sum at the right hand side extends over all multi-indices with length $k + 1 - m$ and $k + 2 - m$ because the arguments in the proof of Lemma 4.5 are not valid for $\hat{v} \in \mathcal{P}^3_{k+1}$ but only for $\hat{v} \in \mathcal{P}^3_k$. Therefore the application of Lemma 4.3 gives for $|\gamma| = m$ only

$$\inf_{\hat{v} \in \mathcal{P}^3_k} \|\hat{D}^\gamma(\hat{u} - \hat{v}); W^{k+2-m,p}(\hat{e})\| \lesssim |\hat{D}^\gamma \hat{u}; W^{k+1-m,p}(\hat{e})| + |\hat{D}^\gamma \hat{u}; W^{k+2-m,p}(\hat{e})|.$$

■

The idea of using additional smoothness of u ($u \in W^{\ell,p}(e)$ with $\ell > k + 1$) was already used by Jamet [108].

Corollary 6.6 *Assume that the element e satisfies the maximal angle condition. Let be $u \in W^{\ell,p}(e) \cap \mathcal{C}(\overline{e})$ where $\ell \in \mathbb{N}$, $1 \leq \ell \leq k+1$, $p \in [1, \infty]$. Fix $m \in \{0, \ldots, \ell-1\}$ and $q \in [1, \infty]$ such that $W^{\ell-m,p}(e) \hookrightarrow L^q(e)$. Then the* isotropic *interpolation error estimate (sometimes called estimate of Jamet type or of Synge type)*

$$|u - \mathrm{I}_h u; W^{m,q}(e)| \lesssim (\mathrm{meas}_3 e)^{1/q-1/p} (\mathrm{diam}\, e)^{\ell-m} |u; W^{\ell,p}(e)|$$

holds provided that

$$\begin{array}{ll} p > 3/\ell & \text{if } m = 0 \text{ and } \ell = 1, 2 \\ p > 2 & \text{if } m = \ell - 1 > 0. \end{array}$$

If $u \in W^{k+2,p}(e) \cap \mathcal{C}(\overline{e})$, $p \in [1, \infty]$, $m \in \{0, \ldots, k\}$, and $q \in [1, \infty]$, then the isotropic interpolation error estimate

$$|u - \mathrm{I}_h u; W^{m,q}(e)| \lesssim (\mathrm{meas}_3 e)^{1/q-1/p} \sum_{\ell=k+1}^{k+2} (\mathrm{diam}\, e)^{\ell-m} |u; W^{\ell,p}(e)|$$

holds provided that $W^{k+2-m,p}(e) \hookrightarrow L^q(e)$.

Proof If we assumed the coordinate system condition the assertion follows immediately from Theorems 6.4 and 6.5. Since the seminorms remain equivalent during a rotation of the coordinate system, the coordinate system condition can be omitted. ■

We remark that partial cases of this corollary were derived in [108, 120] without knowing anisotropic estimates, see Comments 10.10 and 10.11. We point out in particular that the assumptions made here are weaker than those in [108].

The discussion of the maximal angle condition and the coordinate system condition in Section 5 applies in an analogous way. In particular, Example 5.7 proves that the maximal angle condition for the faces, $\gamma_F \leq \gamma_*$, is necessary. We show now by Example 6.7 that also the condition on the angles between the faces, $\gamma_E \leq \gamma_*$, is necessary. Moreover, Example 6.7 proves that there are elements with $\gamma_F \leq \gamma_*$ but $\gamma_E \to \pi$. Also the converse is valid, see [120, Example 8]. That means, both conditions are independent.

Example 6.7 Consider the tetrahedron with the vertices $(0,0,0)$, $(h_1,0,0)$, $(0,h_1,0)$, and $(h_1/3,h_1/3,h_3)$, and the function $u = x_1^2$. One can directly calculate that $\mathrm{I}_h u = h_1 x_1 - (2/9)h_1^2 h_3^{-1} x_3$ and

$$\frac{\|D^{(0,0,1)}(u-\mathrm{I}_h u);L^p(e)\|}{(\mathrm{meas}_3 e)^{1/q-1/p}\sum\limits_{|\alpha|=1} h^\alpha |D^\alpha u;W^{1,p}(e)|} \sim \frac{h_1^2 h_3^{-1}(\mathrm{meas}_3 e)^{1/q}}{(\mathrm{meas}_3 e)^{1/q-1/p}h_1(\mathrm{meas}_3 e)^{1/p}} = \frac{h_1}{h_3},$$

which is divergent for $h_3 = o(h_1)$. We remark that the case $p = q = \infty$ was already considered in [120, Examples 8, 9]. □

6.2 Error estimates in weighted Sobolev spaces

For the treatment of edge and corner singularities it is convenient to describe the solution in weighted Sobolev spaces. So we want to derive in this subsection anisotropic interpolation error estimates for functions of such weighted spaces. Let us start with the spaces $V_\beta^{\ell,p}(e)$, the norm was introduced by (3.11) on page 12. The special case $\ell = 2$, $k = 1$, was already treated in [19, 20].

Lemma 6.8 *Let $\hat e$ be a reference element satisfying Property (P). Consider a multi-index γ with $m := |\gamma| \in \{0,1\}$ and a function $\hat u \in \mathcal{C}(\overline{\hat e})$ with $\hat D^\gamma \hat u \in V_\beta^{\ell-m,p}(\hat e)$, where $\ell \in \mathbb{N}$, $p \in (1,\infty)$, $\beta \in \mathbb{R}$ shall be such that $0 \le m < \ell \le k+1$ and*

$$\begin{array}{rcll} \ell - 3/p & > & 0 & \text{if } m = 0, \\ \beta & < & \ell - 3/p & \text{if } \gamma_3 = 0, \\ \beta & < & \ell - 1 - 2/p & \text{if } m = 1,\ \gamma_3 = 1, \\ p & > & 2 & \text{if } m = 1,\ \ell = 2. \end{array} \tag{6.14}$$

Fix $q \in [1,\infty]$ such that $V_\beta^{\ell-m,p}(\hat e) \hookrightarrow L^q(\hat e)$. Then the estimate

$$\|\hat D^\gamma(\hat u - \mathrm{I}\hat u);L^q(\hat e)\| \lesssim |\hat D^\gamma \hat u;V_\beta^{\ell-m,p}(\hat e)| \tag{6.15}$$

holds.

Note that we concentrate here on main cases. We did not try to cover all possible cases as in Lemma 6.1. (The cases $p = 1$, $p = \infty$, $m \ge 2$ were excluded.)

Proof We want to apply Lemma 4.5, see also Remark 4.7. The functionals F_i $(i = 1,\dots,j)$ are chosen as in the proof of Lemma 6.1 (Lemma 5.1). It remains to show that the functionals F_i are continuous on $V_\beta^{\ell-m,p}(\hat e)$. For proving this we will need intermediately non-integer (weighted) Sobolev spaces $W^{s,p}(\hat e)$ and $V_\beta^{s,p}(\hat e)$, $s \ge 0$, $p \in (1,\infty)$ which are for $s \in \mathbb{N}$ identical with the spaces introduced in Section 3. Without going into detail we state that such spaces exist (see for example [115, Section 8.3] and [164, 165]) and that the following embeddings hold:

$$W^{s,p}(\hat e) \hookrightarrow L^p(\hat e) \quad \text{if } s \ge 0 \quad \text{(from definition)}, \tag{6.16}$$

$$W^{s,p}(\hat e) \hookrightarrow W^{s-2/p,p}(E) \quad \text{if } s - 2/p \notin \mathbb{N} \quad \text{[115, Section 8.3]}, \tag{6.17}$$

where E is an edge of $\hat e$,

$$V_0^{s,p}(\hat e) \hookrightarrow W^{s,p}(\hat e) \quad \text{if } s \ge 0 \quad \text{(from definition)}, \tag{6.18}$$

$$V_\beta^{s,p}(\hat e) \hookrightarrow V_0^{s-\beta,p}(\hat e) \quad \text{if } s \ge \beta \ge 0 \quad \text{[165]}, \tag{6.19}$$

$$V_\beta^{s,p}(\hat e) \hookrightarrow V_\alpha^{s,p}(\hat e) \quad \text{if } \alpha \ge \beta \quad \text{(from definition)}, \tag{6.20}$$

$$\hat v \in V_\beta^{s,p}(\hat e) \Rightarrow \hat r^\alpha \hat v \in V_{\beta-\alpha}^{s,p}(\hat e) \quad \text{[164, Section 1.1]}. \tag{6.21}$$

Embedding (6.19) was proved in [165] only for infinite domains (dihedral angles) but the proof holds true also for bounded convex domains.

Let us start with the case $m = 0$. Define $\alpha := \max\{\beta;\ 0\}$. By (6.14) we have $(\ell - \alpha)p > 3$ and by (6.18), (6.19), and (6.20), the boundedness of F_i $(i = 1, \ldots, j)$ can be proved:

$$\begin{aligned} |F_i(\hat{v})| &\leq \|\hat{v}; \mathcal{C}(\overline{\hat{e}})\| \lesssim \|\hat{v}; W^{\ell-\alpha,p}(\hat{e})\| \\ &\lesssim \|\hat{v}; V_0^{\ell-\alpha,p}(\hat{e})\| \lesssim \|\hat{v}; V_\alpha^{\ell,p}(\hat{e})\| \lesssim \|\hat{v}; V_\beta^{\ell,p}(\hat{e})\|. \end{aligned}$$

For $m = 1$ consider first the case $\beta < \ell - 1 - 2/p$. Define again $\alpha := \max\{\beta;\ 0\}$, that means with (6.14) that $\ell - 1 - \alpha - 2/p > 0$. (If $\beta \geq 0$ then $\alpha = \beta < \ell - 1 - 2/p$. If $\beta < 0$, then $\alpha = 0$ and we have to show $\ell - 1 - 2/p > 0$. This follows for $\ell = 2$ from $p > 2$ and for $\ell \geq 3$ from $p > 1$.) Using the definition of the F_i $(i = 1, \ldots, j)$ as in the proof of Lemma 6.1 (Lemma 5.1) and the embeddings above we conclude

$$\begin{aligned} |F_i(\hat{v})| &\leq \|\hat{v}; L^1(G_i)\| \lesssim \|\hat{v}; L^p(G_i)\| \lesssim \|\hat{v}; W^{\ell-1-\alpha-2/p,p}(G_i)\| \lesssim \|\hat{v}; W^{\ell-1-\alpha,p}(\hat{e})\| \\ &\lesssim \|\hat{v}; V_0^{\ell-1-\alpha,p}(\hat{e})\| \lesssim \|\hat{v}; V_\alpha^{\ell-1,p}(\hat{e})\| \lesssim \|\hat{v}; V_\beta^{\ell-1,p}(\hat{e})\|, \end{aligned}$$

with G_i being the domain of integration, see the proof of Lemma 5.1.

For $\gamma_3 = 0$ the weight β can be larger. Then we have to estimate sharper. Take any α_1,

$$\alpha_1 \in (1 - 1/p - \varepsilon, 1 - 1/p), \quad \varepsilon := \ell - 3/p - \beta > 0, \tag{6.22}$$

and set

$$\alpha_2 := \max\{\beta;\ \alpha_1\}. \tag{6.23}$$

We obtain from (6.22) that p' (defined by $1/p + 1/p' = 1$) satisfies $1/p' > \alpha_1$. Consequently, we get

$$\|\hat{r}^{-\alpha_1}; L^{p'}(G_i)\| \sim 1$$

because G_i is orthogonal to the $\hat{x}_3$-axis. Similarly to above, and by using the Hölder inequality and the embeddings (6.16)–(6.21), we conclude that

$$\begin{aligned} |F_i(\hat{v})| &:= \left|\int_{G_i} \hat{v}\right| \leq \|\hat{r}^{-\alpha_1}; L^{p'}(G_i)\| \, \|\hat{r}^{\alpha_1}\hat{v}; L^p(G_i)\| \sim \|\hat{r}^{\alpha_1}\hat{v}; L^p(G_i)\| \\ &\lesssim \|\hat{r}^{\alpha_1}\hat{v}; W^{\ell-1-(\alpha_2-\alpha_1)-2/p,p}(G_i)\| \lesssim \|\hat{r}^{\alpha_1}\hat{v}; W^{\ell-1-(\alpha_2-\alpha_1),p}(\hat{e})\| \\ &\lesssim \|\hat{r}^{\alpha_1}\hat{v}; V_0^{\ell-1-(\alpha_2-\alpha_1),p}(\hat{e})\| \lesssim \|\hat{r}^{\alpha_1}\hat{v}; V_{\alpha_2-\alpha_1}^{\ell-1,p}(\hat{e})\| \\ &\lesssim \|\hat{v}; V_{\alpha_2}^{\ell-1,p}(\hat{e})\| \lesssim \|\hat{v}; V_\beta^{\ell-1,p}(\hat{e})\|. \end{aligned}$$

Note that $\ell - 1 - (\alpha_2 - \alpha_1) - 2/p > 0$: Indeed, if $\alpha_2 = \alpha_1$ this follows directly from (6.14), and if $\alpha_2 = \beta$ this follows from (6.22) and (6.14), $\alpha_1 > 1 - 1/p - \varepsilon = -(\ell - 1 - 2/p) + \beta$. ∎

We will transform now estimate (6.15) from $\hat{e}$ to e. The only novelty in comparison to Subsection 6.1 is the term $\hat{r}^\beta$ in the norm. Consider the following points.

- Usually weighted spaces are used if the function under consideration is not contained in the corresponding space without weight. Therefore we will assume $\beta \geq 0$.
- The weight r^β makes no sense if the domain has a positive distance to the x_3-axis. So we will investigate only elements e with at least one vertex at the x_3-axis.
- Since we want to transform $\hat{r} := (\hat{x}_1^2 + \hat{x}_2^2)^{1/2}$ to $r := (x_1^2 + x_2^2)^{1/2}$ we will assume that h_1 and h_2 are of the same order, in particular

$$h_1 \sim h_2 \lesssim h_3 \tag{6.24}$$

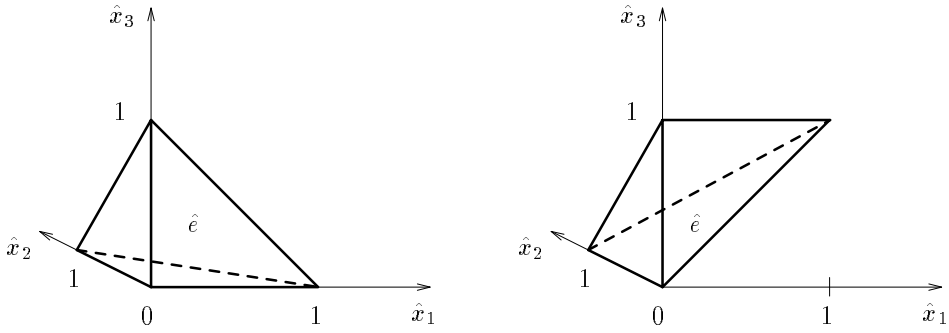

Figure 6.5: Reference elements for tetrahedral elements and $h_1 \lesssim h_2 \lesssim h_3$.

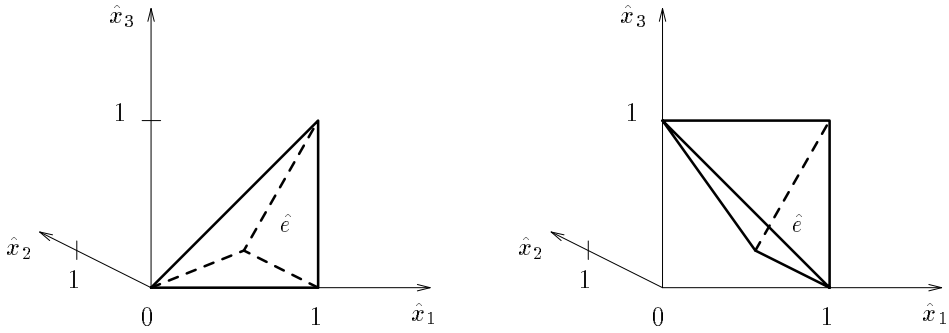

Figure 6.6: Additional reference elements for error estimates in weighted Sobolev spaces.

because $h_1 \sim h_2 \gtrsim h_3$ is not useful. Therefore we will choose

$$\hat{e} := \{(\hat{x}_1, \hat{x}_2, \hat{x}_3)^T \in \mathbb{R}^3 : 0 < \hat{x}_1 < 1,\ 0 < \hat{x}_2 < 1 - \hat{x}_1,\ \hat{x}_1 < \hat{x}_3 < 1 - \hat{x}_2\} \tag{6.25}$$

as the second reference element instead of the one in (6.2), see Figure 6.5.

Note that h_3 is now the largest element size, in contrast to Subsection 6.1. But the relations (6.7), (6.8), were formulated general enough to remain true.

- For the transformation we need a relation between $\hat{r}$ and r, namely

$$\hat{r} \lesssim h_1^{-1} r \tag{6.26}$$

which can be concluded if we assume

$$b_{1,3} = b_{2,3} = 0 \quad \text{and} \quad b_1 = b_2 = 0. \tag{6.27}$$

So we will require (6.27) from now on. That means that a point x is located at the x_3-axis if and only if $\hat{x}$ is located at the $\hat{x}_3$-axis. In other words, elements e with only one vertex at the x_3-axis cannot be mapped to one of the reference elements of Figure 6.5. So we introduce two more reference elements, see Figure 6.6, which are obtained from the previous ones by a reflection at the plane $x_1 = 1/2$. Note that Property (P), page 31, is satisfied by all four elements $\hat{e}$.

- By Property (P) any reference element $\hat{e}$ must have one edge parallel to the $\hat{x}_3$-axis. Together with (6.27) this yields that e must have one edge parallel to the x_3-axis.

We can summarize as follows: Choose the appropriate reference element by the number of edges with length of order h_3 (three or four) and the number of vertices of e laying on in the x_3-axis (one or two). Define the mapping $\hat{e} \to e$ such that points $\hat{x} \in \overline{\hat{e}}$ at the $\hat{x}_3$-axis are mapped to points $x \in \overline{e}$ at the x_3-axis, and that the edge of $\hat{e}$ which is parallel to the $\hat{x}_3$-axis is mapped to the edge of e which is parallel to the x_3-axis. Then (6.7), (6.8) and (6.26) hold provided that the element e satisfies the maximal angle condition.

Theorem 6.9 *Assume that the element e satisfies the maximal angle condition, one edge is parallel to the x_3-axis, and at least one vertex is contained in the x_3-axis. Let $h_1 \sim h_2 \lesssim h_3$, and introduce parameters $m \in \{0;\ 1\}$, $\ell \in \mathbb{N}$ with $1 \le \ell \le k+1$, $p \in (1,\infty)$, $q \in [1,\infty]$, and weights $\beta_\alpha \ge 0$ for all multi-indices α with $|\alpha| = \ell$. Define for each multi-index γ with $|\gamma| = m$ the number*

$$\beta = \beta(\gamma_3) := \begin{cases} \max_{|\alpha|=\ell-m} \beta_{\alpha+\gamma} & \text{if } \gamma_3 = 1, \\ \max_{|\alpha|=\ell} \beta_\alpha & \text{if } \gamma_3 = 0. \end{cases}$$

Assume that the numbers satisfy assumption (6.14) and $V^{\ell-m,p}_{\beta(\gamma_3)}(e) \hookrightarrow L^q(e)$ for all γ with $|\gamma| = m$. Consider a function $u \in \mathcal{C}(\overline{e})$ with $D^\alpha u \in V^{0,p}_{\beta_\alpha}(e)$ for all α with $|\alpha| = \ell$, and $D^\gamma u \in V^{\ell-m,p}_{\beta(\gamma_3)}(e)$ for all γ with $|\gamma| = m$. Then the anisotropic interpolation error estimate

$$|u - \mathrm{I}_h u; W^{m,q}(e)| \lesssim (\mathrm{meas}_3 e)^{1/q-1/p} \sum_{|\alpha|=\ell-m} h^\alpha \sum_{|\gamma|=m} h_1^{-\beta_{\alpha+\gamma}} |D^{\alpha+\gamma} u; V^{0,p}_{\beta_{\alpha+\gamma}}(e)|$$

holds.

The definition of $\beta(\gamma_3)$ and the assumptions on/with $\beta(\gamma_3)$ are necessary to be able to apply Lemma 6.8. The distinction between β_α and $\beta(\gamma_3)$ is made because the error estimate gives a better asymptotics when the weight can be chosen smaller for certain derivatives. We will exploit this in Sections 20 and 21. Of course, the theorem can be written more compact if all weights are equal.

Proof We can prove this theorem similarly to Theorems 5.5, 6.4, and 6.5. But we have to be careful with the assumptions on the weights.

From (6.8) we get

$$\begin{aligned} |u - \mathrm{I}_h u; W^{m,q}(e)| &\sim \sum_{|s|=m} \|D^s (u - \mathrm{I}_h u); L^q(e)\| \\ &\lesssim (\mathrm{meas}_3 e)^{1/q} \sum_{|\gamma|=m} h^{-\gamma} \|\hat{D}^\gamma (\hat{u} - \mathrm{I}\hat{u}); L^q(\hat{e})\|, \end{aligned}$$

see also (5.12).

For any γ with $|\gamma| = m$ we apply Lemma 6.8 and obtain

$$\|\hat{D}^\gamma (\hat{u} - \mathrm{I}\hat{u}); L^q(\hat{e})\| \lesssim |\hat{D}^\gamma \hat{u}; V^{\ell-m,p}_{\beta(\gamma_3)}(\hat{e})| \sim \sum_{|s|=\ell-m} \|\hat{D}^{s+\gamma} \hat{u}; V^{0,p}_{\beta(\gamma_3)}(\hat{e})\|.$$

For $\gamma = (0,0,1)$ we notice that (6.27) yields $\hat{D}^\gamma \hat{u} = b_{3,3} D^\gamma u \sim h_3 D^\gamma u$. Therefore

$$\begin{aligned} \|\hat{D}^\gamma (\hat{u} - \mathrm{I}\hat{u}); L^q(\hat{e})\| &\lesssim (\mathrm{meas}_3 e)^{-1/p} \sum_{|s|=\ell-m} \sum_{|\alpha|=\ell-m} h^{\alpha+\gamma} h_1^{-\beta(1)} \|D^{\alpha+\gamma} u; V^{0,p}_{\beta(1)}(e)\| \\ &\lesssim (\mathrm{meas}_3 e)^{-1/p} \sum_{|\alpha|=\ell-m} h^{\alpha+\gamma} h_1^{-\beta_{\alpha+\gamma}} \|D^{\alpha+\gamma} u; V^{0,p}_{\beta_{\alpha+\gamma}}(e)\| \end{aligned}$$

where we have used $h_1^{-\beta(1)}\|v; V^{0,p}_{\beta(1)}(e)\| \lesssim h_1^{-\beta_{\alpha+\gamma}}\|v; V^{0,p}_{\beta_{\alpha+\gamma}}(e)\|$ which holds since $\beta_{\alpha+\gamma} \le \beta(1)$. For $\gamma_3 = 0$ we obtain in a similar way

$$\begin{aligned}\|\hat{D}^\gamma(\hat{u} - \mathrm{I}\hat{u}); L^q(\hat{e})\| &\lesssim (\mathrm{meas}_3 e)^{-1/p} \sum_{|s|=\ell-m} \sum_{|\alpha|=\ell-m} \sum_{|t|=m} h^{\alpha+\gamma} h_1^{-\beta(0)} \|D^{\alpha+t}u; V^{0,p}_{\beta(0)}(e)\| \\ &\lesssim (\mathrm{meas}_3 e)^{-1/p} \sum_{|\alpha|=\ell-m} \sum_{|t|=m} h^{\alpha+\gamma} h_1^{-\beta_{\alpha+t}} \|D^{\alpha+t}u; V^{0,p}_{\beta_{\alpha+t}}(e)\|.\end{aligned}$$

All estimates together yield

$$\begin{aligned}|u - \mathrm{I}_h u; W^{m,q}(e)| &\lesssim (\mathrm{meas}_3 e)^{1/q-1/p} \sum_{|\gamma|=m} h^{-\gamma} \sum_{|\alpha|=\ell-m} \sum_{|t|=m} h^{\alpha+\gamma} h_1^{-\beta_{\alpha+t}} \|D^{\alpha+t}u; V^{0,p}_{\beta_{\alpha+t}}(e)\| \\ &\sim (\mathrm{meas}_3 e)^{1/q-1/p} \sum_{|\alpha|=\ell-m} \sum_{|t|=m} h^{\alpha} h_1^{-\beta_{\alpha+t}} \|D^{\alpha+t}u; V^{0,p}_{\beta_{\alpha+t}}(e)\|\end{aligned}$$

which is the desired result. ∎

When problems with edge *and corner* singularities are investigated it is convenient to describe the solution in Sobolev spaces with two weights, $V^{\ell,p}_{\beta,\delta}(e)$, see page 13 in Section 3. The application of such spaces is reasonable only if the element e has one vertex at the origin and one edge at the x_3-axis. So we need only one reference element, namely the one described by (6.1). Define by $R = R(x) := (x_1^2 + x_2^2 + x_3^2)^{1/2}$, $r = r(x) := (x_1^2 + x_2^2)^{1/2}$, and $\theta := r/R$ the distance to the origin, the distance to the x_3-axis, and the "angular distance" to the x_3-axis, respectively. $\hat{R}$, $\hat{r}$, and $\hat{\theta}$ are defined analogously. The following lemma was proved in [21] for the special case $\ell = 2$, $k = m = 1$, and with $\delta = 0$ if $\gamma = (0, 0, 1)$.

Lemma 6.10 *Let $\hat{e}$ be the reference element described by (6.1). Consider a multi-index γ with $m := |\gamma| \in \{0;\ 1\}$ and a function $\hat{u} \in \mathcal{C}(\overline{\hat{e}})$ with $\hat{D}^\gamma \hat{u} \in V^{\ell-m,p}_{\beta,\delta}(\hat{e})$, where $\ell \in \mathbb{N}$, $p \in (1, \infty)$, $\beta, \delta \in \mathbb{R}$ shall be such that $0 \le m < \ell \le k + 1$ and*

$$\begin{aligned} \beta &< \ell - 3/p, & & \\ \ell - 3/p &> 0 & &\text{if } m = 0 \\ \delta &< \ell - 3/p & &\text{if } \gamma_3 = 0 \\ \delta &< \ell - 1 - 2/p & &\text{if } m = 1,\ \gamma_3 = 1 \\ p &> 2 & &\text{if } m = 1,\ \ell = 2. \end{aligned} \tag{6.28}$$

Fix $q \in [1, \infty]$ such that $V^{\ell-m,p}_{\beta,\delta}(\hat{e}) \hookrightarrow L^q(\hat{e})$. Then the estimate

$$\|\hat{D}^\gamma(\hat{u} - \mathrm{I}\hat{u}); L^q(\hat{e})\| \lesssim |D^\gamma \hat{u}; V^{\ell-m,p}_{\beta,\delta}(\hat{e})| \tag{6.29}$$

holds.

Proof The lemma can be proved similarly to Lemma 6.8. Let $m = 0$ and define $\alpha := \max\{\beta;\ \delta;\ 0\}$. By (6.28) we have $(\ell - \alpha)p > 3$. Consequently,

$$\begin{aligned}|F_i(\hat{v})| &\le \|\hat{v}; \mathcal{C}(\overline{\hat{e}})\| \lesssim \|\hat{v}; W^{\ell-\alpha,p}(\hat{e})\| \\ &\lesssim \|\hat{v}; V^{\ell-\alpha,p}_{0,0}(\hat{e})\| \lesssim \|\hat{v}; V^{\ell,p}_{\alpha,\alpha}(\hat{e})\| \lesssim \|\hat{v}; V^{\ell,p}_{\beta,\delta}(\hat{e})\|.\end{aligned}$$

For $m = 1$ consider first the case that G_i is not contained in the x_3-axis ($\theta \not\equiv 0$ on G_i). As in the last case of the proof of Lemma 6.8, we take any $\alpha_1 \in (1 - 1/p - \varepsilon, 1 - 1/p)$ with

$\varepsilon := \ell - 3/p - \max\{\beta;\ \delta\} > 0$, set $\alpha_2 := \max\{\beta;\ \delta;\ \alpha_1\}$ and obtain that p' (defined by $1/p + 1/p' = 1$) satisfies $1/p' > \alpha_1$. Consequently, we get

$$\|\hat{r}^{-\alpha_1}; L^{p'}(G_i)\| = \|\hat{R}^{-\alpha_1}\hat{\theta}^{-\alpha_1}; L^{p'}(G_i)\| \sim 1 \tag{6.30}$$

because G_i is orthogonal to the $\hat{x}_3$-axis ($\gamma_3 = 0$) or away from the $\hat{x}_3$-axis ($\gamma_3 = 1, k \geq 2$). (For $\gamma_3 = 0$, $k = 1$ we have $\theta \equiv 1$ on G_i and can admit even any power of θ in (6.30).) We conclude

$$\begin{aligned}
|F_i(\hat{v})| &:= \left|\int_{G_i} \hat{v}\right| \leq \|\hat{r}^{-\alpha_1}; L^{p'}(G_i)\|\, \|\hat{r}^{\alpha_1}\hat{v}; L^p(G_i)\| \sim \|\hat{r}^{\alpha_1}\hat{v}; L^p(G_i)\| \\
&\lesssim \|\hat{r}^{\alpha_1}\hat{v}; W^{\ell-1-(\alpha_2-\alpha_1)-2/p,p}(G_i)\| \lesssim \|\hat{r}^{\alpha_1}\hat{v}; W^{\ell-1-(\alpha_2-\alpha_1),p}(\hat{e})\| \\
&\lesssim \|\hat{r}^{\alpha_1}\hat{v}; V^{\ell-1-(\alpha_2-\alpha_1),p}_{0,0}(\hat{e})\| \lesssim \|\hat{r}^{\alpha_1}\hat{v}; V^{\ell-1,p}_{\alpha_2-\alpha_1,\alpha_2-\alpha_1}(\hat{e})\| \\
&\lesssim \|\hat{v}; V^{\ell-1,p}_{\alpha_2,\alpha_2}(\hat{e})\| \lesssim \|\hat{v}; V^{\ell-1,p}_{\beta,\delta}(\hat{e})\|.
\end{aligned}$$

Note that $\ell - 1 - (\alpha_2 - \alpha_1) - 2/p > 0$: Indeed, if $\alpha_2 = \alpha_1$ this follows from (6.28), and if $\alpha_2 = \max\{\beta;\ \delta\}$ this follows from $\alpha_1 > 1 - 1/p - \varepsilon = -(\ell - 1 - 2/p) + \max\{\beta;\ \delta\}$, see the definition of ε.

If G_i is contained in the x_3-axis ($\gamma_3 = 1$) then (6.30) does not hold. In this case we proceed as follows: Take any $\alpha_1 \in (1-1/p-\varepsilon, 1-1/p)$, $\varepsilon := \ell-3/p-\beta > 0$, set $\alpha_2 := \max\{\beta;\ \delta+\alpha_1;\ \alpha_1\}$ and observe that p' satisfies $1/p' > \alpha_1$. Consequently, we get $\|\hat{R}^{-\alpha_1}; L^{p'}(G_i)\| \sim 1$ and

$$\begin{aligned}
|F_i(\hat{v})| &:= \left|\int_{G_i} \hat{v}\right| \leq \|\hat{R}^{-\alpha_1}; L^{p'}(G_i)\|\, \|\hat{R}^{\alpha_1}\hat{v}; L^p(G_i)\| \sim \|\hat{R}^{\alpha_1}\hat{v}; L^p(G_i)\| \\
&\lesssim \|\hat{R}^{\alpha_1}\hat{v}; W^{\ell-1-(\alpha_2-\alpha_1)-2/p,p}(G_i)\| \lesssim \|\hat{R}^{\alpha_1}\hat{v}; W^{\ell-1-(\alpha_2-\alpha_1),p}(\hat{e})\| \\
&\lesssim \|\hat{R}^{\alpha_1}\hat{v}; V^{\ell-1-(\alpha_2-\alpha_1),p}_{0,0}(\hat{e})\| \lesssim \|\hat{R}^{\alpha_1}\hat{v}; V^{\ell-1,p}_{\alpha_2-\alpha_1,\alpha_2-\alpha_1}(\hat{e})\| \\
&\lesssim \|\hat{v}; V^{\ell-1,p}_{\alpha_2,\alpha_2-\alpha_1}(\hat{e})\| \lesssim \|\hat{v}; V^{\ell-1,p}_{\beta,\delta}(\hat{e})\|.
\end{aligned}$$

Note that $\ell - 1 - (\alpha_2 - \alpha_1) - 2/p > 0$ can be concluded from (6.28) by distinguishing the three cases for α_2: The possibilities $\alpha_2 = \beta$ and $\alpha_2 = \alpha_1$ can be proved as above, the instance $\alpha_2 = \delta + \alpha_1$ is direct. ∎

The transformation of (6.29) from $\hat{e}$ to e can be done in a similar way as above by using (6.24) and (6.27). We obtain $h_3^{-1}R \lesssim \hat{R} \lesssim h_1^{-1}R$ and $\hat{r} \lesssim h_1^{-1}r$, and consequently $\hat{\theta} \lesssim h_3 h_1^{-1}\theta$. This leads to the following theorem.

Theorem 6.11 *Assume that the element e satisfies the maximal angle condition, one vertex is located at the origin of the coordinate system $x = (x_1, x_2, x_3)$, and one edge is contained in the x_3-axis. Let $h_1 \sim h_2 \lesssim h_3$, and introduce parameters $m \in \{0;\ 1\}$, $\ell \in \mathbb{N}$ with $1 \leq \ell \leq k+1$, $p \in (1, \infty)$, $q \in [1, \infty]$, and weights $\beta_\alpha \geq 0$, $\delta_\alpha \geq 0$ for all multi-indices α with $|\alpha| = \ell$. Define the numbers $\beta = \max_{|\alpha|=\ell} \beta_\alpha$ and*

$$\delta = \delta(\gamma_3) := \begin{cases} \max_{|\alpha|=\ell-m} \delta_{\alpha+\gamma} & \text{if } \gamma_3 = 1, \\ \max_{|\alpha|=\ell} \delta_\alpha & \text{if } \gamma_3 = 0 \end{cases}$$

for each multi-index γ with $|\gamma| = m$. Assume that the numbers satisfy assumption (6.28) and $V^{\ell-m,p}_{\beta,\delta(\gamma_3)}(e) \hookrightarrow L^q(e)$ for all γ with $|\gamma| = m$. Consider a function $u \in \mathcal{C}(\overline{e})$ with $D^\alpha u \in V^{0,p}_{\beta_\alpha,\delta_\alpha}(e)$ for all α with $|\alpha| = \ell$, and $D^\gamma u \in V^{\ell-m,p}_{\beta,\delta(\gamma_3)}(e)$ for all γ with $|\gamma| = m$. Then the anisotropic interpolation error estimate

$$\begin{aligned}
&|u - \mathrm{I}_h u; W^{m,q}(e)| \\
&\lesssim (\mathrm{meas}_3 e)^{1/q-1/p} \sum_{|\alpha|=\ell-m} h^\alpha \sum_{|\gamma|=m} h_1^{-\beta_{\alpha+\gamma}-\delta_{\alpha+\gamma}} h_3^{-\delta_{\alpha+\gamma}} \|D^{\alpha+\gamma}u; V^{0,p}_{\beta_{\alpha+\gamma},\delta_{\alpha+\gamma}}(e)\|
\end{aligned}$$

holds.

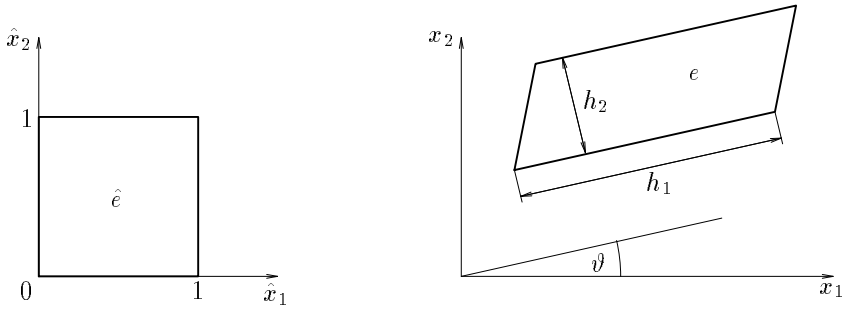

Figure 7.1: Illustration of an affine quadrilateral element.

7 Quadrilateral elements

7.1 Affine elements

In this subsection we show first that the theory of Section 5 carries over to affine quadrilateral elements, that are parallelograms, see Figure 7.1. There is only one small difference in the proof of Lemma 7.1 (estimate on the reference element) where attention is needed. But there are two more reasons why a whole section is devoted to quadrilateral elements. First, for *rectangular elements* we can prove for $k \geq 2$ a slightly sharper estimate, with less terms on the right hand side (Theorem 7.11 and Remark 7.12). Second, for *more general elements* than parallelograms, for example trapezes, the transformation $x = F_e(\hat{x})$ is non-linear and we encounter the difficulties discussed in Example 4.2, page 18. Nevertheless, we were finally able to reproduce the estimates of the affine elements (Theorem 7.17, Corollary 7.18). The section ends with an example showing the necessity of an assumption on the geometry of the non-affine elements.

Consider the Lagrangian finite element $(\hat{e}, \mathcal{P}_{k,\hat{e}}, \Sigma_{k,\hat{e}})$ with

$$\begin{aligned} \hat{e} &:= \{(\hat{x}_1, \hat{x}_2) \in \mathbb{R}^2 : 0 < \hat{x}_1, \hat{x}_2 < 1\}, && (7.1)\\ \mathcal{P}_{k,\hat{e}} &:= \mathcal{Q}_k^2, && (7.2)\\ \Sigma_{k,\hat{e}} &:= \{f_i : \mathcal{C}(\overline{\hat{e}}) \to \mathbb{R} \text{ such that } f_i(\hat{u}) := \hat{u}(\hat{X}^{(i)})\}_{i=1}^{N_e}, && (7.3) \end{aligned}$$

where $N_e = (k+1)^2$ is the number of nodes and

$$\mathcal{X} := \{\hat{X}^{(i)}\}_{i=1}^{N_e} := \{(\tfrac{i}{k}, \tfrac{j}{k})^T \in \mathbb{R}^2\}_{0 \leq i,j \leq k} \tag{7.4}$$

is the set of nodes. Lemma 7.1 contains the estimates of the interpolation error on the reference element. It is identical with Lemma 5.1.

Lemma 7.1 *Let γ be a multi-index with $m := |\gamma|$ and $\hat{u} \in \mathcal{C}(\overline{\hat{e}})$ be a function with $\hat{D}^\gamma \hat{u} \in W^{\ell-m,p}(\hat{e})$, where $\ell, m \in \mathbb{N}$, $p \in [1,\infty]$ shall be such that $0 \leq m \leq \ell \leq k+1$ and*

$$\begin{aligned} &p = \infty \quad \text{if } m = 0 \text{ and } \ell = 0,\\ &p > 2 \quad \text{if } m = 0 \text{ and } \ell = 1,\\ &m < \ell \quad \text{if } \gamma_1 = 0 \text{ or } \gamma_2 = 0, \text{ and } m > 0. \end{aligned} \tag{7.5}$$

Fix $q \in [1,\infty]$ such that $W^{\ell-m,p}(\hat{e}) \hookrightarrow L^q(\hat{e})$. Then the estimate

$$\|\hat{D}^\gamma(\hat{u} - \mathrm{I}\hat{u}); L^q(\hat{e})\| \lesssim |\hat{D}^\gamma \hat{u}; W^{\ell-m,p}(\hat{e})| \tag{7.6}$$

holds.

The assumptions can be discussed as in Section 5 for Lemma 5.1. The proof is also the same. Note that $|\mathcal{X}_\gamma| = j$ still holds but $j = (k-\gamma_1+1)(k-\gamma_2+1)$. The lemma was proved for $m=1$, $\ell = k+1$, $q=p$, in [9].

The transformation from $\hat{e}$ to $e = F(\hat{e})$ can be written as

$$x = F(\hat{x}) = B\hat{x} + b, \quad B = (b_{i,j})_{i,j=1}^2 \in \mathbb{R}^{2\times 2}, \quad b = (b_i)_{i=1}^2 \in \mathbb{R}^2, \tag{7.7}$$

compare (3.6). As in the case of triangles we can formulate a maximal angle condition and a coordinate system condition, and we can prove anisotropic interpolation error estimates on e.

Maximal angle condition: There is a constant $\gamma_* < \pi$ (independent of h and $e \in \mathcal{T}_h$) such that the maximal interior angle γ of any element e is bounded by γ_*, $\gamma \le \gamma_*$.

Coordinate system condition: The angle ϑ between the longer sides and the x_1-axis is bounded by $|\sin\vartheta| \lesssim h_2/h_1$.

Here, h_1 denotes the length of the longer edges of e and $h_2 := \mathrm{meas}_2(e)/h_1$ is the corresponding height. Consequently,

$$|\det B| = \mathrm{meas}_2(e) = h_1 h_2. \tag{7.8}$$

Lemma 7.2 *Assume that an affine quadrilateral element e satisfies the maximal angle condition and the coordinate system condition. Then the entries of the matrix B of (7.7) and of its inverse B^{-1} satisfy the following conditions:*

$$|b_{i,j}| \lesssim \min\{h_i;\ h_j\}, \qquad i,j = 1,2, \tag{7.9}$$

$$|b^{(-1)}_{i,j}| \lesssim \min\{h_i^{-1};\ h_j^{-1}\}, \quad i,j = 1,2. \tag{7.10}$$

Proof Enumerate the vertices of e counterclockwise such that $X_e^{(1)}$ and $X_e^{(4)}$ are the vertices of one of the shortest edges of e. Introduce an element related Cartesian coordinate system $x_e = (x_{1,e}, x_{2,e})$ such that $X_e^{(1)} = (0,0)^T$ and $X_e^{(2)}$ is also located at the $x_{1,e}$-axis. Proceed as in the proof of Lemma 5.4. ∎

Theorem 7.3 *Assume that e is a parallelogram which satisfies the maximal angle condition and the coordinate system condition. Let be $u \in W^{\ell,p}(e) \cap \mathcal{C}(\overline{e})$ where $\ell \in \mathbb{N}$, $1 \le \ell \le k+1$, $p \in [1,\infty]$. Fix $m \in \{0,\dots,\ell-1\}$ and $q \in [1,\infty]$ such that $W^{\ell-m,p}(e) \hookrightarrow L^q(e)$. Then the anisotropic interpolation error estimate*

$$|u - \mathrm{I}_h u; W^{m,q}(e)| \lesssim (\mathrm{meas}_2 e)^{1/q-1/p} \sum_{|\alpha|=\ell-m} h^\alpha |D^\alpha u; W^{m,p}(e)| \tag{7.11}$$

holds provided that $p > 2$ if $\ell = 1$. The result is valid also for $m = \ell = 0$, $p = \infty$, $q \in [1,\infty]$.

Proof See the proof of Theorem 5.5. ∎

Corollary 7.4 *Assume that the parallelogram e satisfies the maximal angle condition. Let be $u \in W^{\ell,p}(e) \cap \mathcal{C}(\overline{e})$ where $\ell \in \mathbb{N}$, $1 \le \ell \le k+1$, $p \in [1,\infty]$. Fix $m \in \{0,\dots,\ell-1\}$ and $q \in [1,\infty]$ such that $W^{\ell-m,p}(e) \hookrightarrow L^q(e)$. Then the* isotropic *interpolation error estimate (sometimes called estimate of Jamet type or of Synge type)*

$$|u - \mathrm{I}_h u; W^{m,q}(e)| \lesssim (\mathrm{meas}_2 e)^{1/q-1/p} (\mathrm{diam}\, e)^{\ell-m} |u; W^{\ell,p}(e)|$$

holds provided that $p > 2$ if $\ell = 1$. The result is valid also for $m = \ell = 0$, $p = \infty$, $q \in [1,\infty]$.

Particular cases of this corollary were derived in [108], see Comment 10.13 on page 61.

7.2 Rectangular elements

For rectangular elements one can prove slightly sharper estimates than for general affine elements. For the proof we have to replace in all statements the usual seminorm $|\,.\,;W^{\ell,p}|$ by the the seminorm $[\,.\,;W^{\ell,p}]$ where only pure derivatives are included. Since we use this improvement in the next subsection as well, it makes sense to present the whole theory in detail. We follow the line of Subsections 4.3 and 7.1 and formulate with Lemmata 7.6, 7.8, and 7.9 the counterparts of Lemmata 4.3, 4.5, and 7.1. Theorem 7.11 is then straightforward. But we start with citing Theorem 1 from from [53], compare also [192].

Lemma 7.5 *Consider a bounded domain $G \subset \mathbb{R}^d$ which satisfies the strong cone condition. Let $u \in W^{\ell,p}(G)$, $\ell \geq 1$, $p \in [1,\infty)$. Fix a set K of multi-indices such that*

$$\{(\ell,0,\ldots,0),\ldots,(0,\ldots,0,\ell)\} \subset K \subset \{\alpha : |\alpha| = \ell\}.$$

Finally, let $\mathcal{P}_K$ be the set of polynomials w such that $D^\alpha w = 0\ \forall \alpha \in K$. Then the equivalence

$$\inf_{w\in\mathcal{P}_K} \|u-w;W^{\ell,p}(G)\| \sim \sum_{|\alpha|\in K} \|D^\alpha u;L^p(G)\| \tag{7.12}$$

holds.

Lemma 7.6 *Consider a bounded domain $G \subset \mathbb{R}^d$ which satisfies a strong cone condition. Let γ be a multi-index with $m := |\gamma|$ and $u \in L^1(G)$ be a function with $D^\gamma u \in W^{\ell-m,p}(G)$, where $\ell, m \in \mathbb{N}$, $0 \leq m \leq \ell$, $p \in [1,\infty)$. Then there exists a polynomial $w \in \mathcal{Q}^d_{\ell-1}$ such that*

$$\|D^\gamma(u-w);W^{\ell-m,p}(G)\| \lesssim [D^\gamma u;W^{\ell-m,p}(G)]. \tag{7.13}$$

The constant depends on G and $\ell - m$. The polynomial w depends on G, ℓ, γ, and u.

Proof For $\gamma = (0,\ldots,0)$ we obtain the assertion by setting $K = \{\alpha = \ell\beta : |\beta| = 1\}$ in Lemma 7.5. Let now γ be arbitrary. By using the lemma with $\gamma = (0,\ldots,0)$ we find a polynomial $w_1 \in \mathcal{Q}^d_{\ell-m-1}$ such that

$$\|D^\gamma u - w_1;W^{\ell-m,p}(G)\| \lesssim [D^\gamma u;W^{\ell-m,p}(G)].$$

Since there exists a $w \in \mathcal{Q}^d_{\ell-1}$ with $D^\gamma w = w_1$ the lemma is proved. ∎

Remark 7.7 Let us compare Lemmata 4.3 and 7.6. First we mention that the strong cone condition is more restrictive than the assumption on the domain in Lemma 4.3. Indeed, if a domain G satisfies the strong cone condition then $G = \bigcup_{j=1}^J G_j$ where each of the G_j is star-shaped with respect to a ball B_j [76, Remark 7.1]. The example of a slit domain shows that the converse is not valid.

Second, the constant in (4.11) depends only on $\operatorname{diam} G_j$ and $\operatorname{diam} B_j$ (not on G generally) and the function w is independent of G and γ. These advantages of Lemma 4.3 are used in Theorem 7.17 and in Lemma 11.1.

We were not able to derive (7.13) from the very general theory in [76] to keep these advantages, but we obtained only

$$\|D^\gamma(u-w);W^{\ell-m-1,p}(G)\| \lesssim [D^\gamma u;W^{\ell-m,p}(G)]$$

by setting $A = \{\alpha : \alpha = \ell\beta, |\beta| = 1\}$ in [76, Theorem 4.2]. However, this result is not sufficient to derive the following Lemma 7.8.

Lemma 7.8 *Assume that $\hat{e}$ is a quadrilateral or a hexahedron. Let $\mathrm{I} : \mathcal{C}(\overline{\hat{e}}) \to \mathcal{P}_{k,\hat{e}}$ be a linear operator. Fix $m, \ell \in \mathbb{N}$, $p \in [1,\infty)$, and $q \in [1,\infty]$ such that $0 \le m \le \ell \le k+1$ and (4.15) hold. Consider a multi-index γ with $|\gamma| = m$ and define $j := \dim \hat{D}^\gamma \mathcal{P}_{k,\hat{e}}$. Assume that there are linear functionals F_i, $i = 1, \ldots, j$, with properties (4.16)–(4.18). Then the error can be estimated for all $\hat{u} \in \mathcal{C}(\overline{\hat{e}})$ with $\hat{D}^\gamma \hat{u} \in W^{\ell-m,p}(\hat{e})$ by*

$$\|\hat{D}^\gamma(\hat{u} - \mathrm{I}\hat{u}); L^q(\hat{e})\| \lesssim [\hat{D}^\gamma \hat{u}; W^{\ell-m,p}(\hat{e})].$$

Proof The proof is the same as that for Lemma 4.5 by using $\hat{v} \in \mathcal{Q}^d_{\ell-1}$ instead of $\hat{v} \in \mathcal{P}^d_{\ell-1}$ and Lemma 7.6 instead of Lemma 4.3. ∎

By using Lemma 7.8 instead of Lemma 4.5 we can prove the following lemma in the same way as Lemma 7.1.

Lemma 7.9 *Under the assumptions of Lemma 7.1 the estimate*

$$\|\hat{D}^\gamma(\hat{u} - \mathrm{I}\hat{u}); L^q(\hat{e})\| \lesssim [\hat{D}^\gamma \hat{u}; W^{\ell-m,p}(\hat{e})] \tag{7.14}$$

holds.

Remark 7.10 It is not clear whether Lemma 7.6 holds for $p = \infty$ as well. In the original source [53, Theorem 1] this case is excluded. The critical point is whether the Aronszajn-Smith-Il'in result

$$\|u; W^{\ell,p}(\hat{e})\| \lesssim \|u; L^p(\hat{e})\| + \sum_{|\alpha|=1} \|D^{\ell\alpha} u; L^p(\hat{e})\|$$

holds for $p = \infty$. This estimate can be found in various sources without a statement about $p = \infty$, see [82, Lemma A.8], [106], [115, Theorem 8.8.4], [178], for example. Consequently, we excluded this case in Lemma 7.8.

In Lemma 7.9, however, we included $p = \infty$ for the following reasons. If $m \ge \ell - 1$, then Lemma 7.9 is identical with Lemma 7.1, and there is nothing to prove. If $m \le \ell - 2$, that means in particular $\ell \ge 2$, we can choose some $p' < \infty$ such that the assumptions of Lemma 7.9 are satisfied with p' instead of p and for arbitrary $q \in [1,\infty]$. (Take for example $p' = 2$.) Since the lemma holds for finite p' and with

$$[\hat{D}^\gamma \hat{u}; W^{\ell-m,p'}(\hat{e})] \lesssim [\hat{D}^\gamma \hat{u}; W^{\ell-m,\infty}(\hat{e})]$$

we get the desired result.

Theorem 7.11 *Assume that e is a rectangle with sides parallel to the coordinate axes. Let γ be a multi-index with $m := |\gamma|$ and $u \in \mathcal{C}(\overline{e})$ be a function with $D^\gamma u \in W^{\ell-m,p}(e)$, where $\ell, m \in \mathbb{N}$, $p \in [1,\infty]$ shall be such that $0 \le m \le \ell \le k+1$ and (7.5) hold. Fix $q \in [1,\infty]$ such that $W^{\ell-m,p}(e) \hookrightarrow L^q(e)$. Then the anisotropic interpolation error estimate*

$$\|D^\gamma(u - \mathrm{I}_h u); L^q(e)\| \lesssim (\mathrm{meas}_2 e)^{1/q-1/p} \sum_{|\alpha|=1} h^{(\ell-m)\alpha} \|D^{\gamma+(\ell-m)\alpha} u; L^p(e)\| \tag{7.15}$$

holds.

Proof From (7.14) by the transformation $x_i = h_i \hat{x}_i + b_i$, $i = 1, 2$. ∎

The theorem was proved for $k = 1$, $\ell = 2$, $p = 2$, in [150, page 90] and for general k, $\ell = k+1$, $m = 1$, $p = 2$, in [155], see Comments 10.14 and 10.15.

Remark 7.12 One can also prove certain estimates for the case of additional smoothness of u, see Comment 10.15 on page 61.

7.3 Subparametric elements

In this subsection we will consider a special class of non-affine quadrilaterals. Often *isoparametric* elements are treated, which means according to [182, Section 3.3] that the shape functions are used for the polynomial transformation F from the reference element $\hat{e}$ to the element e. The term *subparametric* indicates that only a subset of the shape functions is used. We will use the shape functions of the bilinear case which leads to a considerable simplification. But all quadrilaterals with straight sides fall into this class.

Denote the shape functions of the bilinear case by $\hat{\psi}_1 := (1-\hat{x}_1)(1-\hat{x}_2)$, $\hat{\psi}_2 := \hat{x}_1(1-\hat{x}_2)$, $\hat{\psi}_3 := \hat{x}_1\hat{x}_2$, $\hat{\psi}_4 := (1-\hat{x}_1)\hat{x}_2$. Then we can define the subparametric mapping F by

$$F(\hat{x}) := \sum_{i=1}^{4} X_e^{(i)} \hat{\psi}_i(\hat{x}) \in \mathcal{Q}_1^2 \times \mathcal{Q}_1^2.$$

We assume that the $X_e^{(i)}$ form a convex quadrilateral e, then this mapping is invertible [82, page 105]. In the case of e being a parallelogram the mapping F is affine ($X_e^{(1)} - X_e^{(2)} + X_e^{(3)} - X_e^{(4)} = 0$) and the shape functions $\varphi_i(x) := \hat{\varphi}_i(F^{-1}(x))$, $i = 1, \ldots, N_e$, are polynomial. In the general case the φ_i are rational functions.

In view of the explanations in Example 4.2 at the end of Subsection 4.2 we consider the subparametric mapping as a perturbation of an affine mapping. Let $\tilde{e}$ be a rectangular element with edges being parallel to the axes of the coordinate system. The coordinates of the vertices of $\tilde{e}$ are denoted by$\tilde{X}_e^{(i)}$, $i = 1, \ldots, 4$. The subparametric element e is a perturbation of $\tilde{e}$, the coordinates of its vertices are $X_e^{(i)} = \tilde{X}_e^{(i)} + a^{(i)}$, $i = 1, \ldots, 4$. Introduce by

$$\begin{aligned} \tilde{F}(\hat{x}) &:= \tilde{X}_e^{(1)} + B\hat{x}, \quad B := \operatorname{diag}(h_1, h_2), \\ F(\hat{x}) &:= \tilde{F}(\hat{x}) + \sum_{i=1}^{4} a^{(i)} \hat{\psi}_i(\hat{x}), \end{aligned}$$

the transformation of $\hat{e}$ to $\tilde{e}$ and e, respectively, that means $\tilde{e} = \tilde{F}(\hat{e})$, $e = F(\hat{e})$.

The Jacobi matrix of the transformation F is

$$D = D(\hat{x}) := \begin{pmatrix} d_{1,1} & d_{1,2} \\ d_{2,1} & d_{2,2} \end{pmatrix} = B + \sum_{i=1}^{4} \begin{pmatrix} a_1^{(i)} \dfrac{\partial \hat{\psi}_i}{\partial \hat{x}_1} & a_1^{(i)} \dfrac{\partial \hat{\psi}_i}{\partial \hat{x}_2} \\ a_2^{(i)} \dfrac{\partial \hat{\psi}_i}{\partial \hat{x}_1} & a_2^{(i)} \dfrac{\partial \hat{\psi}_i}{\partial \hat{x}_2} \end{pmatrix}.$$

In order to keep properties like (7.8)–(7.10) we demand the existence of constants a_0 and $a = (a_1, a_2)$ with

$$|a_i^{(j)}| \le a_i h_2, \quad 0 \le a_i \lesssim 1, \quad i = 1, 2,\ j = 1, \ldots, 4, \tag{7.16}$$

$$\frac{1}{2} - \frac{h_2}{h_1} a_1 - a_2 \ge a_0 > 0. \tag{7.17}$$

Remark 7.13 Condition (7.17) is necessary to keep the mapping F invertible, in particular, to prove relation (7.18) below. To see this, consider $\tilde{e} = (0, h_1) \times (0, h_2)$, $a^{(1)} = a^{(3)} = (a_1 h_2, -a_2 h_2)^T$, and $a^{(2)} = a^{(4)} = (-a_1 h_2, a_2 h_2)^T$. One can directly calculate that $\det D\big|_{(1,0)} = 2h_1 h_2 (1/2 - a_1 h_2/h_1 - a_2)$.

By taking $a_1 = a_2 = 1/2 - \varepsilon$, $h_2 \ll h_1$, we can learn from this example that the shape of e can be quite different from a rectangle, see Figure 7.2.

Condition (7.17) restricts also the flattening of e which is obtained by taking $a^{(1)} = a^{(2)} = (0, a_2 h_2)^T$, and $a^{(3)} = a^{(4)} = (0, -a_2 h_2)^T$. Note further that there is virtually no restriction on a_1 if $h_2 \ll h_1$. The restriction on a_2 is also discussed in Remark 7.14 below.

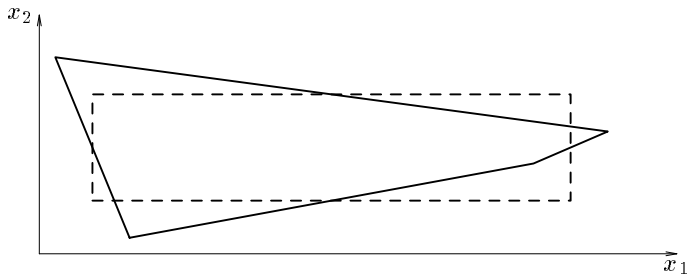

Figure 7.2: Extreme example for the element e. ($\tilde{e}$ is bounded by dashed lines, e by solid lines.)

Remark 7.14 The condition on a_2 can be weakened if the numbers $a_2^{(i)}$, $i = 1, \ldots, 4$, satisfy $\operatorname{sign} a_2^{(1)} = \operatorname{sign} a_2^{(4)}$ and $\operatorname{sign} a_2^{(2)} = \operatorname{sign} a_2^{(3)}$. This is the reason why the affine elements from Subsection 7.1 do satisfy (7.16) but with constants not necessarily satisfying (7.17). As another alternative we could consider perturbations of parallelograms $\tilde{e}$ satisfying the conditions of Subsection 7.1. The following results would remain true but the angle ϑ from the coordinate system condition would have to be involved in (7.17). We chose a rectangle to keep our explanations as clear as possible.

Lemma 7.15 *The conditions (7.16), (7.17), imply for all $\hat{x} \in \hat{e}$ the estimates*

$$|\det D(\hat{x})| \sim h_1 h_2 \tag{7.18}$$

$$|d_{i,j}(\hat{x})| \lesssim \min\{h_i;\ h_j\}, \quad i,j = 1,2, \tag{7.19}$$

$$|d_{i,j}^{(-1)}(\hat{x})| \lesssim \min\{h_i^{-1};\ h_j^{-1}\}, \quad i,j = 1,2, \tag{7.20}$$

where $d_{i,j}^{(-1)}$ are the entries of the inverse of the Jacobi matrix D.

Proof By the calculation of $\dfrac{\partial \hat{\psi}_i}{\partial \hat{x}_j}$ we obtain with (7.16) and (7.17)

$$|d_{1,1} - h_1| = \left|(1-\hat{x}_2)(a_1^{(2)} - a_1^{(1)}) + \hat{x}_2(a_1^{(3)} - a_1^{(4)})\right| \ \le\ 2a_1 h_2$$

and similarly $|d_{1,2}| \le 2a_1 h_2$, $|d_{2,1}| \le 2a_2 h_2$, and $(1-2a_2)h_2 \le d_{2,2} \le (1+2a_2)h_2$. Consequently,

$$\begin{aligned} \det D &= d_{1,1}d_{2,2} - d_{1,2}d_{2,1} \ \ge\ (h_1 - 2a_1h_2)(1-2a_2)h_2 - 4a_1a_2h_2^2 \\ &= h_1h_2(1 - 2a_1h_2/h_1 - 2a_2) \ \ge\ 2a_0h_1h_2, \\ \det D &\le (1 + 2a_1h_2/h_1)h_1(1+2a_2)h_2 + 4a_1a_2h_2^2 \ \lesssim\ h_1h_2, \end{aligned}$$

and (7.18) and (7.19) are proved. The estimate (7.20) is a direct consequence using the explicit representation of the inverse. ∎

For the second order derivatives of the transformation F the relations

$$\frac{\partial^2 x_i}{\partial \hat{x}_j^2} = 0, \quad i,j = 1,2, \tag{7.21}$$

$$\frac{\partial^2 x_i}{\partial \hat{x}_1 \partial \hat{x}_2} = a_i^{(1)} - a_i^{(2)} + a_i^{(3)} - a_i^{(4)}, \qquad \left|\frac{\partial^2 x_i}{\partial \hat{x}_1 \partial \hat{x}_2}\right| \le 4a_i h_2, \quad i = 1,2, \tag{7.22}$$

hold. This implies that the transformation of a mixed derivative $\hat{D}^\alpha$ leads also to derivatives D^β of lower order. In order to avoid mixed derivatives on the left hand side we restrict the error estimates to $m = 0, 1$.

Lemma 7.16 *Consider a rectangular element $\tilde{e}$ with sides of length h_1 and h_2, $h_1 \geq h_2$, which are parallel to the axes of the x_1, x_2-coordinate system. The coordinates of the four vertices are perturbed by vectors $a^{(i)} = (a_1^{(i)}, a_2^{(i)})^T$ satisfying (7.16), (7.17). The resulting element is denoted by e. Let be $u \in W^{\ell,p}(e) \cap \mathcal{C}(\overline{e})$ where $\ell \in \mathbb{N}$, $2 \leq \ell \leq k+1$, $p \in [1,\infty]$. Fix $q \in [1,\infty]$ such that $W^{\ell-1,p}(e) \hookrightarrow L^q(e)$. Then the anisotropic interpolation error estimate*

$$|u - \mathrm{I}_h u; W^{1,q}(e)| \lesssim (\mathrm{meas}_2 e)^{1/q-1/p} \sum_{|\alpha| \leq \ell-1} h^\alpha |D^\alpha u; W^{1,p}(e)| \tag{7.23}$$

holds.

Proof We have to transform estimate (7.14) for $m = 1$. Due to (7.21) we have for pure derivatives $\hat{D}^\alpha \hat{u}$ with $\alpha = n\beta$ ($n \in \mathbb{N}$, $|\beta| = 1$)

$$\hat{D}^{n\beta} \hat{u} = \sum_{|s|=n} c_s^{(n)} D^s u (\hat{D}^\beta x_1)^{s_1} (\hat{D}^\beta x_2)^{s_2} \tag{7.24}$$

with some constants $c_s^{(n)}$. With (7.19) we obtain

$$|\hat{D}^{n\beta} \hat{u}| \lesssim \sum_{|s|=n} h^s |D^s u|. \tag{7.25}$$

Furthermore, we get from (7.24)

$$\hat{D}^{(1,\ell-1)} \hat{u} = \sum_{|s|=\ell-1} \sum_{|t|=1} c_s^{(\ell-1)} D^{s+t} u \left(\frac{\partial x_1}{\partial \hat{x}_2}\right)^{s_1} \left(\frac{\partial x_2}{\partial \hat{x}_2}\right)^{s_2} \left(\frac{\partial x_1}{\partial \hat{x}_1}\right)^{t_1} \left(\frac{\partial x_2}{\partial \hat{x}_1}\right)^{t_2} +$$

$$+ \sum_{|s|=\ell-1} c_s^{(\ell-1)} D^s u \left(s_1 \left(\frac{\partial x_1}{\partial \hat{x}_2}\right)^{s_1-1} \frac{\partial^2 x_1}{\partial \hat{x}_1 \partial \hat{x}_2} \left(\frac{\partial x_2}{\partial \hat{x}_2}\right)^{s_2} + s_2 \left(\frac{\partial x_1}{\partial \hat{x}_2}\right)^{s_1} \left(\frac{\partial x_2}{\partial \hat{x}_2}\right)^{s_2-1} \frac{\partial^2 x_2}{\partial \hat{x}_1 \partial \hat{x}_2} \right),$$

$$|\hat{D}^{(1,\ell-1)} \hat{u}| \sim h_1 \sum_{|s|=\ell-1} \sum_{|t|=1} h^s |D^{s+t} u| + h_2 \sum_{|s|=\ell-2} \sum_{|t|=1} h^s |D^{s+t} u| \lesssim h_1 \sum_{|s|\leq \ell-1} \sum_{|t|=1} h^s |D^{s+t} u|.$$

Similarly we can prove the corresponding estimate for $\hat{D}^{(\ell-1,1)} \hat{u}$. Finally we get

$$\begin{aligned} \|D^\gamma (u - \mathrm{I}_h u); L^q(e)\| &\lesssim (\mathrm{meas}_2 e)^{1/q} \sum_{|\beta|=1} h^{-\beta} \|\hat{D}^\beta (\hat{u} - \mathrm{I}\hat{u}); L^q(\hat{e})\| \\ &\lesssim (\mathrm{meas}_2 e)^{1/q} \sum_{|\beta|=1} h^{-\beta} [\hat{D}^\beta \hat{u}; W^{\ell-1,p}(\hat{e})] \\ &\lesssim (\mathrm{meas}_2 e)^{1/q-1/p} \sum_{|\beta|=1} h^{-\beta} \left(h^\beta \sum_{|s|\leq \ell-1} h^s |D^s u; W^{1,p}(e)| \right). \end{aligned}$$

■

We conjecture that we obtain the same result (7.23) when estimate (7.6) is transformed. However, the transformation of derivatives becomes more involved, see [78] for a general formula for high derivatives of composite functions. We note also that the estimate (7.23) is insufficient: consider $m = k = 1$, $\ell = 2$, then we get no convergence unless $a_1, a_2 \to 0$ for $h_1, h_2 \to 0$. This was investigated in [5] since the following theorem was not seen at that time.

Theorem 7.17 *Consider a rectangular element $\tilde{e}$ with sides of length h_1 and h_2, $h_1 \geq h_2$, which are parallel to the axes of the x_1, x_2-coordinate system. The coordinates of the four vertices are perturbed by vectors $a^{(i)} = (a_1^{(i)}, a_2^{(i)})^T$ satisfying (7.16), (7.17). The resulting element is denoted by e. Let be $u \in W^{\ell,p}(e) \cap \mathcal{C}(\overline{e})$ where $\ell \in \mathbb{N}$, $1 \leq \ell \leq k+1$, $p \in [1,\infty]$. Fix $m \in \{0;\ 1\}$ and $q \in [1,\infty]$ such that $m < \ell$ and $W^{\ell-m,p}(e) \hookrightarrow L^q(e)$. Then the anisotropic interpolation error estimate*

$$|u - \mathrm{I}_h u; W^{m,q}(e)| \lesssim (\mathrm{meas}_2 e)^{1/q-1/p} \sum_{|\alpha|=\ell-m} h^\alpha |D^\alpha u; W^{m,p}(e)| \tag{7.26}$$

holds provided that $p > 2$ if $\ell = 1$. The result is valid also for $m = \ell = 0$, $p = \infty$, $q \in [1,\infty]$.

Proof In the case $m = 0$ we transform (7.14). Since no mixed derivatives appear at the right hand side of (7.14) we can use (7.25) and obtain the desired result.

For $m = 1$ we use Lemma 7.16. The main point is to observe that for $\ell \leq k+1$

$$\mathrm{I}_h w = w \qquad \forall w \in \mathcal{P}^d_{\ell-1}.$$

Indeed, since we investigate only a subparametric mapping F with $F_i \in \mathcal{Q}^d_1$ we have $\hat{w} \in \mathcal{Q}^d_{\ell-1} \subset \mathcal{P}_{k,\hat{e}}$, this means $\hat{w} = \mathrm{I}\hat{w}$. Applying Lemma 7.16 to $v = u - w$ for arbitrary $w \in \mathcal{P}^d_{\ell-1}$ we get $u - \mathrm{I}_h u = v - \mathrm{I}_h v$ and

$$\begin{aligned} |u - \mathrm{I}_h u; W^{1,q}(e)| &\lesssim (\mathrm{meas}_2 e)^{1/q-1/p} \sum_{|\alpha|\leq\ell-1} h^\alpha |D^\alpha v; W^{1,p}(e)| \\ &= (\mathrm{meas}_2 e)^{1/q-1/p} \sum_{|\alpha|\leq\ell-1} h^\alpha |D^\alpha (u-w); W^{1,p}(e)|. \end{aligned} \tag{7.27}$$

Via the change of variables $x_i = \check{x}_i h_i$ we map e to an quadrilateral $\check{e}$. According to (7.16), (7.17), we realize that $\check{e}$ satisfies the assumptions of Lemma 4.3 with $J = 1$, $\mathrm{diam} G_1 \sim \mathrm{diam} B_1 \sim 1$. So we obtain the existence of $\check{w} \in \mathcal{P}^d_{\ell-1}$ such that for all γ with $|\gamma| = 1$ the estimate

$$\|\check{D}^\gamma(\check{u} - \check{w}); W^{\ell-1,p}(\check{e})\| \lesssim |\check{D}^\gamma \check{u}; W^{\ell-1,p}(\check{e})|$$

holds. By transforming this estimate to e and summing up over all γ with $|\gamma| = 1$ we get

$$\exists w \in \mathcal{P}^d_{\ell-1} : \sum_{|\alpha|\leq\ell-1} h^\alpha |D^\alpha (u-w); W^{1,p}(e)| \lesssim \sum_{|\alpha|=\ell-1} h^\alpha |D^\alpha u; W^{1,p}(e)|.$$

With (7.27) we have proved the assertion. ∎

Corollary 7.18 *Of course one can set $h_2 \leq h_1 =: h$ and derive*

$$\|u - \mathrm{I}_h u; W^{m,q}(e)\| \lesssim (\mathrm{meas}_2 e)^{1/q-1/p} h^{\ell-m} |u; W^{\ell,p}(e)|,$$

which holds under the assumptions of Theorem 7.17.

We note that $|u - \mathrm{I}_h u; W^{1,2}(e)| \lesssim h\,|u; W^{2,2}(e)|$ was derived for $k = 1$ in [202] with a fully different proof, see Comment 10.16 on page 62.

We end this section by giving an example showing that the assumption $|a_1^{(i)}| \lesssim a_1 h_2$ in (7.16) cannot be weakened.

Example 7.19 Let e be the quadrilateral with the vertices $(0,0)$, $(h_1,0)$, $(h_1-\varepsilon,h_2)$, $(0,h_2)$ where $\varepsilon\in[0,h_1/2]$. One can directly calculate that $x_1=\hat{x}_1(h_1-\varepsilon\hat{x}_2)$, $x_2=h_2\hat{x}_2$, $\hat{x}_2=h_2^{-1}x_2$, $\hat{x}_1=x_1(h_1-\varepsilon h_2^{-1}x_2)^{-1}$. For the function $u=x_1^2$ we get $\hat{u}=\hat{x}_1^2(h_2-\varepsilon\hat{x}_2)^2$, $\mathrm{I}\hat{u}=\hat{x}_1(h_1^2-2h_1\varepsilon\hat{x}_2+\varepsilon^2\hat{x}_2)$,

$$\begin{aligned}\mathrm{I}_h u &= x_1(h_1-\varepsilon h_2^{-1}x_2)^{-1}(h_1^2-2h_1\varepsilon h_2^{-1}x_2+\varepsilon^2 h_2^{-1}x_2),\\ D^{(0,1)}\mathrm{I}_h u &= -x_1\varepsilon h_2^{-1}(h_1-\varepsilon h_2^{-1}x_2)^{-2}(h_1^2-\varepsilon h_1)\sim -x_1\varepsilon h_2^{-1}.\end{aligned}$$

Consequently, it is

$$\frac{\left\|D^{(0,1)}(u-I_h u);L^q(e)\right\|}{(\mathrm{meas}_2 e)^{1/q-1/p}\sum\limits_{|\alpha|=1}h^\alpha|D^\alpha u;W^{1,p}(e)|}\sim\frac{(\mathrm{meas}_2 e)^{1/q}\varepsilon h_1 h_2^{-1}}{(\mathrm{meas}_2 e)^{1/q-1/p}\cdot(\mathrm{meas}_2 e)^{1/p}h_1}=\frac{\varepsilon}{h_2}.$$

Thus $\varepsilon\lesssim h_2$ is a necessary condition. □

8 Hexahedral elements

8.1 Affine elements

In this section we extend the results of Section 7 to the three-dimensional case, namely to hexahedral elements. There is mainly one point different which, however, is already known from Section 6: the range of the parameter p in the estimates is smaller. But in order to help the reader who does not want to read the whole monograph, the definitions and theorems are formulated completely.

Consider the Lagrangian finite element $(\hat{e},\mathcal{P}_{k,\hat{e}},\Sigma_{k,\hat{e}})$ with

$$\hat{e} := \{(\hat{x}_1,\hat{x}_2,\hat{x}_3)\in\mathbb{R}^3 : 0<\hat{x}_1,\hat{x}_2,\hat{x}_3<1\}, \tag{8.1}$$

$$\mathcal{P}_{k,\hat{e}} := \mathcal{Q}_k^3, \tag{8.2}$$

$$\Sigma_{k,\hat{e}} := \{f_i:\mathcal{C}(\overline{\hat{e}})\to\mathbb{R} \text{ such that } f_i(\hat{u}):=\hat{u}(\hat{X}^{(i)})\}_{i=1}^{N_e}, \tag{8.3}$$

where $N_e=(k+1)^3$ is the number of nodes and

$$\mathcal{X}:=\{\hat{X}^{(i)}\}_{i=1}^{N_e}:=\{(\tfrac{i}{k},\tfrac{j}{k},\tfrac{n}{k})^T\in\mathbb{R}^3\}_{0\le i,j,n\le k} \tag{8.4}$$

is the set of nodes.

Let $\mathrm{I}:\mathcal{C}(\overline{\hat{e}})\to\mathcal{P}_{k,\hat{e}}$ be the Lagrangian interpolation operator on $\hat{e}$, defined by

$$(\mathrm{I}\hat{v})(\hat{X}^{(i)})=\hat{v}(\hat{X}^{(i)}),\quad i=1,\dots,N_e. \tag{8.5}$$

The counterpart of Lemma 7.1 is identical with Lemma 6.1 and reads as follows.

Lemma 8.1 *Let γ be a multi-index with $m:=|\gamma|$ and $\hat{u}\in\mathcal{C}(\overline{\hat{e}})$ be a function with $\hat{D}^\gamma\hat{u}\in W^{\ell-m,p}(\hat{e})$, where $\ell,m\in\mathbb{N}$, $p\in[1,\infty]$ shall be such that $0\le m\le\ell\le k+1$ and*

$$\begin{array}{ll} p=\infty & \text{if } m=0 \text{ and } \ell=0,\\ p>3/\ell & \text{if } m=0 \text{ and } \ell=1,2,\\ m<\ell & \text{if } \gamma_1=0 \text{ or } \gamma_2=0 \text{ or } \gamma_3=0, \text{ and } m>0,\\ p>2 & \text{if } \gamma\in\{(\ell-1,0,0);\ (0,\ell-1,0);\ (0,0,\ell-1)\}.\end{array} \tag{8.6}$$

Fix $q\in[1,\infty]$ such that $W^{\ell-m,p}(\hat{e})\hookrightarrow L^q(\hat{e})$. Then the estimate

$$\|\hat{D}^\gamma(\hat{u}-\mathrm{I}\hat{u});L^q(\hat{e})\|\lesssim|\hat{D}^\gamma\hat{u};W^{\ell-m,p}(\hat{e})| \tag{8.7}$$

holds.

The assumptions can be discussed as in Section 6 for Lemma 6.1. Note that the fourth assumption in (8.6) is necessary only in the three-dimensional case.

Consider now a parallelepiped e. The transformation from $\hat{e}$ to e can be written as

$$x = F(\hat{x}) = B\hat{x} + b, \quad B = (b_{i,j})_{i,j=1}^{3} \in \mathbb{R}^{3\times 3}, \quad b = (b_i)_{i=1}^{3} \in \mathbb{R}^3, \tag{8.8}$$

compare (3.6). For clarity, we formulate the definition of the mesh sizes and the conditions: Let E be one of the longest edges of e, and let Γ_E be the larger of the two faces of e with $E \subset \overline{\Gamma_E}$. Then we define the element sizes by $h_1 := \mathrm{meas}_1(E)$, $h_2 := \mathrm{meas}_2(\Gamma_E)/h_1$, and $h_3 := \mathrm{meas}_3(e)/(h_1h_2)$. For intermediate use we introduce another Cartesian coordinate system $(x_{1,e}, x_{2,e}, x_{3,e})$ such that $(0,0,0)$ is a vertex of $\hat{e}$, E is part of the $x_{1,e}$-axis, and Γ_E is part of the $x_{1,e}, x_{2,e}$-plane. Consequently, we have $|\det B| = \mathrm{meas}_3(e) = h_1h_2h_3$.

Maximal angle condition: There is a constant $\gamma_* < \pi$ (independent of h and $e \in \mathcal{T}_h$) such that the maximal interior angle γ_F of the six faces as well as the maximal angle γ_E between two faces of any element e are bounded by $\gamma_* : 0 < \gamma_* \le \gamma_F \le \pi - \gamma_*$, $0 < \gamma_* \le \gamma_E \le \pi - \gamma_*$.

Coordinate system condition: The transformation of the element related coordinate system $(x_{1,e}, x_{2,e}, x_{3,e})$ to the discretization independent system (x_1, x_2, x_3) can be determined as a translation and three rotations around the $x_{j,e}$-axes by angles ϑ_j $(j = 1,2,3)$, where

$$|\sin\vartheta_1| \le Ch_3/h_2, \quad |\sin\vartheta_2| \le Ch_3/h_1, \quad |\sin\vartheta_3| \le Ch_2/h_1.$$

We formulate now the three-dimensional versions of Lemma 7.2, Theorem 7.3, Corollary 7.4 and Remark 7.12 without proof.

Lemma 8.2 *Assume that a parallelepiped e satisfies the maximal angle condition and the coordinate system condition. Then the entries of the matrix B of (8.8) and of its inverse B^{-1} satisfy the following conditions:*

$$|b_{i,j}| \lesssim \min\{h_i;\, h_j\}, \qquad i,j = 1,2,3, \tag{8.9}$$

$$|b_{i,j}^{(-1)}| \lesssim \min\{h_i^{-1};\, h_j^{-1}\}, \quad i,j = 1,2,3. \tag{8.10}$$

Theorem 8.3 *Assume that e is a parallelepiped which satisfies the maximal angle condition and the coordinate system condition. Let be $u \in W^{\ell,p}(e) \cap \mathcal{C}(\overline{e})$ where $\ell \in \mathbb{N}$, $1 \le \ell \le k+1$, $p \in [1,\infty]$. Fix $m \in \{0,\dots,\ell-1\}$ and $q \in [1,\infty]$ such that $W^{\ell-m,p}(e) \hookrightarrow L^q(e)$. Then the anisotropic interpolation error estimate*

$$|u - \mathrm{I}_h u; W^{m,q}(e)| \lesssim (\mathrm{meas}_3 e)^{1/q-1/p} \sum_{|\alpha|=\ell-m} h^\alpha |D^\alpha u; W^{m,p}(e)| \tag{8.11}$$

holds provided that

$$\begin{aligned} &p > 3/\ell \quad \text{if } m = 0 \text{ and } \ell = 1,2, \\ &p > 2 \qquad \text{if } m = \ell - 1. \end{aligned} \tag{8.12}$$

The result is also valid for $m = \ell = 0$, $p = \infty$, $q \in [1,\infty]$.

Corollary 8.4 *Assume that the parallelepiped e satisfies the maximal angle condition. Let be $u \in W^{\ell,p}(e) \cap \mathcal{C}(\overline{e})$ where $\ell \in \mathbb{N}$, $1 \le \ell \le k+1$, $p \in [1,\infty]$. Fix $m \in \{0,\dots,\ell-1\}$ and $q \in [1,\infty]$ such that $W^{\ell-m,p}(e) \hookrightarrow L^q(e)$. Then the* isotropic *interpolation error estimate (sometimes called estimate of Jamet type or of Synge type)*

$$|u - \mathrm{I}_h u; W^{m,q}(e)| \lesssim (\mathrm{meas}_3 e)^{1/q-1/p} (\mathrm{diam}\, e)^{\ell-m} |u; W^{\ell,p}(e)|$$

holds provided that (8.12) holds. The result is also valid for $m = \ell = 0$, $p = \infty$, $q \in [1,\infty]$.

As in Subsection 7.2 we can state that Lemma 8.1 holds even when (8.7) is replaced by

$$\|\hat{D}^\gamma(\hat{u}-\mathrm{I}\hat{u});L^q(\hat{e})\| \lesssim [\hat{D}^\gamma\hat{u};W^{\ell-m,p}(\hat{e})]. \tag{8.13}$$

For brick elements with edges being parallel to the coordinate axes this leads to the following improved estimate.

Theorem 8.5 *Assume that e is a brick element with edges parallel to the coordinate axes. Let γ be a multi-index with $m := |\gamma|$ and $u \in \mathcal{C}(\overline{e})$ be a function with $D^\gamma u \in W^{\ell-m,p}(e)$, where $\ell, m \in \mathbb{N}$, $p \in [1,\infty]$ shall be such that $0 \le m \le \ell \le k+1$ and (8.6) hold. Fix $q \in [1,\infty]$ such that $W^{\ell-m,p}(e) \hookrightarrow L^q(e)$. Then the anisotropic interpolation error estimate*

$$\|D^\gamma(u-\mathrm{I}_h u);L^q(e)\| \lesssim (\mathrm{meas}_3 e)^{1/q-1/p} \sum_{|\alpha|=1} h^{(\ell-m)\alpha}\|D^{\gamma+(\ell-m)\alpha}u;L^p(e)\| \tag{8.14}$$

holds.

Additional smoothness, $\hat{u} \in W^{k+2,p}(\hat{e})$, is advantageous since the restriction (8.12) can be omitted. For example, it was proved in [9] that for $|\gamma|=1$ the estimate

$$\|D^\gamma(u-\mathrm{I}_h u);L^p(e)\| \lesssim h^\gamma\|D^{(k+1)\gamma}u;L^p(e)\| + \sum_{|\alpha|=k+1} h^\alpha\|D^{\alpha+\gamma}u;L^p(e)\|.$$

holds for all $p \in [1,\infty]$, provided that e is a brick element. For general parallelepipeds we can prove the following theorem in analogy to Theorem 6.5.

Theorem 8.6 *Assume that e is a parallelepiped which satisfies the maximal angle condition and the coordinate system condition. Let be $u \in W^{k+2,p}(e) \cap \mathcal{C}(\overline{e})$, $p \in [1,\infty]$. Fix $m \in \{0,\dots,k\}$ and $q \in [1,\infty]$. Then the anisotropic interpolation error estimate*

$$|u-\mathrm{I}_h u;W^{m,q}(e)| \lesssim (\mathrm{meas}_3 e)^{1/q-1/p} \sum_{k+1-m\le|\alpha|\le k+2-m} h^\alpha|D^\alpha u;W^{m,p}(e)|$$

holds provided that $W^{k+2-m,p}(e) \hookrightarrow L^q(e)$.

8.2 Subparametric elements

As in Subsection 7.3 we consider the multilinear mapping F as a perturbation of an affine mapping. Let $\tilde{e}$ be a brick element with edges parallel to the axes of the coordinate system. The coordinates of the vertices of $\tilde{e}$ are $\tilde{X}_e^{(i)}$, $i=1,\dots,8$. The subparametric element e is a perturbation of $\tilde{e}$, the coordinates of its vertices are $\tilde{X}_e^{(i)}+a^{(i)}$, $i=1,\dots,8$. Denote by

$$\begin{aligned}\tilde{F}(\hat{x}) &= \tilde{X}_e^{(1)} + B\hat{x}, \quad B = \mathrm{diag}\,(h_1,h_2,h_3),\\ F(\hat{x}) &= \tilde{F}(\hat{x}) + \sum_{i=1}^{8} a^{(i)}\hat{\psi}_i(\hat{x}),\end{aligned}$$

the transformation of $\hat{e}$ to $\tilde{e}$ and e, respectively, that means $\tilde{e}=\tilde{F}(\hat{e})$, $e=F(\hat{e})$. Recall that $\hat{\psi}_i$, $i=1,\dots,8$, are the trilinear shape functions. The conditions (7.16), (7.17), read now

$$|a_i^{(j)}| \le a_i h_2, \quad 0 \le a_i \lesssim 1, \quad i=1,2,3,\ j=1,\dots,8, \tag{8.15}$$

$$\frac{1}{2} - \frac{h_3}{h_1}a_1 - \frac{h_3}{h_2}a_2 - a_3 \geq a_0 > 0. \tag{8.16}$$

and Lemma 7.15 is valid for $i, j = 1, 2, 3$.

While first and second order derivatives of F behave as in the two dimensional case third order derivatives do not vanish here:

$$\begin{aligned} \left| \frac{\partial^2 x_i}{\partial \hat{x}_j \partial \hat{x}_k} \right| &\leq 4a_i h_3 (1 - \delta_{j,k}), \quad i, j, k = 1, 2, 3, \\ \left| \frac{\partial^3 x_i}{\partial \hat{x}_1 \partial \hat{x}_2 \partial \hat{x}_3} \right| &\leq 8a_i h_3, \quad \frac{\partial^3 x_i}{\partial \hat{x}_j^2 \partial \hat{x}_k} = 0, \quad i, j, k = 1, 2, 3, \end{aligned}$$

where $\delta_{i,j}$ is the Kronecker delta. However, this does not affect our analysis since in (8.13) only derivatives $\hat{D}^\alpha u$ appear where $\alpha_i = 0$ for at least one $i \in \{1, 2, 3\}$.

Theorem 8.7 *Consider a brick element $\tilde{e}$ with sides of length h_1, h_2, and h_3, $h_1 \geq h_2 \geq h_3$, which are parallel to the axes of the x_1, x_2, x_3-coordinate system. The coordinates of the eight vertices are perturbed by vectors $a^{(i)} = (a_1^{(i)}, a_2^{(i)}, a_3^{(i)})^T$, $i = 1, \ldots, 8$, satisfying (8.15), (8.16). The resulting element is denoted by e. Let be $u \in W^{\ell,p}(e) \cap \mathcal{C}(\overline{e})$ where $\ell \in \mathbb{N}$, $1 \leq \ell \leq k+1$, $p \in [1, \infty]$. Fix $m \in \{0;\ 1\}$ and $q \in [1, \infty]$ such that $W^{\ell-m,p}(e) \hookrightarrow L^q(e)$. Then the anisotropic interpolation error estimate*

$$|u - \mathrm{I}_h u; W^{m,q}(e)| \lesssim (\mathrm{meas}_3 e)^{1/q - 1/p} \sum_{|\alpha| = \ell - m} h^\alpha |D^\alpha u; W^{m,p}(e)|$$

holds provided that

$$\begin{aligned} &p > 3/\ell \quad \text{if } m = 0 \text{ and } \ell = 1, 2, \\ &p > 2 \quad \text{if } m = \ell - 1. \end{aligned}$$

The result is also valid for $m = \ell = 0$, $p = \infty$, $q \in [1, \infty]$.

The theorem can be proved with the same ideas as in the two-dimensional case.

Corollary 8.8 *Of course one can set $h_3 \leq h_2 \leq h_1 =: h$ and derive*

$$\|u - \mathrm{I}_h u; W^{m,q}(e)\| \lesssim (\mathrm{meas}_3 e)^{1/q - 1/p} h^{\ell - m} |u; W^{\ell,p}(e)|,$$

which holds under the assumptions of Theorem 8.7.

9 Pentahedral elements

Due to the limited interest in pentahedral elements we will discuss this element type only very briefly. Some results have been derived in [20].

By the term *pentahedral element* we denote the Lagrangian finite element $(\hat{e}, \mathcal{P}_{k,\hat{e}}, \Sigma_{k,\hat{e}})$ with

$$\hat{e} := \{(\hat{x}_1, \hat{x}_2, \hat{x}_3) \in \mathbb{R}^3 : 0 < \hat{x}_1, \hat{x}_3 < 1,\ 0 < \hat{x}_2 < 1 - \hat{x}_1\}, \tag{9.1}$$

$$\mathcal{P}_{k,\hat{e}} := \left\{ \sum_{\substack{0 \leq \alpha_1 + \alpha_2 \leq k \\ 0 \leq \alpha_3 \leq k}} a_\alpha x^\alpha,\ a_\alpha \in \mathbb{R} \right\}, \tag{9.2}$$

$$\Sigma_{k,\hat{e}} := \{f_i : \mathcal{C}(\overline{\hat{e}}) \to \mathbb{R} \text{ such that } f_i(\hat{u}) := \hat{u}(\hat{X}^{(i)})\}_{i=1}^{N_e}, \tag{9.3}$$

where $N_e = \binom{k+2}{2}(k+1)$ is the number of nodes and

$$\mathcal{X} := \{\hat{X}^{(i)}\}_{i=1}^{N_e} := \{(\tfrac{i}{k}, \tfrac{j}{k}, \tfrac{n}{k})^T \in \mathbb{R}^3\}_{\substack{0 \le i+j \le k \\ 0 \le n \le k}} \tag{9.4}$$

is the set of nodes. Let $\mathrm{I} : \mathcal{C}(\overline{\hat{e}}) \to \mathcal{P}_{k,\hat{e}}$ be the Lagrangian interpolation operator on $\hat{e}$, defined by

$$(\mathrm{I}\hat{v})(\hat{X}^{(i)}) = \hat{v}(\hat{X}^{(i)}), \quad i = 1, \ldots, N_e. \tag{9.5}$$

In Section 6 we derived estimates on tetrahedral reference elements for functions from classical and weighted Sobolev spaces. These lemmata, namely 6.1, 6.8, and 6.10, can be proven for pentahedral elements with the same arguments. Note, however, that the proof is not identical since the dimension of $D^\gamma \mathcal{P}_{k,\hat{e}}$ is here $\binom{k-\gamma_1-\gamma_2+2}{2}(k-\gamma_3+1)$. Observe also that it is sufficient to consider one reference element only.

For the transformation F from $\hat{e}$ to e we have to distinguish different cases. The reason is that, in contrast to tetrahedral and hexahedral elements, the $\hat{x}_3$-direction is distinguished from the other two.

Assume first that (i) the element is affine, (ii) the triangular face is described by mesh sizes h_1 and $h_2 \lesssim h_1$, and (iii) the distance between the triangular faces is $h_3 \lesssim h_2$. This situation corresponds completely to Subsection 6.1. A maximal angle condition and a coordinate system condition can be formulated accordingly, and Theorems 6.4 and 6.5 can be proven.

In a second case assume that (i) the element is affine, (ii) three edges are parallel to the x_3-axis and have length h_3, (iii) the quadrilateral faces satisfy a maximal angle condition, and (iv) the triangular faces are isotropic with size $h_1 \sim h_2 \lesssim h_3$. Then Lemma 6.3 is also valid and, consequently, Theorems 6.4 and 6.5 as well. If one edge is contained in the x_3-axis, then Theorems 6.9 and 6.11 hold, too.

We can also consider the subparametric case as a perturbation of the affine case. The notation can be adapted from Subsection 8.2. Lemma 7.6 can be modified by taking $w \in \mathcal{P}_{\ell-1,e} \subset \mathcal{P}_{k,\hat{e}}$ such that (7.13) becomes

$$\|D^\gamma(u-w); W^{\ell-m,p}(G)\| \lesssim \sum_{\substack{|\alpha|=\ell-m \\ \alpha_3=0 \vee \alpha_3=\ell-m}} \|D^{\alpha+\gamma} u; L^p(G)\| =: \lceil D^\gamma u; W^{\ell-m,p}(G) \rceil .$$

In analogy to Lemma 7.8 we get

$$\|\hat{D}^\gamma(\hat{u} - \mathrm{I}\hat{u}); L^q(\hat{e})\| \lesssim \lceil \hat{D}^\gamma \hat{u}; W^{\ell-m,p}(\hat{e}) \rceil$$

under the assumptions of Lemma 8.1. One can show that

$$\lceil \hat{v}; W^{n,p}(\hat{e}) \rceil \lesssim \sum_{|\alpha|=n} h^\alpha \|D^\alpha v; L^p(e)\|$$

(note that this is not true when the left hand side is replaced by $|\hat{v}; W^{n,p}(\hat{e})|$) and obtains

$$|u - \mathrm{I}_h u; W^{m,q}(e)| \lesssim (\mathrm{meas}_3 e)^{1/q-1/p} \sum_{|\alpha|=\ell-m} h^\alpha |D^\alpha u; W^{m,p}(e)| \tag{9.6}$$

for $m = 0$. For $m = 1$ one can first show an intermediate result as in Lemma 7.16 and conclude (9.6) with the same idea as in the proof of Theorem 7.17.

10 Comments on related work

This final section of Chapter II is devoted to historical remarks and alternative approaches. We discuss related interpolation results of other authors and ideas of their proof. These are sometimes really fascinating though they were not sufficient for our purposes.

Triangular elements

10.1 Other formulations of the maximal angle condition for triangles. The following conditions have been used in the literature instead of the maximal angle condition:

1. Let R_e be the radius of the circumscribed ball $\mathcal{B}_e$ of e (that means, all vertices of e belong to $\partial\mathcal{B}_e$). Then we demand $\operatorname{diam}(e) \gtrsim R_e$ [119].
2. Let V_3 be the set of the three unit vectors which are parallel to the sides of e and define $\sphericalangle(\xi,\eta) \in [0,\frac{\pi}{2}]$ to be the angle between the vectors ξ and $\pm\eta$. Then we demand [108]

$$\theta := \min_{v_1,v_2\in V_3} \max_{\xi\in\mathbb{R}^2} \min_{i=1,2} \sphericalangle(\xi,v_i) \le \theta_* < \frac{\pi}{2}. \tag{10.1}$$

The first condition is interesting due to its similarity to Zlámal's *minimal* angle condition [208] which is equivalent to $\operatorname{diam}(e) \lesssim \varrho_e$, for ϱ_e see Section 1. In [119, Theorem 2.1 and Remark 2.2], it was shown that this condition is equivalent to the maximal angle condition formulated on page 26.

Jamet showed that $\theta = \frac{1}{2}\max\{\alpha;\pi-\alpha\}$ where α is the maximal interior angle in e. Thus this condition is also equivalent to the maximal angle condition [108, page 55].

10.2 Synge's results. Synge [187, pages 209–213] derives for $k=1$ and for triangular elements e satisfying the maximal angle condition the estimate

$$|u-\mathrm{I}_h u; W^{m,\infty}(e)| \lesssim (\operatorname{diam}(e))^{2-m}|u; W^{2,\infty}(e)|, \quad m=0,1. \tag{10.2}$$

The following points of the proof are remarkable:

- He proves first the case $m=1$ and derives the case $m=0$ via

  $$\|u-\mathrm{I}_h u; L^\infty(e)\| \lesssim \operatorname{diam}(e)|u-\mathrm{I}_h u; W^{1,\infty}(e)|.$$

  Therefore he needs the maximal angle condition for $m=0$ as well. (This is not necessary.)
- His proof is constructive. He already used (what we do as well) that

  $$\int_E \frac{\partial(u-\mathrm{I}_h u)}{\partial b} = 0 \tag{10.3}$$

  where E is any edge of e and b is a unit vector parallel to E. In this way he derives for all edge directions b

  $$\left\|\frac{\partial(u-\mathrm{I}_h u)}{\partial b}; L^\infty(e)\right\| \lesssim \operatorname{diam}(e)|u-\mathrm{I}_h u; W^{2,\infty}(e)| = \operatorname{diam}(e)|u; W^{2,\infty}(e)|, \tag{10.4}$$

  where he also used that $|\mathrm{I}_h u; W^{2,\infty}(e)| = 0$. (That means that the proof is fixed to $\ell = k+1$ and simplicial elements.)
- Estimate (10.2) is concluded from (10.4) via elegant geometrical considerations which show that the constant in (10.2) depends on $(\cos\frac{1}{2}\alpha)^{-1}$ where α is the largest interior angle of e.

His method of proof is suited to produce (after slight modification) the anisotropic estimate

$$|u-\mathrm{I}_h u; W^{m,\infty}(e)| \lesssim \sum_{|\alpha|=2-m} h^\alpha |D^\alpha u; W^{m,\infty}(e)|, \quad m=0,1.$$

However, it is not clear how to generalize this approach to functions $u \in W^{2,p}(e)$, $p<\infty$. A generalization to three dimensions is possible Comment 10.11 on page 60.

10.3 The results of Babuška and Aziz. Babuška and Aziz [27] essentially proved Corollary 5.6 for $m = 1$, $p = q = 2$, $\ell = k + 1$, and arbitrary k. *Essentially* means, it was shown for $k = 1$ that

$$\inf_{u \in W^{2,2}(e)} \frac{\|u; W^{2,2}(e)\|}{\|u - \mathrm{I}_h u; W^{1,2}(e)\|} \geq (\operatorname{diam} e)^{-1} \Gamma(\alpha)$$

(note the full norms) where $\Gamma(\alpha)$ ($\pi/3 \leq \alpha < \pi$) is an increasing function and α is the maximal interior angle of e. The proof uses also that $\int_E \hat{D}^\gamma(\hat{u} - \mathrm{I}\hat{u})$ vanishes when E is an edge parallel to γ, $|\gamma| = 1$ (γ identified with a vector in $\mathbb{R}^2$). Furthermore, Babuška and Aziz showed how this proof can be adapted for Lagrangian elements of higher order and for Hermite elements. They gave also an example showing the necessity of the maximal angle condition, compare Remark 5.2 on page 22.

10.4 Jamet's results for triangles. Jamet [108] considered several classes of finite elements, see Comment 10.10 on page 60 and Comment 10.13 on page 61 for the results for tetrahedra and quadrilaterals, respectively. He proved [108, Theorem 3.1] for triangles the estimate

$$|u - \mathrm{I}_h u; W^{m,p}(e)| \lesssim (\cos\theta)^{-m} (\operatorname{diam} e)^{k+1-m} |u; W^{k+1,p}(e)|, \tag{10.5}$$

where θ is defined in (10.1). The parameters m and p must satisfy

$$\begin{array}{lcll} k+1-m & > & 2/p & \text{for } p < \infty, \\ k+1-m & \geq & 0 & \text{for } p = \infty. \end{array} \tag{10.6}$$

The proof utilizes an operator Q with $\hat{D}^\beta \mathrm{I}\hat{u} = Q\hat{D}^\beta \hat{u}$ for $|\beta| = m$. Roughly speaking, the operator Q is defined by $Q\hat{v} = \hat{D}^\beta \mathrm{I}\hat{u}$ with some $\hat{u}$ that satisfies $\hat{D}^\beta \hat{u} = \hat{v}$. To ensure that $\hat{u} \in \mathcal{C}(\overline{\hat{e}})$ (such that I is well-defined) it is demanded that $\hat{v} \in \mathcal{C}(\overline{\hat{e}})$. In this way the quite restrictive condition (10.6) is understandable. (For example, for linear elements and $m = 1$, we obtain the condition $p > 2$ which is not necessary, see Corollary 5.6 on page 28 for a larger set of admissible parameters m and p.)

Estimate (10.5) was proved via

$$\|\hat{D}^\gamma(\hat{u} - \mathrm{I}\hat{u}); L^p(\hat{e})\| \lesssim |\hat{D}^\gamma \hat{u}; W^{k+1-m,p}(\hat{e})|.$$

This means that anisotropic estimates could have been derived by a more detailed look at the mapping $F : \hat{e} \to e$.

Jamet derived that $\theta = \frac{1}{2}\max\{\alpha;\ \pi - \alpha\} \leq \max\{\frac{1}{2}\alpha;\ \frac{1}{3}\pi\}$ where α is the maximal interior angle of e. That means that $(\cos\theta)^{-m} \lesssim 1$ if and only if the maximal angle condition is satisfied. He also formulated a condition like (4.23) as essential for interpolation on anisotropic elements.

To circumvent the restrictions imposed by (10.6) the following estimate was derived for $u \in W^{\ell,p}(e)$, $\ell \geq k + 1$, namely

$$|u - \mathrm{I}_h u; W^{m,p}(e)| \lesssim (\cos\theta)^{-m} \sum_{r=k+1}^{\ell} (\operatorname{diam} e)^{r-m} |u; W^{r,p}(e)|$$

which holds when $\ell - m > 2/p$.

Jamet type estimates are discussed for elements of Hermite type in [201].

10.5 Křížek's results for triangles. Křížek [119] proved Lemma 5.1 for $m = 0, 1$, $\ell = 2$, $k = 1$, $q = p \in (1, \infty)$. The technique is similar to ours by using that $\int_E \hat{D}^\gamma(\hat{u} - \mathrm{I}\hat{u}) = 0$, $|\gamma| = 1$, where E is an edge of $\hat{e}$ parallel to γ. Then he used only an "isotropic mapping" and

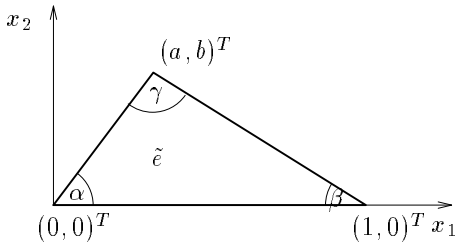

Figure 10.1: Notation and illustration of the triangle $\tilde{e}$ from Barnhill and Gregory.

derives Corollary 5.6 with the parameters above. The progress in comparison to previous work [27, 108, 187] was that he covers the case $1 < p < 2$.

It is interesting to note that he related the maximum angle condition to the radius R_e of the ball circumscribed to e Comment 10.1 on page 56. The paper contains also a numerical example where $\Omega = (0,1)$ is covered by equivalent elements e with $h_2 \sim h_1^2$. (Two triangles are equivalent if their edges have pairwise the same length.)

10.6 The results of Barnhill and Gregory. In a series of papers including [36, 37] Barnhill and Gregory investigated Sard kernel theorems and apply them to Lagrangian interpolation on triangles and rectangles. The proofs are constructive and have some similarities to the proof of interpolation results by Oganesyan and Rukhovets Comment 10.7 on page 59. This approach allowed them to give bounds for the constants in the Sobolev norm estimates which we will review next.

Let e be a triangle with the vertices $(0,0)^T$, $(h_1,0)^T$, and $(0,h_2)^T$, then for $k = 1$, $u \in W^{2,p}(e)$, and $q \le p \le \infty$ the estimate [37, estimate (2.22)]

$$\|D^{(1,0)}(u - \mathrm{I}_h u); L^q(e)\| \le (\mathrm{meas}_2 e)^{1/q-1/p} \sum_{|\alpha|=1} C^\alpha h^\alpha \|D^{\alpha+(1,0)}u; L^p(e)\|$$

holds where the expressions for $C_1(p,q)$, $C_2(p,q)$, are quite complex (including the Beta function). For $p = q = 2$ the constants are [37, equations (2.23)]

$$C_1 = \frac{1}{2}\left(\frac{1}{\sqrt{2}} + \frac{1}{\sqrt{3}}\right) \approx 0.642 \qquad \text{and} \qquad C_2 = 1 + \frac{1}{2\sqrt{2}} + \frac{1}{2\sqrt{6}} \approx 1.56.$$

In a further paper [84] Gregory obtained even $C_2 = 1.03$ and

$$\|u - \mathrm{I}_h u; L^2(\hat{e})\| \le 0.17\,\|D^{(2,0)}u; L^2(\hat{e})\| + 0.38\,\|D^{(1,1)}u; L^2(\hat{e})\| + 0.17\,\|D^{(0,2)}u; L^2(\hat{e})\|.$$

In the same paper he also considered the triangle $\tilde{e}$ with the vertices $(0,0)^T$, $(1,0)^T$, and $(a,b)^T$ with a and b being such that the angle γ at $(a,b)^T$ is maximal and the angle β at $(1,0)^T$ is minimal, see Figure 10.1 for an illustration. The dependence of the constants in the interpolation error estimate on a and b is given in detail. Some further calculation leads to

$$|u - \mathrm{I}_h u; W^{1,2}(\tilde{e})| \le (C_1 + C_2 \cot\alpha)\,|u; W^{2,2}(\tilde{e})|.$$

In this way the maximal angle condition is derived as well. (The maximal angle condition is equivalent to a lower bound for the angle α when $\beta \le \alpha \le \gamma$.)

10.7 The results of Oganesyan and Rukhovets for triangles. Oganesyan and Rukhovets [150, pages 82–84] considered the triangle e with the vertices $(0,0)^T$, $(h_1,0)^T$, and $(0,h_2)^T$, and proved for $k=1$ and $m=0,1$

$$|u-\mathrm{I}_h u; W^{m,2}(e)| \lesssim \sum_{|\alpha|=2-m} h^\alpha |D^\alpha u; W^{m,2}(e')|.$$

Note that the seminorm on the right hand side is measured with respect to the rectangle $e'=(0,h_1)\times(0,h_2)$. Remarkable is:

- The proof is constructive. Observation (10.3) was also used.
- No attempt is made to exploit the different h_1, h_2, further, and no maximal angle condition is derived.
- The appearance of e' instead of e on the right hand side is due to some crude estimations. This can be avoided, see [3, pages 57–59].

It is not obvious whether this approach can be generalized to higher dimensions.

10.8 Bänsch's results for triangles. Lemma 5.1 and Theorem 5.5 were also proved by Bänsch [35] for the case $\ell=k+1$, $1\le m\le k$, $q=p$ (therefore without investigating condition (5.1)). His paper appeared about two years after [9] but nearly at the same time as [12]. Bänsch used in his proof of Lemma 5.1 the following interesting result.

Lemma 10.1 *Let γ be a multi-index, $m:=|\gamma|>0$, and $\hat u\in\mathcal{C}(\overline{\hat e})$ be a function with $\hat D^\gamma \hat u\in W^{\ell-m,p}(\hat e)$, where $\ell\in\mathbb{N}$, $p\in[1,\infty]$ shall be such that $\ell-m>2/p$. Then the estimate*

$$\|\hat D^\gamma \mathrm{I}\hat u; L^\infty(\hat e)\| \lesssim \|\hat D^\gamma \hat u; W^{\ell-m,p}(\hat e)\|$$

holds.

Proof See the proof of Lemma 4 in [35]. The slightly stronger assumption $u\in W^{\ell,p}(\hat e)$ in this paper was used only in the sense $\hat D^\gamma \hat u\in W^{\ell-m,p}(\hat e)$. ∎

From this lemma one can immediately conclude

$$\|\hat D^\gamma(\hat v-\mathrm{I}\hat u); L^q(\hat e)\| \lesssim \|\hat D^\gamma(\hat v-\hat u); W^{\ell-m,p}(\hat e)\|$$

which was derived in the proof of Lemma 4.5 via the functionals f_i. However, Bänsch's proof of Lemma 10.1 is based on three further lemmata which essentially contain the same ideas as needed in our proof of Lemmata 4.5 and 5.1.

Tetrahedral elements

10.9 Alternative formulations of the maximal angle condition for tetrahedra. The following conditions have been used in the literature instead of the maximal angle condition on page 33.

1. All angles of all triangular faces of e are bounded away from π. Moreover, for any face F of e there is at least one edge of e such that the angle between this edge and the plane spanned by F is bounded away from 0 [35].

2. Let V_6 be the set of the 6 unit vectors which are parallel to the sides of e and let $\sphericalangle(\xi,\eta) \in [0,\pi/2]$ be the angle between the vectors ξ and $\pm\eta$. Then we demand that [108]

$$\theta := \min_{v_1,v_2,v_3 \in V_6} \max_{\xi \in \mathbb{R}^3} \min_{i=1,2,3} \sphericalangle(\xi, v_i) \le \theta_* < \frac{\pi}{2}. \tag{10.7}$$

3. Let e_i $(i = 1,\dots,3)$ denote the i-th unit vector of the coordinate system and v_j $(j = 1,\dots,6)$ are the directions of edges of the tetrahedron e. Then we assume [9]

$$\min_{i=1,\dots,3} \max_{j=1,\dots,6} |(v_j, e_i)| \ge C_0 > 0.$$

Formulation 1 is quite similar to our maximal angle condition. We see that Lemma 6.3 can be proved in the same way, relation (6.13) is even direct.

Formulations 2 and 3 are similar to each other. It is not clear whether they are equivalent to the maximal angle condition. At least they are sufficient for the proof of anisotropic interpolation error estimates. They say that one can choose a basis of $\mathbb{R}^3$ by $v_1, v_2, v_3 \in V_6$ such that the transformation from this system to the element related coordinate system $(x_{1,e}, x_{2,e}, x_{3,e})$ is uniformly bounded. On the other hand, the transformation from the reference coordinate system $(\hat{x}_{1,e}, \hat{x}_{2,e}, \hat{x}_{3,e})$ to the system (v_1, v_2, v_3) is affine with a diagonal transformation matrix when the following rule is applied: If the three edges which are parallel to v_1, v_2, v_3, form a polygonal line with the longest edge in the middle then use $\hat{e}$ from (6.2) as the reference element. In all other cases use $\hat{e}$ from (6.1). We do not want to go into more detail here, since this formulations seem to be more difficult to understand and to check than our maximal angle condition or formulation 1 from above.

10.10 Jamet's results for tetrahedra. Jamet [108] derived the results extracted in Comment 10.4 for $d = 2, 3$. That means, we have for $u \in W^{\ell,p}(e)$, $\ell \ge k+1$,

$$|u - \mathrm{I}_h u; W^{m,p}(e)| \lesssim (\cos\theta)^{-m} \sum_{r=k+1}^{\ell} (\operatorname{diam} e)^{r-m} |u; W^{r,p}(e)|$$

when $\ell - m > 3/p$. The angle θ is defined in (10.7). All the discussion in Comment 10.4 applies as well, except that the condition $\theta \le \theta_* < \pi/2$ is not reformulated in geometrical terms, for example as maximal angle condition, see also Comment 10.9.

10.11 Křížek's results for tetrahedra. Křížek [120] proved Corollary 6.6 for $k = 1$, $\ell = 2$, $m = 0, 1$, $q = p = \infty$. The technique is similar to Synge's proof of the same result in two dimensions Comment 10.2 on page 56. The maximal angle condition was introduced as on page 33. This is remarkable because Křížek [119] had chosen a different formulation in two dimensions Comment 10.1 on page 56.

10.12 Bänsch's results for tetrahedra. Lemma 6.1 and Theorem 6.4 were also proved by Bänsch [35] for the case $\ell = k+1$, $1 \le m \le k$, $q = p > 2/(k+1-m)$ (and therefore without investigating condition (6.3)), see also Comment 10.8 on page 59. The transformation from $\hat{e}$ to e was sketched in an elegant way (similarly to [9]) without mentioning that two reference elements are necessary.

Quadrilateral elements

10.13 Jamet's results for quadrilaterals. In [108, Example 2] Jamet stated that his general result, see Comment 10.4 on page 57 Comment 10.10 on page 60 for simplicial elements, is true also for parallelepipeds. For a discussion of quadratic serendipity elements see [108, Example 4].

10.14 The results of Oganesyan and Rukhovets for quadrilaterals. Oganesyan and Rukhovets [150, page 90] considered the rectangle e with sides parallel to the coordinate axes and of length h_1 and h_2. They proved for $k = 1$ and $m = 0, 1$

$$|u - \mathrm{I}_h u; W^{m,2}(e)| \lesssim \sum_{|\alpha|=2-m} h^\alpha |D^\alpha u; W^{m,2}(e)|.$$

For further remarks see Comment 10.7 on page 59. The constants can be traced back, for example it is shown, that

$$\|D^{(1,0)}(u - \mathrm{I}_h u); L^2(e)\|^2 \le 2h_1^2 \|D^{(2,0)} u; L^2(e)\|^2 + 8h_2^2 \|D^{(1,1)} u; L^2(e)\|^2.$$

10.15 The results of von Petersdorff and Rachowicz. Von Petersdorff investigated bilinear interpolation ($k = 1$) and derived for rectangular elements e and for $u \in W^{3,2}(e)$ the estimates [153, pages 71ff.]

$$\|D^{(1,0)}(u - \mathrm{I}_h u); L^2(e)\| \lesssim h_1 \|D^{(2,0)} u; L^2(e)\| + h_2^2 \|D^{(1,2)} u; L^2(e)\|, \tag{10.8}$$
$$\|D^{(0,1)}(u - \mathrm{I}_h u); L^2(e)\| \lesssim h_1^2 \|D^{(2,1)} u; L^2(e)\| + h_2 \|D^{(0,2)} u; L^2(e)\|. \tag{10.9}$$

The proof exploits the tensor product character of the bilinear interpolation. We elucidate this by the following sketch.

Proof Let be

$$\begin{aligned}(\mathrm{I}_1 \hat{u})(\hat{x}_1, \hat{x}_2) &:= (1 - \hat{x}_1)\hat{u}(0, \hat{x}_2) + \hat{x}_1 \hat{u}(1, \hat{x}_2),\\ (\mathrm{I}_2 \hat{u})(\hat{x}_1, \hat{x}_2) &:= (1 - \hat{x}_2)\hat{u}(\hat{x}_1, 0) + \hat{x}_2 \hat{u}(\hat{x}_1, 1),\end{aligned}$$

then we observe that

$$\mathrm{I}\hat{u} = \mathrm{I}_1 \mathrm{I}_2 \hat{u} = \mathrm{I}_2 \mathrm{I}_1 \hat{u},$$
$$\mathrm{I}_1 \hat{D}^{(0,1)} \hat{u} = D^{(0,1)} \mathrm{I}_1 \hat{u}, \qquad \mathrm{I}_2 \hat{D}^{(1,0)} \hat{u} = D^{(1,0)} \mathrm{I}_2 \hat{u}. \tag{10.10}$$

By using interpolation results from one space dimension we get

$$\begin{aligned}\|\hat{D}^{(1,0)}(\hat{u} - \mathrm{I}_1 \hat{u}); L^2(\hat{e})\|^2 &= \int_0^1 \|\hat{D}^{(1,0)}(\hat{u}(., \hat{x}_2) - \mathrm{I}_1 \hat{u}(., \hat{x}_2)); L^2(0,1)\|^2 \, \mathrm{d}\hat{x}_2\\ &\lesssim \int_0^1 \|\hat{D}^{(2,0)} \hat{u}(., \hat{x}_2); L^2(0,1)\|^2 \, \mathrm{d}\hat{x}_2 = \|\hat{D}^{(2,0)} \hat{u}; L^2(\hat{e})\|^2, \qquad (10.11)\\ \|(\hat{D}^{(1,0)} \mathrm{I}_1 \hat{u}) - I_2(\hat{D}^{(1,0)} \mathrm{I}_1 \hat{u}); L^2(\hat{e})\| &\lesssim \|\hat{D}^{(0,2)}(\hat{D}^{(1,0)} \mathrm{I}_1 \hat{u}); L^2(\hat{e})\|\\ &= \|\hat{D}^{(1,0)} \mathrm{I}_1 \hat{D}^{(0,2)} \hat{u}; L^2(\hat{e})\| \lesssim \|\hat{D}^{(1,2)} \hat{u}; L^2(\hat{e})\|. \qquad (10.12)\end{aligned}$$

The last equality follows from (10.10). The last estimate is a consequence of

$$\hat{D}^{(1,0)} \mathrm{I}_1 \hat{v}(\hat{x}_1, \hat{x}_2) = \hat{v}(1, \hat{x}_2) - \hat{v}(0, \hat{x}_2) = \int_0^1 \hat{D}^{(1,0)} \hat{v}(\hat{x}_1, \hat{x}_2) \mathrm{d}\hat{x}_1.$$

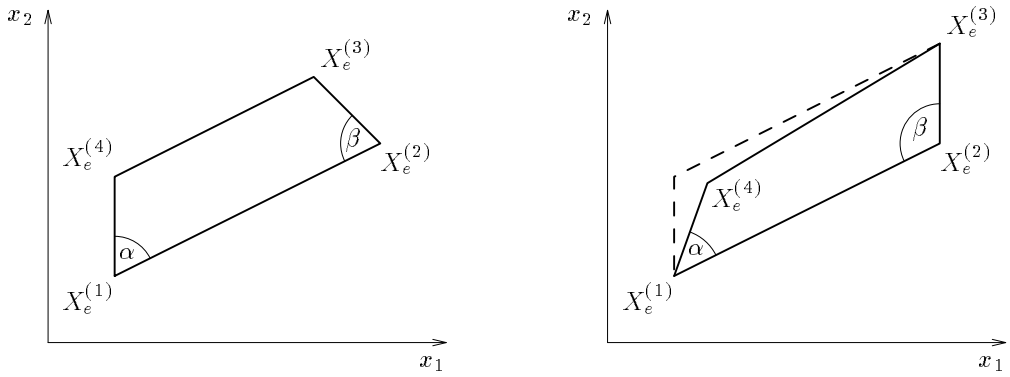

Figure 10.2: Illustration of the quadrilaterals treated by Ženíšek and Vanmaele.

From (10.11) and (10.12) we obtain (10.8) by using the triangle inequality and again (10.10). ∎

Rachowicz [155] extended this approach to arbitrary k. He obtains for $u \in W^{\ell+1,2}$, $\ell = k, k+1$

$$\begin{aligned} \|D^{(1,0)}(u - \mathrm{I}_h u); L^2(e)\| &\lesssim h_1^k \|D^{(k+1,0)}u; L^2(e)\| + h_2^\ell \|D^{(1,\ell)}u; L^2(e)\|, \\ \|D^{(0,1)}(u - \mathrm{I}_h u); L^2(e)\| &\lesssim h_1^\ell \|D^{(\ell,1)}u; L^2(e)\| + h_2^k \|D^{(0,k+1)}u; L^2(e)\|. \end{aligned}$$

An extension to parallelograms is also made but in a non-orthogonal coordinate system determined by the directions of the sides of e.

10.16 The results of Ženíšek and Vanmaele. Ženíšek and Vanmaele [202] considered anisotropic, convex, quadrilateral, isoparametric finite elements e with "bilinear" shape functions ($k = 1$). They derived *isotropic* interpolation error estimates (in the sense of Corollaries 7.4 and 7.18) and treated the constants in the estimates carefully. Therefore we present here the main results.

Lemma 10.2 [202, Theorem 7.1] *Consider first trapezoids as illustrated in Figure 10.2 (left hand side) with*

$$\operatorname{diam} e = |X_e^{(1)} - X_e^{(2)}|, \qquad |X_e^{(2)} - X_e^{(3)}| \le |X_e^{(1)} - X_e^{(4)}| \le \tfrac{1}{12}|X_e^{(1)} - X_e^{(2)}|. \tag{10.13}$$

Then we have for $u \in W^{2,2}(e)$

$$\begin{aligned} \|u - \mathrm{I}_h u; L^2(e)\| &\le \left(C_1 + C_2 \frac{|X_e^{(1)} - X_e^{(4)}|}{\operatorname{diam} e \cdot \sin\beta} \right) (\operatorname{diam} e)^2 |u; W^{2,2}(e)| \\ |u - \mathrm{I}_h u; W^{1,2}(e)| &\le \left(C_3 + \frac{C_4}{\sin\alpha} \right) \frac{\operatorname{diam} e}{\sin\beta} |u; W^{2,2}(e)| \end{aligned}$$

with $C_1 \approx 55.0$, $C_2 \approx 21.7$, $C_3 \approx 12.8$, *and* $C_4 \approx 19.5$.

For the case that the factor $1/12$ in (10.13) is substituted by $1/(2n)$, $n \ge 6$, expressions for the constants are given in dependence of n [202, Remark 7.4]

The proof of Lemma 10.2 uses the following ideas.

- The bilinear interpolation is considered as a perturbation of the linear interpolation $\mathrm{I}_h^{(L)}$ with respect to the vertices $X_e^{(1)}$, $X_e^{(2)}$, and $X_e^{(3)}$. (Therefore the enumeration plays an important role, see (10.13).) By the triangle inequality we have [202, Estimate (8)]

$$\|u - \mathrm{I}_h u; .\,\| \le \|u - \mathrm{I}_h^{(L)} u; .\,\| + \|\mathrm{I}_h^{(L)} u - \mathrm{I}_h u; .\,\| \tag{10.14}$$

  and one can show that

$$(\mathrm{I}_h^{(L)} u - \mathrm{I}_h u)(x) = (\mathrm{I}_h^{(L)} u - u)(X_e^{(4)}) \cdot \varphi_e^{(4)}(x) \tag{10.15}$$

  where $\varphi_e^{(4)}(x)$ is the shape function with respect to $X_e^{(4)}$.

- The first term in (10.14) is estimated using the results in [119] for linear (triangular) elements Comment 10.5 on page 57. The modification is that e is mapped by a linear transformation to a family of reference elements $\tilde{e}$ depending on a parameter.

- The second term in (10.14) is treated via (10.15) where both factors are estimated separately. In particular it is shown that [202, Section 6]

$$\begin{aligned}
|u(X_e^{(4)}) - \mathrm{I}_h^{(L)} u(X_e^{(4)})| &\le 21.7 \frac{|X_e^{(1)} - X_e^{(2)}|^{1/2} |X_e^{(1)} - X_e^{(4)}|^{1/2}}{\sin\beta\,(\sin\alpha)^{1/2}} |u; W^{2,2}(e)|, \\
\|\varphi_e^{(4)}; L^2(e)\| &\le |X_e^{(1)} - X_e^{(2)}|^{1/2} |X_e^{(1)} - X_e^{(4)}|^{1/2} (\sin\alpha)^{1/2}, \\
|\varphi_e^{(4)}; W^{1,2}(e)| &\le 0.90 \frac{|X_e^{(1)} - X_e^{(2)}|^{1/2}}{|X_e^{(1)} - X_e^{(4)}|^{1/2} (\sin\alpha)^{1/2}}.
\end{aligned}$$

Now let e be an arbitrary convex quadrilateral. Then there exists a parallelogram $e' \supset e$ which has three vertices in common with e, see Figure 10.2 (right hand side). Denote these three vertices by $X_e^{(1)}$, $X_e^{(2)}$, and $X_e^{(3)}$ such that $X_e^{(1)} X_e^{(2)}$ and $X_e^{(2)} X_e^{(3)}$ are sides of e with $|X_e^{(2)} - X_e^{(3)}| < |X_e^{(1)} - X_e^{(2)}|$. Denote by G the straight line through $X_e^{(1)}$ and $X_e^{(2)}$.

Lemma 10.3 [202, Theorem 8.1] *Assume that e is a quadrilateral with the notation as described above. Let the inequalities*

$$|X_e^{(2)} - X_e^{(3)}| \le \frac{1}{2n} |X_e^{(1)} - X_e^{(2)}|, \qquad |X_e^{(1)} - X_e^{(4)}| \le \frac{1}{2n} |X_e^{(1)} - X_e^{(2)}|, \qquad n \ge 6,$$

$$\frac{1}{2} \le \frac{\operatorname{dist}(X_e^{(4)}, G)}{\operatorname{dist}(X_e^{(3)}, G)} \le 1$$

be fulfilled. Then we have for $u \in W^{2,2}(e)$

$$\begin{aligned}
\|u - \mathrm{I}_h u; L^2(e)\| &\le \left(C_1 + \frac{C_2 |X_e^{(1)} - X_e^{(4)}|^{1/2} |X_e^{(2)} - X_e^{(3)}|^{1/2}}{|X_e^{(1)} - X_e^{(2)}| (\sin\alpha \sin\beta)^{1/2}} \right) |X_e^{(1)} - X_e^{(2)}|^2 \, |u; W^{2,2}(e)|, \\
|u - \mathrm{I}_h u; W^{1,2}(e)| &\le \left(C_3 + \frac{C_4 |X_e^{(1)} - X_e^{(4)}|^{1/2}}{|X_e^{(2)} - X_e^{(3)}|^{1/2} (\sin\alpha \sin\beta)^{1/2}} \right) \frac{|X_e^{(1)} - X_e^{(2)}|}{\sin\beta} \, |u; W^{2,2}(e)|,
\end{aligned}$$

where the coefficients $C_i = C_i(n)$, $i = 1, \ldots, 4$, are decreasing when n is increasing.

10.17 Anisotropic local error estimates for the *hp*-version of the finite element method. The existence of derivatives of any desired order is one of the basic assumptions for the *hp*-version. The point is merely to describe the size of the derivatives in terms of their order and to ensure integrability, if necessary, by introducing appropriate weight functions. This leads to countably normed spaces. The corresponding local interpolation error estimates are studied, for example, in [126] and, from a slightly different point of view, in [135]. The proofs exploit the tensor product character of the (reference) element as already mentioned in Comment 10.15 on page 61. However, there are also differences to the techniques developed in this monograph, starting with the point that the *hp*-version is not based on Lagrangian finite elements in the sense of (7.1)–(7.4). Therefore we will not discuss these estimates further.

Chapter III

Scott-Zhang interpolation on anisotropic elements

In this chapter, the Scott-Zhang interpolation operator and several modifications of it are discussed. All these operators are defined under weaker regularity assumptions than the Lagrange interpolation operator. Anisotropic local stability and error estimates are proved. In the final section, Section 17, we compare the operators.

11 General considerations

11.1 The aim of this chapter

The Lagrangian (nodal) interpolation operator I_h investigated in the previous chapter is the simplest approximation operator for Lagrangian finite elements. However, it is not appropriate for several investigations. Drawbacks are that it can be applied only to continuous functions and that there are restrictions in the range of the parameters m, q, ℓ, and p of the anisotropic interpolation error estimate (4.2), see for example (4.3) and (4.4). We discussed this already in Section 2 and Subsection 4.1.

In this chapter we investigate the operator Z_h which was introduced by Scott and Zhang. We also introduce and study certain modifications of Z_h. All these operators are defined not only for continuous functions but also for certain classes of discontinuous ones.

Scott and Zhang investigated stability and approximation properties of Z_h for isotropic meshes. In the next section we study whether these properties extend to anisotropic meshes. It turns out that anisotropic estimates of the error in the $L^q(e)$-norm can be proved (Theorem 12.1) but there is a counterexample for derivatives of the interpolation error (Example 12.2).

From the example we can learn, however, how to modify the operator Z_h in order to have a chance to get the desired estimates for derivatives. We define three operators S_h, L_h, and E_h with differences in the applicability concerning the types of elements and the ability to satisfy Dirichlet boundary conditions.

- The operator S_h is applicable for two-dimensional elements and for three-dimensional elements with $h_1 \sim h_2 \lesssim h_3$ ("needle elements"). Dirichlet boundary conditions are preserved on parts of the boundary which are parallel to the x_1-axis/x_1, x_2-plane.

- The operator L_h is applicable for two-dimensional elements and for three-dimensional elements with $h_1 \sim h_2 \gtrsim h_3$ ("flat elements"). Dirichlet boundary conditions are preserved

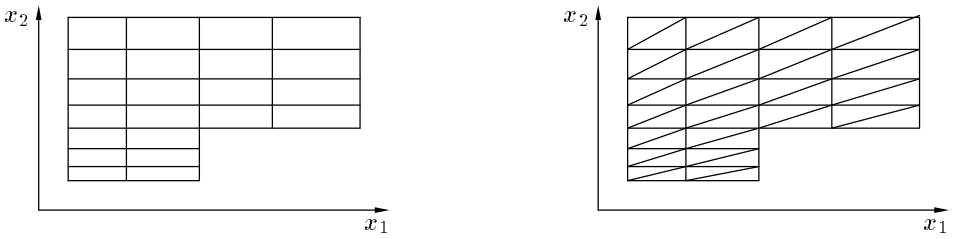

Figure 11.1: Meshes of tensor product type in two dimensions. Left: rectangular elements. Right: triangular elements.

also on parts of the boundary which are parallel to the x_1-axis/x_1, x_2-plane.

- The operator E_h is defined only for three-dimensional elements with the general assumption $h_1 \lesssim h_2 \lesssim h_3$. But we discuss also the case $h_1 \sim h_2 \lesssim h_3$, where we can relax the condition on the mesh. Dirichlet boundary conditions are preserved on parts of the boundary which are orthogonal to the x_1, x_2-plane.

These operators allow stability and approximation estimates for different ranges of m and ℓ and for anisotropic meshes, see Theorems 13.3, 14.2, and 15.1 for functions from classical Sobolev spaces, and Lemmata 13.5 and 15.3 for functions from weighted Sobolev spaces. We will summarize and compare the results in more detail in Section 17.

In this chapter, we restrict ourselves to a certain class of domains, namely *domains of tensor product type*. In two dimensions this means that the domain is the union of rectangles with sides parallel to the coordinate axes. In three dimensions we treat domains which are a union of prismatic domains with a basis face parallel to the x_1, x_2-plane. In such domains it is possible to treat *meshes of tensor product type*, see Subsection 11.2 for the definition. Examples are given in Figure 11.1. Note that also the mesh in Figure 19.3 (right hand side) on page 101 is of tensor product type. The advantage of this class of meshes is not only that the coordinate transformation is simplified but also that certain edges/faces of the elements are orthogonal/parallel to coordinate axes. We will exploit this in the proofs in Sections 13–15.

Later, in Section 20, we shall apply the operators S_h and E_h and derive finite element error estimates for the Poisson problem in certain domains with edges. The result can not be obtained by using the nodal interpolation operator I_h or the original Scott-Zhang operator Z_h. This underlines the importance of this study.

Nevertheless, some questions need further research. First, the investigation in this paper is limited to domains of tensor product type. It is not straightforward how to drop this assumption. Second, estimates with $m = \ell = 1$ are derived only for L_h. This means, such an estimate is not available for three-dimensional "needle elements" ($h_1 \sim h_2 \ll h_2$). Note that the case $\ell = 1$ is of particular interest in the investigation of a-posteriori error estimators and multi-level techniques.

Finally, we remark that Clément [64] and Oswald [151], for example, defined similar interpolation operators and investigated them for isotropic meshes. We comment on this in Section 16.

11.2 Definition of the element sizes and two auxiliary results.

We consider meshes which consist of *affine* elements of *tensor product type*. That means the transformation of a reference element $\hat{e}$ to the element e shall have (block) diagonal form,

$$\begin{pmatrix} x_1 \\ x_2 \end{pmatrix} = \begin{pmatrix} \pm h_{1,e} & 0 \\ 0 & \pm h_{2,e} \end{pmatrix} \begin{pmatrix} \hat{x}_1 \\ \hat{x}_2 \end{pmatrix} + b_e \quad \text{for } d = 2, \tag{11.1}$$

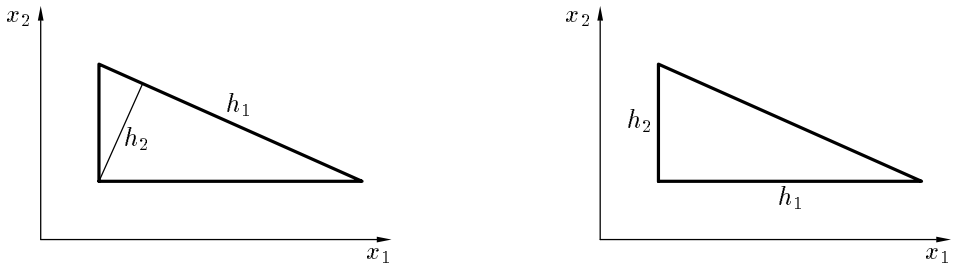

Figure 11.2: Definitions of the mesh sizes for triangles in Chapters II (left) and III (right).

$$\begin{pmatrix} x_1 \\ x_2 \\ x_3 \end{pmatrix} = \begin{pmatrix} B_e & \vdots & 0 \\ \cdots & \cdots & \cdots \\ 0 & \vdots & \pm h_{d,e} \end{pmatrix} \begin{pmatrix} \hat{x}_1 \\ \hat{x}_2 \\ \hat{x}_3 \end{pmatrix} + b_e \quad \text{for } d = 3, \tag{11.2}$$

where $b_e \in \mathbb{R}^d$ and $B_e \in \mathbb{R}^{2\times 2}$ with

$$|\det B_e| \sim h_{1,e}^2, \quad \|B_e\| \sim h_{1,e}, \quad \|B_e^{-1}\| \sim h_{1,e}^{-1}. \tag{11.3}$$

In this way the element sizes $h_{1,e}, \ldots, h_{d,e}$ are implicitly defined. This definition is not identical with the definitions in Chapter II but the orders of the resulting mesh sizes h_i $(i = 1, \ldots, d)$ are the same in both chapters, see Figure 11.2 for an illustration. Note that (11.3) yields $h_{1,e} \sim h_{2,e}$ for three-dimensional elements.

In this definition we did not assume a relation between $h_{1,e}$ and $h_{d,e}$. In Sections 13 and 15 we will consider the case $h_{1,e} \lesssim h_{d,e}$ (interesting is $h_{1,e} = o(h_{d,e})$) and in Section 14 we will examine $h_{d,e} \lesssim h_{1,e}$. Note further that under these assumptions the triangles/tetrahedra can be grouped into pairs/triples which form a rectangle/pentahedron of tensor product type. We will use this property in Section 13.

We demand further that there is no abrupt change in the element sizes, that means, the relation

$$h_{i,e} \sim h_{i,e'} \quad \text{for all } e' \text{ with } \quad \overline{e} \cap \overline{e'} \neq \emptyset \tag{11.4}$$

holds for $i = 1, \ldots, d$. In view this relation and since all considerations in this chapter are local, we will omit the second subscript henceforth.

We will see that the values of the Scott-Zhang interpolant in one single element e, $\mathrm{Z}_h u|_e$, is defined in general not only by the values of u in $\overline{e}$. Values at certain domains σ_i, $i \in I_e$, are used. So it is convenient to introduce the patch S_e of elements around e,

$$S_e := \operatorname{int} \bigcup \{\overline{e'} : e' \in \mathcal{T}_h, \overline{e'} \cap \overline{e} \neq \emptyset\}, \tag{11.5}$$

see also the illustration in Figure 11.3, since we obtain then $\sigma_i \in S_e$ for all $i \in I_e$.

We end this section with a lemma and a corollary which will be widely used in this chapter. The isotropic version of Lemma 11.1 was proved in [171] using results from [76] (see Lemma 4.3) and can easily be generalized to our case.

Lemma 11.1 *For any $u \in W^{\ell,p}(S_e)$ there exists a polynomial $w \in \mathcal{P}^d_{\ell-1}$ such that*

$$\sum_{|\alpha|\le \ell-m} h^\alpha |D^\alpha(u-w); W^{m,p}(S_e)| \lesssim \sum_{|\alpha|=\ell-m} h^\alpha |D^\alpha u; W^{m,p}(S_e)|, \tag{11.6}$$

for all $m = 0, \ldots, \ell$.

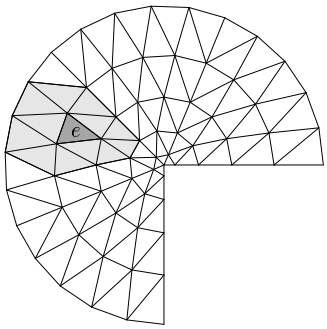

Figure 11.3: Illustration of S_e in a two-dimensional example.

Proof By the change of variables $x_i = \tilde{x}_i h_i$ we transform S_e to $\tilde{S}_e$. According to (11.4) and the tensor product character of our mesh we realize that $\tilde{S}_e$ satisfies the assumptions of Lemma 4.3 with $\operatorname{diam} G_j \sim \operatorname{diam} B_j \sim 1$. So we obtain the existence of $\tilde{w} \in \mathcal{P}^d_{\ell-1}$ such that for all γ with $|\gamma| = m$, $0 \le m \le \ell$,

$$\|\tilde{D}^\gamma(\tilde{u} - \tilde{w}); W^{\ell-m,p}(\tilde{S}_e)\| \lesssim |\tilde{D}^\gamma \tilde{u}; W^{\ell-m,p}(\tilde{S}_e)|.$$

By transforming this estimate to S_e and summing up over all γ we conclude (11.6). ∎

Corollary 11.2 *Let $m_1 + m_2 = m \le \ell$. For any $u \in W^{\ell,p}(S_e)$ there exists a polynomial $w \in \mathcal{P}^d_{m-1}$ such that*

$$\sum_{|\alpha|\le m_2} \sum_{|\beta|\le \ell-m} h^{\alpha+\beta} |D^{\alpha+\beta}(u-w); W^{m_1,p}(S_e)| \lesssim \sum_{|\alpha|=m_2} \sum_{|\beta|\le \ell-m} h^{\alpha+\beta} |D^{\alpha+\beta} u; W^{m_1,p}(S_e)|.$$

Proof We reformulate the left hand side and split it in two terms.

$$\begin{aligned}
&\sum_{|\alpha|\le m_2} \sum_{|\beta|\le \ell-m} h^{\alpha+\beta} |D^{\alpha+\beta}(u-w); W^{m_1,p}(S_e)| \sim \sum_{|\delta|\le \ell-m_1} h^\delta |D^\delta(u-w); W^{m_1,p}(S_e)| \\
&= \sum_{|\delta|\le m_2} h^\delta |D^\delta(u-w); W^{m_1,p}(S_e)| + \sum_{m_2<|\delta|\le \ell-m_1} h^\delta |D^\delta(u-w); W^{m_1,p}(S_e)|
\end{aligned}$$

In view of $m_2 = m - m_1$, the first term can be estimated via Lemma 11.1. The second term contains only derivatives of order higher than m, that means that w plays no role. Consequently, w can be chosen such that

$$\begin{aligned}
&\sum_{|\alpha|\le m_2} \sum_{|\beta|\le \ell-m} h^{\alpha+\beta} |D^{\alpha+\beta}(u-w); W^{m_1,p}(S_e)| \\
&\lesssim \sum_{|\delta|=m_2} h^\delta |D^\delta u; W^{m_1,p}(S_e)| + \sum_{m_2<|\delta|\le \ell-m_1} h^\delta |D^\delta u; W^{m_1,p}(S_e)| \\
&\lesssim \sum_{|\alpha|=m_2} h^\alpha |D^\alpha u; W^{m_1,p}(S_e)| + \sum_{|\alpha|=m_2} \sum_{1\le|\beta|\le \ell-m} h^{\alpha+\beta} |D^{\alpha+\beta} u; W^{m_1,p}(S_e)|,
\end{aligned}$$

and the corollary is proved. ∎

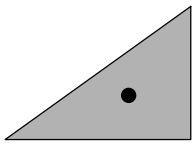

(a) $X^{(i)}$ is an interior point of an element.

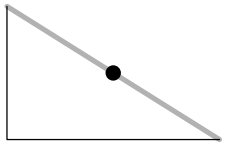

(b) $X^{(i)}$ is an interior point of an edge.

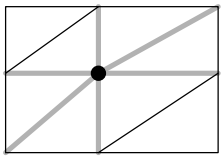

(c) $X^{(i)}$ is a vertex within the domain (here: 6 possibilities for σ_i).

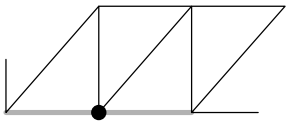

(d) $X^{(i)}$ is a vertex at the boundary (2 possibilities for σ_i).

Figure 12.1: Choice of σ_i in dependence on $X^{(i)}$ for the definition of Z_h.

12 The original Scott-Zhang operator Z_h

In this section we will recall the operator Z_h defined by Scott and Zhang [171] and examine to what extent anisotropic error estimates can be derived by simply carrying out the transformations more carefully. We will see that anisotropic interpolation error estimates are valid for $m = 0$, but modifications of the operator are necessary for estimates of derivatives of the approximation error.

Denote by $\varphi_i \in V_h$, $i \in I$, the nodal basis functions in the finite element space V_h and define

$$(Z_h u)(x) := \sum_{i \in I} a_i \varphi_i(x) \tag{12.1}$$

with real numbers a_i still to be specified. Note that the Lagrange interpolant was defined by choosing $a_i = u(X^{(i)})$ for all $i \in I$.

In order to treat non-smooth functions the idea is to consider subdomains $\sigma_i \subset \overline{\Omega}$ and to choose

$$a_i := (\Pi_{\sigma_i} u)(X^{(i)}) \tag{12.2}$$

where $\Pi_{\sigma_i} : L^2(\sigma_i) \to \mathcal{P}_{k,\sigma_i}$ is the L^2-projection operator. The subdomains σ_i are chosen by the following rules (see also Figure 12.1 for the case of triangles).

- If the node $X^{(i)}$ is an *interior point* of an element $e \subset \mathcal{T}_h$ then $\sigma_i := e$.
- Otherwise $X^{(i)}$ is a *boundary point* of one or more elements $e \subset \mathcal{T}_h$, and σ_i is chosen as some $(d-1)$-dimensional edge/face ς of one of these elements:
  - If there is an edge/face ς so that $X^{(i)}$ is an *interior point* of ς, then σ_i is uniquely determined by $\sigma_i := \varsigma$.
  - If not, then σ_i is taken as one of the edges/faces with $X^{(i)} \in \overline{\varsigma}$. However, we restrict this choice in the case $X^{(i)} \in \partial\Omega$ by demanding $\sigma_i \subset \partial\Omega$ then.

Let us derive now an equivalent definition. The $L^2(\sigma_i)$-projection $\Pi_{\sigma_i} u \in \mathcal{P}_{k,\sigma_i} = V_h|_{\sigma_i}$ is defined by

$$\|u - \Pi_{\sigma_i} u; L^2(\sigma_i)\| = \min_{v \in \mathcal{P}_{k,\sigma_i}} \|u - v; L^2(\sigma_i)\|. \tag{12.3}$$

An explicit representation of $(\Pi_{\sigma_i} u)(X^{(i)})$ can be given by introducing the (unique) function $\psi_i \in V_h|_{\sigma_i}$ with

$$\int_{\sigma_i} \psi_i \varphi_j = \delta_{ij} \quad \text{for all } j \in I. \tag{12.4}$$

Then one finds easily that

$$(\Pi_{\sigma_i} u)(X^{(i)}) = \int_{\sigma_i} u \psi_i. \tag{12.5}$$

To see this recall that a projection operator $P : X \to Y \subset X$ can be defined via $Pu = \sum_j (u, \psi_j)_X \varphi_j$ where $\{\varphi_j\}$ is a basis in Y and $\{\psi_j\}$ is the corresponding biorthogonal basis with respect to the scalar product $(.,.)_X$ in X. By inserting (12.5) into (12.1) and (12.2), we obtain the equivalent definition

$$\mathrm{Z}_h u = \sum_{i \in I} (\Pi_{\sigma_i} u)(X^{(i)}) \cdot \varphi_i = \sum_{i \in I} \left(\int_{\sigma_i} u \psi_i \right) \cdot \varphi_i. \tag{12.6}$$

Though Π_{σ_i} is defined by (12.3) for $u \in L^2(\sigma_i)$, this approach can be extended to functions $u \in L^1(\sigma_i)$ because the polynomial function ψ_i is from $L^\infty(\sigma_i)$ such that the integral in (12.5) is finite. This means that the approximation operator $\mathrm{Z}_h : W^{\ell,p}(\Omega) \to V_h$ can is defined for

$$\ell \geq 1 \quad \text{for } p = 1, \qquad \ell > \frac{1}{p} \quad \text{otherwise.} \tag{12.7}$$

The restrictions to ℓ and p in (12.7) follow from a trace theorem and guarantee that $u|_{\sigma_i} \in L^1(\sigma_i)$ also for $(d-1)$-dimensional σ_i. We consider only integer ℓ, therefore (12.7) is equivalent to

$$\ell \geq 1, \quad p \in [1, \infty].$$

Note further that the approximation operator Z_h does not only preserve homogeneous Dirichlet boundary conditions but also inhomogeneous conditions $u = g$ on $\partial\Omega$ (at least in the sense of $L^1(\partial\Omega)$) if $g \in V_h|_{\partial\Omega}$.

Recall the definition of S_e in (11.5) and note that $\sigma_i \subset S_e$ for all i with $X^{(i)} \in \overline{e}$. For isotropic *simplicial* elements e $(h_1 \sim \ldots \sim h_d)$ Scott and Zhang proved the following stability and approximation result [171]: If $1 \leq \ell \leq k+1$ and $p \in [1, \infty]$ then the estimates

$$|\mathrm{Z}_h u; W^{m,q}(e)| \lesssim (\mathrm{meas}_d e)^{1/q - 1/p} \sum_{j=0}^{\ell} h_1^{j-m} |u; W^{j,p}(S_e)| \tag{12.8}$$

$$|u - \mathrm{Z}_h u; W^{m,p}(e)| \lesssim h_1^{\ell-m} |u; W^{\ell,p}(S_e)| \tag{12.9}$$

hold for $0 \leq m \leq \ell$. Recall that k corresponds to the degree of the polynomials, see (3.4) on page 10. The anisotropic estimate corresponding to (12.9) would be

$$|u - \mathrm{Z}_h u; W^{m,p}(e)| \lesssim \sum_{|\alpha| = \ell - m} h^\alpha |D^\alpha u; W^{m,p}(S_e)|. \tag{12.10}$$

We prove now that this estimate is valid for $m = 0$. This result is restricted here to meshes of tensor product type but it is not restricted to simplicial elements.

Theorem 12.1 *On anisotropic meshes of tensor product type the Scott-Zhang approximation operator Z_h satisfies the stability and approximation error estimates*

$$\|\mathrm{Z}_h u; L^q(e)\| \lesssim (\mathrm{meas}_d e)^{1/q-1/p} \sum_{|\alpha|\le\ell} h^\alpha \|D^\alpha u; L^p(S_e)\|, \tag{12.11}$$

$$\|u - \mathrm{Z}_h u; L^q(e)\| \lesssim (\mathrm{meas}_d e)^{1/q-1/p} \sum_{|\alpha|=\ell} h^\alpha \|D^\alpha u; L^p(S_e)\|, \tag{12.12}$$

$\ell = 1, \dots, k+1$, provided that $u \in W^{\ell,p}(S_e)$. For (12.12) the numbers $p, q \in [1,\infty]$ and $\ell \in \mathbb{N}$ must be such that $W^{\ell,p}(e) \hookrightarrow L^q(e)$.

Proof We start with an estimate for the maximum norm of ψ_i, $i \in I_e$. Let $\hat\psi_i^*$ be the corresponding dual basis function on the reference element $\hat\sigma$ of the $(d-1)$-dimensional finite element σ_i. So we have $1 = \int_{\hat\sigma} \hat\varphi_i \hat\psi_i^* = \int_{\sigma_i} \varphi_i \psi_i^* (\mathrm{meas}_{\dim\sigma_i}\sigma_i)^{-1} = \int_{\sigma_i} \varphi_i \psi_i$, and, consequently, $\psi_i = \psi_i^* (\mathrm{meas}_{\dim\sigma_i}\sigma_i)^{-1}$. With $\|\hat\psi_i^*; L^\infty(\hat\sigma)\| = \|\psi_i^*; L^\infty(\sigma_i)\| \sim 1$ we obtain

$$\|\psi_i; L^\infty(\sigma_i)\| \sim (\mathrm{meas}_{\dim\sigma_i}\sigma_i)^{-1}. \tag{12.13}$$

Using the definition of $\mathrm{Z}_h u$ we find with (12.13) that

$$\begin{aligned}
\|\mathrm{Z}_h u; L^q(e)\| &\le \sum_{i\in I_e} \left\| \varphi_i \int_{\sigma_i} u\psi_i; L^q(e) \right\| \\
&\le (\mathrm{meas}_d e)^{1/q} \sum_{i\in I_e} \left| \int_{\sigma_i} u\psi_i \right| \\
&\lesssim (\mathrm{meas}_d e)^{1/q} \sum_{i\in I_e} (\mathrm{meas}_{\dim\sigma_i}\sigma_i)^{-1} \|u; L^1(\sigma_i)\|,
\end{aligned}$$

where I_e is the index set of the nodes contained in $\overline{e}$. If σ_i has the same dimension as e (that means $X^{(i)}$ is an inner node of e and $\sigma_i = e$) then we use the Hölder inequality and find

$$\begin{aligned}
\|u; L^1(\sigma_i)\| &\le (\mathrm{meas}_d e)^{1-1/p} \|u; L^p(\sigma_i)\| \\
&\lesssim \mathrm{meas}_d \sigma_i \, (\mathrm{meas}_d e)^{-1/p} \|u; L^p(S_e)\|.
\end{aligned} \tag{12.14}$$

If σ_i has lower dimension we use the trace theorem $W^{\ell,p}(S_e) \hookrightarrow W^{\ell,p}(e') \hookrightarrow L^1(\sigma_i)$ ($e' \subset S_e$ is an element with $\sigma_i \subset \overline{e'}$) in the form

$$\|u; L^1(\sigma_i)\| \lesssim \mathrm{meas}_{d-1}\sigma_i (\mathrm{meas}_d e)^{-1/p} \sum_{|\alpha|\le\ell} h^\alpha \|D^\alpha u; L^p(S_e)\| \tag{12.15}$$

which holds for $\ell \ge 1$. Combining the last three estimates we obtain the stability estimate (12.11). From this we derive for any $w \in \mathcal{P}^d_{\ell-1} \subset \mathcal{P}^d_k$

$$\begin{aligned}
\|u - \mathrm{Z}_h u; L^q(e)\| &\le \|u - w; L^q(e)\| + \|\mathrm{Z}_h (u-w); L^q(e)\| \\
&\lesssim (\mathrm{meas}_d e)^{1/q-1/p} \sum_{|\alpha|\le\ell} h^\alpha \|D^\alpha (u-w); L^p(S_e)\|
\end{aligned}$$

where we used the embedding $W^{\ell,p}(e) \hookrightarrow L^q(e)$. With Lemma 11.1 we conclude (12.12). ∎

By the following example we show that Estimate (12.10) does *not* hold for $m \ge 1$ in the general setting of σ_i as introduced above.

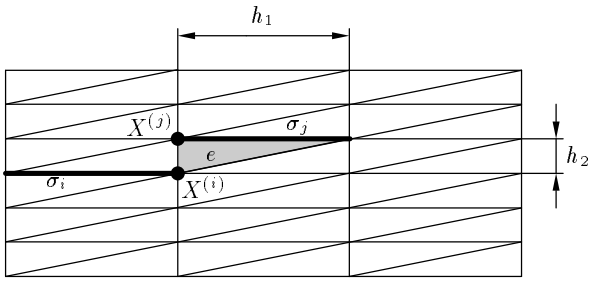

Figure 12.2: Illustration of Example 12.2.

Example 12.2 In this example we will show that (12.10) is in general not satisfied in the case $m = k = 1$ and the whole range of ℓ, namely $\ell = 1, 2$. Consider the situation as illustrated in Figure 12.2, and let $u = u(x_1)$ be any function which is independent of the variable x_2. This leads in general to $a_i \neq a_j$, where a_i and a_j are independent of h_2, that means

$$\left.\frac{\partial \mathrm{Z}_h u}{\partial x_2}\right|_e = h_2^{-1} f(u, x_1, h_1)$$

with a certain function f. In view of $\partial u/\partial x_2 = 0$ we obtain

$$\begin{aligned} |u - \mathrm{Z}_h u; W^{1,p}(e)| &\geq \left\| \frac{\partial \mathrm{Z}_h u}{\partial x_2}; L^p(e) \right\| = h_2^{-1+1/p} F(u, h_1), \\ \sum_{|\alpha|=\ell-1} h^\alpha |D^\alpha u; W^{1,p}(S_e)| &= h_1^{\ell-1} \left\| \frac{\partial^\ell u}{\partial x_1^\ell}; L^p(S_e) \right\| = h_2^{1/p} G(u, h_1). \end{aligned}$$

Consequently, for $f(u, x_1, h_1) \neq 0$ (which is the case in general) and $h_2 = h_1^s$ with sufficiently large s (depending on u) estimate (12.10) can not be satisfied. □

For this example the following points were essential:

1. *Long edges* are chosen for σ_i.
2. X_i and X_j have the same x_1-coordinate but the projections of σ_i and σ_j on the x_1-axis are *different*.

Since we have some freedom in the choice of σ_i we will investigate in the next two sections the operator in the cases where one of these points is avoided. In Section 13 we will use short edges (2D) or small faces (3D) as σ_i. Large sides with identical projection are chosen in Section 14. The resulting operators will be denoted by S_h (small sides) and L_h (large sides).

Having now an idea which choice of σ_i could work, we want to point out that the desired error estimate cannot be obtained with the original proof of [171]. We encounter problems similar to those discussed in Subsection 4.2, in particular Example 4.1. By similar arguments we find for example for the operator S_h that we must prove

$$\|D^\gamma \mathrm{S}_h u; L^q(e)\| \lesssim (\mathrm{meas} e)^{1/q-1/p} \sum_{|\alpha| \leq \ell - |\gamma|} h^\alpha |D^\alpha u; W^{|\gamma|,p}(S_e)|$$

if we want to derive the error estimate by using the stability estimate as in the proof of Theorem 12.1, We will develop such refined proofs for general k, ℓ, m, in the next sections. However, we need in all cases that all σ_i, $i \in I$, are parallel. Therefore we are restricted to meshes of tensor product type. The proof for more general meshes is still open.

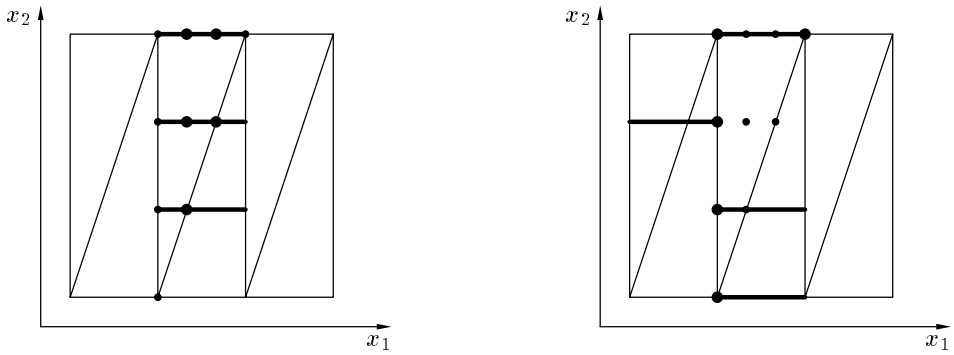

(a) Points where σ_i is uniquely determined.

(b) Points where σ_i can be chosen (here one choice).

Figure 13.1: Choice of σ_i in dependence of $X^{(i)}$ in the case of operator S_h, $k = 3$.

13 The operator S_h: choosing small sides

13.1 Stability and approximation in classical Sobolev spaces

In this section we will investigate the operator S_h which was motivated at the end of the previous section. Since the definition of the σ_i is different from that in Section 12 we will clarify this here: σ_i is (not necessarily uniquely) determined according to the following three properties, compare Figure 13.1.

(P1) σ_i is parallel to the x_1-axis/x_1, x_2-plane.

(P2) $X^{(i)} \in \overline{\sigma_i}$.

(P3) There exists an edge/face ς of some element e such that the projection of ς on the x_1-axis/x_1, x_2-plane is identical with the projection of σ_i.

In connection with (P3) we have to note that σ_i is not necessary an edge/face of one element, see also Figure 13.1. Nevertheless, σ_i together with $\mathcal{P}_k^{d-1}$ or $\mathcal{Q}_k^{d-1}$ is a Lagrangian finite element of dimension $d-1$, which follows from the tensor-product character of the elements e. For simplicity, we will use the terminology "σ_i is an edge/face". We remark in particular that in the case of simplicial elements and $k \geq 2$ there is no d-dimensional finite element $e' \subset S_e$ such that $\sigma_i \subset \overline{e'}$. This implies that $\mathcal{P}_{k,\sigma_i} \neq V_h|_{\sigma_i}$ and in general $\Pi_{\sigma_i} v_h \neq v_h|_{\sigma_i}$ for $v_h \in V_h$. That means that S_h does not reproduce piecewise polynomials, but only global polynomials. However, we need in the proofs only $\Pi_{\sigma_i} w = w$ for $w \in \mathcal{P}_{k,\sigma_i}$ which is of course satisfied.

Since σ_i is said to be a *small* edge/face this implies

$$h_j \leq h_d \quad \text{in } S_e \quad (j = 1, \ldots, d). \tag{13.1}$$

Note that in three dimensions and according to (11.2), (11.3), only elements with $h_1 \sim h_2 \lesssim h_3$ can be treated. But this is sufficient to handle edge singularities, see Section 20.

We will see that for the operator S_h anisotropic interpolation error estimates can be derived when $m < \ell \leq k+1$. The main difficulty is to prove the stability estimate. The approximation property follows then easily using Lemma 11.1 from page 67. To elucidate the different techniques for derivatives in x_1- and x_d-direction we first formulate and prove two lemmata. Then we establish the main theorem of this section. Finally, we give an example which shows that the estimate is not valid for $m = \ell$, $1 \leq m \leq k+1$.

Lemma 13.1 *Consider an element e of a mesh of tensor product type and assume that (13.1) is valid. Then the derivative of $\mathrm{S}_h u$ in x_d-direction satisfies the relation*

$$\left\| \frac{\partial}{\partial x_d} \mathrm{S}_h u; L^q(e) \right\| \lesssim (\mathrm{meas}_d e)^{1/q-1/p} \, |u; W^{1,p}(S_e)|$$

for $u \in W^{1,p}(S_e)$ and all $p, q \in [1, \infty]$.

Proof Using the definition of the operator S_h (in analogy to (12.6) on page 70), the Hölder inequality, estimate (12.13), and the trace theorem (12.15) for $\ell = 1$, we obtain for all $w \in \mathcal{P}_0^d$

$$\begin{aligned}
\left\| \frac{\partial}{\partial x_d} \mathrm{S}_h u; L^q(e) \right\| &= \left\| \frac{\partial}{\partial x_d} \mathrm{S}_h (u - w); L^q(e) \right\| \leq \sum_{i \in I_e} \left\| \frac{\partial \varphi_i}{\partial x_d}; L^q(e) \right\| \left| \int_{\sigma_i} (u - w) \psi_i \right| \\
&\lesssim h_d^{-1} (\mathrm{meas}_d e)^{1/q} \sum_{i \in I_e} \| u - w; L^1(\sigma_i) \| \, \| \psi_i; L^\infty(\sigma_i) \| \\
&\lesssim h_d^{-1} (\mathrm{meas}_d e)^{1/q} \sum_{i \in I_e} (\mathrm{meas}_{d-1} \sigma_i) (\mathrm{meas}_d e)^{-1/p} \sum_{|\alpha| \leq 1} h^\alpha \| D^\alpha (u - w); L^p(S_e) \| (\mathrm{meas}_{d-1} \sigma_i)^{-1} \\
&\lesssim h_d^{-1} (\mathrm{meas}_d e)^{1/q-1/p} \sum_{|\alpha| \leq 1} h^\alpha \| D^\alpha (u - w); L^p(S_e) \|.
\end{aligned}$$

Using Lemma 11.1 with $m = 0$, $\ell = 1$, and relying on (13.1) we obtain the assertion. ∎

Lemma 13.2 *Consider an element e of a mesh of tensor product type and assume that (13.1) is valid. Then the derivative of $\mathrm{S}_h u$ in x_1-direction satisfies the relation*

$$\left\| \frac{\partial}{\partial x_1} \mathrm{S}_h u; L^q(e) \right\| \lesssim (\mathrm{meas}_d e)^{1/q-1/p} \sum_{|\alpha| \leq 1} h^\alpha |D^\alpha u; W^{1,p}(S_e)|$$

for $u \in W^{2,p}(S_e)$ and all $p, q \in [1, \infty]$.

Proof Let $w = w(x_d) \in \mathcal{P}_k^1$. Then we get in analogy to the proof of Lemma 13.1

$$\left\| \frac{\partial}{\partial x_1} \mathrm{S}_h u; L^q(e) \right\| \lesssim h_1^{-1} (\mathrm{meas}_d e)^{1/q} \sum_{i \in I_e} (\mathrm{meas}_{d-1} \sigma_i)^{-1} \| u - w; L^1(\sigma_i) \|.$$

Denote by σ the smallest of the domains σ_i, $i \in I_e$. Introduce now $k+1$ (simply connected, plane) $(d-1)$-dimensional domains $\zeta_j \subset S_e$ such that for all σ_i $(i \in I_e)$ there exists a $\zeta_j \supset \sigma_i$. Note that, due to (11.4), ζ_j $(j = 0, \ldots, k)$ is isotropic with a diameter of order h_1, and therefore $\mathrm{meas}_{d-1} \sigma_i \sim \mathrm{meas} \zeta_j \sim \mathrm{meas}_{d-1} \sigma$ for all i and j. Consequently, we obtain

$$\begin{aligned}
\left\| \frac{\partial}{\partial x_1} \mathrm{S}_h u; L^q(e) \right\| &\lesssim h_1^{-1} (\mathrm{meas}_d e)^{1/q} (\mathrm{meas}_{d-1} \sigma)^{-1} \sum_{j=0}^{k} \| u - w; L^1(\zeta_j) \| \\
&\leq h_1^{-1} (\mathrm{meas}_d e)^{1/q} (\mathrm{meas}_{d-1} \sigma)^{-1} \sum_{j=0}^{k} \sum_{\substack{|\alpha| \leq 1 \\ \alpha_d = 0}} h^\alpha \| D^\alpha (u - w); L^1(\zeta_j) \|.
\end{aligned}$$

Observe now that $w = w_j = \text{const.}$ on ζ_j. On the other hand, since the ζ_j have different x_d-coordinate, we can define w from given w_j $(j = 0, \ldots, k)$. So we can use Lemma 11.1 for dimension $d-1$ to choose $w_j \in \mathcal{P}_0^{d-1}$ such that

$$\sum_{\substack{|\alpha| \leq 1 \\ \alpha_d = 0}} h^\alpha \| D^\alpha (u - w_j); L^1(\zeta_j) \| \lesssim \sum_{\substack{|\alpha| = 1 \\ \alpha_d = 0}} h^\alpha \| D^\alpha u; L^1(\zeta_j) \| \sim h_1 \sum_{\substack{|\alpha| = 1 \\ \alpha_d = 0}} \| D^\alpha u; L^1(\zeta_j) \|$$

and to conclude with the trace theorem (12.15) (applied with $\ell = 1$ for each ζ_j)

$$\left\| \frac{\partial}{\partial x_1} S_h u; L^q(e) \right\| \lesssim (\mathrm{meas}_d e)^{1/q} (\mathrm{meas}_{d-1}\sigma)^{-1} \sum_{j=0}^{k} \sum_{\substack{|\alpha|=1 \\ \alpha_d=0}} \|D^\alpha u; L^1(\zeta_j)\| \tag{13.2}$$

$$\lesssim (\mathrm{meas}_d e)^{1/q-1/p} \sum_{\substack{|\alpha|=1 \\ \alpha_d=0}} \sum_{|\beta|\le 1} h^\beta \|D^{\alpha+\beta} u; L^p(S_e)\|. \tag{13.3}$$

Thus the proposition is proved. ∎

By analogy we can treat the derivative with respect to x_2 in the three-dimensional case.

Theorem 13.3 *Assume that (13.1) is valid. Then the modified Scott-Zhang operator S_h satisfies on anisotropic meshes of tensor-product type the following estimates:*

$$|S_h u; W^{m,q}(e)| \lesssim (\mathrm{meas}_d e)^{1/q-1/p} \sum_{|\alpha|\le \ell-m} h^\alpha |D^\alpha u; W^{m,p}(S_e)|, \tag{13.4}$$

$$|u - S_h u; W^{m,q}(e)| \lesssim (\mathrm{meas}_d e)^{1/q-1/p} \sum_{|\alpha|=\ell-m} h^\alpha |D^\alpha u; W^{m,p}(S_e)|, \tag{13.5}$$

$0 \le m \le \ell - 1 \le k$, provided that $u \in W^{\ell,p}(S_e)$. For (13.5) the numbers $p, q \in [1,\infty]$ must be such that $W^{\ell,p}(e) \hookrightarrow W^{m,q}(e)$. For $m \ge 2$ we exclude triangular and tetrahedral elements.

Proof Consider first the stability estimate (13.4). For $m = 0$, (13.4) can be proved as (12.11). For $m = 1$, (13.4) is proved in Lemmata 13.1 and 13.2. Let $m \ge 2$. Consider a multi-index γ with $|\gamma| = m$ and define $m_2 := \gamma_d$, $m_1 = m - m_2$. For arbitrary $\omega_1 = \omega_{1,1}(x_1, \ldots, x_{d-1})\omega_{1,2}(x_d)$, $\omega_{1,1} \in \mathcal{P}^{d-1}_{m_1-1}$, $\omega_{1,2} \in \mathcal{P}^1_k$, (that is why we exclude simplicial elements) and $\omega_2 \in \mathcal{P}^d_{m-1}$ we obtain in analogy to the proof of Lemma 13.2

$$\begin{aligned} \|D^\gamma S_h u; L^q(e)\| &= \|D^\gamma S_h((u-\omega_2)-\omega_1); L^q(e)\| \\ &\lesssim h^{-\gamma} (\mathrm{meas}_d e)^{1/q} (\mathrm{meas}_{d-1}\sigma)^{-1} \sum_{i\in I_e} \|u - \omega_2 - \omega_1; L^1(\sigma_i)\| \\ &\lesssim h^{-\gamma} (\mathrm{meas}_d e)^{1/q} (\mathrm{meas}_{d-1}\sigma)^{-1} \sum_{j=0}^{k} \sum_{\substack{|\alpha|\le m_1 \\ \alpha_d=0}} h^\alpha \|D^\alpha(u-\omega_2-\omega_1); L^1(\zeta_j)\|. \end{aligned}$$

Then we determine $w_j \in \mathcal{P}^{d-1}_{m_1-1}$ $(j = 0, \ldots, k)$ such that

$$\sum_{\substack{|\alpha|\le m_1 \\ \alpha_d=0}} h^\alpha \|D^\alpha(u-\omega_2-w_j); L^1(\zeta_j)\| \lesssim \sum_{\substack{|\alpha|= m_1 \\ \alpha_d=0}} h^\alpha \|D^\alpha(u-\omega_2); L^1(\zeta_j)\|.$$

Note that the w_j depend on $(u - \omega_2)$ and ω_2 is still to be chosen. The polynomial ω_1 is now determined by the w_j $(j = 0, \ldots, k)$ such that the estimate can be continued by

$$\|D^\gamma S_h u; L^q(e)\| \lesssim h_d^{-m_2} (\mathrm{meas}_d e)^{1/q} (\mathrm{meas}_{d-1}\sigma)^{-1} \sum_{j=0}^{k} \sum_{\substack{|\alpha|= m_1 \\ \alpha_d=0}} \|D^\alpha(u-\omega_2); L^1(\zeta_j)\|. \tag{13.6}$$

Thus the factor $h_1^{-m_1}$ is eliminated. We proceed now as in the proof of Lemma 13.1. Using the trace theorem (12.15) for all j, α and with $\ell - m_1 \geq \ell - m \geq 1$ instead of ℓ we conclude

$$\begin{aligned}\|D^\gamma \mathrm{S}_h u; L^q(e)\| &\lesssim h_d^{-m_2} (\mathrm{meas}_d e)^{1/q-1/p} \sum_{\substack{|\alpha|=m_1 \\ \alpha_d=0}} \sum_{|\beta|\leq \ell-m_1} h^\beta \|D^{\alpha+\beta}(u-\omega_2); L^p(S_e)\| \\ &\lesssim h_d^{-m_2} (\mathrm{meas}_d e)^{1/q-1/p} \sum_{|\delta|\leq \ell-m} \sum_{|\beta|\leq m_2} h^{\beta+\delta} |D^{\beta+\delta}(u-\omega_2); W^{m_1,p}(S_e)|.\end{aligned}$$

Using Corollary 11.2 (page 68) we obtain

$$\begin{aligned}\|D^\gamma \mathrm{S}_h u; L^q(e)\| &\lesssim h_d^{-m_2} (\mathrm{meas}_d e)^{1/q-1/p} \sum_{|\delta|\leq \ell-m} \sum_{|\beta|=m_2} h^{\beta+\delta} |D^{\beta+\delta} u; W^{m_1,p}(S_e)| \\ &\lesssim (\mathrm{meas}_d e)^{1/q-1/p} \sum_{|\delta|\leq \ell-m} h^\delta |D^\delta u; W^{m,p}(S_e)|.\end{aligned}$$

Here we used $h^\beta \leq h_d^{m_2}$ for $|\beta| = m_2$ which follows from (13.1). Thus (13.4) is proved.

For proving estimate (13.5) we need (13.4) and the assumptions on p and q. Since these parameters were chosen such that $W^{\ell,p}(e) \hookrightarrow W^{m,q}(e)$, we have also $W^{\ell-m,p}(e) \hookrightarrow L^q(e)$, this means

$$\|v; L^q(e)\| \lesssim (\mathrm{meas}_d e)^{1/q-1/p} \sum_{|\alpha|\leq \ell-m} h^\alpha \|D^\alpha v; L^p(e)\|$$

for all $v \in W^{\ell-m,p}(e)$. Applying this estimate for all derivatives D^α with $|\alpha| = m$ and summing up the resulting inequalities, we obtain for $v \in W^{\ell,p}(e)$

$$|v; W^{m,q}(e)| \lesssim (\mathrm{meas}_d e)^{1/q-1/p} \sum_{|\alpha|\leq \ell-m} h^\alpha |D^\alpha v; W^{m,p}(e)|.$$

Together with (13.4) we conclude that for all $w \in \mathcal{P}^d_{\ell-1}$ the following estimate holds,

$$\begin{aligned}|u - \mathrm{S}_h u; W^{m,q}(e)| &\leq |u-w; W^{m,q}(e)| + |\mathrm{S}_h(u-w); W^{m,q}(e)| \\ &\lesssim (\mathrm{meas}_d e)^{1/q-1/p} \sum_{|\alpha|\leq \ell-m} h^\alpha |D^\alpha(u-w); W^{m,p}(S_e)|.\end{aligned}$$

With Lemma 11.1 the proposition is proved. ∎

Finally, we want to give an example which shows that

$$|\mathrm{S}_h u; W^{1,2}(e)| \lesssim \|u; W^{1,2}(S_e)\| \tag{13.7}$$

does not hold for any $u \in W^{1,2}(S_e)$.

Example 13.4 Consider $k = 1$ and a triangle with the vertices $X^{(1)} = (0,0)^T$, $X^{(2)} = (h,0)^T$, and $X^{(3)} = (0,1)^T$, and let $\sigma_1 = (-h,0) \times \{0\}$, $\sigma_2 = (0,h) \times \{0\}$, compare Figure 13.2. For $u = r^\varepsilon \sin\frac{\phi}{2}$ (r, ϕ are here polar coordinates) we obtain

$$\begin{aligned}u|_{\sigma_1} = |x_1|^\varepsilon \quad &\Rightarrow \quad (\Pi_{\sigma_1} u)(X^{(1)}) = \int_0^h x^\varepsilon \left(-\frac{6x}{h^2} + \frac{4}{h}\right) \sim h^\varepsilon, \\ u|_{\sigma_2} = 0 \quad &\Rightarrow \quad (\Pi_{\sigma_2} u)(X^{(2)}) = 0.\end{aligned}$$

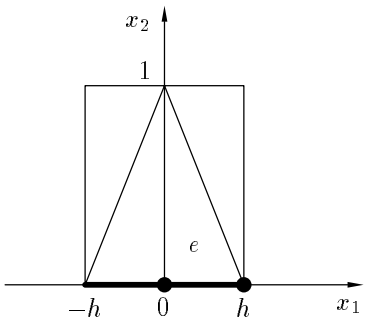

Figure 13.2: Illustration of Example 13.4.

Consequently,

$$\left.\frac{\partial S_h u}{\partial x_1}\right|_e \sim h^{\varepsilon-1}, \qquad |S_h u; W^{1,2}(e)| \gtrsim h^{\varepsilon-1}(\mathrm{meas}_d e)^{1/2} = h^{\varepsilon-1/2} \to \infty$$

for $h \to 0$, $\varepsilon < \frac{1}{2}$. But

$$|u; W^{1,2}(S_e)|^2 \lesssim \int_0^1 \int_0^\pi [(\varepsilon r^{\varepsilon-1} \sin\tfrac{\phi}{2})^2 + (\tfrac{1}{2} r^{\varepsilon-1} \cos\tfrac{\phi}{2})^2]\, r \mathrm{d}\phi \mathrm{d}r \sim \int_0^1 r^{2(\varepsilon-1)+1}\, \mathrm{d}r < \infty$$

for $\varepsilon > 0$. Thus (13.7) does not hold. □

13.2 Stability in weighted Sobolev spaces

We have seen in Example 13.4 that $S_h u$ does not satisfy an estimate with $m = \ell = 1$. However, S_h can be applied in some situations where $u \notin W^{2,p}(S_e)$ for some p we are interested in. For this we consider weighted Sobolev spaces $V_\beta^{\ell,p}(e)$, $\ell \in \mathbb{N}$, $p \in [1,\infty]$, $\beta \in \mathbb{R}$, which were defined by (3.9), (3.11), on page 12. For our application in Section 20 we need the stability of the modified Scott-Zhang operator in these weighted spaces.

Lemma 13.5 *Consider an element e of a mesh of tensor product type and assume that (13.1) is valid. Let m be an integer and β, p, q be real numbers with $0 \le m \le k$, $\beta < 2 - \frac{2}{p}$, $\beta \le 1$, $p, q \in [1,\infty]$, and assume that S_e has zero distance to the x_3-axis. Then for $u \in W^{m,p}(S_e) \cap V_\beta^{m+1,p}(S_e)$ the stability estimate*

$$|S_h u; W^{m,q}(e)| \lesssim (\mathrm{meas}_d e)^{1/q-1/p} h_1^{-\beta} \sum_{|\alpha|=m-1} \sum_{|t|=1} h^t \|D^{\alpha+t} u; V_\beta^{1,p}(S_e)\| \tag{13.8}$$

holds. For $m \ge 2$ we exclude tetrahedral elements.

Proof We start with estimate (13.6) which was obtained in the proof of Theorem 13.3. Let γ be a multi-index with $|\gamma| = m$ and $\omega_2 \in \mathcal{P}_{m-1}^d$. Then there holds

$$\|D^\gamma S_h u; L^q(e)\| \lesssim h_3^{-\gamma_3} (\mathrm{meas}_d e)^{1/q} (\mathrm{meas}_{d-1}\sigma)^{-1} \sum_{j=0}^{k} \sum_{\substack{|\alpha|=m-\gamma_3 \\ \alpha_3=0}} \|D^\alpha (u-\omega_2); L^1(\zeta_j)\|. \tag{13.9}$$

Let $\gamma_3 > 0$, then we can continue, similar to the proof of Theorem 13.3, with the trace theorem because we assumed $u \in W^{m,p}(S_e)$.

$$\|D^\gamma \mathrm{S}_h u; L^q(e)\| \lesssim h_3^{-\gamma_3} (\mathrm{meas}_d e)^{1/q-1/p} \sum_{\substack{|\alpha|=m-\gamma_3 \\ \alpha_3=0}} \sum_{|\delta|\le\gamma_3} h^\delta \|D^{\alpha+\delta}(u-\omega_2); L^p(S_e)\|.$$

Using Corollary 11.2 we obtain

$$\begin{aligned} \|D^\gamma \mathrm{S}_h u; L^q(e)\| &\lesssim h_3^{-\gamma_3} (\mathrm{meas}_d e)^{1/q-1/p} \sum_{\substack{|\alpha|=m-\gamma_3 \\ \alpha_3=0}} \sum_{|\delta|=\gamma_3} h^\delta \|D^{\alpha+\delta} u; L^p(S_e)\| \\ &\lesssim (\mathrm{meas}_d e)^{1/q-1/p} \sum_{|\alpha|=m} \|D^\alpha u; L^p(S_e)\| \end{aligned} \tag{13.10}$$

We estimate the right hand side via the trivial embeddings $V_\beta^{1,p}(S_e) \hookrightarrow V_{\beta-1}^{0,p}(S_e) \hookrightarrow L^p(S_e)$, $\beta \le 1$, which leads with (13.1) to

$$\begin{aligned} \sum_{|\alpha|=m} \|D^\alpha u; L^p(S_e)\| &\sim \sum_{|\alpha|=m-1} \sum_{|t|=1} \|D^{\alpha+t} u; L^p(S_e)\| \\ &\lesssim h_1^{-\beta+1} \sum_{|\alpha|=m-1} \sum_{|t|=1} \|r^{\beta-1} D^{\alpha+t} u; L^p(S_e)\| \\ &\lesssim h_1^{-\beta} \sum_{|\alpha|=m-1} \sum_{|t|=1} h^t \|D^{\alpha+t} u; V_\beta^{1,p}(S_e)\|, \end{aligned} \tag{13.11}$$

which is the desired result.

For $\gamma_3 = 0$ we use (13.9) with $\omega_2 = 0$ and estimate the $L^1(\zeta_j)$-norms against weighted norms via the Hölder inequality:

$$\|v; L^1(\zeta_j)\| \le \|r^{-\beta}; L^{p'}(\zeta_j)\| \cdot \|r^\beta v; L^p(\zeta_j)\| \tag{13.12}$$

with p' from $1/p + 1/p' = 1$. The $L^{p'}(\zeta_j)$-norm of $r^{-\beta}$ is finite if and only if $p'\beta < 2$ which is equivalent to $\beta < 2 - 2/p$. Using $\mathrm{meas}_{d-1}\sigma \sim \mathrm{meas}\zeta_j \sim h_1^2$ for all j, and $r \lesssim h_1$ we get

$$\|r^{-\beta}; L^{p'}(\zeta_j)\| \lesssim h_1^{(-\beta p'+2)/p'} \sim (\mathrm{meas}_{d-1}\sigma)^{1-1/p} h_1^{-\beta}. \tag{13.13}$$

The application of $W^{1,p}(S_e) \hookrightarrow L^p(\zeta_j)$ to $r^\beta v$ implies the trace theorem $V_\beta^{1,p}(S_e) \hookrightarrow V_\beta^{0,p}(\zeta_j)$ which leads to

$$\|r^\beta v; L^p(\zeta_j)\| \lesssim (\mathrm{meas}_{d-1}\sigma)^{1/p} (\mathrm{meas}_d e)^{-1/p} \sum_{|s|\le 1} h_1^{1-|s|} h^s \|r^{\beta-1+|s|} D^s v; L^p(S_e)\|.$$

Combining these estimates we obtain

$$\|v; L^1(\zeta_j)\| \le \mathrm{meas}_{d-1}\sigma\, (\mathrm{meas}_d e)^{-1/p} h_1^{-\beta} \sum_{|s|\le 1} h_1^{1-|s|} h^s \|r^{\beta-1+|s|} D^s v; L^p(S_e)\|$$

and thus with (13.9)

$$\begin{aligned} \|D^\gamma \mathrm{S}_h u; L^q(e)\| &\lesssim (\mathrm{meas}_d e)^{1/q} (\mathrm{meas}_{d-1}\sigma)^{-1} \sum_{j=0}^{k} \sum_{|\alpha|=m} \|D^\alpha u; L^1(\zeta_j)\| \\ &\lesssim (\mathrm{meas}_d e)^{1/q-1/p} h_1^{-\beta} \sum_{|\alpha|=m} \sum_{|s|\le 1} h_1^{1-|s|} h^s \|r^{\beta-1+|s|} D^{\alpha+s} u; L^p(S_e)\|. \end{aligned} \tag{13.14}$$

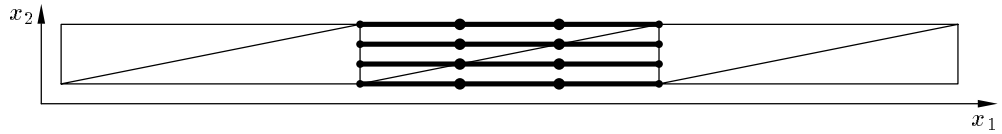

(a) Points where σ_i is uniquely determined.

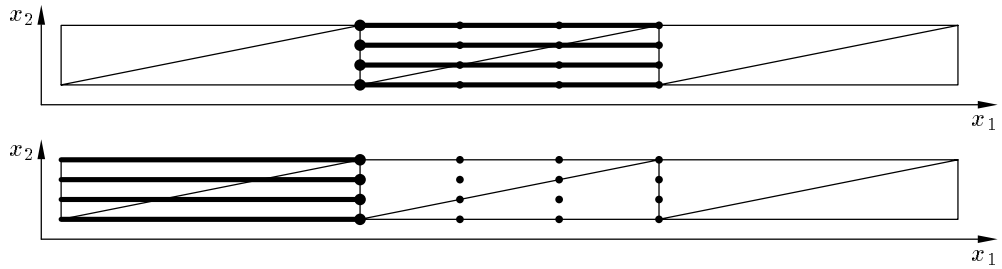

(b) Two choices for σ_i for points on vertical mesh lines.

Figure 14.1: Choice of σ_i in dependence of $X^{(i)}$ in the case of operator L_h.

The last step to derive (13.8) is done by a rearrangement of the terms at the right hand side, namely

$$\begin{aligned}
&\sum_{|t|=1}\sum_{|s|\le 1} h_1^{1-|s|} h^s \|r^{\beta-1+|s|} D^{t+s} u; L^p(S_e)\| \\
&\quad = \sum_{|t|=1}\sum_{|s|=1} h^s \|r^\beta D^{t+s} u; L^p(S_e)\| + \sum_{|t|=1} h_1 \|r^{\beta-1} D^t u; L^p(S_e)\| \\
&\quad \lesssim \sum_{|t|=1}\sum_{|s|=1} h^s \|r^\beta D^{t+s} u; L^p(S_e)\| + \sum_{|s|=1} h^s \|r^{\beta-1} D^s u; L^p(S_e)\| \\
&\quad \sim \sum_{|s|=1} h^s \|D^s u; V_\beta^{1,p}(S_e)\|.
\end{aligned}$$

Together with (13.14) we conclude (13.8) in the case $\gamma_3 = 0$. ∎

14 The operator L_h: choosing large sides with a projection property

In contrast to Section 13 we will now employ large edges/faces and denote the resulting operator by L_h. The notation is used as follows: We keep Properties (P1), (P2), and (P3) from page 73 and simply turn the relation (13.1):

$$h_j \ge h_d \quad \text{in } S_e \quad (j = 1, \dots, d). \tag{14.1}$$

But in correspondence with Item 2 at the end of Section 12, we do not have so much freedom for the choice of the σ_i as in the case of S_h. We must assume the following projection property (P4), compare also Figure 14.1.

(P4) If the projections of any two points $X^{(i)}$ and $X^{(j)}$ on the x_1-axis/x_1, x_2-plane coincide then so do the projections of σ_i and σ_j.

We can prove the results of Theorem 13.3 for this case as well. Moreover, these results extend to the case $m = \ell$. But in contrast to the needle elements of Section 13 the three-dimensional elements are now flat, $h_1 \sim h_2 \gtrsim h_3$. The idea for this choice of σ_i was found in [41, Chapter 5] where the special case of rectangular and brick elements was considered for $k = 1$, $p = q = 2$. We extend this theory to further types of element and to general $k \in \mathbb{N}$, $p, q \in [1, \infty]$. Our proof differs from that in [41].

We start as in Section 13 with the separate consideration of the stability of first derivatives of $\mathrm{L}_h u$. This time the derivative in x_1-direction is the simpler one.

Lemma 14.1 *Consider an element e of a mesh of tensor product type and assume that (14.1) is valid. Then the estimate*

$$\left\| \frac{\partial}{\partial x_n} \mathrm{L}_h u; L^q(e) \right\| \lesssim (\mathrm{meas}_d e)^{1/q - 1/p} |u; W^{1,p}(S_e)|, \quad n = 1, \ldots, d, \tag{14.2}$$

holds for $u \in W^{1,p}(S_e)$ and all $p, q \in [1, \infty]$.

Proof For $n = 1, \ldots, d-1$ the proof can be carried out with the same arguments as the proof of Lemma 13.1. The only difference is that the role of x_d and h_d is now played by x_n and h_n.

For the case $n = d$ we will reformulate $\mathrm{L}_h u$. For this consider first a one-dimensional situation, that means a single finite element formed by an interval (ξ, η). Let ϕ_i, $i = 0, \ldots, k$, be the nodal basis functions in (ξ, η). We change now to a new basis

$$\chi_i = \sum_{j=0}^{i} \phi_j, \quad i = 0, \ldots, k.$$

Consequently,

$$\sum_{i=0}^{k} a_i \phi_i = \sum_{i=0}^{k-1} (a_i - a_{i+1}) \chi_i + a_k,$$

where we also used that $\sum_{i=0}^{k} \phi_i = 1$. Note further that

$$\|\chi_i; L^\infty(\xi, \eta)\| \lesssim 1, \quad \|\chi_i'; L^\infty(\xi, \eta)\| \lesssim |\eta - \xi|^{-1}. \tag{14.3}$$

We use this kind of a new basis in the case of a rectangular element $e = (\xi_1, \eta_1) \times (\xi_2, \eta_2)$. The nodal basis functions are (for simplicity with a double index)

$$\varphi_{i,j}(x_1, x_2) = \phi^i(x_1) \phi_j(x_2), \quad i, j = 0, \ldots, k, \tag{14.4}$$

where ϕ^i and ϕ_j are the nodal basis functions with respect to (ξ_1, η_1) and (ξ_2, η_2), respectively. Thus

$$\begin{aligned} \mathrm{L}_h u &= \sum_{i=0}^{k} \sum_{j=0}^{k} a_{i,j} \phi^i(x_1) \phi_j(x_2) \\ &= \sum_{i=0}^{k} \phi^i(x_1) \left(\sum_{j=0}^{k-1} (a_{i,j} - a_{i,j+1}) \chi_j(x_2) + a_{i,k} \right), \\ \frac{\partial}{\partial x_2} \mathrm{L}_h u &= \sum_{i=0}^{k} \phi^i(x_1) \sum_{j=0}^{k-1} (a_{i,j} - a_{i,j+1}) \chi_j'(x_2). \end{aligned} \tag{14.5}$$

Because of Property (P4) the subdomains $\sigma_{i,j}$ belonging to the node (i,j) depend only on i. We can write

$$\begin{aligned} a_{i,j} &= \int_{\sigma_{i,j}} \psi_i(x_1)\, u(x_1, y_j)\, \mathrm{d}x_1, \\ a_{i,j} - a_{i,j+1} &= -\int_{\sigma_{i,j}} \psi_i(x_1) \int_{y_j}^{y_{j+1}} \frac{\partial u}{\partial x_2}(x_1, y)\, \mathrm{d}y \mathrm{d}x_1, \\ \sum_{j=0}^{k-1} |a_{i,j} - a_{i,j+1}| &\le \int_{S_e} \left| \psi_i \frac{\partial u}{\partial x_2} \right|, \end{aligned} \tag{14.6}$$

where y_j is the value of the x_2-coordinate of points $X_e^{(i,j)}$. The proof of (14.2) is now standard:

$$\begin{aligned} \left\| \frac{\partial}{\partial x_d} \mathrm{L}_h u; L^q(e) \right\| &\lesssim \sum_{i=0}^{k} \sum_{j=0}^{k-1} |a_{i,j} - a_{i,j+1}| \cdot \|\phi^i(x_1) \chi_j'(x_2); L^q(e)\| \\ &\lesssim h_2^{-1} (\mathrm{meas}_d e)^{1/q} \sum_{i=0}^{k} \int_{S_e} \left| \psi_i \frac{\partial u}{\partial x_2} \right| \\ &\lesssim h_2^{-1} (\mathrm{meas}_d e)^{1/q+1-1/p} \sum_{i=0}^{k} (\mathrm{meas}_{d-1} \sigma_i)^{-1} \left\| \frac{\partial u}{\partial x_2}; L^p(S_e) \right\|. \end{aligned}$$

For pentahedral and hexahedral elements the proof is similar. We only replace (14.4) by

$$\varphi_{i,j}(x_1, x_2, x_3) = \phi^i(x_1, x_2) \phi_j(x_3), \quad i = 0, \ldots, K,\ j = 0, \ldots, k,$$

with appropriate basis functions $\phi^i(x_1, x_2)$ and

$$K = (k+1)^2 - 1 \quad \text{for hexahedra,} \quad K = \binom{k+2}{2} - 1 \quad \text{for pentahedra.} \tag{14.7}$$

In the case of simplicial elements we have to modify these considerations slightly. We will explain it in the two-dimensional case. Consider an element e with nodes $X_e^{(i,j)}$,

$$\begin{aligned} e &= \left\{ (x_1, x_2) : \xi_1 \le x_1 \le \eta_1,\ \xi_2 \le x_2 \le \eta_2 - (x_1 - \xi_1) \frac{\eta_2 - \xi_2}{\eta_1 - \xi_1} \right\}, \\ X_e^{(i,j)} &= \left(\xi_1 + \frac{i}{k}(\eta_1 - \xi_1), \xi_2 + \frac{j}{k}(\eta_2 - \xi_2) \right), \end{aligned}$$

and nodal basis functions $\varphi_{i,j}$, $i = 0, \ldots, k$, $j = 0, \ldots, k - i$, as illustrated in Figure 14.2. The new basis functions are

$$\chi_{i,j} = \sum_{s=0}^{j} \varphi_{i,s}, \quad i = 0, \ldots, k,\ j = 0, \ldots, k - i.$$

We get

$$\begin{aligned} \mathrm{L}_h u &= \sum_{i=0}^{k} \sum_{j=0}^{k-i} a_{i,j} \varphi_{i,j} = \sum_{i=0}^{k} \left(\sum_{j=0}^{k-i-1} (a_{i,j} - a_{i,j+1}) \chi_{i,j} + a_{i,k-i} \chi_{i,k-i} \right), \\ \left\| \frac{\partial \mathrm{L}_h u}{\partial x_2}; L^q(e) \right\| &\lesssim \sum_{i=0}^{k} \left(\sum_{j=0}^{k-i-1} |a_{i,j} - a_{i,j+1}| \left\| \frac{\partial \chi_{i,j}}{\partial x_2}; L^q(e) \right\| + |a_{i,k-i}| \left\| \frac{\partial \chi_{i,k-i}}{\partial x_2}; L^q(e) \right\| \right). \end{aligned}$$

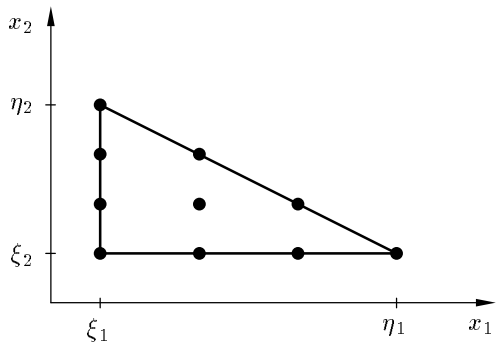

Figure 14.2: Illustration of the case of a triangle with $k = 3$.

To conclude (14.2) with the same arguments as above it remains to show that

$$\frac{\partial \chi_{i,k-i}}{\partial x_2} = 0 \quad \text{for all } i = 0, \ldots, k. \tag{14.8}$$

For this we observe that $\chi_{i,k-i}$ is uniquely determined by

$$\chi_{i,k-i}(X^{(s,j)}) = \begin{cases} 1 & \text{for } s = i,\ j = 0, \ldots, k-i, \\ 0 & \text{else.} \end{cases}$$

Thus $\chi_{i,k-i} = \phi^i(x_1)$ with ϕ^i in the sense of (14.4), and (14.8) is proved.

The proof for tetrahedral elements is analogous. ∎

Theorem 14.2 *Assume that (14.1) is valid. On anisotropic meshes of tensor-product type the modified Scott-Zhang operator* L_h *satisfies the following estimates:*

$$|\mathrm{L}_h u; W^{m,q}(e)| \lesssim (\mathrm{meas}_d e)^{1/q-1/p} |u; W^{m,p}(S_e)|, \tag{14.9}$$

$$|u - \mathrm{L}_h u; W^{m,q}(e)| \lesssim (\mathrm{meas}_d e)^{1/q-1/p} \sum_{|\alpha|=\ell-m} h^\alpha |D^\alpha u; W^{m,p}(S_e)|, \tag{14.10}$$

$0 \le m \le \ell$, $1 \le \ell \le k+1$, *provided that* $u \in W^{\ell,p}(S_e)$. *For* (14.10) *the numbers* $p, q \in [1, \infty]$ *must be such that* $W^{\ell,p}(e) \hookrightarrow W^{m,q}(e)$.

Proof Estimate (14.10) follows from (14.9) via Lemma 11.1 as it was done for S_h in the proof of Theorem 13.3. So the main point is to prove (14.9). For $m = 0$, this can be done as in the proof of (12.11). The case $m = 1$ is treated in Lemma 14.1.

Let $m \ge 2$. Consider a multi-index γ with $|\gamma| = m$ and define $m_2 := \gamma_d$, $m_1 := m - m_2$. In the proof of Lemma 14.1, we made for the case $m_2 = 1$ a transformation of the nodal basis $\varphi_{i,j}$ to a basis $\chi_{i,j}$ in order to obtain differences of first order:

$$\frac{\partial}{\partial x_d} \sum_{i=0}^{K} \sum_{j=0}^{k} a_{i,j} \varphi_{i,j} = \frac{\partial}{\partial x_d} \sum_{i=0}^{K} \sum_{j=0}^{k-1} (a_{i,j} - a_{i,j+1}) \chi_{i,j}.$$

This process is repeated until differences of order m_2 are created: For simplicity consider again the one-dimensional situation. We define recursively coefficients $a_i^{(n)}$ and functions $\chi_i^{(n)}$,

$i = 0, \ldots, k-n$, $n = 0, \ldots, m_2$, by

$$a_i^0 := a_i, \qquad a_i^{(n+1)} := a_i^{(n)} - a_{i+1}^{(n)}, \quad i = 0, \ldots, k-n, \tag{14.11}$$

$$\chi_i^0 := \varphi_i, \qquad \chi_i^{(n+1)} := \sum_{s=0}^{i} \chi_s^{(n)}, \qquad i = 0, \ldots, k, \tag{14.12}$$

and obtain

$$\frac{\partial^{m_2}}{\partial x^{m_2}} \sum_{i=0}^{k} a_i \varphi_i = \frac{\partial^{m_2}}{\partial x^{m_2}} \sum_{i=0}^{k-m_2} a_i^{(m_2)} \chi_i^{(m_2)}. \tag{14.13}$$

We get this by induction in analogy to the proof of Lemma 14.1. The only point is to prove that

$$\frac{\partial^{n+1}}{\partial x^{n+1}} \chi_{k-n}^{(n+1)} = 0 \quad \text{for } n = 0, \ldots, m_2 - 1. \tag{14.14}$$

This can be shown for any fixed n via $\chi_i^{(n+1)} = \sum_{s=0}^{i} \binom{i-s+n}{n} \chi_s^{(0)}$ (proof by induction) which yields $\chi_k^{(n+1)} = \sum_{s=0}^{k} \binom{k-s+n}{n} \varphi_s$, $\chi_k^{(n+1)}(X_e^{(r)}) = \binom{k-r+n}{n}$, $r = 0, \ldots, k$, $\chi_k^{(n+1)} \in \mathcal{P}_n^1$. From $\chi_i^{(n+1)} = \chi_{i+1}^{(n+1)} - \chi_{i+1}^{(n)}$ we conclude by induction $\chi_i^{(n+1)} \in \mathcal{P}_n^1$ for $i = k, k-1, \ldots, k-n$. Thus $\frac{\partial^{n+1}}{\partial x^{n+1}} \chi_i^{(n+1)} = 0$ for $i = k-n, \ldots, k$.

Consider now rectangular elements ($d = 2$) and transfer this basis transformation to the x_2-direction. We derive (again by induction) from (14.13)

$$\frac{\partial^{m_2}}{\partial x_d^{m_2}} \sum_{i=0}^{k} \sum_{j=0}^{k} a_{i,j} \varphi_{i,j} = \frac{\partial^{m_2}}{\partial x_d^{m_2}} \sum_{i=0}^{k} \sum_{j=0}^{k-m_2} a_{i,j}^{(m_2)} \chi_{i,j}^{(m_2)}. \tag{14.15}$$

The so created differences $a_{i,j}^{(n+1)} = a_{i,j}^{(n)} - a_{i,j+1}^{(n)}$ are used now to establish an integral representation; compare (14.6):

$$a_{i,j}^{(1)} = -\int_{\sigma_{i,j}} \psi_i(x_1) \int_0^{\delta} \frac{\partial u}{\partial x_d}(x_1, y_j + \eta_1)\, \mathrm{d}\eta_1 \mathrm{d}x_1,$$

$\delta = y_{j+1} - y_j$ is assumed to be independent of j. We continue recursively and obtain

$$\begin{aligned}
a_{i,j}^{(2)} &= -\int_{\sigma_{i,j}} \psi_i(x_1) \left[\int_0^{\delta} \frac{\partial u}{\partial x_d}(x_1, y_j + \eta_1)\, \mathrm{d}\eta_1 - \int_0^{\delta} \frac{\partial u}{\partial x_d}(x_1, y_{j+1} + \eta_1)\, \mathrm{d}\eta_1 \right] \mathrm{d}x_1 \\
&= (-1)^2 \int_{\sigma_{i,j}} \psi_i(x_1) \int_0^{\delta} \int_0^{\delta} \frac{\partial^2 u}{\partial x_d^2}(x_1, y_j + \eta_1 + \eta_2)\, \mathrm{d}\eta_1 \mathrm{d}\eta_2 \mathrm{d}x_1, \\
a_{i,j}^{(n)} &= (-1)^n \int_{\sigma_{i,j}} \psi_i(x_1) \underbrace{\int_0^{\delta} \cdots \int_0^{\delta}}_{n \text{ times}} \frac{\partial^n u}{\partial x_d^n}(x_1, y_j + \eta_1 + \cdots + \eta_n)\, \mathrm{d}\eta_1 \cdots \mathrm{d}\eta_n \mathrm{d}x_1.
\end{aligned}$$

Using (12.13) and $\delta \sim h_2$ we get

$$|a_{i,j}^{(n)}| \lesssim (\mathrm{meas}_{d-1} \sigma_{i,j})^{-1} h_d^{n-1} \left\| \frac{\partial^n u}{\partial x_d^n}; L^1(S_e) \right\|.$$

Replace now $\mathrm{meas}_{d-1}\sigma_{i,j}$ by $\mathrm{meas}_{d-1}\sigma := \min_{i,j} \mathrm{meas}_{d-1}\sigma_{i,j}$ and u by $u-w$, $w \in \mathcal{P}^2_{m-1}$ arbitrary. Together with (14.15) we conclude that

$$\begin{aligned}
\|D^\gamma \mathrm{L}_h u; L^q(e)\| &= \|D^\gamma \mathrm{L}_h (u-w); L^q(e)\| \\
&\lesssim \sum_{i=0}^{k} \sum_{j=0}^{k-m_2} |a_{i,j}^{(m_2)}| \|D^\gamma \chi_{i,j}^{(m_2)}; L^q(e)\| \\
&\lesssim h^{-\gamma} (\mathrm{meas}_d e)^{1/q} \sum_{i=0}^{k} \sum_{j=0}^{k-m_2} |a_{i,j}^{(m_2)}| \\
&\lesssim h^{-\gamma} (\mathrm{meas}_d e)^{1/q} (\mathrm{meas}_{d-1}\sigma)^{-1} h_d^{m_2-1} \left\| \frac{\partial^{m_2}}{\partial x_d^{m_2}} (u-w); L^1(S_e) \right\| \\
&\lesssim h^{-\gamma} h_d^{m_2} (\mathrm{meas}_d e)^{1/q-1/p} \left\| \frac{\partial^{m_2}}{\partial x_d^{m_2}} (u-w); L^p(S_e) \right\| \qquad (14.16) \\
&\lesssim h_1^{-m_1} (\mathrm{meas}_d e)^{1/q-1/p} \sum_{|\alpha| \le m-m_2} h^\alpha \left\| D^\alpha \frac{\partial^{m_2}}{\partial x_d^{m_2}} (u-w); L^p(S_e) \right\| .
\end{aligned}$$

In order to derive (14.16) we have used that $h_d \,\mathrm{meas}_{d-1}\sigma \sim \mathrm{meas}_d e$. Via Corollary 11.2, (14.1), and $m = m_1 + m_2$ we obtain

$$\begin{aligned}
\|D^\gamma \mathrm{L}_h u; L^q(e)\| &\lesssim h_1^{-m_1} (\mathrm{meas}_d e)^{1/q-1/p} \sum_{|\alpha| = m-m_2} h^\alpha \left\| D^\alpha \frac{\partial^{m_2} u}{\partial x_d^{m_2}}; L^p(S_e) \right\| \\
&\le (\mathrm{meas}_d e)^{1/q-1/p} \sum_{|\alpha| = m-m_2} \left\| D^\alpha \frac{\partial^{m_2} u}{\partial x_d^{m_2}}; L^p(S_e) \right\| \\
&\le (\mathrm{meas}_d e)^{1/q-1/p} |u; W^{m,p}(S_e)|
\end{aligned}$$

and (14.9) is proved for rectangular elements. The proof for all other types of elements is similar using the ideas explained in the proof of Lemma 14.1. ∎

15 The operator E_h: choosing long edges in the three-dimensional case

15.1 Stability and approximation in classical Sobolev spaces

In Sections 13 and 14 we assumed $h_1 \sim h_2$ in the three-dimensional case. We will now investigate the general three-dimensional situation of independent element sizes h_1, h_2, and h_3. In order to obtain in Subsection 15.2 a notation which is compatible with that in Subsection 13.2 we let

$$h_1 \le h_2 \le h_3. \qquad (15.1)$$

Assume, for simplicity, *tensor product meshes* in the sense that transformation (11.2) is reduced to

$$x_i = \pm h_i \hat{x}_i + b_i, \quad i = 1,2,3. \qquad (15.2)$$

The investigation of the operators S_h and L_h was based on taking σ_i as isotropic faces, that means that h_2 is of the same order as h_1 or h_3. In [41] it was suggested to overcome this restriction by taking *one-dimensional* σ_i but this was not elaborated thoroughly. We will now investigate which estimates can be obtained in this case. We assume the following properties which are analogous to those in Section 14.

(P1′) σ_i is parallel to the x_3-axis.

(P2) $X^{(i)} \in \overline{\sigma_i}$.

(P3′) There exists an edge ς of some element e such that the projection of ς on the x_3-axis is identical with the projection of σ_i.

(P4′) If the projections of any two points $X^{(i)}$ and $X^{(j)}$ on the x_3-axis coincide then so do the projections of σ_i and σ_j.

The corresponding operator is denoted by $E_h : W^{\ell,p}(\Omega) \to V_h$. Note that it is defined only for $u \in W^{\ell,p}(\Omega)$ with

$$\ell \geq 2 \quad \text{for } p = 1, \qquad \ell > \frac{2}{p} \quad \text{otherwise,} \tag{15.3}$$

to guarantee that $u|_{\sigma_i} \in L^1(\sigma_i)$. Condition (15.3) can be reformulated to

$$\ell \geq 2,\ p \in [1,\infty] \quad \text{or} \quad \ell = 1,\ p \in (2,\infty]. \tag{15.4}$$

We will prove now stability an approximation properties in classical Sobolev spaces. Then, we discuss in Remark 15.2 that the result is also valid for meshes of tensor product type. Of course, we can apply in that case also the operator S_h which is defined for a larger class of functions. But the operators S_h and E_h differ in the part of the boundary where Dirichlet boundary conditions are preserved, see also the comparison in Section 17. As we already did for S_h in Subsection 13.2 we prove a stability estimate for functions from weighted Sobolev spaces $V_\beta^{\ell,p}(S_e)$ in Subsection 15.2.

Theorem 15.1 *Consider an element e of a tensor product mesh and assume that (15.1) and (15.2) are fulfilled. Then the operator E_h satisfies for all $q \in [1,\infty]$ the following estimates:*

$$|E_h u; W^{m,q}(e)| \lesssim (\mathrm{meas}_3 e)^{1/q-1/p} \sum_{|\alpha|\leq 1} h^\alpha |D^\alpha u; W^{m,p}(S_e)| \tag{15.5}$$

if $m \geq 1$ or $p > 2$, and

$$\|E_h u; L^q(e)\| \lesssim (\mathrm{meas}_3 e)^{1/q-1/p} \sum_{|\alpha|\leq \ell} h^\alpha \|D^\alpha u; L^p(S_e)\| \tag{15.6}$$

with ℓ and p satisfying (15.4). The approximation error estimate

$$|u - E_h u; W^{m,q}(e)| \lesssim (\mathrm{meas}_3 e)^{1/q-1/p} \sum_{|\alpha|=\ell-m} h^\alpha |D^\alpha u; W^{m,p}(S_e)| \tag{15.7}$$

holds if $0 \leq m \leq \ell - 1 \leq k$, p satisfies (15.4), q is such that $W^{\ell,p}(e) \hookrightarrow W^{m,q}(e)$, and $u \in W^{\ell,p}(S_e)$.

We will see in the proof that for certain derivatives $D^\gamma E_h u$ the stability estimate (15.5) can still be improved.

Proof We prove the theorem for brick elements. Other element types are treated similarly, see the discussion in the proof of Lemma 14.1. We have to consider different cases separately.

First, let γ be a multi-index with $|\gamma| = m$ and $\gamma_1 \neq 0$, $\gamma_2 \neq 0$. We use the difference technique developed in the proof of Theorem 14.2 for both directions x_1 and x_2. In analogy to (14.16) we obtain for all $w \in \mathcal{P}^3_{m-1}$

$$\begin{aligned}\|D^\gamma \mathrm{E}_h u; L^q(e)\| &= \|D^\gamma \mathrm{E}_h (u-w); L^q(e)\| \\ &\lesssim h^{-\gamma} h_1^{\gamma_1} h_2^{\gamma_2} (\mathrm{meas}_3 e)^{1/q-1/p} \left\| \frac{\partial^{\gamma_1}}{\partial x_1^{\gamma_1}} \frac{\partial^{\gamma_2}}{\partial x_2^{\gamma_2}} (u-w); L^p(S_e) \right\| \\ &\leq h_3^{-\gamma_3} (\mathrm{meas}_3 e)^{1/q-1/p} \sum_{|\alpha| \leq \gamma_3} h^\alpha |D^\alpha u; W^{\gamma_1+\gamma_2,p}(S_e)|.\end{aligned}$$

Using Corollary 11.2 and (15.1) we conclude

$$\begin{aligned}\|D^\gamma \mathrm{E}_h u; L^q(e)\| &\lesssim h_3^{-\gamma_3} (\mathrm{meas}_3 e)^{1/q-1/p} \sum_{|\alpha| = \gamma_3} h^\alpha |D^\alpha u; W^{\gamma_1+\gamma_2,p}(S_e)| \\ &\leq (\mathrm{meas}_3 e)^{1/q-1/p} |u; W^{m,p}(S_e)|.\end{aligned}$$

In a second case we assume $\gamma_n \neq 0$, $n = 1$ or $n = 2$, but $\gamma_{3-n} = 0$, $\gamma_3 \neq 0$. Then we can use the difference technique only within some faces f_i $(i = 0, \ldots, k)$ which are parallel to the x_n, x_3-plane. Defining $f := \bigcup_{i=0}^k f_i$ we find as above that for all $w \in \mathcal{P}^3_{m-1}$

$$\begin{aligned}\|D^\gamma \mathrm{E}_h u; L^q(e)\| &= \|D^\gamma \mathrm{E}_h (u-w); L^q(e)\| \\ &\lesssim h^{-\gamma} h_n^{\gamma_n} (\mathrm{meas}_3 e)^{1/q} (\mathrm{meas}_2 f)^{-1/p} \left\| \frac{\partial^{\gamma_n}}{\partial x_n^{\gamma_n}} (u-w); L^p(f) \right\|. \quad (15.8)\end{aligned}$$

Using the trace theorem $W^{\gamma_3,p}(S_e) \hookrightarrow L^p(f)$ and again Corollary 11.2 as well as (15.1) we obtain

$$\begin{aligned}\|D^\gamma \mathrm{E}_h u; L^q(e)\| &\lesssim h_3^{-\gamma_3} (\mathrm{meas}_3 e)^{1/q-1/p} \sum_{|\alpha| \leq \gamma_3} h^\alpha |D^\alpha (u-w); W^{\gamma_n,p}(S_e)| \\ &\lesssim h_3^{-\gamma_3} (\mathrm{meas}_3 e)^{1/q-1/p} \sum_{|\alpha| = \gamma_3} h^\alpha |D^\alpha u; W^{\gamma_n,p}(S_e)| \\ &\leq (\mathrm{meas}_3 e)^{1/q-1/p} |u; W^{m,p}(S_e)|.\end{aligned}$$

Consider now the remaining pure derivatives. Let first be $\gamma_n = m \neq 0$, $n = 1$ or $n = 2$, $\gamma_3 = 0$. Estimate (15.8) holds in this case as well. By using $p = 1$ and $w = 0$ it reads now

$$\|D^\gamma \mathrm{E}_h u; L^q(e)\| \lesssim (\mathrm{meas}_3 e)^{1/q} (\mathrm{meas}_2 f)^{-1} \|D^\gamma u; L^1(f)\|. \quad (15.9)$$

With the trace theorem $W^{1,p}(S_e) \hookrightarrow L^1(f)$ for all $p \in [1, \infty]$ we conclude the assertion (15.5).

Finally, for $\gamma_3 = m \neq 0$, $\gamma_1 = \gamma_2 = 0$, the proof of the stability is completely analogous to the proof of Lemma 13.1. We have for all $w \in \mathcal{P}^3_{m-1}$

$$\|D^\gamma \mathrm{E}_h u; L^q(e)\| \lesssim h_3^{-m} (\mathrm{meas}_3 e)^{1/q} \sum_{i \in I_e} (\mathrm{meas}_1 \sigma_i)^{-1} \|u - w; L^1(\sigma_i)\|.$$

The trace theorem $W^{m+1,p}(S_e) \hookrightarrow L^1(\sigma_i)$ (which is the reason for the assumption $m \geq 1$ or $p > 2$) and Corollary 11.2 yield

$$\|D^\gamma \mathrm{E}_h u; L^q(e)\| \lesssim h_3^{-m} (\mathrm{meas}_3 e)^{1/q-1/p} \sum_{|\alpha| \leq m} \sum_{|\beta| \leq 1} h^{\alpha+\beta} \|D^{\alpha+\beta} (u-w); L^p(S_e)\|$$

$$\begin{aligned} &\lesssim h_3^{-m}(\mathrm{meas}_3 e)^{1/q-1/p} \sum_{|\alpha|=m} \sum_{|\beta|\le 1} h^{\alpha+\beta} \|D^{\alpha+\beta} u; L^p(S_e)\| \\ &\lesssim (\mathrm{meas}_3 e)^{1/q-1/p} \sum_{|\beta|\le 1} h^{\beta} |D^{\beta} u; W^{m,p}(S_e)|. \end{aligned}$$

Note that in this last case ($\gamma_3 = m$) for $m \ge 2$ and for $m = 1$, $p > 2$, it can even be proved that

$$\|D^\gamma \mathrm{E}_h u; L^q(e)\| \lesssim (\mathrm{meas}_3 e)^{1/q-1/p} |u; W^{m,p}(S_e)|$$

because then $W^{m,p}(S_e) \hookrightarrow L^1(\sigma_i)$ holds.

Estimate (15.6) is trivial since

$$\|\mathrm{E}_h u; L^q(e)\| \lesssim (\mathrm{meas}_3 e)^{1/q} \sum_{i \in I_e} (\mathrm{meas}_1 \sigma_i)^{-1} \|u; L^1(\sigma_i)\|,$$

and the embedding $W^{\ell,p}(S_e) \hookrightarrow L^1(\sigma_i)$ holds just for ℓ, p satisfying (15.4).

Estimate (15.7) is concluded from (15.5) and (15.6) as in the proof of Theorem 13.3. ∎

It is interesting to point out that the proof shows that

$$\|D^\gamma \mathrm{E}_h u; L^q(e)\| \lesssim (\mathrm{meas}_3 e)^{1/q-1/p} |u; W^{m,p}(S_e)| \tag{15.10}$$

holds for γ with $|\gamma| = m$ if at most one of the numbers $\gamma_1, \gamma_2, \gamma_3$ vanishes. Our way of proof does not work for pure derivatives. Consider for example the case $\gamma = (1,0,0)$. To prove (15.10) with $p > 2$ ($\mathrm{E}_h u$ is defined only for $u \in W^{1,p}(\Omega)$ with $p > 2$.) one would have to skip the trace on f and to use a trace theorem in the form (12.15). But this leads to

$$\|D^\gamma \mathrm{E}_h u; L^q(e)\| \lesssim h_1^{-1} (\mathrm{meas}_3 e)^{1/q-1/p} \sum_{|\alpha|\le 1} h^\alpha \|D^\alpha u; L^p(S_e)\|$$

with some diverging terms at the right hand side. The case $\gamma = (1,0,0)$ could be treated only if

$$\|D^\gamma \mathrm{E}_h u; L^q(e)\| \lesssim (\mathrm{meas}_3 e)^{1/q-1/p} \|D^\gamma u; L^p(S_e)\|$$

was valid. It is not clear whether this estimate holds.

Remark 15.2 Our motivation for introducing the operator E_h was to be able to treat the general case of three independent mesh sizes $h_1 \le h_2 \le h_3$. Of course this includes the special case $h_1 \sim h_2$. We point out that in this case the transformation (15.2) can be generalized to (11.2), (11.3). To see that then the statement of Theorem 15.1 remains true consider an arbitrary element $e \in \mathcal{T}_h$ and denote its projection into the x_1, x_2-plane by ζ. Since $\mathcal{T}_h$ is of tensor product type, and since all σ_i are perpendicular to the x_1, x_2-plane, it suffices to choose S_e such that its projection to the x_1, x_2-plane is again ζ (and $\sigma_i \subset \overline{S_e}$), compare Figure 15.1. Via the transformation

$$\begin{pmatrix} x_1 \\ x_2 \\ x_3 \end{pmatrix} = \begin{pmatrix} h_1^{-1} B_e & \vdots & 0 \\ \cdots & \cdots & \cdots \\ 0 & \vdots & 1 \end{pmatrix} \begin{pmatrix} \tilde{x}_1 \\ \tilde{x}_2 \\ \tilde{x}_3 \end{pmatrix} =: \tilde{B} \begin{pmatrix} \tilde{x}_1 \\ \tilde{x}_2 \\ \tilde{x}_3 \end{pmatrix},$$

B_e from (11.2), the domains e and S_e can be mapped to $\tilde{e}$ and $\tilde{S}_e = S_{\tilde{e}}$ which satisfy (locally) the assumptions made at the beginning of this section. That means that Theorem 15.1 holds true with respect to the coordinate system $\tilde{x}_1, \tilde{x}_2, \tilde{x}_3$. By observing that

$$\det \tilde{B} \sim 1, \quad \|\tilde{B}\| \sim 1, \quad \|\tilde{B}^{-1}\| \sim 1$$

we find that Theorem 15.1 extends to the meshes described above.

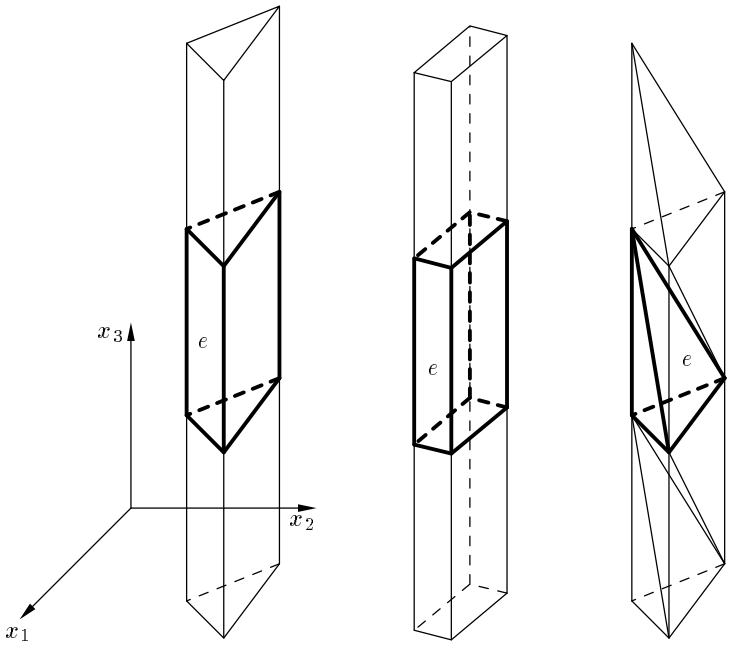

Figure 15.1: Illustration of the possible choice of a smaller S_e in the case of E_h (three element types).

15.2 Stability in weighted Sobolev spaces

As in Subsection 13.2 we do not have an estimate with $m = \ell = 1$ for E_h. Therefore we consider a stability estimate for functions from weighted Sobolev spaces $V_\beta^{\ell,p}(S_e)$. These spaces were introduced in (3.9), (3.11). To be able to apply the transformation (15.2) to the weight we will restrict the consideration to the case $h_1 \sim h_2$. However, we can then relax (15.2) to (11.2), see Remark 15.2 above.

Lemma 15.3 *Consider an element e of a tensor product mesh and assume that (15.1) and (15.2) are fulfilled. Let m be an integer and β, p, q be real numbers with $0 \le m \le k$, $p, q \in [1, \infty]$, $\beta < 2 - \frac{2}{p}$, $\beta \le 1$. Then for $u \in W^{m,p}(S_e) \cap V_\beta^{m+1,p}(S_e)$ the stability estimate*

$$|\mathrm{E}_h u; W^{m,q}(e)| \le (\mathrm{meas}_3 e)^{1/q-1/p} h_1^{-\beta} \sum_{|\alpha|=m-1} \sum_{|t|=1} h^t \|D^{\alpha+t} v; V_\beta^{1,p}(S_e)\| \tag{15.11}$$

holds if $m \ge 1$ or $p \ge 2$.

Proof Observe that the relations

$$\|v; L^1(S_e)\| \le \|r^{-\beta}; L^{p'}(S_e)\| \cdot \|r^\beta v; L^p(S_e)\|, \tag{15.12}$$

$$\|r^{-\beta}; L^{p'}(S_e)\| \lesssim (\mathrm{meas}_3 S_e)^{1-1/p} h_1^{-\beta} \tag{15.13}$$

(compare (13.12), (13.13)) lead to the embedding

$$V_\beta^{m+1,p}(S_e) \hookrightarrow V_0^{m+1,1}(S_e) \hookrightarrow W^{m+1,1}(S_e), \quad \beta < 2 - \frac{2}{p},$$

that means $u \in W^{m+1,1}(S_e)$. Therefore we can apply Theorem 15.1 (see also Remark 15.2) with $p = 1$:

$$|\mathrm{E}_h u; W^{m,q}(e)| \lesssim (\mathrm{meas}_3 e)^{1/q-1} \sum_{|\alpha|\le 1} h^\alpha |D^\alpha u; W^{m,1}(S_e)| \tag{15.14}$$

Notice further that (15.12), (15.13) lead to the estimate

$$\|v; L^1(S_e)\| \lesssim (\mathrm{meas}_3 S_e)^{1-1/p} h_1^{-\beta} \|r^\beta v; L^p(S_e)\|, \quad \beta < 2 - \frac{2}{p}.$$

So we get

$$\begin{aligned}
&\sum_{|\alpha|\le 1} \sum_{|t|=1} h^\alpha \|D^{\alpha+t} v; L^1(S_e)\| \\
&\quad\lesssim (\mathrm{meas}_3 S_e)^{1-1/p} h_1^{-\beta} \left(\sum_{|\alpha|=1} \sum_{|t|=1} h^\alpha \|r^\beta D^{\alpha+t} v; L^p(S_e)\| + \sum_{|t|=1} h_1 \|r^{\beta-1} D^t v; L^p(S_e)\| \right) \\
&\quad\lesssim (\mathrm{meas}_3 S_e)^{1-1/p} h_1^{-\beta} \sum_{|s|=1} h^s \|D^s v; V^{1,p}(S_e)\|.
\end{aligned}$$

Together with (15.14) the assertion (15.11) is concluded. ∎

16 Comments on related work

The well-known Clément operator [64] fits perfectly in the framework developed in Section 12. We have just to replace the definition of the domains σ_i by $\overline{\sigma_i} := \bigcup_{\overline{e} \ni X^{(i)}} \overline{e}$ and to use $\mathcal{P}_k^d$ instead of $\mathcal{P}_{k,\sigma_i}$. The resulting operator C_h,

$$(\mathrm{C}_h u)(x) := \sum_{i \in I} (\Pi_{\sigma_i} u)(X^{(i)}) \cdot \varphi_i(x),$$

is even defined for $u \in L^1(\Omega)$ and allows the estimate

$$|u - \mathrm{C}_h u; W^{m,q}(e)| \lesssim (\mathrm{meas}_d e)^{1/q-1/p} h^{\ell-m} |u; W^{\ell,p}(S_e)|,$$

$0 \le m \le \ell \le k+1$, on isotropic meshes.

The operator C_h in this original form does not reproduce the piecewise polynomials $v_h \in V_h$, $\mathrm{C}_h v_h = v_h$ is in general not satisfied for $v_h \in V_h$. But this can be corrected by defining $\Pi_{\sigma_i} : L^2(\sigma_i) \to V_h|_{\sigma_i}$.

A modification of the Clément operator is discussed by Oswald [151]. He fixed just one (arbitrary) element $e =: \sigma_i$ with $X^{(i)} \in \overline{e}$. The resulting operator O_h allows the same estimates as C_h, and we have $V_h|_{\sigma_i} = \mathcal{P}_{k,\sigma_i}$.

For C_h and O_h one can verify easily that all estimates in Section 12 remain true. Condition (12.7) can even be omitted; the operator is defined for all $u \in L^1(\Omega)$. Therefore, estimates (12.8), (12.9), (12.11), and (12.12) hold for $\ell = 0$ as well. Example 12.2 can be modified in the obvious way. (Of course, Z_h has to be substituted by C_h or O_h in all relations.) Note that we need in the proof only $\mathrm{C}_h w = w$ for $w \in \mathcal{P}_{\ell-1}^d$, which is satisfied, no matter whether Π_{σ_i} is acting into $\mathcal{P}_k^d$ or $V_h|_{\sigma_i}$.

The disadvantage of both C_h and O_h is that they do not preserve Dirichlet boundary conditions. To satisfy such boundary conditions one has to consider a modification of C_h near the boundary which is small enough to keep the approximation order [64, 117, 174].

Remark 16.1 In the original papers by Clément [64] and Scott/Zhang [171], only affine, isotropic, simplicial elements were considered. It turns out that the theory can easily be extended to affine, isotropic elements of other types (quadrilaterals, hexahedra, pentahedra). For a study of isoparametric elements, see [44, 145].

Remark 16.2 Siebert [174] and Kunert [117] derived also some results for the operator C_h for anisotropic meshes. However, they considered only the case $k = 1$, $p = 2$, and only subsets $H^1_{\mathcal{T}}(\Omega) \subset W^{1,2}(\Omega)$ of so-called mesh adapted functions. This allows them to prove global results of the form

$$\begin{aligned} \sum_e \varrho_e^{-1} \|v - \mathrm{C}_h v; L^2(e)\| &\lesssim |v; W^{1,2}(\Omega)|, \\ \sum_e h_{i,e}\, \varrho_e^{-1} \left\| \frac{\partial}{\partial x_i}(v - \mathrm{C}_h v)); L^2(e) \right\| &\lesssim |v; W^{1,2}(\Omega)|, \quad i = 1, \dots, d, \end{aligned}$$

where $\varrho_e \sim \min_{j=1,\dots,d} h_{j,e}$. Using these estimates they prove asymptotic properties of a-posteriori error estimators. For v they insert the (exact) finite element error $u - u_h$. Unfortunately, the condition $u - u_h \in H^1_{\mathcal{T}}(\Omega)$ can not be proved/tested in general, see also the discussion of anisotropic a-posteriori error estimators in Section 28.

17 Comparison of the operators

The starting point of our investigation was the interpolation operator Z_h introduced by Scott and Zhang [171]. We have seen in Section 12 that anisotropic estimates are valid for $m = 0$ but in general not for $m \geq 1$. Therefore we introduced three modifications and investigated the resulting operators S_h, L_h, and E_h, for the definitions see pages 73, 79, and 84. In order to summarize and to compare the different Scott-Zhang type interpolation operators we give a tabular overview. For comparison we add also the results for the nodal interpolant I_h and for the operators C_h (Clément) and O_h (Oswald).

In Table 17.1 we find the element types which the operator is applicable for. Note the slight difference of *tensor product type* and *tensor product* elements in three dimensions. Tensor product type corresponds to transformation (11.2), (11.3), and tensor product means the restriction to transformation (15.2), see also (3.6)–(3.8).

Table 17.2 compares the conditions for which the stability estimate

$$|\mathrm{Q}_h u; W^{m,q}(e)| \lesssim (\mathrm{meas}_d e)^{1/q-1/p} \sum_{|\alpha| \leq \ell - m} h^\alpha |D^\alpha u; W^{m,p}(S_e)| \tag{17.1}$$

holds, $\mathrm{Q}_h \in \{\mathrm{C}_h, \mathrm{O}_h, \mathrm{Z}_h, \mathrm{S}_h, \mathrm{L}_h, \mathrm{E}_h, \mathrm{I}_h\}$. In the case of S_h and E_h we additionally proved stability in weighted Sobolev spaces. The estimate

$$|\mathrm{Q}_h u; W^{m,q}(e)| \leq (\mathrm{meas}_d e)^{1/q-1/p} h_1^{-\beta} \sum_{|\alpha|=m-1} \sum_{|t|=1} h^t \|D^{\alpha+t} u; V^{1,p}_\beta(S_e)\|$$

holds under the conditions given in Table 17.3.

The approximation error estimate

$$|u - \mathrm{Q}_h u; W^{m,q}(e)| \lesssim (\mathrm{meas}_d e)^{1/q-1/p} \sum_{|\alpha| = \ell - m} h^\alpha |D^\alpha u; W^{m,p}(S_e)| \tag{17.2}$$

holds if the conditions of Table 17.2 are satisfied and the parameters ℓ, p, m, q are such that the embedding $W^{\ell,p}(e) \hookrightarrow W^{m,q}(e)$ holds. The operator I_h plays an exceptional role here, because

	$d=2$	$d=3$
Z_h, C_h, O_h	tensor product meshes h_1, h_2 arbitrary	meshes of tensor product type $h_1 \sim h_2 \lesssim h_3$ or $h_1 \sim h_2 \gtrsim h_3$
		tensor product meshes h_1, h_2, h_3 independent
S_h	tensor product meshes $h_1 \lesssim h_2$	meshes of tensor product type $h_1 \sim h_2 \lesssim h_3$
L_h	tensor product meshes $h_1 \gtrsim h_2$	meshes of tensor product type $h_1 \sim h_2 \gtrsim h_3$
E_h		meshes of tensor product type $h_1 \sim h_2 \lesssim h_3$
		tensor product meshes $h_1 \lesssim h_2 \lesssim h_3$
I_h	tensor product meshes h_1, h_2 arbitrary	meshes of tensor product type $h_1 \sim h_2 \lesssim h_3$ or $h_1 \sim h_2 \gtrsim h_3$
		tensor product meshes h_1, h_2, h_3 independent
	even for more general meshes, see Sections 5 and 7	even for more general meshes, see Sections 6, 8 and 9

Table 17.1: Comparison of the operators: Treated finite elements.

C_h, O_h	$m=0$, $0 \le \ell \le k+1$, $p,q \in [1,\infty]$
Z_h	$m=0$, $1 \le \ell \le k+1$, $p,q \in [1,\infty]$
S_h	$0 \le m \le \ell-1$, $1 \le \ell \le k+1$, $p,q \in [1,\infty]$ for $m \ge 2$ triangles and tetrahedra are excluded
L_h	$0 \le m \le \ell$, $1 \le \ell \le k+1$, $p,q \in [1,\infty]$
E_h	$1 \le m \le \ell-1$, $1 \le \ell \le k+1$, $p,q \in [1,\infty]$
	$m=0$, $2 \le \ell \le k+1$, $p,q \in [1,\infty]$
	$m=0$, $\ell=1$, $p \in (2,\infty]$, $q \in [1,\infty]$
I_h	$0 \le m \le \ell-1$, $1 \le \ell \le k+1$, $q \in [1,\infty]$, $p > d/\ell$ if $\ell < d$ and $m=0$, $p > 2$ if $d=3$ and $m=\ell-1>0$
	$m=0$, $\ell=0$, $p=\infty$, $q \in [1,\infty]$

Table 17.2: Comparison of the operators: Conditions for the stability and error estimates.

C_h, O_h, Z_h	not treated
S_h	$0 \le m \le k$, $p,q \in [1,\infty]$, $\beta < 2-2/p$, $\beta \le 1$ for $m \ge 2$ triangles and tetrahedra are excluded
L_h	not treated
E_h	$1 \le m \le k$, $p,q \in [1,\infty]$, $\beta < 2-2/p$, $\beta \le 1$
	$m=0$, $p \in (2,\infty]$, $q \in [1,\infty]$, $\beta < 2-2/p$, $\beta \le 1$
I_h	not treated in this form

Table 17.3: Comparison of the operators: Conditions for the stability in weighted Sobolev spaces.

C_h, O_h, Z_h	only $m = 0$
S_h	$m = \ell$ excluded, only $m = 0, 1$ for simplices, in 3D only needle elements
L_h	in 3D only flat elements
E_h	$m = \ell$ excluded, restrictions on p when $m = 0$, $\ell = 1$
I_h	$m = \ell$ excluded, restrictions on p when $m = 0$, $\ell < d$ or $m = \ell - 1 > 0$

Table 17.4: Comparison of the operators: Restrictions in the applicability.

estimate (17.2) is proved directly. The stability in the sense of (17.1) can be concluded via $|I_h u| \leq |u| + |u - I_h u|$. Moreover, anisotropic interpolation error estimates are derived also for functions from weighted Sobolev spaces, see Subsection 6.2.

Some shortcomings of the operators are given in Table 17.4. Additionally, we state that Dirichlet boundary conditions $u = g \in V_h|_{\Gamma_1}$ on Γ_1 can be satisfied on any part of $\partial\Omega$ for Z_h and I_h, on parts of the boundary which are parallel to the x_1-axis/x_1, x_2-plane for S_h and L_h, and on parts of $\partial\Omega$ which are perpendicular to the x_1, x_2-plane for E_h.

Finally, we mention that S_h and E_h have been successfully applied in the study of the Poisson problem in a domain with an edge where the singularity was treated with anisotropic mesh refinement, see Section 20. The operator L_h was applied by Becker [41] to show the stability and an approximation error estimate of the stabilized Q_1/Q_0-element pair in the context of the Stokes equation. The anisotropic estimates for I_h have been applied in the study of diffusion problems in domains with corners and edges [9, 19, 20, 21, 153], see also Sections 20 and 21, as well as for singularly perturbed convection-diffusion-reaction problems with anisotropic refinement in boundary layers [5, 13, 14, 73], see also Sections 25 and 26.

Chapter IV

Anisotropic finite element approximations near edges

This chapter is concerned with a specific finite element strategy for solving elliptic boundary value problems in domains with edges. A class of anisotropically graded meshes is introduced and the optimal convergence rate of the finite element error is proved. Numerical tests are presented.

18 The aim of this chapter

Chapters IV and V (Sections 25–22) contain anisotropic discretization strategies and global error estimates for model problems, for example the Poisson problem and the convection-diffusion-reaction problem. The differential operators in these problems are simple, the solution is always only a scalar function. Our main interest is to treat typical peculiarities (typical also for more complex problems) like boundary layers or edge and corner singularities. We focus on the applicability of the techniques to general polygonal/polyhedral domains and to piecewise polynomial trial functions of arbitrary (but fixed) degree k.

In this chapter we study elliptic problems posed over three-dimensional domains with corners and edges. As discussed in Subsection 19.1 the solution of such problems has both singular and anisotropic behaviour. The singularity leads to a reduced convergence order of the finite element method on quasi-uniform meshes. Two-dimensional problems with corner singularities can be treated with *local mesh grading* in order to improve the approximation order, see Subsection 19.2. This approach can be generalized to the three-dimensional case in two ways; we introduce them in Subsection 19.3. It turns out that the adequate refinement is *anisotropic* [9, 19, 21].

In Section 20, we consider the Poisson problem,

$$-\Delta u = f \quad \text{in } \Omega, \qquad u = 0 \quad \text{on } \Gamma_1, \qquad \frac{\partial u}{\partial n} = 0 \quad \text{on } \Gamma_2 := \partial\Omega \setminus \Gamma_1,$$

for simplicity over a *three-dimensional tensor product domain* $\Omega = G \times (0, z_0)$. We prove in Subsection 20.1 (Theorem 20.2 and Corollary 20.3) for model cases and *piecewise (multi-)linear trial functions* the approximation estimate

$$\|u - u_h; W^{m,2}(\Omega)\| \lesssim h^{2-m} \|f; L^2(\Omega)\|, \qquad m = 0, 1,$$

by using the Scott-Zhang interpolation results.

The principal difficulties are the following:

- The solution u is contained in $W^{2,2}(S_e)$ if the neighbourhood S_e of the element e has positive distance to the edge. Thus we can estimate the interpolation error by

$$|u - \mathrm{E}_h u; W^{1,2}(e)| \lesssim \sum_{|\alpha|=1} h_e^{\alpha} |D^{\alpha} u; W^{1,2}(S_e)|. \tag{18.1}$$

  The norm at the right hand side grows, however, to infinity for some derivatives D^{α} if the distance of S_e to the edge E tends to zero. So we have to find a suitable description in oder to compensate the large norms with small element sizes $h_{i,e}$.

- The solution u is not contained in $W^{2,2}(S_e)$ if the neighbourhood S_e of the element e has zero distance to the edge. In this case we used local estimates for functions from weighted Sobolev spaces $V_{\beta}^{2,2}(S_e)$.

- The estimate (18.1) does not hold if E_h is replaced by the Lagrange interpolant I_h. In this case we need at the right hand side the space $W^{1,p}(e)$ with some $p > 2$, see Section 4. Nevertheless, one can prove

$$\|u - \mathrm{I}_h u; W^{1,2}(\Omega)\| \lesssim h$$

  but we needed more smoothness of the data ($f \in W^{4,2}(\Omega)$ in [9]) or a stronger refinement condition [19].

By using *trial functions of higher degree* k and a corresponding stronger anisotropic mesh grading one can prove for model cases (Examples 20.9 and 20.10) that solutions with edge singularities can be approximated according to

$$\|u - u_h; W^{1,2}(\Omega)\| \lesssim h^k.$$

The basis for this estimate is set by the global interpolation error estimates in Theorems 20.7 (for the Lagrange interpolant and a singularity exponent $\lambda > 1/2$) and 20.8 (for the modified Scott-Zhang interpolants S_h and E_h and $\lambda \leq 1$). Of course, the right hand side f has to be sufficiently smooth.

For *general polyhedral domains* or more general differential operators one has to combine the anisotropic refinement near singular edges with an isotropic refinement for treating the additional corner singularities. One of the challenges has been to describe a family of meshes which is both suited for approximation and for a simple realization in a computer program. With our proposal [21], see also the summary in Section 21, the construction of such meshes is principally known. The analysis is done, however only in the case of piecewise linear trial functions, $k = 1$ (Theorem 21.4 and Corollary 21.5). The difficulty for $k \geq 2$ consists in a sufficiently fine description of the properties of the solution u. Section 21 is completed with a computation of the Poisson equation in the Fichera domain.

One of the surprising results is that the anisotropic mesh grading does not disturb the asymptotics of the *condition number* κ of the stiffness matrix. We show in Subsection 20.3 that $\kappa \lesssim h^{-2}$ as in the case of a family of quasi-uniform meshes and a smooth solution. However, this does not imply that optimal preconditioning techniques for families of isotropic meshes can be used for anisotropic meshes. We analyze this in Section 29.

Note that we present asymptotic estimates always in terms of $h := \max_{e \in \mathcal{T}_h} \mathrm{diam} e$. Since we advocate only strategies where the number of elements is $N_{\mathrm{el}} \sim h^{-d}$, the error can easily be expressed in terms of N_{el} or the number N of unknowns (degrees of freedom).

We end the current section with a philosophical comment. The performance of the h-version of the finite element method is strongly determined by the family of meshes. Therefore

the choice of an appropriate family of meshes $\mathcal{T}_h$ has to be made carefully. It should satisfy the following requirements, or it should at least be a good compromise between them.

1. In order to allow an optimal decrease of the finite element error as the parameter h describing the family tends to zero, the *meshes must be refined* in certain parts of the domain. This can be done a-priori by incorporating analytic knowledge of the problem into the design of the meshes, see Sections 19–26. Alternatively, the family can be defined in an a-posteriori (adaptive) strategy, this means that a new mesh is defined by exploiting the information given by the approximate solution u_h on the previous mesh(es), see Section 28.

2. Determining a finite element solution involves the solution of an algebraic system of equations. If the usual nodal basis functions are used to assemble this system then the resulting matrix (sometimes called the *stiffness matrix*) is ill-conditioned. Solution techniques/preconditioners that are based on a *hierarchy of meshes* (multi-grid, BPX) turn out to overcome this problem effectively.

3. The meshing strategy should be *general* enough to handle domains of arbitrary shape. However, it should be simple enough to allow an effective implementation on serial *and parallel* computers.

In the examples of Chapters IV and V, the families of meshes are defined according to Item 1 above, namely, to establish optimal a-priori error estimates with only $\mathcal{O}(h^{-d})$ finite elements. It is still a challenge to improve this approach by formulating a corresponding adaptive refinement strategy; we comment on this in Section 28. We remark further that the example families of meshes can be constructed in a hierarchical way. However, the foundation of optimal solution techniques is still in its infancy, see Section 29. Finally, both types of mesh can be defined in a subdomain approach, see Sections 21, 25 and 26. This makes them suitable in the sense of Item 3.

19 The Poisson problem in a domain with an edge: an introduction

19.1 Statement of the problem

In this section, we give an overview over the mathematical problem we want to treat in this chapter. First we introduce analytical properties of the Poisson problem in a domain with edges. We will see then that the finite element method on quasi-uniform meshes suffers in general from a reduced order of convergence. Two-dimensional problems with corner singularities can be treated with *local mesh grading* in order to improve the approximation order, see Subsection 19.2. This approach can be generalized to the three-dimensional case in two ways; we discuss this in Subsection 19.3. Before, at the end of this subsection, we mention several other ways to cope with edge singularities.

Consider the Dirichlet problem for the Poisson equation,

$$-\Delta u = f \quad \text{in } \Omega, \qquad u = 0 \quad \text{on } \partial\Omega, \tag{19.1}$$

over a bounded polyhedral domain $\Omega \subset \mathbb{R}^3$. For simplicity, let Ω be a prismatic domain,

$$\Omega = G \times Z, \tag{19.2}$$

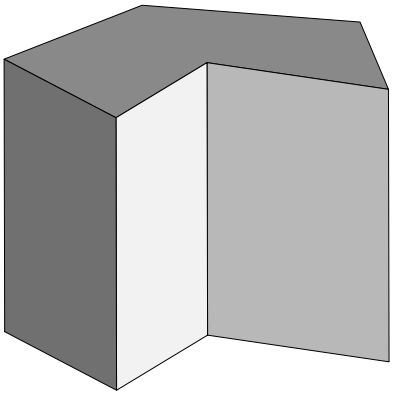

Figure 19.1: Illustration of a prismatic domain with a singular edge.

where $G \subset \mathbb{R}^2$ is a polygonal domain and $Z = (0, z_0) \subset \mathbb{R}^1$ is an interval. The domain G shall have one corner C with interior angle $\omega > \pi$. The other interior angles of G shall be smaller than π, see Figure 19.1. Denote by $E = C \times Z$ the edge with the large interior angle.

It is well known that the (variational) solution u of (19.1) has, in general, singular behaviour near E. The solution u can be decomposed into a singular part $u_{\rm s}$ and a regular part $u_{\rm r} \in W^{2,2}(\Omega)$, $u = u_{\rm s} + u_{\rm r}$, where

$$u_{\rm s} = \xi(r)\gamma(x)r^{\lambda}\Phi(\phi), \quad \lambda = \frac{\pi}{\omega}. \tag{19.3}$$

Here we denote by r, ϕ the polar coordinates in a plane perpendicular to the edge ($r := \mathrm{dist}\,(x, E)$, $\phi \in (0, \omega)$), $\xi(r)$ is a smooth cut-off function ($\xi(r) = 1$ for $r < R_0$, $\xi(r) = 0$ for $r > 2R_0$, R_0 is a constant), $\gamma(x) \in W^{2,2}_{\lambda}(\Omega)$ is a coefficient function, and $\Phi(\phi) = \sin \lambda\phi$ [116].

Remark 19.1 Note that γ depends on all three spatial coordinates unless the right hand side f is sufficiently smooth ($D^{(0,0,j)}f \in L^2(\Omega)$, $j = 1, 2$). The coefficient function γ, sometimes called *stress intensity distribution*, can be represented explicitly by a convolution integral,

$$\gamma(r, x_3) = \frac{1}{\pi}\int_{\mathbb{R}} \frac{r}{r^2 + s^2} q(x_3 - s)\ \mathrm{d}s,$$

where the smoothness of q can be characterized in Besov spaces depending on λ [88].

We remark also that in the two-dimensional case the coefficient γ is a constant (sometimes called the *stress intensity coefficient*). Furthermore, the singular part $u_{\rm s}$ may consist of a sum of several singular functions, $u_{\rm s} = \xi(r)\sum_i \gamma_i(x) r^{\lambda_i}\Phi_i(\phi)$, for example in the case of mixed boundary conditions. For more general operators the situation becomes more complicated because the exponents λ_i are not explicitly known. They correspond to eigenvalues of a related operator eigenvalue problem where $\Phi_i(\phi)$ are the eigenfunctions. Moreover, there are special angles ω where logarithmic terms have to be included in the representation. For an overview see, for example, the monographs [66, 87, 116].

For our purposes it is sufficient to know integrability properties of derivatives of the solution. That means that we do not need to know the terms of the representation formula. So we get by integration

$$u \notin W^{2,2}(\Omega) \tag{19.4}$$

even in the case of smooth data $f \in C^\infty(\overline{\Omega})$. Furthermore, one can prove that

$$u \in W^{1+s,2}(\Omega) \quad \text{for } s < \lambda \tag{19.5}$$

for $f \in L^2(\Omega)$.

Nevertheless, second order (generalized) derivatives of u exist. They are integrable in the following sense:

$$r^\beta \frac{\partial u}{\partial x_i} \in W^{1,2}(\Omega) \qquad \text{for } \beta > 1-\lambda, \quad i = 1,2, \tag{19.6}$$

$$\frac{\partial u}{\partial x_3} \in W^{1,2}(\Omega), \tag{19.7}$$

see Lemma 20.1. We mention here an anisotropic feature of the solution; *only the derivatives in directions perpendicular to the edge are singular.*

Finishing the description of the analytic properties of u we would like to point out that the domain was chosen such that the example is as simple as possible.

- The domain Ω has one "singular edge". The case of more than one singular edge can be treated similarly because the singularities are of local nature.
- For general polyhedral domains one has to consider not only edge singularities but also corner singularities. However, these do not contribute to the anisotropic character of the solution which is the interest here. Prismatic domains have the advantage that no corner singularities appear [181, 191], see Comment 22.2 on page 122.

Consider now the solution of Problem (19.1) with a finite element method. For simplicity let us use tetrahedral elements and piecewise linear basis functions. If the mesh is *quasi-uniform*, $h := \max_{e \in \mathcal{T}_h} \operatorname{diam}(e) \sim \min_{e \in \mathcal{T}_h} \varrho_e$, then the poor regularity of u as given by (19.5) leads to the finite element error estimates

$$\|u - u_h; W^{1,2}(\Omega)\| \lesssim h^{\lambda-\varepsilon}, \tag{19.8}$$

$$\|u - u_h; L^2(\Omega)\| \lesssim h^{2(\lambda-\varepsilon)}, \tag{19.9}$$

with arbitrarily small $\varepsilon > 0$ [3, page 82], [166]. Using regularity results in Besov spaces instead of Sobolev-Slobodetskiĭ spaces it is possible to prove these estimates even for $\varepsilon = 0$ [72]. One can also give an example that shows that estimate (19.8) is sharp in the sense $\|u-u_h; W^{1,2}(\Omega)\| \gtrsim h^\lambda$ [3, page 85].

In view of this loss of accuracy of the standard finite element method, many specially adapted numerical methods have been developed which yield error estimates of the same quality as for problems with a regular solution. In this monograph we shall focus on *a-priori local mesh grading techniques*. We introduce this approach in Subsections 19.2 and 19.3. In the remainder of this subsection we shortly review other methods.

A well-known technique is the *singular function method* [49, 71], [182, Section 8.2], also called *Fix method* [181], *augmenting technique* [194], or *additive separation of the singularities* [150, pages 267–272]. In the two-dimensional case, the basic idea is to augment the finite element space V_{0h} by singular functions $\xi(r) r^{\lambda_i} \Phi_i(\phi)$. Note that $u_s = \xi(r) \sum_i \gamma_i r^{\lambda_i} \Phi_i(\phi)$, $\gamma_i \in \mathbb{R}$, in two dimensions, see Remark 19.1 above. The proof of finite element error estimates is then simple because the coefficients of these functions are real numbers. The extension to three dimensions is not straightforward, however. Edge singularities contain a coefficient *function* $\gamma = \gamma(x)$ which

has to be approximated [181]. If, additionally, corner singularities appear, then the coefficients of these singular functions are constant. However, the exponents λ_i and the eigenfunctions Φ_i have to be determined numerically [38] and approximate (non-exact) singular functions have to be used [39].

A similar approach is to calculate the singular part of the solution explicitly. In addition to the solution of the eigenvalue problem mentioned in Remark 19.1, this includes the computation of the corresponding coefficient, the so-called stress intensity factor [30, 51].

If the solution u and the right hand side f can be represented by a Fourier series, as in Problem (19.1), (19.2),

$$u = \sum_{i=0}^{\infty} u_i(x_1, x_2) \sin \frac{i\pi}{z_0} x_3, \qquad f = \sum_{i=0}^{\infty} f_i(x_1, x_2) \sin \frac{i\pi}{z_0} x_3,$$

then the coefficients u_i satisfy the boundary value problem

$$-\Delta u_i + \left(\frac{i\pi}{z_0}\right)^2 u_i = f_i \quad \text{in } G, \qquad u_i = 0 \quad \text{on } \partial G;$$

recall that $\Omega = G \times (0, z_0)$. The coefficients u_i, $i = 1, \ldots, N$, can be determined approximately by a finite element method over G. The error in this method consists of the finite element error and a truncation error because only a finite number of coefficients can be calculated. This approach, the *Fourier finite element method*, was analyzed for problems in rotationally symmetric domains in [99, 147, 193]. The functions u_i have singular behaviour near the corners of G which can be treated by mesh refinement [100, 101, 193] or by the singular function method [122, 124].

The idea of *windowing* [11], [59, Section 2.5.3.], [150, pages 286–287] or *local defect correction techniques* [48, 91], [92, pages 293–302], is to solve the problem on an unrefined mesh covering the whole domain and to improve the solution by solving (a) problem(s) in some window(s) in the neighbourhood of the corners or edges.

Other methods include the *hp*-version of the finite element method and the boundary element method, both with anisotropic mesh refinement, see for example [89, 153, 169], and the finite volume method on graded meshes [132].

19.2 Local mesh grading in two dimensions

Local mesh grading near geometrical singularities was first investigated in the two dimensions [28, 158] [150, page 274f.]. Therefore it is convenient for the motivation to discuss first this case.

As pointed out in Remark 19.1, the singular part u_s of the solution u may be represented by

$$u_s = \gamma\, \xi(r) r^{\lambda} \Phi(\phi), \quad \gamma \in \mathbb{R},$$

in the two-dimensional case. We now follow an idea of Oganesyan and Rukhovets [149] and consider the coordinate transformation

$$\left(\frac{r}{R_0}\right)^{\mu} = \frac{\varrho}{R_0}, \quad \mu \in (0, 1]. \tag{19.10}$$

This means that the neighbourhood

$$U = \{x \in \mathbb{R} : \operatorname{dist}(x, C) < R_0\}$$

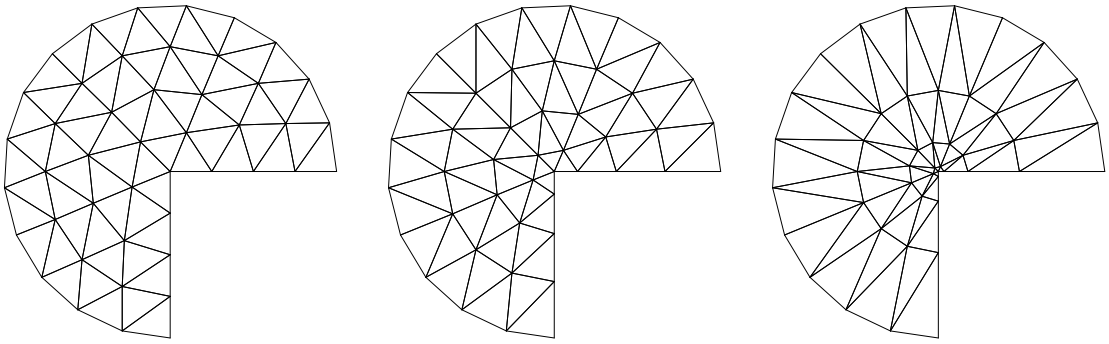

Figure 19.2: Quasi-uniform mesh in the transformed plane (ϱ, ϕ) (left) and graded meshes in the original (r, ϕ) plane: $\mu = 0.7$ (middle) and $\mu = 0.4$ (right).

of the corner $C = (X_1, X_2)$ is transformed into itself, but $u_{\rm s}$ is now

$$u_{\rm s} = u_{\rm s}(\varrho, \phi) = \bar{\gamma}\bar{\xi}(\varrho)\,\varrho^{\lambda/\mu}\Phi(\phi).$$

The advantage is that, in contrast to $\partial^{k+1}u_{\rm s}/\partial r^{k+1}$, the derivatives $\partial^{k+1}u_{\rm s}/\partial\varrho^{k+1}$ $(k = 1, 2, \ldots)$ are square-integrable for sufficiently small values of μ $(\mu < \lambda/k)$. So we can suppose that $u_{\rm s}(\varrho, \phi)$ can be approximated on a quasi-uniform mesh of element size h with optimal order (depending on the degree of the shape functions).

Trying to avoid this coordinate transformation for practical calculations (for example one would also have to transform the input data) has led to the idea of creating the mesh only in the transformed domain, of transforming back immediately and of computing the finite element solution on the transformed mesh but in the original coordinate system. (Actually, we transform only the coordinates of the nodes and connect them again by straight lines.) Two examples of transformed meshes are given in Figure 19.2. In the following, we derive another description of the graded mesh so constructed, in the original coordinates. We try to find a relation between the diameter $\operatorname{diam}(e)$ of an element e and its distance $\operatorname{dist}(e, C)$ from the corner point. (Instead of $\operatorname{dist}(e, C) := \min_{x \in e} |x - C|$ we can use the more easily computed quantity $\min_{i=1,\ldots,n_e} |X_e^{(i)} - C|$, where $\{X_e^{(i)}\}_{i=1}^{n_e}$ is the set of vertices of the element e.)

Elements with a vertex at the corner of the domain are contained in the transformed domain in a circle of radius $\varrho = h$, which means in the original domain

$$\operatorname{diam}(e) \sim h^{1/\mu} \quad \text{if } \operatorname{dist}(e, C) = 0.$$

For elements without a vertex at the corner we find a circular annulus that contains the element and has an inner radius ϱ_i and an outer radius ϱ_o such that $\varrho_o - \varrho_i \sim h$. In the same way we can write for the original domain $r_o - r_i \sim \operatorname{diam}(e)$, $r_o^\mu = \varrho_o$, $r_i^\mu = \varrho_i$. Consequently, we have

$$\frac{h}{\operatorname{diam}(e)} \sim \frac{r_o^\mu - r_i^\mu}{r_o - r_i} = \mu r_*^{\mu-1}$$

for some $r_* \in (r_i, r_o)$. This relation can be rewritten in the form $\operatorname{diam}(e) \sim h r_*^{1-\mu}$. Since $r_i < r_* < r_o = \varrho_o^{1/\mu} \le (2\varrho_i)^{1/\mu} = 2^{1/\mu} r_i$ we get $r_* \sim \operatorname{dist}(e, C)$.

We can summarize and state that within a refinement neighbourhood U around the corner $C := (X_1, X_2)$ the elements e should have a size according to

$$\operatorname{diam}(e) \sim \begin{cases} h^{1/\mu} & \text{if } C \in \overline{e}, \\ h \operatorname{dist}(e, C)^{1-\mu} & \text{if } C \notin \overline{e}, \end{cases} \tag{19.11}$$

where h is the parameter of the family $\mathcal{T}_h$ and μ is the refinement parameter. Note that such meshes have $\mathcal{O}(h^{-2})$ elements. It has been proved in [28, 158] [150, page 274f.] that the error estimates

$$\begin{aligned} \|u - u_h\,; W^{1,2}(\Omega)\| &\lesssim h, && (19.12)\\ \|u - u_h\,; L^2(\Omega)\| &\lesssim h^2, && (19.13) \end{aligned}$$

hold provided that μ is chosen according to

$$\mu < \lambda \qquad (19.14)$$

and that piecewise linear trial functions are used. This type of mesh, with $\mu = \lambda/2$, is also optimal in the sense of $\|u - u_h\,; L^\infty(\Omega)\|$ [167], [190, Section 14].

The easiest way to construct such a mesh is as described by the motivation above: generate a quasi-uniform (ungraded) mesh and move the nodes from U via the coordinate transformation (19.10). This transformation can be written in a programmer's style by

$$\begin{aligned} r &:= [(x_1 - X_1)^2 + (x_2 - X_2)^2]^{1/2},\\ x_1 &:= X_1 + (x_1 - X_1)(r/R_0)^{-1+1/\mu}, \qquad (19.15)\\ x_2 &:= X_2 + (x_2 - X_2)(r/R_0)^{-1+1/\mu}. \end{aligned}$$

Note that the number of elements and nodes remains unchanged and that condition (1.4) (bounded aspect ratio, the bound depends on μ) is still fulfilled after the transformation.

Another variant to construct such meshes is the method of dyadic partitioning [80]: starting with a coarse mesh the elements are divided until condition (19.11) is fulfilled.

19.3 Isotropic and anisotropic mesh grading in three dimensions

When the approach of Subsection 19.2 is extended to our example with a three-dimensional domain we have to distinguish between two types of mesh which can be generated.

1. By describing the meshes via condition (19.11) it is possible to construct a family of isotropic meshes (bounded aspect ratio) and to prove the error estimates (19.12), (19.13), for all $f \in L^2(\Omega)$ if the parameter μ satisfies (19.14) [11, 23, 123]. We suggest that these isotropic meshes should be constructed using the method of dyadic partitioning [80], see Figure 19.3 (left).

   The disadvantage of such meshes is that for $\mu \le 1/3$ the asymptotic number of elements N_{el} as well as the condition number κ of the stiffness matrix increase,

   $$\begin{aligned} &N_{\mathrm{el}} \sim h^{-3}|\ln h|, \quad h^{-d}|\ln h| \lesssim \kappa \lesssim h^{-2-\varepsilon} && \text{for } \mu = \tfrac{1}{3},\\ &N_{\mathrm{el}} \sim h^{-1/\mu}, \qquad\quad h^{1-1/\mu} \lesssim \kappa \lesssim h^{1-1/\mu-\varepsilon} && \text{for } \mu < \tfrac{1}{3}, \end{aligned} \qquad (19.16)$$

   $\varepsilon > 0$ is an arbitrary small number, see [11, 23]. This means that this type of mesh is not optimal for $\mu \le 1/3$.

2. When we consider a neighbourhood of the edge and employ the transformation (19.15) to the nodes of quasi-uniform meshes, we get an anisotropic mesh, see Figure 19.3 (right). Under a maximal angle condition, see page 33, to the elements e, the estimates (19.12), (19.13), have been proved for $\mu < \lambda$ as well, see Remark 19.3 below. The asymptotic

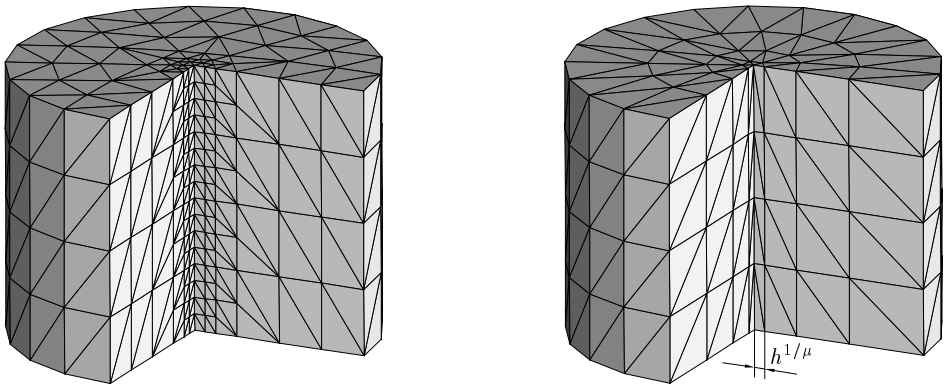

Figure 19.3: Comparison of isotropic (left) and anisotropic (right) mesh grading: meshes.

number of elements $N_{\rm el}$ as well as the condition number κ of the stiffness matrix are in this case optimal for all μ,

$$N_{\rm el} \sim h^{-3}, \quad \kappa \sim h^{-2} \quad \text{for all } \mu \in (0,1]. \tag{19.17}$$

The first statement follows by construction. The estimate of the condition number was originally proved in the preprint version of [19, 20]. Since this version was never published the proof is included in Subsection 20.3.

One can compare both approaches from a theoretical point of view. The conclusions are that the first strategy does not exploit property (19.7), and it has deficiencies for small $\mu \leq 1/3$. The choice $\mu \leq 1/3$ becomes necessary for highly singular solutions of problems with mixed boundary conditions. But all these considerations are in an asymptotic sense where most of the constants are unknown. Therefore we will now compare the strategies in a computational example [15, 18] which was calculated with the finite element package *FEMPS3D*. For a short description of the code see Comment 30.2 on page 172.

Example 19.2 Consider the Laplace equation with essential boundary conditions,

$$-\Delta u = 0 \quad \text{in } \Omega, \qquad u = g \quad \text{on } \partial\Omega,$$

in the three-dimensional domain $\Omega = \{(x_1, x_2, x_3) = (r\cos\phi, r\sin\phi, z) \in \mathbb{R}^3 : r < 1,\, 0 < \phi < 3\pi/2,\, 0 < z < 1\}$. The right hand side g is taken such that

$$u = (10 + z)\, r^{2/3} \sin \tfrac{2}{3}\phi$$

is the exact solution of the problem. It has the typical singular behaviour at the edge. We constructed the three types of mesh discussed above (quasi-uniform, isotropically refined with $\mu = 0.5$, anisotropically refined with $\mu = 0.5$) with different numbers N of unknowns. From the numerical solution and the known exact solution, the energy norm $|u - u_h\,; W^{1,2}(\Omega)|$ of the finite element error was computed. The relative norms

$$|u - u_h\,; W^{1,2}(\Omega)|_{\%} := \frac{|u - u_h\,; W^{1,2}(\Omega)|}{|u_h\,; W^{1,2}(\Omega)|}$$

are arranged in a double logarithmic scale in Figure 19.4. The example verifies the theoretical results (19.8) and (19.12). The anisotropic strategy gives a slightly smaller error. This can be taken as an indication that the isotropic strategy leads to overrefinement near the edge, and that anisotropic meshes are more appropriate to treat edge singularities. □

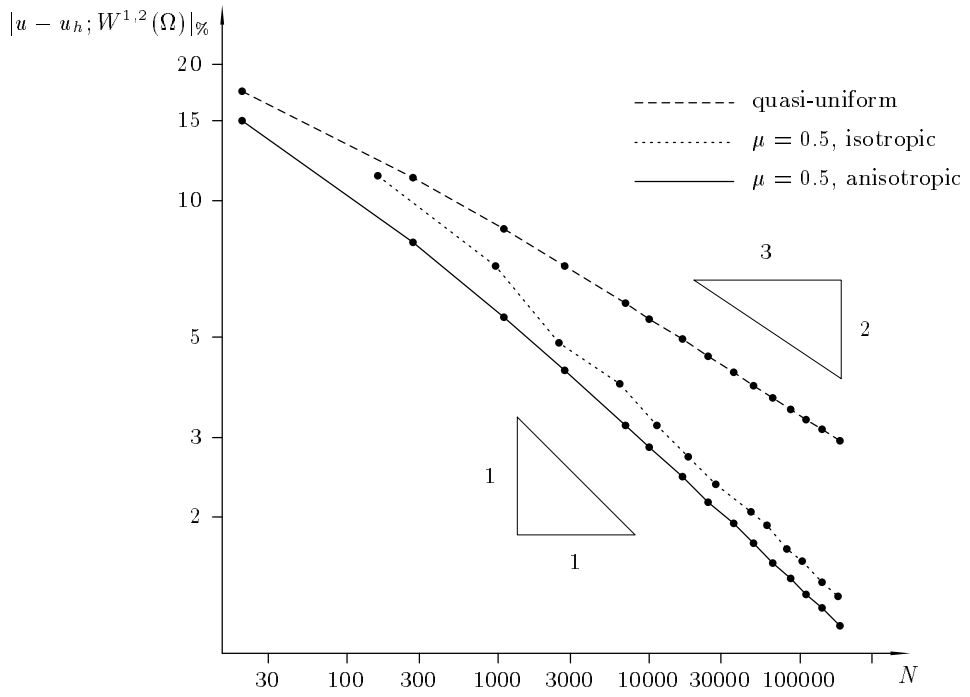

Figure 19.4: Comparison of isotropic and anisotropic mesh grading: diagram.

We end this section with two remarks motivating the extensive treatment of local interpolation error estimates in this monograph.

Remark 19.3 The investigation of the anisotropic mesh refinement strategy led to the development of a basic theory about anisotropic local error estimates for the Lagrange interpolant, see [9]. With these estimates it was possible to prove estimate (19.12) under rather high assumptions on the regularity of the right hand side f. These assumptions were relaxed in [19, 20] where local interpolation error estimates were also proven for functions from weighted Sobolev spaces, see also Subsection 6.2. However, the most interesting case $f \in L^2(\Omega)$ could still not be treated. This is deficient because Nitsche's method for obtaining an $L^2(\Omega)$-estimate of the finite element error is not applicable. Moreover, the refinement condition in [19, 20] is slightly stronger than (19.14). Only after proving anisotropic local estimates for modifications of the Scott-Zhang operator, see Chapter III, was it possible to prove the estimates (19.12) and (19.13) for $f \in L^2(\Omega)$ and under the refinement condition (19.14) [7]. We present this proof in Subsection 20.1.

Remark 19.4 The introductory example (19.1), (19.2), is the simplest one possible for the illustration in this section. It is usually the starting point for the investigation of new methods. A broader class of problems includes arbitrary self-adjoint elliptic operators of second order, mixed boundary conditions, and general polyhedral domains. In [23], the isotropic mesh refinement strategy is investigated comprehensively for such problems. One of the difficulties that arise is that the regularity of the solution u can become so poor that $u \notin W^{s,2}(\Omega)$ for any $s > 3/2$, which causes the Lagrangian interpolation theory to fail. In this case another approximation operator must be employed. The one chosen in [23] was the Scott-Zhang operator [171]. This example further motivates the investigation in Chapter III.

20 The Poisson problem with edge singularities

20.1 The case of (multi-)linear trial functions

Consider the Poisson problem

$$\Delta u = f \quad \text{in } \Omega, \qquad u = 0 \quad \text{on } \Gamma_1, \qquad \frac{\partial u}{\partial n} = 0 \quad \text{on } \Gamma_2 := \partial\Omega \setminus \Gamma_1, \tag{20.1}$$

over a bounded polyhedral domain $\Omega \subset \mathbb{R}^3$. For simplicity, let Ω be a prismatic domain,

$$\Omega = G \times Z, \tag{20.2}$$

where $G \subset \mathbb{R}^2$ is a polygonal domain and $Z = (0, z_0) \subset \mathbb{R}^1$ is an interval. This restriction is made because we want to focus on edge singularities in this section. More general domains are considered in Section 21.

In the previous section we summarized already some facts about the pure Dirichlet problem, $\Gamma_2 = \emptyset$. We discussed the singular behaviour near edges for $f \in L^2(\Omega)$, see (19.3)–(19.7) and Remark 19.1. Furthermore, we motivated in Subsection 19.3 the utilization of anisotropic finite element meshes by theoretical considerations and by a numerical test example. Finally, we reviewed previous contributions of the author to the numerical analysis of (isotropic and anisotropic) mesh refinement techniques [3, 7, 9, 11, 15, 18, 19, 20, 23], see, for example, Remarks 19.3 and 19.4, and we pointed to related literature.

In all previous papers, the investigation of anisotropic mesh refinement near edges is restricted to the case $k = 1$, (multi-)linear elements. The final result was derived in [7] as an application of the modified Scott-Zhang operators S_h and E_h. We present this estimate next. In Subsection 20.2 we discuss how the case $k \geq 2$ can be treated.

Consider the model situation that

$$\Gamma_1 = \{x \in \partial\Omega : 0 < x_3 < z_0\}. \tag{20.3}$$

We assume that the cross-section G has only one corner with interior angle $\omega > \pi$ at the origin. Thus Ω has only one "singular edge" E which is part of the x_3-axis. The case of several singular edges parallel to the x_3-axis does not introduce additional difficulties because the singularities are of local nature.

Let $V_0 \subset W^{1,2}(\Omega)$ be the space of all $W^{1,2}(\Omega)$-functions which vanish at the Dirichlet part of the boundary, and introduce the bilinear form $a(.,.) : V_0 \times V_0 \to \mathbb{R}$ by $a(u,v) := \int_\Omega \nabla u \cdot \nabla v$. Then the variational form of problem (20.1) is given by:

$$\textit{Find } u \in V_0 : a(u,v) = (f,v)_\Omega \quad \forall v \in V_0. \tag{20.4}$$

The existence of a unique variational solution u follows from the Lax-Milgram lemma. The properties of the solution u can be described favourably using the weighted Sobolev spaces $V^{\ell,p}_\beta(\Omega)$ introduced in Section 3.

Lemma 20.1 *Assume that (20.2) and (20.3) are satisfied. Then the solution u of (20.4) satisfies*

$$\frac{\partial u}{\partial x_i} \in V^{1,2}_{\beta_2}(\Omega), \qquad \left\| \frac{\partial u}{\partial x_i}; V^{1,2}_{\beta_2}(\Omega) \right\| \lesssim \|f; L^2(\Omega)\|, \quad i = 1,2,\ \beta_2 > 1 - \lambda, \tag{20.5}$$

$$\frac{\partial u}{\partial x_3} \in V^{1,2}_0(\Omega), \qquad \left\| \frac{\partial u}{\partial x_3}; V^{1,2}_0(\Omega) \right\| \lesssim \|f; L^2(\Omega)\|, \tag{20.6}$$

where $\lambda = \pi/\omega$.

The index of β_2 indicates that the weight r^{β_2} belongs to *second* order derivatives, compare Assumption 20.6 in Subsection 20.2.

Proof The singularity of the edge at the x_3-axis can be described by (20.5), (20.6), see for example [116, Sections 26 and 30], Comment 22.3 on page 123 or [19, Section 2]. One can show by mirror techniques that the corners and edges at the bottom and the top face do not introduce singularities, see also Comment 22.2 on page 122. Finally, the remaining edges parallel to x_3-axis were assumed to have an opening angle smaller than π such that no singularity occurs. ∎

We define now a family of meshes of tensor product type, $\mathcal{T}_h$, see Sections 3 and 11 for a definition of this type. Such a mesh can be constructed by introducing in G the standard graded mesh for two-dimensional corner problems, see the end of Subsection 19.2, which is then extended in the third direction using a uniform mesh size h. In this way we obtain a *pentahedral or*, by dividing each pentahedron, a *tetrahedral* triangulation of Ω, see Figure 19.3 on page 101 for an illustration. The grading near the singular edge E is described by a parameter $\mu \in (0,1]$ such that the elements of the mesh $\mathcal{T}_h$ satisfy the following relations:

$$h_{1,e} \sim h_{2,e} \sim \begin{cases} h^{1/\mu} & \text{if } \operatorname{dist}(e,E) = 0, \\ h(\operatorname{dist}(e,E))^{1-\mu} & \text{if } 0 < \operatorname{dist}(e,E) \lesssim 1, \\ h & \text{if } \operatorname{dist}(e,E) \sim 1. \end{cases} \qquad h_{3,e} \sim h. \tag{20.7}$$

By

$$V_{0h} := \{v_h \in V_0 : v_h|_e \in \mathcal{P}_{1,e} \quad \forall e \in \mathcal{T}_h\}$$

we define the standard finite element space $V_{0h} \subset \mathcal{C}(\overline{\Omega})$ over $\mathcal{T}_h$. We derive now an interpolation result for the solution of (20.4).

Theorem 20.2 *Let u be the solution of (20.4) and $k = 1$ (multi-linear trial functions). Then the estimate*

$$|u - \mathrm{E}_h u; W^{1,2}(\Omega)| \lesssim h \, \|f; L^2(\Omega)\|$$

holds if $\mu < \lambda$. The operator E_h was defined in Section 15.

Proof We reduce the estimation of the global error to the evaluation of the local errors and distinguish between the elements far from the edge E and the elements close to E. Moreover, we write shortly r_e for $\operatorname{dist}(e,E)$.

For all elements e with $\overline{S_e} \cap E = \emptyset$ we can use Theorem 15.1 with $m = k = 1$ and $\ell = p = q = 2$:

$$\begin{aligned} |u - \mathrm{E}_h u; W^{1,2}(e)| &\lesssim \sum_{|\alpha|=1} h_e^\alpha |D^\alpha u; W^{1,2}(S_e)| \\ &\lesssim \sum_{i=1}^{2} h_{i,e} r_e^{-\beta_2} \left| \frac{\partial u}{\partial x_i}; V_{\beta_2}^{1,2}(S_e) \right| + h_{3,e} \left| \frac{\partial u}{\partial x_3}; V_0^{1,2}(S_e) \right| \end{aligned} \tag{20.8}$$

for any $\beta_2 > 1 - \lambda$. Here, we have used the fact that $r_e \lesssim \operatorname{dist}(S_e, E)$ holds, which follows from

$$r_e \le \operatorname{dist}(S_e, E) + h_{1,e'} \sim \operatorname{dist}(S_e, E) + h\,[\operatorname{dist}(S_e, E)]^{1-\mu}$$

for sufficiently small h, compare also Figure 11.3 on page 68 for an illustration. We apply now the assumption (20.7) and obtain for $r_e \lesssim 1$ and $\beta_2 = 1-\mu$ the relation $h_{i,e} r_e^{-\beta_2} \sim h r_e^{1-\mu-\beta_2} = h$

$(i = 1, 2)$. The choice $\beta_2 = 1 - \mu$ is admissible due to the refinement condition $\mu < \lambda$. In the case $r_e \sim 1$ we have also $h_{i,e} r_e^{-\beta_2} \lesssim h$. Combining this with (20.8) we obtain

$$|u - \mathrm{E}_h u; W^{1,2}(e)| \lesssim h \sum_{i=1}^{2} \left| \frac{\partial u}{\partial x_i}; V^{1,2}_{\beta_2}(S_e) \right| + h \left| \frac{\partial u}{\partial x_3}; V^{1,2}_{0}(S_e) \right|. \tag{20.9}$$

Consider now the elements e with $\overline{S_e} \cap E \neq \emptyset$. We use the triangle inequality and Lemma 15.3 with $m = k = 1$, $p = q = 2$, $\beta_2 \in (1 - \lambda, 1)$:

$$\begin{aligned} |u - \mathrm{E}_h u; W^{1,2}(e)| &\lesssim |u; W^{1,2}(e)| + |\mathrm{E}_h u; W^{1,2}(e)| \\ &\lesssim \sum_{|\alpha|=1} \|D^\alpha u, L^2(e)\| + h_{1,e}^{-\beta_2} \sum_{|\alpha|=1} h_e^\alpha \|D^\alpha u, V^{1,2}_{\beta_2}(S_e)\|. \end{aligned} \tag{20.10}$$

For the first term we use that $r \lesssim h_{1,e}$ in e and $1 - \beta_2 > 0$ and obtain

$$\begin{aligned} \sum_{|\alpha|=1} \|D^\alpha u, L^2(e)\| &\lesssim \sum_{i=1}^{2} h_{1,e}^{1-\beta_2} \left\| \frac{\partial u}{\partial x_i}; V^{0,2}_{\beta_2 - 1}(e) \right\| + h_{1,e} \left\| \frac{\partial u}{\partial x_3}; V^{0,2}_{-1}(e) \right\| \\ &\lesssim h \sum_{i=1}^{2} \left\| \frac{\partial u}{\partial x_i}; V^{1,2}_{\beta_2}(e) \right\| + h \left\| \frac{\partial u}{\partial x_3}; V^{1,2}_{0}(e) \right\|. \end{aligned} \tag{20.11}$$

We also used that $h_{1,e}^{1-\beta_2} \sim h^{(1-\beta_2)/\mu} = h$ for $\beta_2 = 1 - \mu$. The second term is treated with similar arguments:

$$\begin{aligned} h_{1,e}^{-\beta_2} \sum_{|\alpha|=1} h_e^\alpha \|D^\alpha u, V^{1,2}_{\beta_2}(S_e)\| &\lesssim \sum_{i=1}^{2} h_{1,e}^{1-\beta_2} \left\| \frac{\partial u}{\partial x_i}; V^{1,2}_{\beta_2}(S_e) \right\| + h_{1,e}^{-\beta_2} h \left\| \frac{\partial u}{\partial x_3}; V^{1,2}_{\beta_2}(S_e) \right\| \\ &\lesssim h \sum_{i=1}^{2} \left\| \frac{\partial u}{\partial x_i}; V^{1,2}_{\beta_2}(S_e) \right\| + h \left\| \frac{\partial u}{\partial x_3}; V^{1,2}_{0}(S_e) \right\|. \end{aligned} \tag{20.12}$$

The last term was estimated using $r^{\beta_2} \leq h_{1,e}^{\beta_2}$.

Inserting (20.11) and (20.12) in (20.10) we find that (20.9) (with full norms instead of seminorms at the right hand side) holds for elements with $\overline{S_e} \cap E \neq \emptyset$ as well. Summing up over all elements we obtain

$$|u - \mathrm{E}_h u; W^{1,2}(\Omega)| \lesssim h \sum_{i=1}^{2} \left\| \frac{\partial u}{\partial x_i}; V^{1,2}_{\beta_2}(\Omega) \right\| + h \left\| \frac{\partial u}{\partial x_3}; V^{1,2}_{0}(\Omega) \right\|,$$

$\beta_2 = 1 - \mu \in (1 - \lambda, 1)$. Here we used that any patch S_e overlaps only with a finite number (independent of h) of patches $S_{e'}$. By applying Lemma 20.1 the theorem is proved. ∎

The finite element solution u_h is determined by:

$$\textit{Find } u_h \in V_{0h} : a(u_h, v_h) = (f, v_h)_\Omega \quad \forall v_h \in V_{0h}. \tag{20.13}$$

Corollary 20.3 *Let u be the solution of (20.4) and let u_h be the finite element solution defined by (20.13). Assume that the mesh is refined according to $\mu < \lambda$. Then the finite element error can be estimated by*

$$\begin{aligned} |u - u_h; W^{1,2}(\Omega)| &\lesssim h \, \|f; L^2(\Omega)\|, \\ \|u - u_h; L^2(\Omega)\| &\lesssim h^2 \, \|f; L^2(\Omega)\|. \end{aligned}$$

Proof The first estimate follows from Theorem 20.2 via the projection property of the finite element method. Note that $\mathrm{E}_h u \in V_{0h}$ due to (20.3). The $L^2(\Omega)$-estimate is obtained by Nitsche's method. ∎

Remark 20.4 By analogy one can prove for $\lambda < \mu \leq 1$ that

$$\begin{aligned} |u - u_h; W^{1,2}(\Omega)| &\lesssim h^{\lambda/\mu-\varepsilon} \|f; L^2(\Omega)\|, \\ \|u - u_h; L^2(\Omega)\| &\lesssim h^{2(\lambda/\mu-\varepsilon)} \|f; L^2(\Omega)\|, \end{aligned}$$

for arbitrary small $\varepsilon > 0$. That means that we get for the unrefined mesh ($\mu = 1$) only an approximation order $\lambda - \varepsilon$ ($W^{1,2}(\Omega)$-norm) or $2(\lambda - \varepsilon)$ ($L^2(\Omega)$-norm). We conjecture that the ε can be omitted. But this needs another way of proof, for example using the theory of interpolation spaces, compare [28] for the two-dimensional case. However, one can show by an example that these estimates cannot be improved further [3]. Numerical tests support the results, see Example 19.2 and [9, 15, 20].

Remark 20.5 Consider other variants of boundary conditions.

1. If $\Gamma_1 \subset \{x \in \partial\Omega : x_3 = 0 \vee x_3 = z_0\}$, then $\mathrm{S}_h u \in V_{0h}$ and the whole theory can be applied as well, provided that (20.5) and (20.6) can be shown for this case as well. (This situation is not covered by the theory reviewed in Comment 22.3 on page 123.)

   Note that we used in the proof of Theorem 20.2 only the following properties of E_h:

$$\begin{aligned} |u - \mathrm{E}_h u; W^{1,2}(e)| &\lesssim \sum_{|\alpha|=1} h_e^{\alpha} |D^{\alpha} u; W^{1,2}(S_e)|, \\ |\mathrm{E}_h u; W^{1,2}(e)| &\lesssim h_{1,e}^{-\beta_2} \sum_{|\alpha|=1} \|D^{\alpha} u, V_{\beta_2}^{1,2}(S_e)\|. \end{aligned}$$

   Both estimates hold true for S_h as well, see Theorem 13.3 and Lemma 13.5.

   We point out that in particular the first of these two estimates, the anisotropic local interpolation estimate, is an essential ingredient of the proof of the optimal global error estimate. This estimate is neither satisfied for E_h replaced by I_h (see Sections 4 and 6) nor for Z_h, C_h, or O_h (see the discussion in Section 16).

2. Conditions of third kind can be treated like Neumann boundary conditions.

3. If the type of the boundary condition changes at the edge E we can proceed in the same way as described by Lemma 20.1 (see also Comment 22.3 on page 123), Theorem 20.2 and Corollary 20.3. We have only to set $\lambda = \pi/(2\omega)$.

   Note that in this case edges produce a singularity if $\omega > \pi/2$. Therefore it is very likely that more than one singular edge has to be treated.

4. If Dirichlet boundary conditions are given on (parts of) both $\{x \in \partial\Omega : 0 < x_3 < z_0\}$ and $\{x \in \partial\Omega : x_3 = 0 \vee x_3 = z_0\}$ then neither $\mathrm{S}_h u \in V_{0h}$ nor $\mathrm{E}_h u \in V_{0h}$. In such cases we have to modify S_h or E_h near the Dirichlet boundary, as it was done by Clément for C_h [64]. But we will not develop this here.

20.2 Higher order trial functions

We will now discuss the case of higher order trial functions, $k \geq 2$. On the one hand, this case simpler than $k = 1$ since we can use the Lagrange interpolant I_h (when $\lambda > 1/2$) to obtain optimal interpolation error estimates. The difficulty with I_h mentioned in Remarks 19.3 and 20.5 (Item 1) do not occur. However, the critical point for the case $k \geq 2$ is the description of all singularities appearing. Therefore, let us focus on edge singularities and assume for the moment the following property of u which is a straightforward generalization of (20.5), (20.6). For a discussion of this assumption see Examples 20.9 and 20.10 at the end of this subsection, and Comment 22.3 on page 123.

Assumption 20.6 *The function u has only one singularity at $E = \{x \in \partial\Omega : x_1 = x_2 = 0\}$. There holds*

$$u \in V^{k+1,2}_{\beta_{k+1}}(\Omega), \qquad \frac{\partial u}{\partial x_3} \in V^{k,2}_{\beta_k}(\Omega), \quad \ldots, \quad \frac{\partial^k u}{\partial x_3^k} \in V^{1,2}_{\beta_1}(\Omega),$$

where $\beta_n = \max\{n + \beta_*;\ 0\}$, $\beta_* > -\lambda - 1$. Reformulated, this means for all α with $|\alpha| \leq k+1$

$$D^\alpha u \in V^{0,2}_{\beta_\alpha}(\Omega), \qquad \beta_\alpha = \max\{\alpha_1 + \alpha_2 + \beta_*;\ 0\}, \qquad \beta_* > -\lambda - 1. \tag{20.14}$$

Then we obtain the following interpolation error estimate.

Theorem 20.7 *Let u satisfy Assumption 20.6 with some $\lambda > 1/2$. Assume that the mesh is constructed as described in Subsection 20.1. For $k \geq 2$ the interpolation error estimate*

$$|u - \mathrm{I}_h u; W^{1,2}(\Omega)| \lesssim h^k \sum_{|\alpha|=k+1} \|D^\alpha u; V^{0,2}_{\beta_\alpha}(\Omega)\| \tag{20.15}$$

holds provided that the grading parameter μ satisfies

$$\mu < \frac{\lambda}{k} \quad \text{if } \lambda \leq k, \qquad \mu = 1 \quad \text{if } \lambda > k. \tag{20.16}$$

Proof The assertion is clear for $\lambda > k$ because we have a quasi-uniform mesh and $u \in W^{k+1,2}(\Omega)$ in this case.

Let now $\lambda \leq k$ and consider all elements e which do not touch the edge E. We use Theorem 6.4, (20.7), and Assumption 20.6 in order to get

$$\begin{aligned} |u - \mathrm{I}_h u; W^{1,2}(e)| &\lesssim \sum_{|\alpha|=k} \sum_{|\gamma|=1} h_e^\alpha \|D^{\alpha+\gamma} u; L^2(e)\| && (20.17)\\ &\lesssim h^k \sum_{|\alpha|=k} \sum_{|\gamma|=1} (\mathrm{dist}\,(e,E))^{(1-\mu)(\alpha_1+\alpha_2)} \|D^{\alpha+\gamma} u; L^2(e)\| \\ &\lesssim h^k \sum_{|\alpha|=k} \sum_{|\gamma|=1} \|D^{\alpha+\gamma} u; V^{0,2}_{(1-\mu)(\alpha_1+\alpha_2)}(e)\|. && (20.18) \end{aligned}$$

We show now

$$(1-\mu)(\alpha_1 + \alpha_2) \geq \beta_{\alpha+\gamma} \tag{20.19}$$

with $\beta_{\alpha+\gamma}$ as introduced in (20.14). From $\mu < \lambda/k$ we get $-\lambda - 1 < -k\mu - 1$. Hence we can choose $\beta_* \in (-\lambda - 1, -k\mu - 1]$ such that

$$-\frac{\beta_* + 1}{\mu} \geq k \tag{20.20}$$

and conclude $\alpha_1+\alpha_2 \le k \le -(\beta_*+1)/\mu < -(\beta_*+\gamma_1+\gamma_2)/\mu$, $(1-\mu)(\alpha_1+\alpha_2) > \beta_*+\alpha_1+\alpha_2+\gamma_1+\gamma_2$. Since $\mu \le 1$ we obtain also $(1-\mu)(\alpha_1+\alpha_2) \ge 0$. These estimates together give (20.19). With (20.18) we get

$$|u - \mathrm{I}_h u; W^{1,2}(e)| \lesssim h^k \sum_{|\alpha|=k+1} \|D^\alpha u; V^{0,2}_{\beta_\alpha}(e)\|. \tag{20.21}$$

If the element touches the edge E, $E \cap \overline{e} \neq \emptyset$, we use Theorem 6.9 and Assumption 20.6 in order to obtain

$$|u - \mathrm{I}_h u; W^{1,2}(e)| \lesssim \sum_{|\alpha|=k} \sum_{|\gamma|=1} h_e^\alpha h_{1,e}^{-\beta_{\alpha+\gamma}} \|D^{\alpha+\gamma} u; V^{0,2}_{\beta_{\alpha+\gamma}}(e)\|. \tag{20.22}$$

This estimate is valid for $\beta_{\alpha+\gamma} < k - 1/2$ only, see the assumption in (6.28), which means for $\alpha = (k,0,0)$, $\gamma = (1,0,0)$ that $\beta_* + (k+1) < k - 1/2$, $\beta_* < -3/2$. Together with $\beta_* > -\lambda - 1$ this yields the assumption made, $\lambda > 1/2$. Now we simplify,

$$h_e^\alpha h_{1,e}^{-\beta_{\alpha+\gamma}} = \begin{cases} h_e^\alpha \lesssim h^k & \text{if } \beta_{\alpha+\gamma} = 0, \\ h_{1,e}^{-\beta_*-\gamma_1-\gamma_2} h_{3,e}^{\alpha_3} \lesssim h^{\alpha_3-(\beta_*+\gamma_1+\gamma_2)/\mu} & \text{if } \beta_{\alpha+\gamma} = \beta_*+\alpha_1+\alpha_2+\gamma_1+\gamma_2. \end{cases}$$

The last exponent can be simplified further by using (20.20) and $|\gamma| = 1$, namely $\alpha_3 - (\beta_* + \gamma_1+\gamma_2)/\mu \ge -(\beta_*+1)/\mu \ge k$. By inserting this into (20.22) we obtain that (20.21) holds also in this case. By summing up all the elementwise estimates we get (20.15). ∎

The case $\lambda \le 1/2$ was excluded in Theorem 20.7 since the Lagrangian interpolation operator can be applied only for continuous functions. For mixed boundary value problems, where $\lambda = \pi/(2\omega)$, this means $\omega < \pi$. We cannot treat concave edges in this way. This restriction can be overcome when a modified Scott-Zhang interpolant is used instead of the Lagrange interpolant, as in Theorem 20.2.

Theorem 20.8 *Let u satisfy Assumption 20.6 with some $\lambda \le 1$. Assume that the mesh is constructed as described in Subsection 20.1 and that the grading parameter μ satisfies (20.16). Then the estimates*

$$\begin{aligned} |u - \mathrm{S}_h u; W^{1,2}(\Omega)| &\lesssim h^k \sum_{|\alpha|=k+1} \|D^\alpha u; V^{0,2}_{\beta_\alpha}(\Omega)\| \\ |u - \mathrm{E}_h u; W^{1,2}(\Omega)| &\lesssim h^k \sum_{|\alpha|=k+1} \|D^\alpha u; V^{0,2}_{\beta_\alpha}(\Omega)\| \end{aligned}$$

hold for all $k \ge 1$.

Proof For $k = 1$ the theorem was verfied in Subsection 20.1. The ideas to prove this theorem for $k \ge 2$ are contained in the proofs of Theorems 20.2 and 20.7. Elements e with $\overline{S_e} \cap E = \emptyset$ can be treated as in the proof of Theorem 20.7, and the remaining elements as in the proof of Theorem 20.2. Note that we have assumed $\lambda \le 1$ in order to obtain $h_{1,e} \sim h^{1/\mu} \le h^{k/\lambda} \le h^k$ in front of the term $\|\partial u/\partial x_3; V_0^{1,2}(\Omega)\|$. ∎

Let us discuss now applications of the last two theorems.

Example 20.9 Assumption 20.6 covers the typical behaviour of the solution of (20.4) near an edge, at least for Dirichlet and mixed boundary conditions. This can be derived from the study of such problems in a dihedral angle $\{x = (r\cos\phi, r\sin\phi, x_3) \in \mathbb{R}^3 : 0 < r < \infty, 0 < \phi <$

$\omega, x_3 \in \mathbb{R}\}$, see Comment 22.3 on page 123 and also Item 3 in Remark 20.5. This means, if $\operatorname{supp} f \subset (\Omega \cup E)$ then one concludes

$$\begin{aligned} |u - u_h; W^{1,2}(\Omega)| &\lesssim h^k, \\ \|u - u_h; L^2(\Omega)\| &\lesssim h^{k+1}. \end{aligned}$$

The first estimate is obtained for $k \geq 2$, $\lambda > 1/2$, from Theorem 20.7, and for $k \geq 1$, $\lambda \leq 1$, from Theorem 20.8. The second estimate is proved by Nitsche's method. □

Example 20.10 Consider $k = 2$, general $f \in V_0^{1,2}(\Omega)$ (the weight has to be taken with respect to all singular edges), and assume (20.3). Then all edges E_j which are parallel to the x_3-axis and with interior angle $\omega_j > \pi/2$ are singular edges. The behaviour of the solution near these edges is described by Assumption 20.6, see Comment 22.3 on page 123. All edges which are orthogonal to the x_3-axis are non-singular since the leading terms of the decomposition are $r \sin \phi = y$ and $r^3 \ln r \, \Phi(\phi) \in W^{4-\varepsilon,2}(\Omega)$. The corner singularities are included in the edge singularities described above, see Comment 22.2 on page 122. Consequently, the only singularities are near the singular edges. We can apply the mesh refinement as described above and obtain

$$\begin{aligned} |u - u_h; W^{1,2}(\Omega)| &\lesssim h^2, \\ \|u - u_h; L^2(\Omega)\| &\lesssim h^3. \end{aligned}$$

from Theorem 20.7. □

In the general case we have to treat edge and corner singularities where the singular edges can also intersect. A suitable refinement strategy is described for $k = 1$ in the next section. We conjecture that this strategy is also adequate for $k \geq 2$ (with μ depending on k as in (20.16)). For $\lambda > 1/2$ the convergence can be proved by using the Lagrange interpolation operator, see [21, Proof of Theorem 5.1] for $k = 1$. For $k \geq 2$ the proof is even simpler than for $k = 1$ since the Hölder technique [21, Proof of Theorem 5.1] can be avoided, see the proof of Theorem 20.7. The critical part is the proof of the corresponding anisotropic regularity results.

For $\lambda \leq 1/2$ the Lagrangian interpolation operator cannot be applied. Since the modified Scott-Zhang operators are investigated for meshes of tensor product type only, it is not clear how to prove convergence in this case.

20.3 Condition number of the stiffness matrix

Consider the nodal basis $\{\varphi_i(x)\}_{i=1}^N$ with $\varphi_i(X^{(j)}) = \delta_{i,j}$ in V_h (or V_{0h}, respectively), with N being the number of degrees of freedom. Thus each function $v_h \in V_h$ (or V_{0h}) can be represented by $v_h(x) = \sum_{i=1}^N v_i \varphi_i(x)$, with $v_i = v_h(X^{(i)})$.

The stiffness matrix $K := (a_{i,j})_{i,j=1}^N$ has the entries $a_{i,j} = a(\varphi_j, \varphi_i)$. We want to estimate the condition number κ of this matrix,

$$\kappa := \frac{\lambda_{\max}(K)}{\lambda_{\min}(K)} \tag{20.23}$$

where $\lambda_{\max}$ and $\lambda_{\min}$ are the maximal and minimal eigenvalues of K, respectively.

Lemma 20.11 *The condition number of the stiffness matrix A which is related to problem (20.1) is bounded by*

$$\kappa \lesssim h^{-2}, \tag{20.24}$$

That means, the order of the condition number is the same as in the case of smooth solutions and isotropic meshes.

Proof Due to the boundedness and the ellipticity of the bilinear form we get

$$a(v_h\,,v_h) \sim \|v_h\,;W^{1,2}(\Omega)\|^2 \quad \forall v_h \in V_h \ \ (V_{0h}).$$

Denoting by $\langle\ .\ ,\ .\ \rangle$ the Euclidean scalar product in $\mathbb{R}^N$ and by $\underline{v} := (v_i)_{i=1}^N$ the grid function related to v_h, we obtain the identity $a(v_h\,,v_h) = \langle K\underline{v},\underline{v}\rangle$ and get by using the Rayleigh quotient

$$\begin{aligned}\lambda_{\max} &\lesssim \max_{\underline{v}\in\mathbb{R}^N} \frac{\|v_h\,;W^{1,2}(\Omega)\|^2}{\langle\underline{v},\underline{v}\rangle},\\ \lambda_{\min} &\gtrsim \min_{\underline{v}\in\mathbb{R}^N} \frac{\|v_h\,;W^{1,2}(\Omega)\|^2}{\langle\underline{v},\underline{v}\rangle}.\end{aligned}$$

We are now looking for an upper and a lower bound of $\|v_h\,;W^{1,2}(\Omega)\|^2$ in terms of $\langle\underline{v},\underline{v}\rangle$.

Using the inverse inequality we have

$$\|v_h\,;W^{1,2}(\Omega)\|^2 = \sum_{e\in\mathcal{T}_h} \|v_h\,;W^{1,2}(e)\|^2 \lesssim \sum_{e\in\mathcal{T}_h} h_{1,e}^{-2}\|v_h\,;L^2(e)\|^2. \tag{20.25}$$

On the reference element $\hat{e}$ we have

$$\|\hat{v}_h\,;L^2(\hat{e})\|^2 \sim \sum_{j\,\in I_e} v_j^2, \tag{20.26}$$

since norms in N_e-dimensional spaces are equivalent. I_e is the set of numbers of the nodes belonging to e. Transforming (20.26) to e we get

$$\|v_h\,;L^2(e)\|^2 \sim \mathrm{meas}(e) \sum_{j\,\in I_e} v_j^2. \tag{20.27}$$

Inserting (20.27) into (20.25) and using $\mathrm{meas}(e) \sim h_{1,e}^2 h$ and that each node belongs only to a bounded number of elements we get

$$\begin{aligned}\|v_h\,;W^{1,2}(\Omega)\|^2 &\lesssim h\langle\underline{v},\underline{v}\rangle\\ \lambda_{\max} &\lesssim h\end{aligned} \tag{20.28}$$

For the lower estimate of $\|v_h\,;W^{1,2}(\Omega)\|^2$ we use the embedding

$$W^{1,2}(\Omega) \hookrightarrow W^{1,2}_{1-\delta}(\Omega) \hookrightarrow W^{0,2}_{-\delta}(\Omega)$$

which holds for $0 \le \delta < 1$ [116, Subsection 0.11]. Consequently, we have

$$\|v_h\,;W^{1,2}(\Omega)\|^2 \gtrsim \|r^{-\delta}v_h\,;L^2(\Omega)\|^2. \tag{20.29}$$

Denoting $R_e := \max_{x\in e} r(x)$, and using (20.27) we get from (20.29)

$$\|v_h\,;W^{1,2}(\Omega)\|^2 \gtrsim \sum_{i\in I} R_e^{-2\delta}\|v_h\,;L^2(e)\|^2 \gtrsim \sum_{i\in I} R_e^{-2\delta} h_{1,e}^2 h \sum_{j\,\in I_e} v_j^2$$

Using $h_{1,e} \gtrsim h R_e^{1-\mu}$ (which follows from (20.7) and holds for all $e \in I$) and choosing $\delta = 1-\mu$, we obtain

$$\begin{aligned}\|v_h\,;W^{1,2}(\Omega)\|^2 &\gtrsim h^3\langle\underline{v},\underline{v}\rangle\\ \lambda_{\min} &\gtrsim h^3\end{aligned} \tag{20.30}$$

independent of the choice of μ.

From (20.28) and (20.30) we get the estimate (20.24). ∎

In the proof we used some ideas of the proof for the case of mesh grading in two dimensions [150]. With analogous arguments we had investigated in [11] the case of *isotropic* mesh grading near edges. In contrast to Lemma 20.11 we get $\lambda_{\min} \gtrsim h^3$ for isotropic elements only in the case $\mu > 1/3$, see [11]. For $\mu \leq 1/3$ we obtain $\lambda_{\min} \gtrsim h^{1/\mu+\varepsilon}$ and thus $\kappa \gtrsim h^{1-1/\mu+\varepsilon}$, $\varepsilon > 0$ arbitrarily small. But we stress that Lemma 20.11 is related to anisotropic mesh refinement. The author is not aware of a similar result for such meshes.

21 Diffusion problems in domains with corners and edges

In Sections 19 and 20 we considered the Poisson problem in a prismatic polyhedral domain $\Omega \subset \mathbb{R}^3$. There, we focused on the approximation of edge singularities by using anisotropic finite element meshes. The aim of this section is to treat a general diffusion problem,

$$-\sum_{i,j=1}^{3} a_{i,j} \frac{\partial^2 u}{\partial x_i \partial x_j} = f \quad \text{in } \Omega, \qquad u = 0 \quad \text{on } \partial\Omega, \tag{21.1}$$

where $\Omega \subset \mathbb{R}^3$ is an *arbitrary polyhedral domain*. The coefficients $a_{i,j} = a_{j,i}$ are assumed to be constant. The operator shall be elliptic, $\sum_{i,j=1}^{3} a_{i,j}\xi_i\xi_j \geq C_0 > 0$ for all $\xi_1, \xi_2, \xi_3 \in \mathbb{R}$ such that $\xi_1^2 + \xi_2^2 + \xi_3^2 = 1$. If Ω is not convex then the solution has in general singular behaviour near the edges and the corners. We summarize here the results which are published in [21]. Therefore we restrict ourselves to tetrahedral meshes and to linear shape functions ($k = 1$).

The idea is quite obvious, we want to combine anisotropic mesh refinement near singular edges with isotropic refinement near corners. One difficulty is to describe and to construct the meshes in the transition from anisotropy to isotropy. A complication is that corner singularities can be stronger or weaker than edge singularities. In [23], where isotropic mesh refinement was considered, this was circumvented by controlling the refinement with the strongest singularity appearing in the problem under consideration. We try to avoid this by allowing different refinement parameters in different regions. Moreover, in Section 20 the tensor product character of prismatic domains was used to describe the mesh. But these orthogonalities are no longer available because we want to treat general polyhedral domains.

A second difficulty is the choice of an approximation operator.

- For linear shape functions we have applied in Section 20 the operators S_h and E_h. This allowed us to prove the desired error estimate under the optimal grading condition (20.16). But these operators were investigated in Chapter III for meshes of tensor product type only. It is not clear how to extend this theory to treat the more general meshes which are necessary here.

- When we use the Lagrangian interpolation operator I_h then one of the key estimates,

$$|u - \mathrm{I}_h u; W^{1,2}(e)| \lesssim (\mathrm{meas}_3 e)^{1/2-1/p} \sum_{|\alpha|=1} h^\alpha |D^\alpha u; W^{1,p}(e)|, \tag{21.2}$$

  is not valid for $p = 2$ but for $p > 2$ only. Therefore we need the regularity theory in Banach spaces $W^{\ell,p}(\Omega)$ with $p > 2$. In particular, the regular part u_{r} of the solution must satisfy $u_r \in W^{2,p}(\Omega)$. For this we assume that the right hand side f of problem (21.1) satisfies

$$f \in L^p(\Omega) \quad \text{for some } p > 2. \tag{21.3}$$

  The drawback is that we obtain the optimal convergence order only with a grading condition which is slightly too strong.

In any a-priori technique for coping with edge and corner singularities we assume some knowledge about the singular exponents. In particular, for mesh refinement techniques a lower bound of the leading exponent is needed. For edges these exponents can in general be given analytically, but for corners an eigenvalue problem for the Laplace-Beltrami operator has to be solved numerically, see Comment 22.1 on page 122. An edge E or a corner C is called singular if the leading singularity exponent λ_E or λ_C satisfies $\lambda_E \leq 2-2/p$ or $\lambda_C \leq 2-3/p$, respectively.

The plan of this section is as follows. We discuss the construction of a suitable family of finite element meshes as extensive as in [21]. Then we state the regularity and the approximation result without proofs. They are very technical and can be found in [21]. After some discussion we present a numerical test example. We end the section with a discussion of shape functions of higher degree and possible extensions to more general boundary value problems.

In order to explain our approach we subdivide Ω into a finite number of disjoint tetrahedral subdomains, $\overline{\Omega} = \bigcup_{j=1}^{J} \overline{\Omega_j}$, such that each subdomain contains at most one singular edge and at most one singular corner. In this way we localize the problem and reduce all considerations to few standard cases. Here we exploit that the singularities are of local nature only.

The freedom in the choice of the finite element mesh is restricted by the following three needs:

A. general admissibility conditions arising from the finite element theory and the subdomain approach,

B. refinement conditions, such that the global error estimates can be proven,

C. geometrical conditions on the elements such that anisotropic local interpolation error estimates can be proven.

We will now elaborate a set of conditions that satisfies all the needs. Afterwards we give simple examples how one can construct such a mesh. We point out that we do not attempt to give a minimal set of conditions. Rather, we want to describe a set of conditions that is both sufficient for our error estimates and simple to be verified for our examples. We also admit (but do not request) overrefinement in certain regions if the mesh generation algorithm can be kept simple then.

The general conditions on the triangulation $\mathcal{T}_h = \{e\}$ are the following.

A1. The domain is covered by the closure of the finite elements e, $\overline{\Omega} = \bigcup_{e \in \mathcal{T}_h} \overline{e}$.

A2. The triangulation is such that the subdomains Ω_j are resolved exactly: if $e \cap \Omega_j \neq \emptyset$ then $e \subset \Omega_j$.

A3. The elements are disjoint, $e \cap e' = \emptyset \quad \forall e, e' \in \mathcal{T}_h,\ e \neq e'$.

A4. Any face of any element e is either a subset of the boundary $\partial\Omega$ or face of another element $e' \in \mathcal{T}_h$.

A5. The number N_{el} of elements is related to the global mesh parameter h by $N_{\mathrm{el}} \sim h^{-3}$.

To describe the refinement conditions we need some further notation. First, define in each subdomain Ω_j $(j = 1, \ldots, J)$ a Cartesian coordinate system $(x_1^{(j)}, x_2^{(j)}, x_3^{(j)})$ with the following properties:

- One corner of Ω_j is located at the origin. In particular, if Ω_j possesses a refinement corner, then this one is chosen.

- One edge of Ω_j is contained in the $x_3^{(j)}$-axis. In particular, if Ω_j possesses a refinement edge, then this one is used.

We use here the term *refinement edge/corner* instead of *singular edge/corner* since we want to allow refinement near edges/corners which are not singular. This can be advantageous for a simpler construction of the meshes or just since only a lower estimate of the singular exponent is known.

Next, we denote for each finite element $e \subset \Omega_j$ by

$$\begin{aligned} r_e &:= \inf_{x \in e} \left[(x_1^{(j)})^2 + (x_2^{(j)})^2 \right]^{1/2}, \\ R_e &:= \inf_{x \in e} \left[(x_1^{(j)})^2 + (x_2^{(j)})^2 + (x_3^{(j)})^2 \right]^{1/2}, \end{aligned}$$

the distances of e to the $x_3^{(j)}$-axis and the origin. Note that $R_e \geq r_e$. Moreover, we introduce in each Ω_j refinement parameters $\mu_j, \nu_j \in (0,1]$ corresponding to the refinement edge/corner, respectively. If there is no refinement edge/corner we let $\mu_j = 1$ or $\nu_j = 1$, respectively.

As mentioned above we want to admit overrefinement. Therefore we distinguish between size parameters $H_{1,e}$, $H_{3,e}$ ($e \in \mathcal{T}_h$),

$$H_{1,e} := \begin{cases} h^{1/\mu_j} & \text{if } r_e = 0, \\ h r_e^{1-\mu_j} & \text{if } r_e > 0, \end{cases} \qquad H_{3,e} := \begin{cases} h^{1/\nu_j} & \text{if } 0 \leq R_e \lesssim h^{1/\nu_j}, \\ h R_e^{1-\nu_j} & \text{if } R_e \gtrsim h^{1/\nu_j}, \end{cases}$$

and actual mesh sizes $\tilde{h}_{1,e}$, $\tilde{h}_{2,e}$, $\tilde{h}_{3,e}$ which are defined as the lengths of the projections of $e \subset \Omega_j$ on the $x_1^{(j)}$-, $x_2^{(j)}$-, or $x_3^{(j)}$-axis, respectively. (The tilde is used because this definition is different from the mesh sizes $h_{1,e}$, $h_{2,e}$, $h_{3,e}$ as used in Section 6.) Note that $h^{1/\nu_j} \sim h R_e^{1-\nu_j}$ for $R_e \sim h^{1/\nu_j}$.

The relation between these sizes is given by condition B1:

B1. If $\mu_j < 1$ then $\tilde{h}_{1,e} \sim \tilde{h}_{2,e} \sim H_{1,e}$, $\tilde{h}_{3,e} \lesssim H_{3,e}$ ($e \in \mathcal{T}_h$). But in particular we demand that $\tilde{h}_{3,e} \sim H_{3,e}$ if $r_e = 0$.

If $\mu_j = 1$ then $\tilde{h}_{j,e} \lesssim H_{3,e}$ ($e \in \mathcal{T}_h$, $j = 1,2,3$) and in particular $\tilde{h}_{j,e} \sim H_{3,e}$ if $R_e = 0$.

Note that Assumption A5 is indeed a condition but not a consequence of B1. That was different in Section 20 where overrefinement was not allowed. In this sense we will also demand two similar conditions:

B2. The number of elements $e \subset \Omega_j$ with $r_e = 0$ is of order h^{-1}.

B3. The number of elements $e \subset \Omega_j$ such that $0 \leq R_e \lesssim h^{1/\nu_j}$ is bounded by $h^{2\mu_j/\nu_j - 2}$. In particular, there is only one element e with $R_e = 0$.

Though further conditions on the parameters μ_j and ν_j are imposed in Theorem 21.4, we want to ensure a priori that $H_{1,e} \lesssim H_{3,e}$ for $\mu_j < 1$:

B4. If $\mu_j < 1$ then $\mu_j \leq \nu_j$ $(j = 1, \ldots, J)$.

The next set of conditions is imposed such that the anisotropic local interpolation error estimates of Section 6 hold.

C1. The finite elements e must satisfy the maximal angle condition, see page 33.

C2. If Ω_j contains a refinement edge then all elements $e \subset \Omega_j$ have two vertices such that the straight line through them is parallel to the $x_3^{(j)}$-axis.

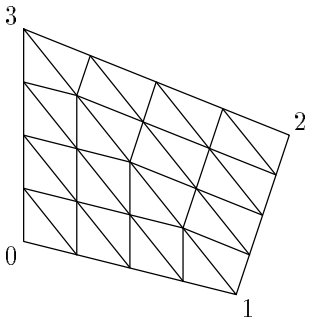

Case 1: Equidistant mesh.

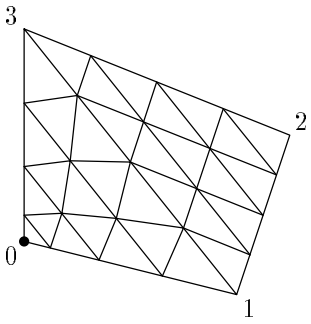

Case 2: Refinement towards a corner ($\nu_j = 0.67$).

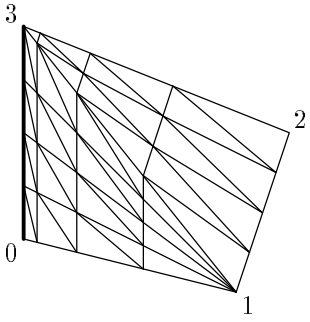

Case 3: Refinement towards an edge ($\mu_j = 0.5$).

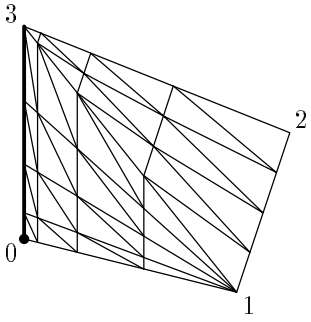

Case 4: Refinement towards a corner and an edge ($\nu_j = 0.67$, $\mu_j = 0.5$).

Figure 21.1: Illustration of the meshing of the subdomains ($n = 4$).

C3. If Ω_j does not contain a refinement edge then all elements are isotropic, that means, they have bounded aspect ratio.

Note that we used in Section 6 the maximal angle condition C1 and a coordinate system condition which is very technical. It is possible to avoid the latter condition by imposing C2 and $\tilde{h}_{1,e} \sim \tilde{h}_{2,e}$.

Lemma 21.1 *For any polyhedral domain $\Omega \subset \mathbb{R}^3$ it is possible to generate meshes which satisfy all the Assumptions A1–C3.*

Proof We start with the meshing of one subdomain Ω_j and then we discuss the satisfaction of Condition A4 after gluing together the meshes of the subdomains. Let us distinguish four cases: 1) Ω_j contains neither a refinement corner nor a refinement edge, 2) Ω_j contains a refinement corner but no refinement edge, 3) Ω_j contains a refinement edge but no refinement corner, 4) Ω_j contains both a refinement corner and a refinement edge.

The meshing in these four situations is illustrated in Figure 21.1. A mathematical description of this mesh generation procedure can be given as follows: Introduce barycentric coordinates $\lambda_0^{(j)}, \ldots, \lambda_3^{(j)}$ ($\lambda_i^{(j)} > 0$, $\sum_{i=0}^3 \lambda_i^{(j)} = 1$) in Ω_j such that the refinement corner has the coordinate $\lambda_0^{(j)} = 1$ and the refinement edge is described by $\lambda_1^{(j)} = \lambda_2^{(j)} = 0$. Let $n \in \mathbb{N}$ be an integer such that $h \sim n^{-1}$.

Case 1: The vertices P_{i_1,i_2,i_3} have the coordinates

$$\lambda_1^{(j)} = \tfrac{i_1}{n}, \quad \lambda_2^{(j)} = \tfrac{i_2}{n}, \quad \lambda_3^{(j)} = \tfrac{i_3}{n}, \quad 0 \le i_1 + i_2 + i_3 \le n.$$

The tetrahedra are described as quadruples of vertices; they are

$$\begin{array}{ll}
(P_{i_1,i_2,i_3}, P_{i_1+1,i_2,i_3}, P_{i_1,i_2+1,i_3}, P_{i_1,i_2,i_3+1}), & 0 \le i_1+i_2+i_3 \le n-1,\\
(P_{i_1+1,i_2,i_3}, P_{i_1,i_2+1,i_3}, P_{i_1,i_2,i_3+1}, P_{i_1+1,i_2,i_3+1}), & 0 \le i_1+i_2+i_3 \le n-2,\\
(P_{i_1,i_2+1,i_3}, P_{i_1,i_2,i_3+1}, P_{i_1+1,i_2,i_3+1}, P_{i_1,i_2+1,i_3+1}), & 0 \le i_1+i_2+i_3 \le n-2,\\
(P_{i_1+1,i_2,i_3}, P_{i_1,i_2+1,i_3}, P_{i_1+1,i_2+1,i_3}, P_{i_1+1,i_2,i_3+1}), & 0 \le i_1+i_2+i_3 \le n-2,\\
(P_{i_1,i_2+1,i_3}, P_{i_1+1,i_2+1,i_3}, P_{i_1+1,i_2,i_3+1}, P_{i_1,i_2+1,i_3+1}), & 0 \le i_1+i_2+i_3 \le n-2,\\
(P_{i_1+1,i_2+1,i_3}, P_{i_1+1,i_2,i_3+1}, P_{i_1,i_2+1,i_3+1}, P_{i_1+1,i_2+1,i_3+1}), & 0 \le i_1+i_2+i_3 \le n-3.
\end{array}$$

Case 2: The topology is as in Case 1 but the coordinates of the vertices P_{i_1,i_2,i_3} change to

$$\lambda_1^{(j)} = \tfrac{i_1}{n}\left(\tfrac{i_1+i_2+i_3}{n}\right)^{-1+1/\nu_j}, \quad \lambda_2^{(j)} = \tfrac{i_2}{n}\left(\tfrac{i_1+i_2+i_3}{n}\right)^{-1+1/\nu_j}, \quad \lambda_3^{(j)} = \tfrac{i_3}{n}\left(\tfrac{i_1+i_2+i_3}{n}\right)^{-1+1/\nu_j},$$

$0 \le i_1+i_2+i_3 \le n$.

Case 3: We introduce here a larger set of nodes P_{i_1,i_2,i_3}

$$0 \le i_1+i_2 \le n, \quad 0 \le i_3 \le n \quad \text{if} \quad i_1+i_2 < n, \quad i_3 = 0 \quad \text{if} \quad i_1+i_2 = n,$$

with the coordinates

$$\lambda_1^{(j)} = \tfrac{i_1}{n}\left(\tfrac{i_1+i_2}{n}\right)^{-1+1/\mu_j}, \quad \lambda_2^{(j)} = \tfrac{i_2}{n}\left(\tfrac{i_1+i_2}{n}\right)^{-1+1/\mu_j}, \quad \lambda_3^{(j)} = \tfrac{i_3}{n}(1-\lambda_1^{(j)}-\lambda_2^{(j)}).$$

The tetrahedra are described in three cases:

Subdivision of pentahedra:

$$\begin{array}{ll}
(P_{i_1,i_2,i_3}, P_{i_1+1,i_2,i_3}, P_{i_1,i_2+1,i_3}, P_{i_1,i_2,i_3+1}), & 0 \le i_1+i_2 \le n-2,\\
(P_{i_1+1,i_2,i_3}, P_{i_1,i_2+1,i_3}, P_{i_1,i_2,i_3+1}, P_{i_1+1,i_2,i_3+1}), & 0 \le i_1+i_2 \le n-2,\\
(P_{i_1,i_2+1,i_3}, P_{i_1,i_2,i_3+1}, P_{i_1+1,i_2,i_3+1}, P_{i_1,i_2+1,i_3+1}), & 0 \le i_1+i_2 \le n-2,\\
(P_{i_1+1,i_2,i_3}, P_{i_1,i_2+1,i_3}, P_{i_1+1,i_2+1,i_3}, P_{i_1+1,i_2,i_3+1}), & 0 \le i_1+i_2 \le n-3,\\
(P_{i_1,i_2+1,i_3}, P_{i_1+1,i_2+1,i_3}, P_{i_1+1,i_2,i_3+1}, P_{i_1,i_2+1,i_3+1}), & 0 \le i_1+i_2 \le n-3,\\
(P_{i_1+1,i_2+1,i_3}, P_{i_1+1,i_2,i_3+1}, P_{i_1,i_2+1,i_3+1}, P_{i_1+1,i_2+1,i_3+1}), & 0 \le i_1+i_2 \le n-3,
\end{array}$$

$0 \le i_3 \le n-1$ in all cases.

Subdivision of pyramids:

$$\begin{array}{ll}
(P_{i_1+1,i_2,i_3}, P_{i_1,i_2+1,i_3}, P_{i_1+1,i_2,i_3+1}, P_{i_1+1,i_2+1,0}), & i_1+i_2 = n-2,\\
(P_{i_1,i_2+1,i_3}, P_{i_1+1,i_2,i_3+1}, P_{i_1,i_2+1,i_3+1}, P_{i_1+1,i_2+1,0}), & i_1+i_2 = n-2,
\end{array}$$

$0 \le i_3 \le n-1$ in both cases.

Remaining tetrahedra:

$$(P_{i_1,i_2,i_3}, P_{i_1,i_2,i_3+1}, P_{i_1+1,i_2,0}, P_{i_1,i_2+1,0}), \quad i_1+i_2 = n-1, \quad 0 \le i_3 \le n-1.$$

Case 4: The topology is as in Case 3 but the $\lambda_3^{(j)}$-coordinate of the points P_{i_1,i_2,i_3} changes to

$$\lambda_3^{(j)} = \left(\tfrac{i_3}{n}\right)^{1/\nu_j}(1-\lambda_1^{(j)}-\lambda_2^{(j)}).$$

We have now to prove that such a mesh satisfies all conditions: A1, A2, A3, and A5 are obvious. Assumption A4 is equivalent to the necessity that the faces $\overline{\Omega_j} \cap \overline{\Omega_{j'}}$ are meshed in the same way. This leads in general to some cascade effect: let $M \subset \partial\Omega$ be a connected set of refinement edges and vertices (edges are here considered as closed sets), then we have to choose

$$\mu_j = \nu_j = \mu_M \quad \text{for all } j : \overline{\Omega_j} \cap M \neq \emptyset.$$

That means that the refinement is determined by the strongest singularity in this region. An exception is the case when the face $\lambda_3^{(j)} = 0$ is part of the boundary $\partial\Omega$. Then ν_j can be chosen larger than μ_j. We remark that the cascade effect could be avoided by using mortar elements [45].

The coordinate transformation $\lambda_0^{(j)}, \ldots, \lambda_3^{(j)} \mapsto x_1^{(j)}, \ldots, x_3^{(j)}$ is independent of h. Therefore, Assumption B1 can easily be verified by noting that

$$\begin{aligned} (s+h)^{1/\mu_j} - s^{1/\mu_j} &\sim hs^{1-\mu_j}, \\ \lambda_1^{(j)} + \lambda_2^{(j)} + \lambda_3^{(j)} &\sim R_e \quad \text{for all } e \text{ with } R_e > 0, \\ \lambda_1^{(j)} + \lambda_2^{(j)} &\sim r_e \quad \text{for all } e \text{ with } R_e > 0. \end{aligned}$$

Indeed, in Case 2 all elements are isotropic, that means $\tilde{h}_{i,e}$ is of the size of the distance of the two planes $\lambda_4^{(j)} = (\frac{i_1+i_2+i_3+1}{n})^{1/\nu_j}$ and $\lambda_4^{(j)} = (\frac{i_1+i_2+i_3}{n})^{1/\nu_j}$,

$$\tilde{h}_{i,e} \sim \left(\tfrac{i_1+i_2+i_3+1}{n}\right)^{1/\nu_j} - \left(\tfrac{i_1+i_2+i_3}{n}\right)^{1/\nu_j} \sim hR_e^{1-\nu_j} \quad (i = 1,2,3).$$

In cases 3 and 4, the projection of the element into the $\lambda_1^{(j)}, \lambda_2^{(j)}$-plane is isotropic, that means

$$\tilde{h}_{i,e} \sim \left(\tfrac{i_1+i_2+1}{n}\right)^{1/\mu_j} - \left(\tfrac{i_1+i_2}{n}\right)^{1/\mu_j} \sim hr_e^{1-\mu_j} \quad (i = 1,2).$$

Finally, we see in Case 4 that

$$\begin{aligned} \tilde{h}_{3,e} &\lesssim \lambda_3^{(j)}(P_{\cdot,\cdot,i_3+1}) - \lambda_3^{(j)}(P_{\cdot,\cdot,i_3}) + (\tilde{h}_{1,e} + \tilde{h}_{2,e}) \\ &\lesssim \left(\tfrac{i_3+1}{n}\right)^{1/\nu_j} - \left(\tfrac{i_3}{n}\right)^{1/\nu_j} + hr_e^{1-\mu_j} \\ &\lesssim h(x_3^{(j)})^{1-\nu_j} + hr_e^{1-\nu_j} \\ &\lesssim hR_e^{1-\nu_j}, \end{aligned}$$

because $\nu_j \geq \mu_j$.

Condition B2 is satisfied by construction. B3 is checked by realizing that the number of elements is of order i^2 where i satisfies $(i/n)^{1/\mu_j} \lesssim (1/n)^{1/\nu_j}$, that means $i \lesssim n^{1-\mu_j/\nu_j}$. Condition B4 is independent of our meshing strategy. Conditions C1–C3 are also satisfied by construction. Note that overrefinement is accepted in Cases 3 and 4 near the edge $\lambda_0^{(j)} = \lambda_4^{(j)} = 0$ and due to the cascade effect described above. ∎

Remark 21.2 Note that the number of elements is n^3 for Cases 1 and 2, and $3n^3 - 3n^2 + n$ for Cases 3 and 4. We introduced the richer topology in the latter cases to ensure the maximal angle condition C1. However, we can use the topology of Cases 1/2 if $\mu_j = \nu_j < 1$, compare Figure 21.2. The vertices P_{i_1,i_2,i_3} have then the coordinates

$$\lambda_1^{(j)} = \tfrac{i_1}{n}\left(\tfrac{i_1+i_2}{n}\right)^{-1+1/\mu_j}, \quad \lambda_2^{(j)} = \tfrac{i_2}{n}\left(\tfrac{i_1+i_2}{n}\right)^{-1+1/\mu_j}, \quad \lambda_3^{(j)} = \left(\tfrac{i_1+i_2+i_3}{n}\right)^{1/\mu_j} - \lambda_1^{(j)} - \lambda_2^{(j)}.$$

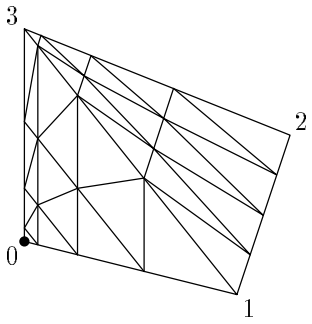

Figure 21.2: Modification of Case 4 for $\mu_j = \nu_j < 1$.

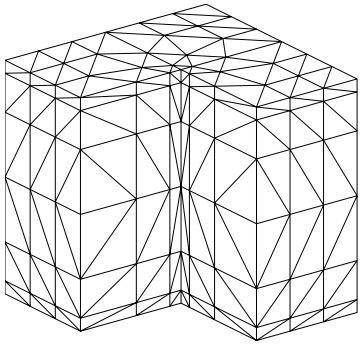

Figure 21.3: Tensor product domain with mesh refinement near the singular edge and the corners.

$0 \le i_1 + i_2 + i_3 \le n$.

We point out that also simpler meshing strategies can be applied where overrefinement takes place in more regions. Figure 21.5 shows an example where artificial refinement edges are introduced. Moreover, we introduced the Assumptions A1–C3 in order to allow other refinement strategies which are not based on the domain decomposition approach, see Figure 21.3 for an example with a coordinate transformation.

We introduce now the finite element space V_h of all continuous functions whose restriction to any e ($e \in \mathcal{T}_h$) is a polynomial of first degree. Furthermore, we let V_{0h} be defined by $V_{0h} := \{v_h \in V_h : v_h|_{\partial\Omega} = 0\}$. Note that $V_h \subset H^1(\Omega)$ and $V_{0h} \subset V_0$. The variational formulation of problem (21.1) reads as follows.

$$Find\ u \in V_0 : a(u,v) = (f,v)_\Omega \quad \forall v \in V_0, \tag{21.4}$$

where the bilinear form $a(.,.)$ is defined by

$$a(u,v) := \int_\Omega \sum_{i,j=1}^{3} a_{i,j} \frac{\partial u}{\partial x_i} \frac{\partial v}{\partial x_j}.$$

Furthermore, the finite element solution is defined by

$$Find\ u_h \in V_{0h} : a(u_h, v_h) = (f, v_h)_\Omega \quad \forall v_h \in V_{0h}. \tag{21.5}$$

Let $\lambda_{E,n}^{(j)}$ and $\lambda_{C,n}^{(j)}$, $n = 1, 2, \ldots$, be the singularity exponents with respect to the singular edge and the singular corner of Ω_j, $j = 1, \ldots, J$. Define in particular the leading singular exponents by $\lambda_E^{(j)} := \lambda_{E,1}^{(j)}$, $\lambda_C^{(j)} := \lambda_{C,1}^{(j)}$. Note that these exponents are defined by Ω (and the differential operator) and not only by Ω_j, compare Comment 22.1 on page 122. If no edge/corner of Ω_j is edge/corner of Ω then we define $\lambda_E^{(j)} := \infty$, $\lambda_C^{(j)} := \infty$, respectively.

The regularity of derivatives of u can be described by means of the weighted Sobolev spaces $V_{\beta,\delta}^{\ell,p}(\Omega_j)$, see Section 3, page 13, for the definition.

Theorem 21.3 [21, Theorem 2.10] *Assume that $2 \le p < 6$, $\lambda_{E,n}^{(j)} \ne 2 - 2/p$, $\lambda_{C,n}^{(j)} \ne 2 - 3/p$, for all $n = 1, 2, \ldots$, $j = 1, \ldots, J$, and $\lambda_E^{(j)} > 1 - 2/p$. Then the solution u of the general problem (21.1) admits the following decomposition in Ω_j:*

$$u = u_r + u_s, \tag{21.6}$$

where $u_r \in W^{2,p}(\Omega_j)$ and

$$\frac{\partial u_s}{\partial x_i^{(j)}} \in V_{\beta,\delta}^{1,p}(\Omega_j), \quad i = 1, 2, \tag{21.7}$$

$$\frac{\partial u_s}{\partial x_3^{(j)}} \in V_{\beta,0}^{1,p}(\Omega_j), \tag{21.8}$$

for any $\beta, \delta \ge 0$ satisfying $\beta > 2 - 3/p - \lambda_C^{(j)}$ and $\delta > 2 - 2/p - \lambda_E^{(j)}$.

In the following, we investigate first the global interpolation error for the family of anisotropically graded meshes introduced above. Then we obtain the global finite element error estimate via the Céa lemma.

Theorem 21.4 [21, Theorem 5.1] *Let u be the solution of the boundary value problem (21.4) with $f \in L_p(\Omega)$, $2 < p < p_+$,*

$$p_+ := \min_j \left\{ 6;\ \frac{2}{1 - \lambda_C^{(j)}};\ \frac{1}{1 - \lambda_E^{(j)}} \right\}. \tag{21.9}$$

In addition to the condition B4, assume that the refinement parameters μ_j, ν_j satisfy the following conditions for all j:

$$\mu_j < \lambda_E^{(j)} \frac{p}{2p - 2}, \tag{21.10}$$

$$\nu_j < \left(\lambda_C^{(j)} + \frac{1}{2} \right) \frac{2p}{5p - 6}, \tag{21.11}$$

$$\frac{1}{\nu_j} \left(\frac{5}{2} - \frac{3}{p} \right) + \frac{1}{\mu_j} \left(\lambda_C^{(j)} - 2 + \frac{3}{p} \right) > 1. \tag{21.12}$$

Then for the interpolation error $u - I_h u$ the following estimate holds:

$$|u - I_h u; W^{1,2}(\Omega)| \lesssim h \, \|f; L^p(\Omega)\|. \tag{21.13}$$

Proof The theorem can be proved by distinguishing the four cases as mentioned in the proof of Lemma 21.1 and by using the local interpolation error estimates for functions from (weighted) Sobolev spaces, see [21, Section 5]. Before, one has to ensure that Theorems 6.4, 6.9, and 6.11 can be proved if $h_{1,e}, h_{2,e}, h_{3,e}$ are replaced by $\tilde{h}_{1,e}, \tilde{h}_{2,e}, \tilde{h}_{3,e}$, as defined above. This was done in [21, Section 4]. ∎

Corollary 21.5 *Let u be the solution of the boundary value problem (21.4) with $f \in L_p(\Omega)$, $2 < p < p_+$, p_+ from (21.9), and let u_h be the finite element solution of (21.5). Then the error estimate*

$$\|u - u_h; W^{1,2}(\Omega)\| \lesssim h \, \|f; L^p(\Omega)\|$$

holds if all refinement parameters μ_j and ν_j, $j = 1, \ldots, J$, satisfy the conditions (21.10)–(21.12).

Let us discuss the assumptions of this approximation result. First, we note that the restriction $p < p_+$ is not essential for this estimate, because $f \in L^p(\Omega)$ yields $f \in L^q(\Omega)$ for $q \le p$ and $\|f; L^q(\Omega)\| \lesssim \|f; L^p(\Omega)\|$. We can apply Theorem 21.4 for $q < p_+$. Nevertheless, we have to replace p in the conditions of the Theorem 21.4 by $\min\{p;\ p_+ - \kappa\}$, $\kappa > 0$ arbitrarily small.

In order to use meshes which are not too much refined, the estimates are most favourable for p close to 2. For $p = 2 + \delta$ (δ is an arbitrarily small real number), the refinement conditions reduce to

$$\begin{aligned} \mu_j &< \lambda_E^{(j)} \left(1 - \frac{\delta}{2 + 2\delta}\right), \\ \nu_j &< \left(\lambda_C^{(j)} + \frac{1}{2}\right) \left(1 - \frac{3\delta}{4 + 5\delta}\right), \\ \frac{1}{\nu_j} + \frac{1}{\mu_j}\left(\lambda_C^{(j)} - \frac{1}{2}\right) &> 1 + \frac{3\delta}{4 + 2\delta}\left(\frac{1}{\mu_j} - \frac{1}{\nu_j}\right). \end{aligned}$$

On the other hand it is not clear in which way the constant in the local interpolation error estimate depends on p; we suspect that it grows to infinity for $p \to 2$.

The conditions (21.10) and (21.11) are the edge and corner refinement conditions, respectively. They are expected because they balance the edge and corner singularities (compare with [19, 23, 123]). On the contrary, the condition (21.12) seems to be artificial but actually it comes from the anisotropy of the mesh near the corner. Indeed, (21.12) follows from (21.11) and $p > 2$ in the case $\mu_j = \nu_j$. In the case $\mu_j \ne \nu_j$, it imposes a condition between μ_j and ν_j, this means that the mesh cannot be too much anisotropic. For the Fichera domain treated in Example 21.6, we have $\lambda_C \approx 0.45$ and $\lambda_E = 2/3$. We then see that for p close to 2, the condition (21.12) holds for $\mu_j = 0.6$ and $\nu_j = 0.9$.

Example 21.6 We consider the Poisson equation with a specific right hand side, together with homogeneous Dirichlet boundary conditions:

$$\begin{aligned} -\Delta u &= R^{-1} \quad \text{in } \Omega, \\ u &= 0 \qquad \text{on } \partial\Omega. \end{aligned}$$

The domain $\Omega := (-1, 1)^3 \setminus [0, 1]^3$ has three edges with interior angle $\omega_0 = \frac{3}{2}\pi$, which meet in the center of coordinates; we denote by R the distance to this point. Sometimes such a corner is called Fichera corner. Note that the right hand side is contained in $L_p(\Omega)$ for $p < 3$.

In order to determine the regularity of the solution, we consider first the corner singularity and find that $\lambda_C \approx 0.45$ [169]. The edge singularities are described by $\lambda_E = \pi/\omega_0 = 2/3$.

This problem was solved first with ungraded meshes and mesh sizes $h_i = 1/i$, $i = 2, 3, \ldots, 48$. We compare this with three refinement strategies. The first one is obtained by a simple coordinate transformation

$$x_i := x_i \cdot |x_i|^{-1+1/\mu_j}, \quad i = 1, 2, 3,$$

for all vertices (x_1, x_2, x_3). It leads to overrefinement near the coordinate planes, see Figure 21.5. The second one was described by our constructive proof of Lemma 21.1, see pages 114–116. The corresponding mesh is illustrated in Figure 21.6. The optically bad elements near the

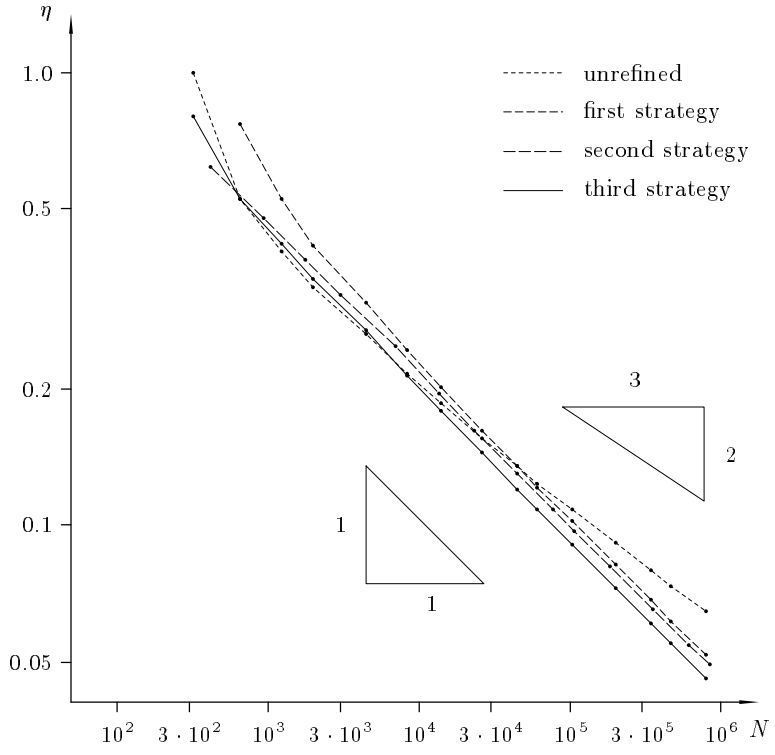

Figure 21.4: Example 21.6: Estimated error η in the energy norm for various mesh sizes.

diagonals can be avoided by using the strategy of Case 4a instead of Case 4, compare Remark 21.2 and Figure 21.7. For all j we used the parameters $\mu_j = \nu_j = 0.6$.

The calculations were done using the code *FEMPS3D* which is described shortly in Comment 30.2 on page 172. We remark only that the energy of the finite element error was estimated with an error estimator of residual type which was tuned for treating anisotropic meshes, see also Section 28. The norms are given in form of a diagram in Figure 21.4.

We see that the theoretical approximation order $h \sim N^{-1/3}$, N is the number of nodes, can be verified in the practical calculation for all three refinement strategies. The error is the smallest in the third refinement strategy, however, the difference between the strategies is small. □

Remark 21.7 We believe that the approach to mesh refinement as introduced in this section is applicable to a larger class of problems since the singularities can be characterized in a similar way for general second order boundary value problems including systems of equations. For isotropic mesh refinement the approximation theory was given in [23] in this generality. For anisotropic mesh refinement, however, there are some remaining tasks.

1. We conjecture that Theorem 21.3 can be proved also for other boundary conditions (Neumann, Robin, mixed). Then Theorem 21.4 is valid as long as $\lambda_E^{(j)} > 1/2$ for all j. (Otherwise (21.9) yields $p_+ \leq 2$ which contradicts another assumption of Theorem 21.4.) For $\lambda_E^{(j)} \leq 1/2$ there is no $\varepsilon > 0$ such that $u \in W^{3/2+\varepsilon,2}(\Omega)$. Therefore the Lagrangian interpolation operator is not applicable. It is an open problem to extend the Scott-Zhang

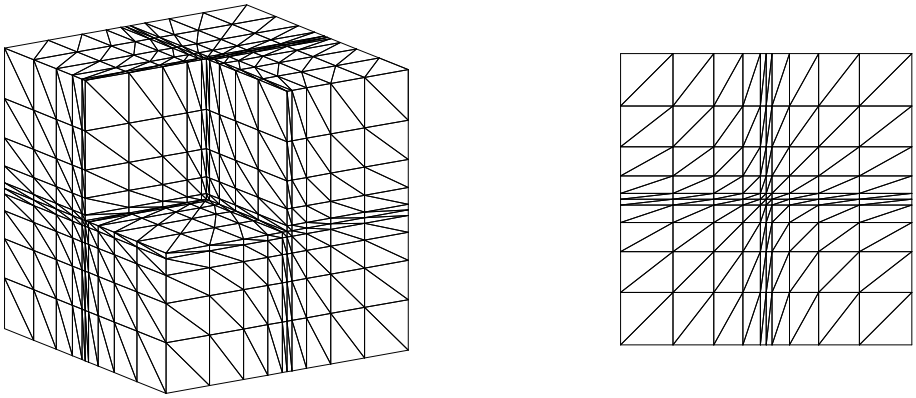

Figure 21.5: Example 21.6: First strategy, a simple coordinate transformation. Left: perspective view. Right: cut at $x_3 = 0$.

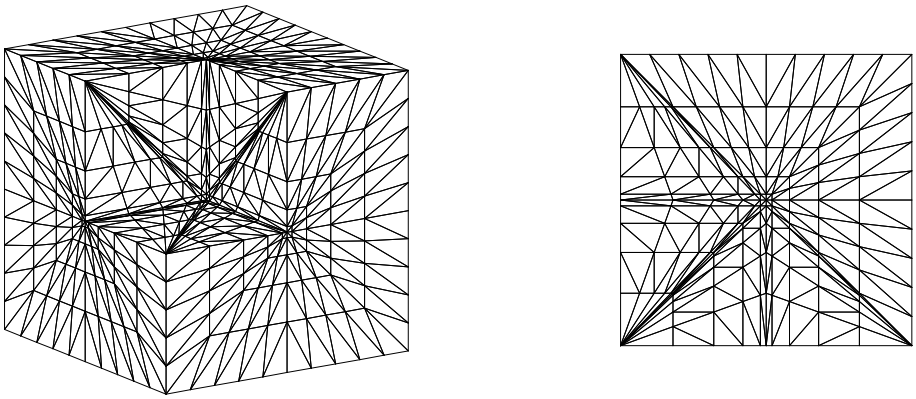

Figure 21.6: Example 21.6: Second strategy, refinement according to Cases 1–4. Left: perspective view. Right: cut at $x_3 = 0$.

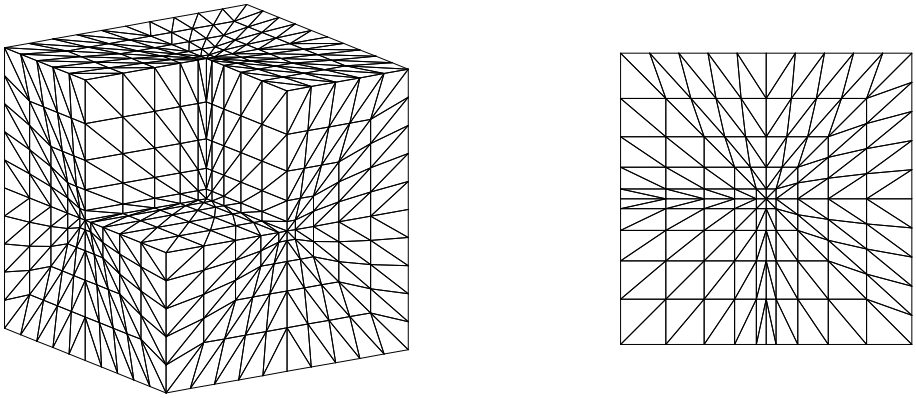

Figure 21.7: Example 21.6: Third strategy, refinement with Case 4a instead of Case 4. Left: perspective view. Right: cut at $x_3 = 0$.

interpolation theory to non-tensor product meshes.

2. For more general boundary value problems like the Lamé system of elasticity we do not know about an anisotropic regularity theory in the sense of Theorem 21.3. In particular, the theory must be developed in non-Hilbert spaces since we need $p > 2$.

3. For $k \geq 2$ the regularity theory in Hilbert spaces ($p = 2$) can be applied, compare Theorem 20.7 on page 107. If the regularity result of Theorem 21.3 can be extended to higher order derivatives like in Assumption 20.6, then the proof of the approximation result is straightforward.

22 Three comments on the analytical properties of u

In this section we present some analytical background which was omitted in Sections 19–21 since we wanted to focus on the numerical part of the theory.

22.1 Calculation of the singularity exponents. Consider first the Poisson problem. For homogeneous Dirichlet or Neumann boundary conditions the singularity exponents with respect to an edge E are given by $\lambda_{E,n} = n\pi/\omega_E > 1/2$, $n = 1, 2, \ldots$, where ω_E is the angle between the two faces of Ω containing E. In the case of mixed Dirichlet/Neumann boundary conditions we have $\lambda_{E,n} = (n - 1/2)\pi/\omega_E > 1/4$, $n = 1, 2, \ldots$.

Let $\mathsf{C}_C \subset \mathbb{R}^3$ be the infinite polyhedral cone which coincides with Ω in a neighbourhood of a corner C of Ω, and let S_C^2 be the unit sphere centered at C. Set $G_C := \mathsf{C}_C \cap S_C^2$ and denote by $\lambda_n > 0$, $n = 1, 2, \ldots$, the eigenvalues (in increasing order) of the Laplace-Beltrami operator on G_C (with Dirichlet boundary conditions). Then the singular exponents related to C are given by $\lambda_{C,n} = (\lambda_n + 1/4)^{1/2} - 1/2$, $n = 1, 2, \ldots$. Papers on a numerical calculation of the singular exponents $\lambda_{C,n}$ include [40, 121, 169]. In some cases these exponents can be calculated analytically, see Comment 22.2.

In Section 21 we considered a more general differential operator, see (21.1). Since we assumed constant coefficients, there exists a linear change of variables $y = Bx$ which transforms the problem (21.1) into the Poisson problem with homogeneous Dirichlet boundary conditions in another polyhedral domain Ω'. The singularity exponents can then be calculated as described above but with respect to the transformed domain.

22.2 Corner singularities in tensor product domains. Tensor product domains in the sense of Section 20 have the advantage that the corner singularities can be described explicitly. Consider a corner C at the origin of the coordinate system. A neighbourhood $U(C) \subset \Omega$ can be described in spherical coordinates by

$$U(C) = \{x = (R\cos\phi\sin\theta, R\sin\phi\sin\theta, R\cos\theta) : O < R < R_0, 0 < \phi < \omega, 0 < \theta < \pi/2\}.$$

The singular functions have the form [181, 191]

$$u_{C,i} = R^{\lambda_{C,i}} F_i(\phi, \theta), \qquad \lambda_{C,i} = \left(\lambda_i + \frac{1}{4}\right)^{1/2} - \frac{1}{2},$$

where λ_i, F_i are the eigenvalues/eigensolutions of the eigenvalue problem for the Laplace-Beltrami operator,

$$F_{\theta\theta} + F_\theta \cot\theta + F_{\phi\phi}(\sin\theta)^{-2} = -\lambda_i F \quad \text{in } G,$$

$G = \{x = (\cos\phi \sin\theta, \sin\phi \sin\theta, \cos\theta) : 0 < \phi < \omega, 0 < \theta < \pi/2\}$, and boundary conditions corresponding to the original problem. Separation of variables, $F(\phi,\theta) = \Phi(\phi)\Theta(\theta)$, leads to

$$\begin{aligned} \Phi'' + \lambda_{E,i}^2 \Phi &= 0 \quad \text{in } (0,\omega), \\ \Theta'' + \Theta' \cot\theta + (\lambda_i - \lambda_{E,i}^2 (\sin\theta)^{-2})\Theta &= 0 \quad \text{in } \left(0, \frac{\pi}{2}\right). \end{aligned}$$

For the Dirichlet problem we get the solution

$$\begin{aligned} &\lambda_{E,1} = \frac{\pi}{\omega}, && \Phi_1(\phi) = \sin\lambda_{E,i}\phi, \\ &\lambda_1 = (\lambda_{E,1}+1)(\lambda_{E,1}+2), && \Theta_1(\theta) = (\sin\theta)^{\lambda_{E,1}} \cos\theta, \\ &\lambda_{C,1} = \lambda_{E,1} + 1, \end{aligned}$$

see also [191]. This means that the leading corner singularity is

$$U_{C,1} = R^{\lambda_{E,1}+1} \sin\lambda_{E,1}\phi (\sin\theta)^{\lambda_{E,1}} \cos\theta = (R\sin\theta)^{\lambda_{E,1}} (R\cos\theta) \sin\lambda_{E,1}\phi = x_3 r^{\lambda_{E,1}} \sin\lambda_{E,1}\phi,$$

which has precisely the structure of the leading edge singularity function.

In the case of the mixed boundary value problem with $u = 0$ for $\phi = 0, \omega$, and $\partial u/\partial n = 0$ for $\theta = \pi/2$ we obtain [191]

$$\begin{aligned} &\lambda_{E,1} = \frac{\pi}{\omega}, && \Phi_1(\phi) = \sin\lambda_{E,i}\phi, \\ &\lambda_1 = \lambda_{E,1}(\lambda_{E,1}+1), && \Theta_1(\theta) = (\sin\theta)^{\lambda_{E,1}}, \\ &\lambda_{C,1} = \lambda_{E,1}, \end{aligned}$$

that means

$$U_{C,1} = R^{\lambda_{E,1}} \sin\lambda_{E,1}\phi (\sin\theta)^{\lambda_{E,1}} = r^{\lambda_{E,1}} \sin\lambda_{E,1}\phi.$$

In the case $u = 0$ for $\phi = 0$, and $\partial u/\partial n = 0$ for $\phi = \omega$ and $\theta = \pi/2$ the same results are valid with $\lambda_{E,1} = \pi/(2\omega)$.

22.3 Regularity of the solution u of the Poisson problem in a domain with one single edge. The regularity theory for elliptic boundary value problems in non-smooth domains with corners and edges is well developed, especially in the framework of weighted Sobolev spaces. Boundary value problems in domains with non-intersecting edges are treated in [113, 129, 131], and in polyhedral domains in [66, 130, 154], see also the monograph [116] and the summary of results in [23, Section 2].

Let us formulate here a regularity result for domains Ω with one single edge E with constant internal angle (either Ω is a dihedral angle and f is assumed to have bounded support, or Ω is a bounded domain with only one closed edge). The result was originally proved in [129] in more general form. We use here the formulation of [116, Theorem 26.3] where we have set specifically $m = 1$, $p = p_1 = 2$.

The critical point is hidden in two assumptions.

A1 Let $u \in V^{\ell+2,2}_{\beta+\ell}(\Omega)$ be a solution of (20.1) with right hand side $f \in V^{\ell,2}_{\beta+\ell}(\Omega)$ where $\beta - 1$ is not a singularity exponent.

This assumption is essential since we investigate the regularity in the scale $V^{\ell,p}_{\beta}(\Omega)$ of weighted Sobolev spaces. But we have existence and uniqueness of the solution u of (20.1) in the space $V_0 \subset V = W^{1,2}(\Omega)$ which does not belong to this scale. Note that ℓ can be an arbitrary integer,

see [116, Lemma 27.2(ii)]. Spaces with negative ℓ are defined by $V_\beta^{\ell,2}(\Omega) = (V_{-\beta}^{-\ell,2}(\Omega))'$ [116, Subsection 0.8].

The investigation of the regularity is done by applying a Fourier transform to (20.1) and a further change of variables, see [116, Subsections 22.4 and 26.1]. The resulting operator pencil is denoted by $\mathcal{A}(\zeta,\theta)$, $\zeta \in E$, $\theta = \pm 1$.

A2 For all $\zeta \in E$ and $\theta \in \{\pm 1\}$ both $\ker\mathcal{A}(\zeta,\theta)$ and $\operatorname{coker}\mathcal{A}(\zeta,\theta)$ are trivial.

Both conditions, A1 and A2, are satisfied for the Dirichlet problem for the Poisson equation where $\ell = -1$, $\beta = 1$ [116, Subsection 28.1], and for mixed boundary conditions, where $\ell = -1, 0$, $\beta = 1$ [116, Subsection 32.2], see also [166, Lemma 4].

Theorem 22.1 [116, Theorem 26.3] *Let Assumptions A1 and A2 be valid and assume that* $f \in V_{\beta+\ell}^{\ell,2}(\Omega) \cap V_{\beta_1+\ell_1}^{\ell_1,2}(\Omega)$ *with* $-\lambda < \beta_1 - 1 < \lambda$ *where* λ *is the leading (smallest positive) singularity exponent. Then* $u \in V_{\beta_1+\ell_1}^{\ell_1+2,2}(\Omega)$ *and*

$$\|u; V_{\beta_1+\ell_1}^{\ell_1+2,2}(\Omega)\| \lesssim \|f; V_{\beta_1+\ell_1}^{\ell_1,2}(\Omega)\|.$$

The application of this theorem for $f \in L^2(\Omega)$ leads to

$$\|u; V_{\max\{\beta;\,0\}}^{2,2}(\Omega)\| \lesssim \|f; V_{\max\{\beta;\,0\}}^{0,2}(\Omega)\| \lesssim \|f; L^2(\Omega)\|, \qquad \beta > 1-\lambda, \tag{22.1}$$

in particular

$$\|D^\alpha u; V_{\max\{\beta;\,0\}-2+|\alpha|}^{2-|\alpha|,2}(\Omega)\| \lesssim \|f; L^2(\Omega)\|, \qquad |\alpha| \le 2, \quad \beta > 1-\lambda, \tag{22.2}$$

Theorem 22.1 does not give the optimal regularity for derivatives of u in tangential direction. Therefore we state another theorem in the formulation of [116]. This one was originally proved by [131].

Theorem 22.2 [116, Theorem 30.1(iii)] *Let Assumptions A1 and A2 be valid and assume that* $f \in V_{\beta+\ell}^{\ell,2}(\Omega) \cap V_{\beta_1+\ell_1}^{\ell_1,2}(\Omega)$ *with* $\ell \ge 0$ *and* $-\lambda - 1 < \beta_1 - 1 < \lambda$. *Then* $\partial u/\partial x_3 \in V_{\beta_1+\ell_1}^{\ell_1+1,2}(\Omega)$ *and*

$$\left\| \frac{\partial u}{\partial x_3}; V_{\beta_1+\ell_1}^{\ell_1+1,2}(\Omega) \right\| \lesssim \|f; V_{\beta_1+\ell_1}^{\ell_1,2}(\Omega)\|.$$

The application of this theorem for $f \in L^2(\Omega)$ leads to

$$\begin{aligned} \left\| \frac{\partial u}{\partial x_3}; V_\beta^{1,2}(\Omega) \right\| &\lesssim \|f; V_\beta^{0,2}(\Omega)\| \lesssim \|f; L^2(\Omega)\|, && \beta \in (-\lambda, 1+\lambda), \\ \left\| \frac{\partial u}{\partial x_3}; V_{\max\{\beta;\,0\}}^{1,2}(\Omega) \right\| &\lesssim \|f; L^2(\Omega)\|, && \beta > -\lambda. \end{aligned} \tag{22.3}$$

For the Dirichlet problem we can now apply both theorems recursively. We change the notation slightly in order to be in accordance with Assumption 20.6. For $f \in L^2(\Omega)$ we obtain from Theorems 22.1 and 22.2

$$u \in V_{\beta_2}^{2,2}(\Omega), \qquad \frac{\partial u}{\partial x_3} \in V_{\beta_1}^{1,2}(\Omega), \qquad \beta_n = \max\{\beta + n;\, 0\}, \quad \beta > -1-\lambda. \tag{22.4}$$

Let now $f \in V_0^{1,2}(\Omega) \subset L^2(\Omega)$. We conclude with $\partial u/\partial x_3 = 0$ on $\partial\Omega$ that $\partial u/\partial x_3$ is the weak solution of

$$-\Delta \frac{\partial u}{\partial x_3} = \frac{\partial f}{\partial x_3} \in L^2(\Omega) \quad \text{in } \Omega, \qquad \frac{\partial u}{\partial x_3} = 0 \quad \text{on } \partial\Omega.$$

The theorems give now

$$\frac{\partial u}{\partial x_3} \in V^{2,2}_{\beta_2}(\Omega), \qquad \frac{\partial^2 u}{\partial x_3^2} \in V^{1,2}_{\beta_1}(\Omega).$$

Since $f \in V^{1,2}_0(\Omega)$ implies $f \in V^{1,2}_{\beta_3}(\Omega)$ we get also $u \in V^{3,2}_{\beta_3}(\Omega)$, β_3 as in (22.4).

Proceeding that way for $f \in V^{k-1,2}_0(\Omega)$ gives

$$u \in V^{k+1,2}_{\beta_{k+1}}(\Omega), \qquad \frac{\partial u}{\partial x_3} \in V^{k,2}_{\beta_k}(\Omega), \quad \ldots, \quad \frac{\partial^k u}{\partial x_3^k} \in V^{k+1,2}_{\beta_1}(\Omega),$$

with β_n from (22.4). This is just what we stated in Assumption 20.6.

Chapter V

Anisotropic finite element approximations in boundary layers

This chapter deals with singularly perturbed reaction-diffusion and convection-diffusion-reaction problems. Special anisotropic meshes of Shishkin type are investigated in order to derive finite element error estimates which are uniformly valid with respect to the perturbation parameter.

23 The aim of this chapter

In this chapter we consider singularly perturbed problems. We are mainly interested in a resolution of boundary layers. The main results include the following.

In Section 24 we discuss several approximation strategies for the model problem

$$-\varepsilon^2 \Delta u + cu = f \quad \text{in } \Omega \subset \mathbb{R}^d \quad (d = 2, 3), \qquad u = 0 \quad \text{auf } \partial\Omega.$$

The solution u is characterized for $0 < \varepsilon \ll 1$ by a boundary layer of width $\mathcal{O}(\varepsilon |\ln \varepsilon|)$. We show that the finite element method both on quasi-uniform meshes and on meshes with isotropic refinement in the boundary layer does not lead to error estimates which are quasi-uniform with respect to the perturbation parameter $\varepsilon \ll 1$ (Lemmata 24.1 and 24.3). As our favorite variant we propose to use in the layer anisotropic elements with size $h_1 = h$ in tangential direction and $h_2 = ah$ normal to the boundary. The parameter a describes the width of the refinement zone. In [5, 6, 14] we proved for $a \sim \varepsilon |\ln \varepsilon|$ the uniform error estimate

$$|||\, u - u_h \,|||_\Omega \lesssim h^k \varepsilon^{1/2} |\ln \varepsilon|^{k+1/2} + h^{k+1} \tag{23.1}$$

in the energy norm $|||\ .\ |||_\Omega \sim \varepsilon |\ .\ ; W^{1,2}(\Omega)| + \|\ .\ ; L^2(\Omega)\|$. We note, however, that in these papers corner/edge singularities were excluded by demanding certain compatibility conditions on the data. We postpone the proof of (23.1) to Section 25 but we confirm the result by a numerical test example. With some remarks (Remarks 24.2, 24.5, 24.6, and 24.7) we refer also to related literature.

The error analysis for the anisotropic mesh refinement strategy is presented in Section 25. Additionally to [5, 6, 14], wee focus on two new points.

1. We incorporate an additional mesh refinement to treat also corner singularities. This is restricted to two dimensions but the techniques should work also in three dimensions.

2. Results in related literature led to the assumption that for $h \geq \varepsilon$ (which is the interesting case in practice) a numerical layer of width $a = \mathcal{O}(\varepsilon |\ln h|)$ is more appropriate. Therefore we investigate also this case in Section 25.

We mention here that the two cases in Item 2 look similar but they need different strategies for the proof.

- In the case $a = a_* \varepsilon |\ln \varepsilon|$ we get for $\operatorname{dist}(x, \partial\Omega) \geq a$ the a-priori estimate $|D^\alpha u(x)| \lesssim \varepsilon^{a_* - |\alpha|}$ for the solution u. That means we can use the standard interpolation theory for the large elements in the interior of the domain if only a_* is sufficiently large such that $|D^\alpha u|$ is bounded uniformly in ε.
- In the case $a = a_* \varepsilon |\ln h|$ we get for $\operatorname{dist}(x, \partial\Omega) \geq a$ the a-priori estimate $|D^\alpha u(x)| \lesssim h^{a_*} \varepsilon^{-|\alpha|}$. Therefore we must use low derivatives (if possible *no* derivative) of u in order to get a bound uniform in ε. Fortunately, the powers of h can be extracted due to the h^{a_*}-term in the a-priori estimate above.

The final result is

$$|||\, u - u_h \,|||_\Omega \lesssim h^k \varepsilon^{1/2} \min\{ |\ln h|^{k+1/2};\ |\ln \varepsilon|^{k+1} \} + h^{k+1},$$

if $a = a_* \varepsilon \min\{|\ln h|;\ |\ln \varepsilon|\}$ with a suitable constant a_* (Corollary 25.11). The section ends with a discussion of insufficient refinement near the corners.

We mention again that we present the asymptotic estimates in general in terms of $h := \max_{e \in \mathcal{T}_h} \operatorname{diam} e$. Since we advocate only strategies where the number of elements is $N_{\mathrm{el}} \sim h^{-d}$, the error can easily be expressed in terms of N_{el} or the number N of unknowns (degrees of freedom).

The reaction-diffusion problem (24.1) was chosen as one of the simplest singularly perturbed problems to motivate the usefulness of anisotropic meshes. In Section 26 we consider a slightly different example as well. In the convection-diffusion-reaction problem

$$-\varepsilon \Delta u + b \cdot \nabla u + cu = f \quad \text{in } \Omega = (0,1)^2, \qquad u = 0 \quad \text{on } \partial\Omega,$$

three types of boundary have to be distinguished. At the *inflow boundary* ($b \cdot n < 0$, n is the outer normal on $\partial\Omega$) there is no layer. At the *outflow boundary* ($b \cdot n > 0$) there is an *ordinary* (or *outflow*) *layer* of width $\mathcal{O}(\varepsilon |\ln \varepsilon|)$. Parts of the boundary with $b \cdot n = 0$ are called *characteristic*. There will appear a *parabolic layer* of width $\mathcal{O}(\varepsilon^{1/2} |\ln \varepsilon|)$ in these regions.

In Subsection 26.2 and 26.3 we summarize some approximation results for a *pure* and a *stabilized* Galerkin finite element method on anisotropic meshes (Theorem 26.6). The surprising point is that one can even for the pure Galerkin method prove uniform convergence (with respect to $\varepsilon \ll 1$) in an $\varepsilon^{1/2}$-weighted $W^{1,2}(\Omega)$-norm [73, 186]. However, as reported in [162], practical calculations with linear and bilinear elements show that these estimates are very sensitive to the choice of a certain mesh parameter. Such non-robust behaviour reduces the practical importance of the pure Galerkin method. Therefore we consider also a stabilized Galerkin method and summarize and reformulate results which were obtained in [13]. For our proposed choice of the stabilization parameters we were able to prove, under some assumptions on u, that the finite element error converges in an energy type norm with the optimal order almost uniform with respect to ε (Theorem 26.6),

$$|||\, u - u_h \,|||_{\Omega,\delta} \lesssim h^k |\ln \varepsilon|^{k+1/2}.$$

Here, we used refinement zones of the width of the boundary layers.

24 Discretization techniques for a reaction-diffusion problem: state of the art

Let us study the reaction-diffusion model problem

$$L_\varepsilon u := -\varepsilon^2 \Delta u + cu = f \quad \text{in } \Omega \subset \mathbb{R}^d, \qquad u = 0 \quad \text{on } \partial\Omega, \tag{24.1}$$

where $\varepsilon \in (0,1]$ is the diffusion parameter, c and f are sufficiently smooth functions, $c \geq c_0 > 0$, and $d = 2, 3$. We introduce in this section the specific difficulties of boundary layers and refer to relevant literature. In particular, we will see that the numerical approximation of functions with boundary layers leads naturally to anisotropic finite elements.

For $d = 2$ the boundary value problem (24.1)) describes, for example, a temperature distribution in a thin domain $\Omega \times (0, z_0)$, $z_0 \ll 1$, where the temperature can be considered as constant in the x_3-direction. Heat transfer across the boundary parts $x_3 = 0$ and $x_3 = z_0$ enters the model by the term cu. In addition, problem (24.1) appears within a Newton iteration of nonlinear reaction-diffusion problems,

$$-\varepsilon^2 \Delta u + g(x,u) = f \quad \text{in } \Omega, \qquad u = 0 \quad \text{on } \partial\Omega,$$

or in an implicit semi-discretization of a time-dependent partial differential equation

$$\frac{\partial u}{\partial t} - \Delta u = \tilde{f}$$

with $\tau = \varepsilon^2$ being the step size.

In the singularly perturbed case $\varepsilon \ll 1$ the solution of (24.1) is characterized by a boundary layer of width $\mathcal{O}(\varepsilon |\ln \varepsilon|)$, see, for example, [96]. This is caused by the fact that the solution u_0 of the algebraic limit equation

$$c(x) u_0(x) = f(x) \quad \text{in } \Omega \tag{24.2}$$

in general cannot satisfy the given boundary condition. The effect is illustrated in Figure 24.1 for the one-dimensional example

$$-\varepsilon^2 u'' + u = 1 \quad \text{in } (0,1), \qquad u(0) = u(1) = 0, \tag{24.3}$$

where the exact solution can be given analytically,

$$u(x) = \frac{e^{x/\varepsilon} - e^{-x/\varepsilon}}{e^{1/\varepsilon} - e^{-1/\varepsilon}}.$$

In higher space dimensions, the boundary layer is of the same nature. The consequence is that one cannot expect an a-priori estimate of the solution better than

$$|u; W^{\ell,2}(\Omega)| \lesssim \varepsilon^{1/2-\ell}, \quad \ell \geq 1. \tag{24.4}$$

For this estimate we excluded additional effects of higher space dimensions like corner and edge singularities.

We investigate now error estimates for the finite element solution u_h determined by:

$$\textit{Find } u_h \in V_{0h} : a(u_h, v_h) = (f, v_h)_\Omega \quad \forall v_h \in V_{0h}. \tag{24.5}$$

Here, $a(u,v) := \varepsilon^2 (\nabla u, \nabla v)_\Omega + (cu, v)_\Omega$ is the bilinear form which defines the energy norm

$$|||\, v \,|||_\Omega := \big(a(v,v)\big)^{1/2} \sim \varepsilon |v; W^{1,2}(\Omega)| + \|v; L^2(\Omega)\|. \tag{24.6}$$

The finite element space $V_{0h} \subset \mathcal{C}(\overline{\Omega})$ is defined by

$$V_{0h} := \{ v_h \in V_0 : v_h|_e \in \mathcal{P}_{k,e} \quad \forall e \in \mathcal{T}_h \}. \tag{24.7}$$

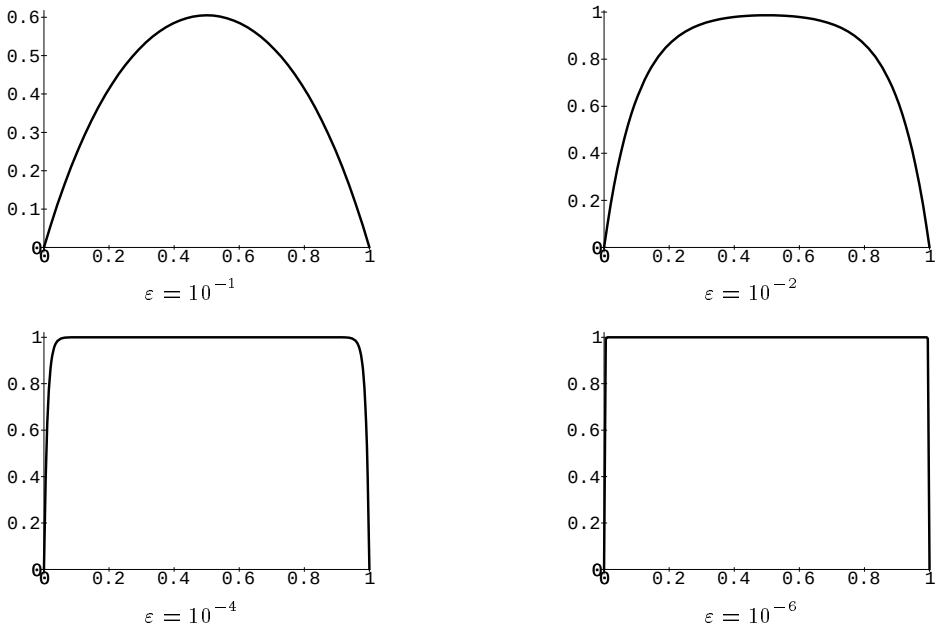

Figure 24.1: Illustration of boundary layers: solution of Problem (24.3) for different values of ε.

Lemma 24.1 *Consider problem (24.1) and assume that the solution u satisfies the estimate (24.4). Then the finite element error satisfies the error estimate*

$$|||\, u - u_h \,|||_\Omega \lesssim h^k \varepsilon^{1/2-k} \tag{24.8}$$

when a family of quasi-uniform meshes is used.

Proof Due to the Galerkin orthogonality, the error in the energy norm can be estimated via

$$|||\, u - u_h \,|||_\Omega \le |||\, u - v_h \,|||_\Omega \quad \forall v_h \in V_{0h}. \tag{24.9}$$

Therefore we need only to bound the interpolation error $|||\, u - \mathrm{I}_h u \,|||_\Omega$.

Since the mesh is quasi-uniform we obtain

$$\begin{aligned} |||\, u - \mathrm{I}_h u \,|||_\Omega &\lesssim \varepsilon |u - \mathrm{I}_h u; W^{1,2}(\Omega)| + \|u - \mathrm{I}_h u; L^2(\Omega)\| \\ &\lesssim \varepsilon h^k |u; W^{k+1,2}(\Omega)| + h^k |u; W^{k,2}(\Omega)|. \end{aligned}$$

With (24.4) and (24.9) we obtain (24.8). In the case $k = 1$ the estimate

$$\|u - \mathrm{I}_h u; L^2(\Omega)\| \lesssim h |u; W^{1,2}(\Omega)|$$

(which was used above) does not hold for the Lagrangian interpolation operator. Instead, one has to use another interpolation operator, for example C_h, O_h, or S_h, see Chapter III. ■

Due to the factor $\varepsilon^{1/2-k}$ in (24.8) we must expect that the convergence order h^k can be observed only for small h, when the boundary layer is resolved. This can be seen in the test described below, see Table 24.1 in Example 24.4.

Remark 24.2 Schatz and Wahlbin [168] analyzed carefully two- (and one-)dimensional problems. They derived $L^2(\Omega)$-, $L^\infty(\Omega)$-, and pointwise error estimates for quasi-uniform meshes

with linear finite elements. Also the case of rough data is addressed. We cite two estimates which hold uniformly in ε. For convex Ω and $c, f \in H^{1/2,\infty}(\Omega)$ (in the sense of interpolation spaces) the estimate

$$\|u - u_h\,; L^2(\Omega)\| \lesssim \min(\sqrt{h}, h^2\varepsilon^{-3/2})$$

holds. Moreover, uniform estimates in the sense

$$\begin{aligned} \|u - u_h\,; L^2(\Omega)\| &\lesssim \min(h, h^2\varepsilon^{-1}) \\ |\!|\!| u - u_h |\!|\!| &\lesssim \min(h, \varepsilon) \end{aligned}$$

hold if $f \in W_0^{1,2}(\Omega)$, that means, if f satisfies homogeneous Dirichlet boundary conditions.

An improvement to the approximation on quasi-uniform meshes is to use locally refined meshes in the boundary layer $\Omega_L := \{x \in \Omega : \operatorname{dist}(x, \partial\Omega) \le a\}$, $a \sim \varepsilon|\ln\varepsilon|$.

Lemma 24.3 *Let $\mathcal{T}_h$ contain (isotropic) elements of diameter $\varepsilon^{1-1/(2k)}h$ in the boundary layer but elements of diameter h outside (where the solution has no large derivatives). Under the assumption that*

$$|u; W^{\ell,2}(\Omega_L)| \lesssim \varepsilon^{1/2-\ell}, \quad \ell \ge 1, \tag{24.10}$$

$$|u; W^{\ell,2}(\Omega \setminus \Omega_L)| \lesssim 1, \tag{24.11}$$

we obtain

$$|\!|\!| u - u_h |\!|\!|_\Omega \lesssim h^k. \tag{24.12}$$

However, the number of elements increases (for $d = 2, 3$) to $\mathcal{O}(\varepsilon^{1-d+d/(2k)}|\ln\varepsilon|h^{-d})$ in the layer.

Proof We proceed as in the proof of Lemma 24.1. Using (24.10) and (24.11) we derive

$$\begin{aligned} |\!|\!| u - \mathrm{I}_h u |\!|\!|_{\Omega_L} &\lesssim (\varepsilon^{1-1/(2k)}h)^k \left(\varepsilon|u; W^{k+1,2}(\Omega_L)| + |u; W^{k,2}(\Omega_L)|\right) \\ &\lesssim h^k\varepsilon^{k-1/2}(\varepsilon\,\varepsilon^{1/2-(k+1)} + \varepsilon^{1/2-k}) \;=\; h^k, \\ |\!|\!| u - \mathrm{I}_h u |\!|\!|_{\Omega\setminus\Omega_L} &\lesssim h^k \left(\varepsilon|u; W^{k+1,2}(\Omega \setminus \Omega_L)| + |u; W^{k,2}(\Omega \setminus \Omega_L)|\right) \\ &\lesssim h^k(\varepsilon + 1). \end{aligned}$$

With the projection property (24.9) we conclude (24.12). The number of elements is obtained by dividing the area/volume of the layer by the area/volume of the elements in the layer. ∎

A closer look at the structure of the boundary layer demonstrates that large derivatives only occur perpendicularly to the boundary and not in the tangential direction. Hence, *anisotropic refinement*, with elements of diameter h in the tangential direction and with thickness of order $\varepsilon|\ln\varepsilon|h$ in the normal direction, is much more efficient in the layer. While using only $\mathcal{O}(h^{-d})$ elements one can prove, under some assumptions on the solution, that the error behaves like

$$|\!|\!| u - u_h |\!|\!|_\Omega \lesssim h^k(\varepsilon^{1/2-\delta} + h) \tag{24.13}$$

with $\delta > 0$ arbitrarily small, see [5, 6, 14]. We will discuss this for the two-dimensional case extensively in Section 25. Before, we will present a numerical test and some remarks.

The a-priori error analysis is valuable especially in cases when the asymptotical approximation order can be confirmed by numerical tests with a moderate number of elements. Therefore we document now a test example which was computed with the finite element multi-grid package *FEMGPM*, which is described briefly in Comment 30.1 on page 171.

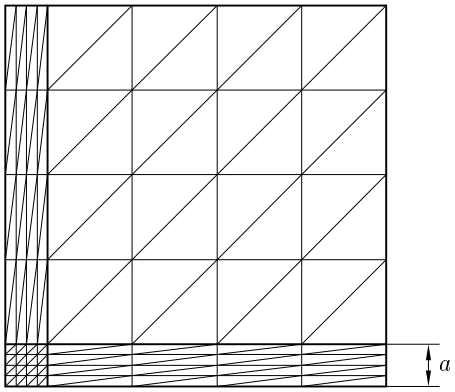

Figure 24.2: Anisotropically refined mesh for the numerical test, $N_{\rm el} = 2^7$.

$N_{\rm el}$	$\varepsilon = 10^{-1}$	$\varepsilon = 10^{-3}$	$\varepsilon = 10^{-5}$
2^7	0.114 e+0	0.278 e+0	0.282 e+0
2^9	0.570 e−1	0.189 e+0	0.195 e+0
2^{11}	0.285 e−1	0.128 e+0	0.136 e+0
2^{13}	0.143 e−1	0.856 e−1	0.955 e−1
2^{15}	0.713 e−2	0.543 e−1	0.674 e−1

Table 24.1: Error norm for $a = 0.5$.

$N_{\rm el}$	$\varepsilon = 10^{-1}$	$\varepsilon = 10^{-3}$	$\varepsilon = 10^{-5}$
2^7	0.747 e−1	0.894 e−2	0.130 e−2
2^9	0.387 e−1	0.518 e−2	0.657 e−3
2^{11}	0.196 e−1	0.362 e−2	0.330 e−3
2^{13}	0.980 e−2	0.298 e−2	0.167 e−3
2^{15}	0.490 e−2	0.256 e−2	0.877 e−4

Table 24.2: Error norm for $a = \varepsilon|\log_{10}\varepsilon|$.

$N_{\rm el}$	$\varepsilon = 10^{-1}$	$\varepsilon = 10^{-3}$	$\varepsilon = 10^{-5}$
2^7	0.511 e−1	0.134 e−1	0.218 e−2
2^9	0.257 e−1	0.681 e−2	0.112 e−2
2^{11}	0.129 e−1	0.342 e−2	0.568 e−3
2^{13}	0.644 e−2	0.171 e−2	0.285 e−3
2^{15}	0.322 e−2	0.864 e−3	0.143 e−3

Table 24.3: Error norm for $a = 2\varepsilon|\log_{10}\varepsilon|$.

$N_{\rm el}$	$\varepsilon = 10^{-1}$	$\varepsilon = 10^{-3}$	$\varepsilon = 10^{-5}$
2^7	0.912 e−1	0.257 e−1	0.395 e−2
2^9	0.456 e−1	0.134 e−2	0.217 e−2
2^{11}	0.228 e−1	0.680 e−2	0.112 e−3
2^{13}	0.114 e−1	0.342 e−2	0.568 e−3
2^{15}	0.571 e−2	0.171 e−2	0.285 e−3

Table 24.4: Error norm for $a = 4\varepsilon|\log_{10}\varepsilon|$.

Example 24.4 As a numerical example we took the boundary value problem from [168, Example 11.3]:

$$-\varepsilon^2\Delta u + u = 0 \quad \text{in } \Omega = (0,1)^2, \qquad u = e^{-x_1/\varepsilon} + e^{-x_2/\varepsilon} \quad \text{on } \partial\Omega.$$

A boundary layer appears only at $M = \{x \in \partial\Omega : x_1 = 0 \vee x_2 = 0\}$. We introduce a parameter a describing the width of the numerical boundary layer and use a partition of the domain into four rectangles $(0,a)^2$, $(0,a)\times(a,1)$, $(a,1)\times(0,a)$, and $(a,1)^2$. The rectangles were uniformly hierarchically refined, see Figure 24.2. We varied the number of elements $N_{\rm el}$ and computed numerical solutions with piecewise linear trial functions for different values of ε and a [14]. From these solutions we calculated the energy norm $|||\, u - u_h \,|||$ of the finite element error by a numerical integration formula which was determined such that the integration error was independent of $N_{\rm el}$ (but dependent on $u(\varepsilon)$ and a). The error is given in Tables 24.1–24.4.

We can draw three conclusions. In Table 24.1 the error is displayed when a quasi-uniform mesh is used. We see the asymptotic behaviour of the error in the case of a large value of ε, but the error is far from this asymptotic behaviour in case of small ε. For $a = a_*\varepsilon|\log_{10}\varepsilon|$ we obtain the expected order of the approximation error for small ε as well. That means the

a-priori error estimates in (24.8) and (24.13) are confirmed.

Second, The error estimate (24.13) indicates that the error should diminish with decreasing ε. This effect can be seen in Tables 24.2–24.4.

Third, by comparing Tables 24.2–24.4 we see that the performance depends upon the scaling factor a_*. The error analysis demands only a lower bound on this parameter but obviously it should be chosen carefully. □

We end this section with remarks on related results from other authors, on interior layers, and on stabilized Galerkin methods.

Remark 24.5 Mesh refinement near the boundary is not new. An obvious idea to mesh a rectangular/cuboidal domain is to use the cross product of adapted one-dimensional meshes. This leads naturally to anisotropic elements in the boundary layer. The main difference between approaches is how they refine in one dimension. Bakhvalov [32] used a gradually refined mesh which is optimally adapted to the exponential character of the functions describing the layer,

$$X^{(i)} = \begin{cases} \frac{\varepsilon}{c_0} \ln \frac{q}{q - i/N}, & i = 0, \ldots, i_0, \\ \alpha + \beta \frac{i}{N}, & i = i_0 + 1, \ldots, N, \end{cases}$$

with two parameters c_0 and $q \in (0,1)$ which determine the remaining constants α, β and i_0. Shishkin [139, 173] simplified this mesh and uses piecewise uniform meshes,

$$X^{(i)} = \begin{cases} a \frac{i}{N}, & i = 0, \ldots, N, \\ a + (1-a) \frac{i-N}{N}, & i = N+1, \ldots, 2N, \end{cases}$$

with a parameter $a \sim \varepsilon \ln N$.

Previous results concerning the resolution of boundary layers for the model problem (24.1) are due to Shishkin [172, 173] in the context of finite difference methods in two and three dimensions, due to Blatov [47] in the context of the h-version of the finite element method (bilinear elements), and due to Melenk/Schwab [135] and Xenophontos [196] for the hp-version of the finite element method, both in two dimensions only. In [47, 172] the authors used meshes of *Bakhvalov type*, and in [173] *Shishkin* meshes. The error estimates were derived in the maximum norm [47, 172, 173], see also [139], or in the energy norm [135, 196].

A critical review of decompositions of the solution, approximations on locally refined meshes, and error estimates for one- and two-dimensional problems is given in [162].

Remark 24.6 In the case that c and f are not sufficiently regular, for example piecewise constant, we find a discrepancy in the properties of the solutions u and u_0 of (24.1) and (24.2), respectively. While u is at least contained in $W^{1,2}(\Omega)$, this can be violated for u_0. It can be interpreted as a smoothing property of the diffusion term $-\varepsilon^2 \Delta u$. The result is that u can also have *interior layers*. They have similar properties to boundary layers, for example a thickness of $\mathcal{O}(\varepsilon |\ln \varepsilon|)$. However, the geometry of these layers can be arbitrarily complicated. Therefore,

1. we have to approximate curved manifolds, and
2. we cannot assume that certain sides of the finite elements are always parallel to the coordinate axes.

Algorithmic ideas about how to do the approximation have been proposed in [125], see, for example, Figures 9, 10, and 12 of this paper, and in [176]. A numerical localization procedure for interior layers is also described in [205] in the context of compressible (viscous and inviscid) flow problems. All the computational results are promising.

We remark that it is much easier to approximate a curved interior manifold by anisotropic elements, than it is to approximate a curved boundary. The reason for this is that in the latter case only one side of the curved manifold belongs to the domain Ω. The other side should not be covered by the triangulation.

We will not study such problems in this report. But we underline that for the treatment of them it is necessary to investigate not only elements where the longest side is parallel to an axis of the coordinate system. (Here we mean a well chosen coordinate system which is adapted to the boundary or interior layer.) Therefore we discussed in Chapter II the coordinate system condition quite extensively.

Remark 24.7 In the literature one can find a number of variants to stabilize the Galerkin finite element method, see for example [31, 79, 105]. The basic idea is to modify the bilinear and linear forms to become

$$\begin{aligned} a(u,v) &:= \sum_{e\in\mathcal{T}_h} (L_\varepsilon u, v+\delta_e L v)_e, \\ \langle f, v\rangle &:= \sum_{e\in\mathcal{T}_h} (f, v+\delta_e L v)_e, \end{aligned}$$

where $L = L_\varepsilon$ (*Galerkin/Least-squares method* [105]) or $L = -L_\varepsilon{}^*$ (*unusual stabilized finite element method* [31]). For the self-adjoint differential operator L_ε, as in (24.1), the optimization (with respect to minimizing the energy norm) of the choice of the set of numerical diffusion parameters $\delta_e \geq 0$ leads to $\delta_e = 0$ for all e, that is the pure Galerkin method (Galerkin orthogonality). The result may be different for other norms.

In the case of a constant coefficient c Franca and Farhat [79] choose $L = -L_\varepsilon{}^*$ and $\delta_e = [\mathrm{diam}\,(e)]^2/[c(\mathrm{diam}\,(e))^2 + \varepsilon^2]$ and obtain a diminution of the error in the maximum norm. This, however, was demonstrated only in a computational example ("picture norm"), but not analytically. The explanation is that for piecewise linear trial functions this method is equivalent to a pure Galerkin method with an enriched trial space (piecewise linears plus cubic element bubble functions) [79].

The approximation error of this method was analyzed in [14] for higher order trial functions and with respect to anisotropic meshes. It turned out that there is a range of values from which δ_e can be chosen such that the error estimate (24.13) is preserved. This freedom can then be used to control the error in some other norm. But this was not pursued further.

25 Boundary layers and corner singularities in a reaction-diffusion problem

25.1 Properties of the exact solution

In the previous section we summarized results on the numerical treatment of the reaction-diffusion model problem

$$L_\varepsilon u := -\varepsilon^2 \Delta u + cu = f \quad \text{in } \Omega, \qquad u = 0 \quad \text{on } \partial\Omega, \tag{25.1}$$

$(0 < \varepsilon \ll 1,\ c = c(x) \geq c_0 > 0)$.

In this section we will continue this discussion with two additional points. First, we discuss the analytical properties of u in general polygonal domains, and we treat the arising corner singularities. Second, we investigate two slightly different versions of anisotropic mesh refinement. The difference is in the width a of the refinement layer, see the illustration in Figure 24.2 on

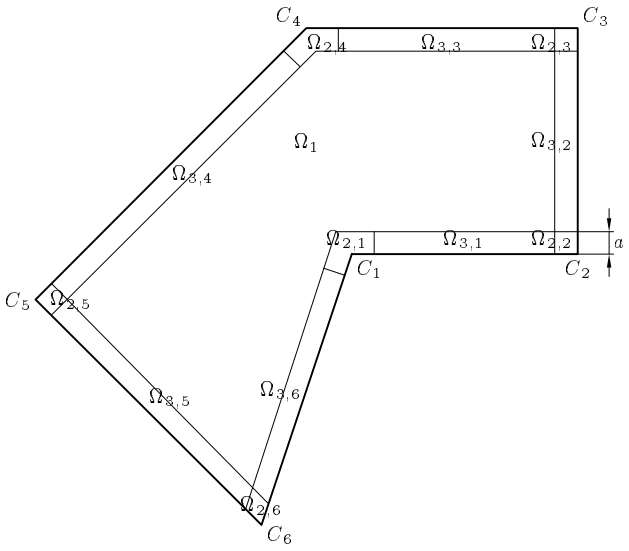

Figure 25.1: Illustration of the partition of Ω for a reaction-diffusion problem.

page 132: the original *Shishkin meshes* [139, 173] are characterized by $a \sim \varepsilon|\ln h|$ whereas for the *Shishkin type meshes* in [14] the relation $a \sim \varepsilon|\ln \varepsilon|$ was assumed.

The plan is to introduce some notation and to discuss the analytical properties of u in this subsection. In the other two subsections we derive estimates for the interpolation error and the finite element error, respectively.

We begin with a parameter dependent partition of Ω as illustrated in Figure 25.1. The subdomains are obtained by introducing lines with a distance a (this is the parameter), $\varepsilon < a \ll 1$, to the boundary and eventually, near corners with large angles, some more lines perpendicularly to them. The interior domain is denoted by Ω_1, the union of the small subdomains $\Omega_{2,j}$ near the corners C_j by $\Omega_2 := \bigcup_{j=1}^J \Omega_{2,j}$, and the union if boundary strips by $\Omega_3 := \bigcup_{j=1}^J \Omega_{3,j}$. Furthermore, we define by $\Omega_2^- := \bigcup_{j=1}^J \Omega_{2,j}^-$ the union of corner regions $\Omega_{2,j}^- := \{x \in \Omega : \operatorname{dist}(x, C_j) < \varepsilon\}$ and note that $\Omega_{2,j}^- \subset \Omega_{2,j}$.

The parameter a will later be chosen as the thickness of the refinement layer ($a = a_* \varepsilon|\ln \varepsilon|$ or $a = \min\{a_\Omega;\ a_* \varepsilon|\ln h|\}$ with suitably chosen constants a_* and a_Ω) but here it is essential that we can define in Ω_3 a boundary fitted coordinate system (x_1, x_2) with $x_2 = \operatorname{dist}(x, \partial\Omega)$. Derivatives D^α are to be understood with respect to this coordinate system. Points in $\Omega_1 \cup \Omega_2$ can be considered in any Cartesian coordinate system. Moreover, for points in Ω we define by r the distance to the set of corners $\{C_j\}_{j=1}^J$. Note that we have in particular $r = \operatorname{dist}(x, C_j)$ for $x \in \Omega_{2,j}$.

Assumption 25.1 *Let u be the solution of (25.1) where f and c are sufficiently smooth functions, $0 < \varepsilon \ll 1$, and $c \geq c_0 > 0$. For given $k, n \in \mathbb{N}$, $n \geq k+1$, the solution u can be decomposed into a smooth term u_s, a boundary layer term u_b, a corner singularity u_c, and a remainder u_r, $u = u_\mathrm{s} + u_\mathrm{b} + u_\mathrm{c} + u_\mathrm{r}$. There is a constant $\gamma_0 > 0$ such that the terms satisfy the following estimates for all $\alpha \in \mathbb{N}^2 : |\alpha| \leq k+1$:*

$$|D^\alpha u_\mathrm{s}| \lesssim 1 \qquad \text{in } \Omega, \tag{25.2}$$

$$|D^\alpha u_\mathrm{b}| \lesssim \begin{cases} \varepsilon^{-\alpha_2} e^{-\gamma_0 x_2/\varepsilon} + \varepsilon^{-|\alpha|} e^{-\gamma_0 r/\varepsilon} & \text{in } \Omega_3, \\ \varepsilon^{-|\alpha|} e^{-\gamma_0 \operatorname{dist}(x,\partial\Omega)/\varepsilon} & \text{in } \Omega \setminus \Omega_3, \end{cases} \tag{25.3}$$

$$|D^\alpha u_{\rm c}| \lesssim \begin{cases} \varepsilon^{-\lambda_j} r^{\lambda_j - |\alpha|} e^{-\gamma_0 r/\varepsilon} & \text{in } \Omega^-_{2,j} \quad \text{when } \lambda_j < k+1, \\ \varepsilon^{-|\alpha|} |\ln(r/\varepsilon)|\, e^{-\gamma_0 r/\varepsilon} & \text{in } \Omega^-_{2,j} \quad \text{when } \lambda_j = k+1, \\ 0 & \text{in } \Omega^-_{2,j} \quad \text{when } \lambda_j > k+1, \\ 0 & \text{in } \Omega \setminus \Omega^-_2, \end{cases} \tag{25.4}$$

$$\|u_{\rm r}; W^{\ell,2}(\Omega)\| \lesssim \varepsilon^{n-\ell}, \qquad \ell \le k+3, \tag{25.5}$$

where $\lambda_j = \pi/\omega_j$ and ω_j is the interior angle at the corner C_j.

We underline that the constants hidden in $\lesssim$ and $\sim$ are always independent of ε (and h) but they can depend on α. Note further that the term $\varepsilon^{-|\alpha|} e^{-\gamma_0 r/\varepsilon}$ in (25.3) contains for $x \in \Omega_{3,j}$ also the influence of layer terms with respect to other boundary sides and of so-called corner layers. Since the boundary layer has the same structure on the whole boundary $\partial\Omega$ we can use the compact notation $u_{\rm b}$. This is not any longer possible if convection-diffusion-reaction problems are considered, see the more involved notation in Assumption 26.2. We remark also that the decomposition of u is usually made much more detailed than here. In particular, the smaller we want to make the remainder $u_{\rm r}$, this means, the larger we want to make n, the more terms of the detailed decomposition we have to include into $u_{\rm s}$, $u_{\rm b}$, and $u_{\rm c}$. This is possible if the data f and c are sufficiently smooth. It is also clear that a large k, this means the existence of high derivatives of $u_{\rm s}$, $u_{\rm b}$, $u_{\rm c}$, and $u_{\rm r}$, requires more smoothness of the data than a small k.

Remark 25.2 If we replaced α_2 in (25.3) by $|\alpha|$ we could prove Assumption 25.1; the estimates could then be extracted from [110, 111].

This is not a convincing result, since we want to use the original form of Assumption 25.1. But for the sake of completeness we will prove the statement of the remark.

Proof Set $u_{\rm s} = \sum_{j=1}^J \sum_{i=0}^{2n} \varepsilon^i u_{j,i}$. From [110, (3.6)] we obtain

$$u_{j,0} = f^0_{j,0}/c, \quad u_{j,1} = f^0_{j,1}/c, \quad u_{j,i} = (f^0_{j,i} + \Delta u_{j,i-2})/c, \quad i = 2,3,\ldots,$$

where $f^0_{j,i}$ is defined in [110, (4.4)] by

$$f^0_{j,i} = \begin{cases} \chi_j f, & \text{if } i = 0, \\ 0 & \text{if } i = 1,3,5,\ldots, \\ -\sum_{j'=0}^J [2\nabla\chi_j \cdot \nabla u_{j',i-2} + u_{j',i-2}\Delta\chi_j] & \text{if } i = 2,4,6,\ldots, \end{cases}$$

where χ_j is a smooth cut-off function. From $|D^\alpha f| \lesssim 1$ we get $|D^\alpha u_{j,2m}| \lesssim c_0^{-(m+1)} \lesssim 1$, $m = 0,1,\ldots$. Since $u_{2m+1} = 0$ we obtain (25.2).

In $u_{\rm b}$ we collect the boundary layer terms $\hat V_{j,2n}$, $\hat W_{j,2n}$, and $Z_{j,2n,M}$, as well as that terms of $U^{(s)}_{{\rm asy},j,2n,M}$ that are not contained in (25.4). With [110, (3.26) and (3.38)] we obtain the estimate for $z_{j,i}$: $|D^\alpha z_{j,i}| \lesssim \varepsilon^{-|\alpha|} e^{-\gamma_0 r/\varepsilon} \lesssim \varepsilon^{-|\alpha|} e^{-\gamma_0 \operatorname{dist}(x,\partial\Omega)/\varepsilon}$. For the other terms let us distinguish two cases, $x \in \bar\Omega \setminus \Omega^-_2$ and $x \in \bar\Omega^-_2$.

In the first case we have

$$u_{\rm b} = \sum_{j=1}^J \sum_{i=0}^{2n} \varepsilon^i \zeta_j(r/\varepsilon)\,(v_{j,i} + w_{j,i}) + \sum_{j=1}^J \sum_{i=0}^{2n+M} \varepsilon^i z_{j,i},$$

where ζ_j is a smooth cut-off function with $\zeta(z) = 0$ for $z < 1/2$ and $\zeta(z) = 1$ for $z > 1$, see [110, page 132]. From [110, (3.13) and (3.16)] we obtain for $x \in \Omega_3$

$$|D^\alpha v_{j,i}| \lesssim \varepsilon^{-|\alpha|} e^{-\gamma_0 x_2/\varepsilon}, \quad |D^\alpha w_{j,i}| \lesssim \varepsilon^{-|\alpha|} e^{-\gamma_0 x_2/\varepsilon}, \tag{25.6}$$

since $r\Theta = r\theta/\varepsilon \sim r(\sin\theta)/\varepsilon = x_2/\varepsilon$ and

$$|D^\alpha w| \lesssim \sum_{|\beta|=|\alpha|} r^{-\beta_2} |D_r^{\beta_1} D_\theta^{\beta_2} w| \lesssim \sum_{|\beta|=|\alpha|} \varepsilon^{-\beta_2} e^{-\gamma_0 r\Theta} \lesssim \varepsilon^{-|\alpha|} e^{-\gamma_0 r\Theta}$$

for $w = v_{j,i}$. (Even if the transformation $(r,\theta) \to (x_1, x_2)$ is done more carefully the author was not able to replace $|\alpha|$ by α_2 in (25.6): since $f^1_{j,0} = 0$, see [110, page 141], we have $v_{j,0} = Ce^{-\sqrt{q_0} r\theta/\varepsilon}$ and $|D^{(1,0)} v_{j,0}| \sim |\sqrt{q_0}\varepsilon^{-1} e^{-\sqrt{q_0} r\theta/\varepsilon}(\theta\cos\theta + \sin\theta)| \sim \varepsilon^{-1} e^{-\gamma_0 x_2/\varepsilon}$ for $\theta \sim 1$.) A similar argument can be applied for $w_{j,i}$. For $x \notin \Omega_3$ it remains to show that $r\theta \gtrsim \operatorname{dist}(x, \partial\Omega)$. Indeed, if $\theta \geq 1$ this is obvious, and for $\theta < 1$ we find that $r\theta \sim r\sin\theta$ which is the distance to the boundary edge with $\theta = 0$.

Consider now the case $x \in \Omega_2^-$. Then we can use [110, Theorem 6.2] to prove (25.3), (25.4), in that case. Note that u_c contains only the singular terms of $U^{(s)}_{\mathrm{asy},j,2n,M}$, and they vanish outside Ω_2^-.

Finally, [110, Theorem 6.1] yields (25.5) where n and ℓ have a different meaning here and in [110].

We remark that there is a revised version [111] of [110] where instead of polar coordinates (r,θ) an in general non-orthogonal coordinate system (e, y) is used to describe the terms $v_{j,i}$ and $w_{j,i}$. With this additional material one can prove Assumption 25.1 for $\omega = \pi/2$ and $\omega = 3\pi/2$ but it is not clear how to do this for general ω. ■

Writing α_2 in (25.3), however, makes sense since it is well known that layer terms have a behaviour as $e^{-\gamma_0 \operatorname{dist}(x,\partial\Omega)/\varepsilon}$. The difficulty with Kellogg's result is that he used polar coordinates (r,θ) centered at the vertices of Ω which seems to be not suited in regions with $\varepsilon \lesssim r \ll 1$, $\varepsilon \lesssim \theta \lesssim 1$. The problems remain also in the revised version [111] of [110]. In the former paper [96], Han and Kellogg treated the case when Ω is the unit square. They derived a slightly different splitting with boundary layer terms u_b in Cartesian coordinates and with an estimate as given by (25.3). But in that paper, it was not obtained that the corner singularities (25.4) restrict to an ε-neighbourhood of C_j. Nevertheless, Assumption 25.1 seems to be correct, a proof will appear elsewhere [67].

25.2 Interpolation error estimates on locally refined meshes

For applying the finite element method, the inner domain Ω_1 is meshed in general (see Remark 25.3 for the exception) using $\mathcal{O}(h^{-2})$ isotropic triangles or quadrilaterals e with mesh size $\operatorname{diam} e \sim h$. The boundary layer strips $\Omega_{3,j}$, $j = 1, \ldots, J$, are subdivided into $\mathcal{O}(h^{-1}) \times \mathcal{O}(h^{-1})$ trapezoids of comparable size. If desired each trapezoid can be divided into two triangles. Thus we get

$$h_{1,e} \sim h \quad \text{and} \quad h_{2,e} \sim ah \quad \text{in } \Omega_{3,j}.$$

The subdomains $\Omega_{2,j}$, $j = 1, \ldots, J$, are split into $\mathcal{O}(h^{-2})$ (possibly isotropic) elements satisfying the maximal angle condition. If $\lambda_j > k+1$ (recall that k corresponds to the degree of the polynomial trial functions) then all elements have the same size, otherwise we demand

$$\begin{array}{lcll} \operatorname{diam} e & \sim & \varepsilon h^{1/\mu_j} & \text{if } C_j \in \overline{e}, \\ \operatorname{diam} e & \sim & \varepsilon h (r/\varepsilon)^{1-\mu_j} & \text{if } e \subset \Omega_{2,j},\ 0 < \operatorname{dist}(C_j, e) \lesssim \varepsilon, \\ \operatorname{diam} e & \lesssim & ah & \text{if } e \subset \Omega_{2,j},\ \varepsilon \lesssim \operatorname{dist}(C_j, e). \end{array} \tag{25.7}$$

The parameters μ_j are chosen such that

$$\mu_j < \frac{\lambda_j}{k} \quad \text{if } \lambda_j \leq k, \qquad \mu_j = 1 \quad \text{if } \lambda_j > k. \tag{25.8}$$

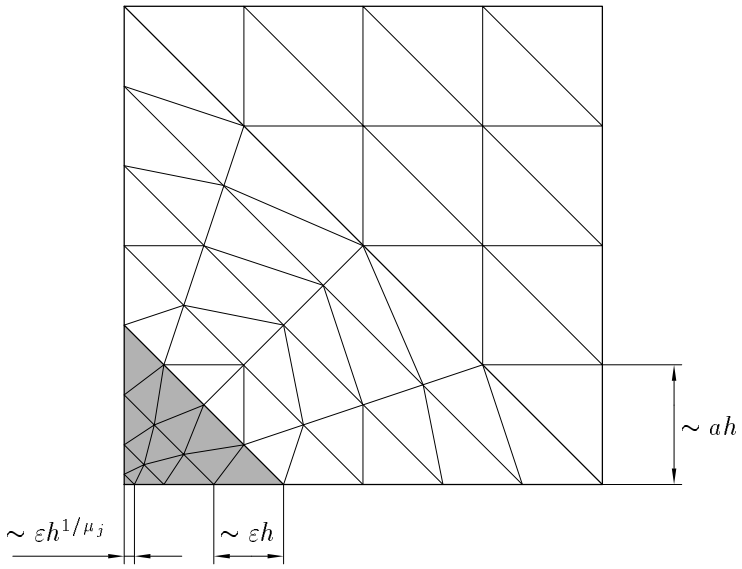

Figure 25.2: Illustration of the mesh refinement near corners.

We explain the construction near corners by the example of an isotropic triangle with edges of length $\mathcal{O}(a)$ and one vertex in C_j. A subtriangle with edges of length $\mathcal{O}(\varepsilon)$ and one vertex in C_j (shaded in Figure 25.2) can be covered by a refined mesh as explained in Section 19. The remaining quadrilateral can be divided into $\mathcal{O}(h^{-1}) \times \mathcal{O}(h^{-1})$ quadrilateral elements which can (but do not have to) be split into two triangles each. If the quadrilaterals are obtained by a uniform splitting we get elements with an aspect ratio a/ε. This is allowed but it can be avoided by some transition layer where the element size εh is doubled until ah is reached.

Remark 25.3 We mention that for compatibility reasons elements e with $\operatorname{diam} e \sim h$ and $\varrho_e \sim ah$ must be used in regions $\Omega_{1,j} \subset \Omega_1$ close to corners C_j with large interior angles. Observe that these regions are small, $\operatorname{meas}_2 \Omega_{1,j} \sim ah$.

The finite element space $V_{0h} \subset \mathcal{C}(\overline{\Omega})$ is defined again by (24.7). In the remaining part of this subsection we derive interpolation error estimates for u on the family of meshes just described. We distinguish two different choices of the parameter a.

Lemma 25.4 *Let u_c satisfy (25.4), and let $\mathcal{T}_h$ be as described above. Then the interpolation error can be estimated by*

$$|u_c - \mathrm{I}_h u_c; W^{m,2}(\Omega)| \lesssim \varepsilon^{1-m} h^{k+1-m}, \qquad m = 0, 1,$$

if

$$\mu_j < \frac{\lambda_j + 1 - m}{k + 1 - m} \quad \text{for } \lambda_j \le k, \qquad \mu_j = 1 \quad \text{for } \lambda_j > k, \qquad j = 1, \dots, J. \tag{25.9}$$

Moreover, the estimate

$$\|u_c - \mathrm{I}_h u_c; L^\infty(\Omega)\| \lesssim h^{k+1}$$

holds if μ_j satisfies

$$\mu_j < \frac{\lambda_j}{k+1} \quad \text{for } \lambda_j \le k + 1, \qquad j = 1, \dots, J. \tag{25.10}$$

The parameter k corresponds to the degree of the polynomials, see (24.7) and (3.4).

In the case $\varepsilon \sim 1$ the result is classical, see [28], [150, pages 274f.] and [158] for $k = 1$, and [81] for general k. However, in these references the construction of the mesh is more restrictive than here. Note that (25.8) is the stronger of the conditions (for $m = 0$ and $m = 1$) mentioned in the lemma.

Proof We estimate the error in $\Omega_{2,j}^-$ with arbitrary $j \in \{1, \ldots, J\}$ and distinguish two cases. Note that we can assume that $\lambda_j \le k+1$ since otherwise $u_c = 0$ in $\Omega_{2,j}^-$.

First, let $C_j \in \overline{e}$. By (25.4) and (25.7) we obtain with $\|\mathrm{I}_h u_c; L^\infty(e)\| \lesssim \|u_c; L^\infty(e)\|$ that

$$\|u_c - \mathrm{I}_h u_c; L^\infty(e)\| \lesssim \|u_c; L^\infty(e)\| \lesssim \varepsilon^{-\lambda_j} (\varepsilon h^{1/\mu_j})^{\lambda_j} \sim h^{\lambda_j/\mu_j} \lesssim h^{k+1} \tag{25.11}$$

for μ_j from (25.10). By analogy we get

$$\|u_c - \mathrm{I}_h u_c; L^2(e)\| \lesssim (\mathrm{meas}_2 e)^{1/2} \|u_c; L^\infty(e)\| \lesssim \varepsilon^{-\lambda_j} (\varepsilon h^{1/\mu_j})^{\lambda_j+1} \sim \varepsilon h^{(\lambda_j+1)/\mu_j} \lesssim h^{k+1} \tag{25.12}$$

for $\mu_j \le \min\{(\lambda_j+1)/(k+1);\ 1\}$. For the estimate of the derivative of the interpolation error we have to modify this proof slightly since we cannot assume that $u_c \in W^{1,\infty}(e)$. But we have $u_c \in W^{1,2}(e)$. By integration we get

$$|u_c; W^{1,2}(e)|^2 \lesssim \varepsilon^{-2\lambda_j} \int_0^{\operatorname{diam} e} r^{2\lambda_j - 2} r \, \mathrm{d}r \lesssim \varepsilon^{-2\lambda_j} (\operatorname{diam} e)^{2\lambda_j} \sim h^{2\lambda_j/\mu_j}$$

and hence by using the inverse inequality and (25.11)

$$|u_c - \mathrm{I}_h u_c; W^{1,2}(e)| \lesssim |u_c; W^{1,2}(e)| + (\operatorname{diam} e)^{-1} (\mathrm{meas}_2 e)^{1/2} \|\mathrm{I}_h u_c; L^\infty(e)\| \lesssim h^{\lambda_j/\mu_j} \lesssim h^k \tag{25.13}$$

for $\mu_j \le \min\{\lambda_j/k;\ 1\}$. Note that we have to add a logarithmic term for $\lambda_j = 1$,

$$\begin{aligned} |u_c; W^{1,2}(e)|^2 &\lesssim \varepsilon^{-2} \int_0^{\operatorname{diam} e} \left| \ln \frac{r}{\varepsilon} \right|^2 r \, \mathrm{d}r \\ &\lesssim \varepsilon^{-2} r^2 \left[\frac{(\ln(r/\varepsilon))^2}{2} - \frac{\ln(r/\varepsilon)}{2} + \frac{1}{4} \right]_0^{\operatorname{diam} e} \lesssim h^{1/\mu_j} (\ln h)^2, \end{aligned}$$

but for $\mu_j < 1/k$ the result remains the same.

Let now $r_e := \operatorname{dist}(e, C_j) > 0$. In this case we can use the interpolation error estimates. We get with (25.7) and for $m = 0, 1$

$$\begin{aligned} |u_c - \mathrm{I}_h u_c; W^{m,2}(e)|^2 &\lesssim (\operatorname{diam} e)^{2(k+1-m)} |u_c; W^{k+1,2}(e)|^2 \\ &\lesssim [\varepsilon h (r_e/\varepsilon)^{1-\mu_j}]^{2(k+1-m)} \varepsilon^{-2\lambda_j} \int_e r^{2(\lambda_j - k - 1)} \\ &\lesssim \varepsilon^{2[\mu_j(k+1-m)-\lambda_j]} h^{2(k+1-m)} \int_e r^{2[(1-\mu_j)(k+1-m)+\lambda_j-k-1]} \\ &\sim \varepsilon^{2[\mu_j(k+1-m)-\lambda_j]} h^{2(k+1-m)} \int_e r^{2[\lambda_j - m - \mu_j(k+1-m)]} \end{aligned}$$

since $r_e \le r$ in e. Hence

$$\begin{aligned} \sum_{\substack{e \subset \Omega_{2,j}^- \\ C_j \notin \overline{e}}} |u_c - \mathrm{I}_h u_c; W^{m,2}(e)|^2 &\lesssim \varepsilon^{2[\mu_j(k+1-m)-\lambda_j]} h^{2(k+1-m)} \int_0^\varepsilon r^{2[\lambda_j - m - \mu_j(k+1-m)]+1} \, \mathrm{d}r \\ &\sim \varepsilon^{2[\mu_j(k+1-m)-\lambda_j]} h^{2(k+1-m)} \varepsilon^{2[\lambda_j - m - \mu_j(k+1-m)]+2} \\ &\sim \varepsilon^{2(1-m)} h^{2(k+1-m)} \end{aligned} \tag{25.14}$$

if $\lambda_j - m - \mu_j(k+1-m) > -1$ which follows from (25.9). For $\lambda_j = k+1$ we have to include the logarithmic term as above but the result remains the same. The L^∞-estimate is derived via

$$\begin{aligned}\|u_c - I_h u_c; L^\infty(e)\| &\lesssim (\operatorname{diam} e)^{k+1} |u_c; W^{k+1,\infty}(e)| \\ &\lesssim [\varepsilon h (r_e/\varepsilon)^{1-\mu_j}]^{k+1} \varepsilon^{-\lambda_j} r_e^{\lambda_j - k - 1} \\ &\sim \varepsilon^{\mu_j(k+1)-\lambda_j} h^{k+1} r_e^{\lambda_j - \mu_j(k+1)} \lesssim h^{k+1}\end{aligned}$$

since $\lambda_j - \mu_j(k+1) > 0$ and $r_e \lesssim \varepsilon$.

Together, the estimates (25.12)–(25.14) give the desired result since $u_c = 0$ in $\Omega \setminus \Omega_2^-$. ∎

Lemma 25.5 *Let u_b satisfy (25.3) and let $\mathcal{T}_h$ be as described above with $a = a_* \varepsilon |\ln \varepsilon|$, $a_* \geq (k+1)/\gamma_0$. Then the interpolation error estimates*

$$|u_b - I_h u_b; W^{m,2}(\Omega)| \lesssim \varepsilon^{1/2-m} |\ln \varepsilon|^{k+1/2} h^k, \qquad m = 0, 1, \tag{25.15}$$

$$\|u_b - I_h u_b; L^\infty(\Omega)\| \lesssim |\ln \varepsilon|^{k+1} h^{k+1}, \tag{25.16}$$

hold.

Proof In Ω_1 we have $|D^\alpha u_b| \lesssim \varepsilon^{-|\alpha|} e^{-\gamma_0 a_* |\ln \varepsilon|} = \varepsilon^{k+1-|\alpha|}$. Hence the desired estimates are satisfied when restricted to Ω_1.

In Ω_2 we have $|D^\alpha u_b| \lesssim \varepsilon^{-k-1}$ for $|\alpha| = k+1$. Hence we get for $m = 0, 1$

$$\begin{aligned}|u_b - I_h u_b; W^{m,2}(\Omega_2)| &\lesssim (\operatorname{meas}_2 \Omega_2)^{1/2} (ah)^k |u_b; W^{k+m,\infty}(\Omega_2)| \\ &\lesssim a^{k+1} h^k \varepsilon^{-k-m} \sim \varepsilon^{1-m} |\ln \varepsilon|^{k+1} h^k, \\ \|u_b - I_h u_b; L^\infty(\Omega_2)\| &\lesssim (ah)^{k+1} |u_b; W^{k+1,\infty}(\Omega_2)| \\ &\lesssim |\ln \varepsilon|^{k+1} h^{k+1}.\end{aligned}$$

Finally, in Ω_3 we have $|D^\alpha u_b| \lesssim \varepsilon^{-\alpha_2} + \varepsilon^{-|\alpha|} e^{-\gamma_0 a_* |\ln \varepsilon|} \lesssim \varepsilon^{-\alpha_2}$. By using Theorem 5.5 or 7.17 we get

$$\begin{aligned}\|u_b - I_h u_b; L^2(\Omega_3)\| &\lesssim (\operatorname{meas}_2 \Omega_3)^{1/2} \sum_{|\alpha|=k} h^{\alpha_1} (ah)^{\alpha_2} \|D^\alpha u_b; L^\infty(\Omega_3)\| \\ &\lesssim (\operatorname{meas}_2 \Omega_3)^{1/2} \sum_{|\alpha|=k} h^{\alpha_1} (ah)^{\alpha_2} \varepsilon^{-\alpha_2} \\ &\sim (\operatorname{meas}_2 \Omega_3)^{1/2} h^k \sum_{|\alpha|=k} |\ln \varepsilon|^{\alpha_2} \\ &\sim h^k \varepsilon^{1/2} |\ln \varepsilon|^{k+1/2} \\ |u_b - I_h u_b; W^{1,2}(\Omega_3)| &\lesssim (\operatorname{meas}_2 \Omega_3)^{1/2} \sum_{|\alpha|=k} h^{\alpha_1} (ah)^{\alpha_2} |D^\alpha u_b; W^{1,\infty}(\Omega_3)| \\ &\lesssim (\operatorname{meas}_2 \Omega_3)^{1/2} h^k \sum_{|\alpha|=k} a^{\alpha_2} \varepsilon^{-\alpha_2 - 1} \\ &\sim h^k \varepsilon^{-1/2} |\ln \varepsilon|^{k+1/2} \\ \|u_b - I_h u_b; L^\infty(\Omega_3)\| &\lesssim \sum_{|\alpha|=k+1} h^{\alpha_1} (ah)^{\alpha_2} \|D^\alpha u_b; L^\infty(\Omega_3)\| \\ &\lesssim h^{k+1} |\ln \varepsilon|^{k+1}.\end{aligned}$$

Summing up these estimates we get the assertion. ∎

Lemma 25.6 *Let $u_{\rm b}$ satisfy assumption (25.3) and let $\mathcal{T}_h$ be as described above with $a = \min\{a_\Omega; a_*\varepsilon|\ln h|\}$, $a_* \geq (k+1)/\gamma_0$, a_Ω suitably chosen. Then the interpolation error estimates*

$$\begin{aligned} \|u_{\rm b} - {\rm I}_h u_{\rm b}; L^2(\Omega)\| &\lesssim h^k(h + \varepsilon^{1/2}|\ln h|^{k+1}), && (25.17)\\ |u_{\rm b} - {\rm I}_h u_{\rm b}; W^{1,2}(\Omega)| &\lesssim \varepsilon^{-1/2}h^k|\ln h|^{k+1}, && (25.18)\\ \|u_{\rm b} - {\rm I}_h u_{\rm b}; L^\infty(\Omega)\| &\lesssim h^{k+1}|\ln h|^{k+1}, && (25.19) \end{aligned}$$

hold.

Some ideas for the following proof were taken from [73].

Proof We prove the lemma first for the case $a = a_*\varepsilon|\ln h|$. In Ω_1 we have $|D^\alpha u_{\rm b}(x)| \lesssim \varepsilon^{|\alpha|}e^{-\gamma_0 {\rm dist}\,(x,\partial\Gamma)/\varepsilon}$. Since $\int_a^\infty e^{-2\gamma_0 x_2/\varepsilon}\,{\rm d}x_2 \sim \varepsilon e^{-2\gamma_0 a/\varepsilon} \sim \varepsilon h^{2(k+1)}$ we obtain

$$\begin{aligned} \|D^\alpha u_{\rm b}; L^2(\Omega_1)\| &\lesssim \varepsilon^{-|\alpha|+1/2}h^{k+1},\\ \|D^\alpha u_{\rm b}; L^\infty(\Omega_1)\| &\lesssim \varepsilon^{-|\alpha|}h^{k+1}. \end{aligned}$$

Consequently, we derive by using the triangle inequality

$$\begin{aligned} \|u_{\rm b} - {\rm I}_h u_{\rm b}; L^2(\Omega_1)\| &\lesssim ({\rm meas}_2\Omega_1)^{1/2}\|u_{\rm b}; L^\infty(\Omega_1)\| \lesssim h^{k+1}\\ |u_{\rm b} - {\rm I}_h u_{\rm b}; W^{1,2}(\Omega_1)| &\lesssim |u_{\rm b}; W^{1,2}(\Omega_1)| + h^{-1}\|{\rm I}_h u_{\rm b}; L^2(\Omega_1)\|\\ &\lesssim \varepsilon^{-1/2}h^{k+1} + h^k \lesssim \varepsilon^{-1/2}h^k,\\ \|u_{\rm b} - {\rm I}_h u_{\rm b}; L^\infty(\Omega_1)\| &\lesssim \|u_{\rm b}; L^\infty(\Omega_1)\| \lesssim h^{k+1}. \end{aligned}$$

The $W^{1,2}$-norm estimate has to modified slightly in the exceptional subregions $\Omega_{1,j}$ close to corners C_j with large interior angles, see the remark at the end of the description of the mesh. With $\varrho_e \sim ah$ and ${\rm meas}_2\Omega_{1,j} \sim ah$ we obtain

$$\begin{aligned} |u_{\rm b} - {\rm I}_h u_{\rm b}; W^{1,2}(\Omega_{1,j})| &\lesssim |u_{\rm b}; W^{1,2}(\Omega_{1,j})| + (ah)^{-1}\|{\rm I}_h u_{\rm b}; L^2(\Omega_{1,j})\|\\ &\lesssim \varepsilon^{-1/2}h^{k+1} + (ah)^{-1}(ah)^{1/2}h^{k+1} \lesssim \varepsilon^{-1/2}h^k, \end{aligned}$$

that means, the result above is valid.

In Ω_2 we have $|D^\alpha u_{\rm b}| \lesssim \varepsilon^{-k-1}$ for $|\alpha| = k+1$ and we get by analogy to the proof of Lemma 25.5

$$\begin{aligned} |u_{\rm b} - {\rm I}_h u_{\rm b}; W^{m,2}(\Omega_2)| &\lesssim \varepsilon^{1-m}h^k|\ln h|^{k+1},\\ \|u_{\rm b} - {\rm I}_h u_{\rm b}; L^\infty(\Omega_2)\| &\lesssim h^{k+1}|\ln h|^{k+1}. \end{aligned}$$

In Ω_3 we evaluate the terms separately. Let $u_{\rm b} =: u_1 + u_2$ with

$$\begin{aligned} |D^\alpha u_1| &\lesssim \varepsilon^{-\alpha_2}e^{-\gamma_0 x_2/\varepsilon} \lesssim \varepsilon^{-\alpha_2},\\ |D^\alpha u_2| &\lesssim \varepsilon^{-|\alpha|}e^{-\gamma_0 r/\varepsilon} \lesssim \varepsilon^{-|\alpha|}e^{-\gamma_0 a_*|\ln h|} \lesssim \varepsilon^{-|\alpha|}h^{k+1}. \end{aligned}$$

The first term can be treated as $u_{\rm b}$ in the proof of Lemma 25.5. We get

$$\begin{aligned} |u_1 - {\rm I}_h u_1; W^{m,2}(\Omega_3)| &\lesssim h^k\varepsilon^{1/2-m}|\ln h|^{k+1/2}\\ \|u_1 - {\rm I}_h u_1; L^\infty(\Omega_3)\| &\lesssim h^{k+1}|\ln h|^{k+1}. \end{aligned}$$

The second term can be bounded as $u_{\rm b}$ in Ω_1. One has only to mention that the inverse inequality in the $W^{1,2}$-estimate leads to a factor $(ah)^{-1} \leq (\varepsilon h)^{-1}$ instead of h^{-1}. This, however,

h^{-1}	$\varepsilon = 10^{-1}$	$\varepsilon = 10^{-3}$	$\varepsilon = 10^{-5}$
4	0.648	0.564	0.552
8	0.650	0.574	0.566
16	0.653	0.576	0.574
32	0.653	0.576	0.576
64	0.653	0.583	0.578

Table 25.1: Example 24.4: Scaled error norm $|||\, u - u_h \,|||_\Omega/(\varepsilon^{1/2}|\log_{10}\varepsilon|h)$ for $a = 2\varepsilon|\log_{10}\varepsilon|$.

does not influence the result since $(\mathrm{meas}_2\Omega_3)^{1/2}$ produces another $a^{1/2}$. Summing up the estimates we get the assertion for $a = a_*\varepsilon|\ln h|$.

In the remaining case $a = a_\Omega \neq a(\varepsilon)$ the mesh is quasi-uniform. We get

$$\begin{aligned} |u_\mathrm{b} - \mathrm{I}_h u_\mathrm{b}; W^{m,2}(\Omega)| &\lesssim h^k |u_\mathrm{b}; W^{k+m,2}(\Omega)| \lesssim \varepsilon^{1/2-k-m} h^k, \\ \|u_\mathrm{b} - \mathrm{I}_h u_\mathrm{b}; L^\infty(\Omega_2)\| &\lesssim h^{k+1} |u_\mathrm{b}; W^{k+1,\infty}(\Omega)| \lesssim \varepsilon^{-k-1} h^{k+1}. \end{aligned}$$

(The factor $\varepsilon^{1/2}$ is obtained by integration of (25.3).) With $\varepsilon < a_\Omega/(a_*|\ln h|) \sim |lnh|^{-1}$ we obtain the desired result. ∎

Remark 25.7 We mention that the quality of the interpolation error estimates for u_b can be improved. First, the L^2-estimate can be made of order h^{k+1} in both lemmata but this is not exploited further.

Second, it is possible to diminish the exponent of the logarithmic term in (25.15) from $k+1/2$ to k, see the preprint version of [14], but this refined proof does not extend to three dimensions when $k = 1$. Therefore we do not pursue this further. We conclude from a computational argument that the result is optimal with this modification. Table 25.1 displays the scaled error norm $|||\, u - u_h \,|||_\Omega/(\varepsilon^{1/2}|\log_{10}\varepsilon|h)$ for calculations of Example 24.4 with different values of h and ε. It becomes constant for decreasing ε and h.

Theorem 25.8 *Let u satisfy Assumption 25.1 and consider $\mathcal{T}_h$ as described above with μ satisfying (25.8). For $a = a_*\varepsilon|\ln\varepsilon|$, $a_* \geq (k+1)/\gamma_0$, we obtain*

$$\begin{aligned} |u - \mathrm{I}_h u; L^2(\Omega)| &\lesssim \varepsilon^{1/2}|\ln\varepsilon|^{k+1/2} h^k + h^{k+1}, \\ |u - \mathrm{I}_h u; W^{1,2}(\Omega)| &\lesssim \varepsilon^{-1/2}|\ln\varepsilon|^{k+1/2} h^k \\ \|u - \mathrm{I}_h u; L^\infty(\Omega)\| &\lesssim |\ln\varepsilon|^{k+1} h^{k+1}. \end{aligned}$$

For $a = \min\{a_\Omega;\ a_*\varepsilon|\ln h|\}$, $a_* \geq (k+1)/\gamma_0$, a_Ω suitably chosen, we get

$$\begin{aligned} \|u - \mathrm{I}_h u; L^2(\Omega)\| &\lesssim h^k(h + \varepsilon^{1/2}|\ln h|^{k+1}), \\ |u - \mathrm{I}_h u; W^{1,2}(\Omega)| &\lesssim \varepsilon^{-1/2} h^k |\ln h|^{k+1}, \\ \|u - \mathrm{I}_h u; L^\infty(\Omega)\| &\lesssim h^{k+1}|\ln h|^{k+1}. \end{aligned}$$

Proof For u_b and u_c use Lemmata 25.4–25.6, for u_s and u_r use that

$$|(u_\mathrm{s} + u_\mathrm{r}) - \mathrm{I}_h(u_\mathrm{s} + u_\mathrm{r}); W^{m,q}(\Omega)| \lesssim h^{k+1-m}|u_\mathrm{s} + u_\mathrm{r}; W^{k+1,q}(\Omega)| \tag{25.20}$$

$$\lesssim \begin{cases} h^{k+1-m}[(\mathrm{meas}_2\Omega)^{1/2} + \varepsilon^2] & \text{if } q = 2 \\ h^{k+1-m}[1+1] & \text{if } q = \infty. \end{cases} \tag{25.21}$$

In order to bound u_r we take $n \geq k+3$ in Assumption 25.1. In the case $q = \infty$ we use apply the embedding $W^{k+3,2}(\Omega) \hookrightarrow W^{k+1,\infty}(\Omega)$ which gives $\|u_\mathrm{r}; W^{k+1,\infty}(\Omega)\| \lesssim \|u_\mathrm{r}; W^{k+3,2}(\Omega)\| \lesssim 1$. ∎

25.3 Finite element error estimates

We conclude now the error estimate in the energy norm (24.6) for the finite element solution u_h determined by (24.5).

Theorem 25.9 *Let u satisfy Assumption 25.1 and let u_h be the finite element solution on a family of meshes as described in Subsection 25.2 where μ satisfies (25.8). For $a = a_* \varepsilon |\ln \varepsilon|$, $a_* \geq (k+1)/\gamma_0$, we obtain*

$$|||\, u - u_h \,|||_\Omega \lesssim h^k (\varepsilon^{1/2} |\ln \varepsilon|^{k+1/2} + h), \tag{25.22}$$

whereas for $a = \min\{a_\Omega;\ a_* \varepsilon |\ln h|\}$, $a_* \geq (k+1)/\gamma_0$, the estimate

$$|||\, u - u_h \,|||_\Omega \lesssim h^k (\varepsilon^{1/2} |\ln h|^{k+1} + h), \tag{25.23}$$

holds.

Proof Use Theorem 25.8 and the projection property of the finite element method with respect to the energy norm. ∎

Remark 25.10 We proved error estimates for the Galerkin solution on two types of anisotropically refined finite element meshes. Let us compare both approaches. In Shishkin type meshes we use $a = a_* \varepsilon |\ln \varepsilon|$, $a_* \geq (k+1)/\gamma_0$. That means that the refined mesh covers the layer. Indeed, we have $D^{(0,j)} e^{-\gamma_0 x_2/\varepsilon} \leq \varepsilon^{k+1-j}$ in Ω_1. With Shishkin meshes, $a = \min\{a_\Omega;\ a_* \varepsilon |\ln h|\}$, we resolve only part of the layer as long as $h > \varepsilon$. Is this "more economical" [186]? We obtain with N^2 elements

$$|||\, u - u_h \,|||_\Omega \lesssim \begin{cases} N^{-k} \varepsilon^{1/2} |\ln \varepsilon|^{k+1/2} + N^{-(k+1)} & \text{if } a = a_* \varepsilon |\ln \varepsilon|, \\ N^{-k} \varepsilon^{1/2} |\ln N|^{k+1} + N^{-(k+1)} & \text{if } a = a_* \varepsilon |\ln N|. \end{cases} \tag{25.24}$$

If the constants in these two estimates (hidden in $\lesssim$) are equal (which is not clear) then the error is smaller for Shishkin meshes.

The difference in (25.24) is much more essential in convection-diffusion-reaction problems, where the term $\varepsilon^{1/2}$ does not appear in estimates like (25.24), see Section 26. In this case we get even $\lim_{\varepsilon \to 0} |||\, u - u_h \,|||_\Omega = \infty$ for fixed h and Shishkin type meshes.

We would like to propose another definition for a, namely

$$a = a_* \varepsilon \min\{|\ln h|;\ |\ln \varepsilon|\}, \tag{25.25}$$

resulting in a slightly sharper estimate than both (25.22) and (25.23).

Corollary 25.11 *Let u satisfy Assumption 25.1 and let u_h be the finite element solution of problem (25.1) on a family of meshes as described above where μ satisfies (25.8). For a as in (25.25) we obtain*

$$|||\, u - u_h \,|||_\Omega \lesssim h^k \varepsilon^{1/2} \min\{|\ln h|^{k+1/2};\ |\ln \varepsilon|^{k+1}\} + h^{k+1}.$$

Remark 25.12 As we have seen in Sections 6, 8, and 9, the validity of the local interpolation error estimates for anisotropic finite elements depends critically on the dimension of the domain. For some cases of the parameters k, m, and q, more regularity has to be assumed in three dimensions. But in the proofs of Lemmata 25.5 and 25.6 we used only that $u_b \in W^{k+1,\infty}(\Omega_3)$ such that the anisotropic error estimates hold in three dimensions as well. However, estimate

(25.20) in the proof of Theorem 25.8 is not valid in the single instance $d = 3, k = 1, m = 1, q = 2$. The way out is to use additional smoothness $u_s + u_r \in W^{k+2,2}(\Omega)$ and an interpolation error estimate as in the second part of Corollary 6.6. With these arguments we see that the results of Lemmata 25.5 and 25.6 can be extended to three dimensions provided that an assumption like 25.1 is given.

The critical part in the investigation of the three-dimensional problem is that the singular part u_c contains not only corner singularities but also edge singularities. They have to be approximated, for example, by refined meshes similar to them discussed in Section 21.

An analysis for the case $\Omega = (0,1)^3$ and without corner and edge singularities (as it is possible under some compatibility conditions on the data) can be found in [14].

Let us discuss the implications of an insufficient treatment of the corner singularity u_c.

Example 25.13 Consider an integer $j \in \{1, \dots, J\}$ such that $\lambda_j < k$. Let u_c satisfy (25.4). Assume that $\mathcal{T}_h$ is constructed as described at the beginning of Subsection 25.2, with the exception that $\mathcal{T}_h$ is quasi-uniform in $\Omega^-_{2,j}$. The element size in this subdomain is denoted by $\hbar$. □

Lemma 25.14 *In the situation of Example 25.13 the interpolation error can be estimated by*

$$\begin{aligned} \|u_c - I_h u_c; L^2(\Omega^-_{2,j})\| &\lesssim \hbar(\varepsilon^{-1}\hbar)^{\lambda_j - \delta}, \\ |u_c - I_h u_c; W^{1,2}(\Omega^-_{2,j})| &\lesssim (\varepsilon^{-1}\hbar)^{\lambda_j - \delta}, \\ \|u_c - I_h u_c; L^\infty(\Omega^-_{2,j})\| &\lesssim (\varepsilon^{-1}\hbar)^{\lambda_j - \delta}. \end{aligned}$$

Before we prove the lemma we formulate a corollary which follows due to the projection property of the finite element method.

Corollary 25.15 *In the situation of Example 25.13 the finite element error can be estimated by*

$$|||\, u - u_h \,|||_\Omega \lesssim (\varepsilon + \hbar)(\varepsilon^{-1}\hbar)^{\lambda_j - \delta} \lesssim \varepsilon h^{\lambda_j - \delta} \cdot \begin{cases} 1 & \text{if } \mu_j = 1, \text{ that means } \hbar \sim \varepsilon h, \\ |\ln \varepsilon|^{\lambda_j - \delta} & \text{if } \hbar \sim ah \text{ and } a \sim \varepsilon |\ln \varepsilon|, \\ |\ln h|^{\lambda_j - \delta} & \text{if } \hbar \sim ah \text{ and } a \sim \varepsilon |\ln h|. \end{cases}$$

Proof (Lemma 25.14) By analogy to the proof of Lemma 25.4 we obtain for elements e with $C_j \in \overline{e}$ (that means $r_e := \operatorname{dist}(e, C_j) = 0$) the estimates

$$\begin{aligned} \|u_c - I_h u_c; L^\infty(e)\| &\lesssim \|u_c; L^\infty(e)\| \lesssim \varepsilon^{-\lambda_j}\hbar^{\lambda_j}, \\ \|u_c - I_h u_c; L^2(e)\| &\lesssim (\operatorname{meas}_2 e)^{1/2}\|u_c; L^\infty(e)\| \lesssim \varepsilon^{-\lambda_j}\hbar^{1+\lambda_j}, \\ |u_c - I_h u_c; W^{1,2}(e)| &\lesssim \varepsilon^{-\lambda_j}\hbar^{\lambda_j}. \end{aligned}$$

For elements with $r_e > 0$ we use that $\hbar \lesssim r_e \lesssim r$ in e and $\lambda_j < k$ to obtain for $m = 0, 1$ and arbitrary $\delta \in (0, k - \lambda_j)$

$$\begin{aligned} |u_c - I_h u_c; W^{m,2}(e)|^2 &\lesssim \hbar^{2(k+1-m)}|u_c; W^{k+1,2}(e)|^2 \\ &\lesssim \hbar^{2(1-m+\lambda_j-\delta)}\hbar^{2(k-\lambda_j+\delta)}\varepsilon^{-2\lambda_j}\int_e r^{2(\lambda_j-k-1)} \\ &\lesssim \hbar^{2(1-m+\lambda_j-\delta)}\varepsilon^{-2\lambda_j}\int_e r^{2(-1+\delta)} \end{aligned}$$

and similarly

$$\|u_c - I_h u_c; L^\infty(e)\|^2 \lesssim \hbar^{2k} |u_c; W^{k+1,2}(e)|^2 \lesssim \hbar^{2(\lambda_j-\delta)} \varepsilon^{-2\lambda_j} \int_e r^{2(-1+\delta)}.$$

Summing up these estimates we get

$$\begin{aligned}
\|u_c - I_h u_c; L^2(\Omega_{2,j}^-)\|^2 &\lesssim \varepsilon^{-2\lambda_j}\hbar^{2(1+\lambda_j)} + \varepsilon^{-2\lambda_j}\hbar^{2(1+\lambda_j-\delta)} \int_0^\varepsilon r^{2(-1+\delta)+1}\,\mathrm{d}r \\
&\lesssim \varepsilon^{2(-\lambda_j+\delta)}\hbar^{2(1+\lambda_j-\delta)}, \\
|u_c - I_h u_c; W^{1,2}(\Omega_{2,j}^-)|^2 &\lesssim \varepsilon^{-2\lambda_j}\hbar^{2\lambda_j} + \varepsilon^{-2\lambda_j}\hbar^{2(\lambda_j-\delta)} \int_0^\varepsilon r^{2(-1+\delta)+1}\,\mathrm{d}r \\
&\lesssim \varepsilon^{2(-\lambda_j+\delta)}\hbar^{2(\lambda_j-\delta)}, \\
\|u_c - I_h u_c; L^\infty(\Omega_{2,j}^-)\|^2 &\lesssim \max\left\{ \varepsilon^{-2\lambda_j}\hbar^{2\lambda_j};\ \varepsilon^{-2\delta}\hbar^{2(\lambda_j-\delta)} \int_0^\varepsilon r^{2(-1+\delta)+1}\,\mathrm{d}r \right\} \\
&\lesssim \varepsilon^{2(-\lambda_j+\delta)}\hbar^{2(\lambda_j-\delta)}.
\end{aligned}$$

■

We conjecture that $\delta = 0$ can be achieved by a more involved proof, see [150, page 275] for a proof with a more special finite element mesh. In that monograph we find also an example [150, page 265] which can be modified slightly to show that these estimates are sharp in the following sense.

Lemma 25.16 *For $v = \varepsilon^{-\lambda} r^\lambda \sin\lambda\phi$ ($r := \operatorname{dist}(x, C_j)$) we get in general no better result than*

$$\min_{v_h \in V_{0h}} |||\, v - v_h \,|||_\Omega \gtrsim \varepsilon h^\lambda \cdot \begin{cases} 1 & \text{if } \mu_j = 1, \text{ that means } \hbar \sim \varepsilon h, \\ |\ln\varepsilon|^\lambda & \text{if } \hbar \sim ah \text{ and } a \sim \varepsilon|\ln\varepsilon|, \\ |\ln h|^\lambda & \text{if } \hbar \sim ah \text{ and } a \sim \varepsilon|\ln h|, \end{cases} \tag{25.26}$$

if the mesh is chosen as described in Example 25.13.

Proof Without loss of generality assume that $C_j = (0,0)$. Let e be a triangle with the vertices $(0,0)$, $(b,0)$ on the boundary of Ω and $(0,b)$ in the interior. Since any $v_h \in V_{0h}$ satisfies the boundary condition we get via $v_h(0,0) = v_h(b,0) = 0$ the relation $D^{(1,0)}v_h = 0$. Consequently, we obtain by a direct calculation

$$\begin{aligned}
|v - v_h; W^{1,2}(e)|^2 &\geq \|D^{(1,0)}v; L^2(e)\|^2 \geq \int_0^{\pi/2}\int_0^{b/\sqrt{2}} (D^{(1,0)}v)^2 r\,\mathrm{d}r\,\mathrm{d}\phi \\
&= \int_0^{\pi/2}\int_0^{b/\sqrt{2}} (\varepsilon^{-\lambda}\lambda r^{\lambda-1}\sin(\lambda-1)\phi)^2 r\,\mathrm{d}r\,\mathrm{d}\phi \\
&= \varepsilon^{-2\lambda}\lambda^2(2\lambda)^{-1}(b/\sqrt{2})^{2\lambda}\int_0^{\pi/2}\sin^2(\lambda-1)\phi\,\mathrm{d}\phi \sim (\varepsilon^{-1}b)^{2\lambda}.
\end{aligned}$$

Consequently,

$$\min_{v_h \in V_{0h}|_e} |v - v_h; W^{1,2}(e)| \gtrsim \varepsilon^{-\lambda}\hbar^\lambda \sim \begin{cases} h^\lambda & \text{if } \hbar \sim \varepsilon h, \\ (ah/\varepsilon)^\lambda & \text{if } \hbar \sim ah. \end{cases} \tag{25.27}$$

■

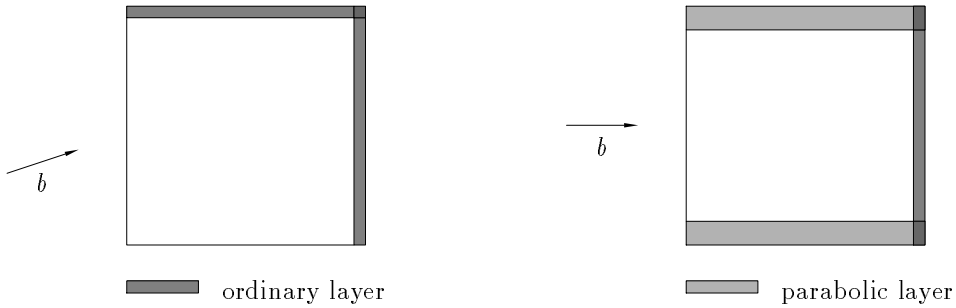

Figure 26.1: Illustration of the location of ordinary and parabolic boundary layers.

This function v can also be considered in our example since the leading singularity is $\varepsilon^{-\lambda} r^{\lambda} \sin \lambda\phi$ [110]. Such a term is in general contained in the solution when the data do not satisfy certain compatibility conditions. Consequently, we cannot expect a better approximation order for the finite element solution than that given in (25.26) when no mesh grading near the corners is applied.

26 A convection-diffusion-reaction problem

26.1 Statement of the problem

This section is concerned with the finite element solution of the linear(ized) diffusion-convection-reaction model problem

$$L_\varepsilon u := -\varepsilon \Delta u + b \cdot \nabla u + cu = f \quad \text{in } \Omega, \qquad u = 0 \quad \text{on } \partial\Omega, \tag{26.1}$$

where $\Omega \subseteq \mathbb{R}^2$ is a bounded polygonal domain, $\varepsilon \in (0, 1]$ is the perturbation parameter, and b, c, and f are sufficiently smooth functions satisfying

$$\nabla \cdot b = 0, \quad c \geq 0 \quad \text{almost everywhere in } \Omega. \tag{26.2}$$

Problem (26.1) is of singularly perturbed type when

$$\varepsilon^{-1} |b(x)| \gg 1 \quad \text{and/or} \quad \varepsilon^{-1} |c(x)| \gg 1. \tag{26.3}$$

The solution u has in general sharp boundary or interior layers, as introduced in Sections 24 and 25 for the special case $b \equiv 0$ but with a much greater variety, see Example 26.1 for an introduction. The resolution of such layers is again a typical application of anisotropic meshes.

Example 26.1 The location of boundary layers is well known. To get an example we consider problem (26.1) in the unit square $\Omega = (0, 1)$. Assume that $b = (\cos\alpha, \sin\alpha)^T$. In the case $\alpha \in (0, \pi/2)$ there occur only *ordinary* (or *outflow*) *boundary layers* of thickness $\mathcal{O}(\varepsilon |\ln \varepsilon|)$ at the two sides $x_1 = 1$ and $x_2 = 1$. For $\alpha = 0$ *parabolic* (or *characteristic*) *layers* of thickness $\mathcal{O}(\varepsilon^{1/2} |\ln \varepsilon|)$ are located at $x_2 = 0$ and $x_2 = 1$. At the outflow part of the boundary layer, $x_1 = 1$, again an ordinary boundary layer occurs. In all cases there is no layer at the inflow part of the boundary, see also Figure 26.1. In the case $b \equiv 0$ there is a layer along the whole boundary $\partial\Omega$, see Sections 24 and 25. □

The investigation of properties of the analytical solution and of methods for the numerical solution of (26.1) are topics of extensive current research. A good review of the state of the art

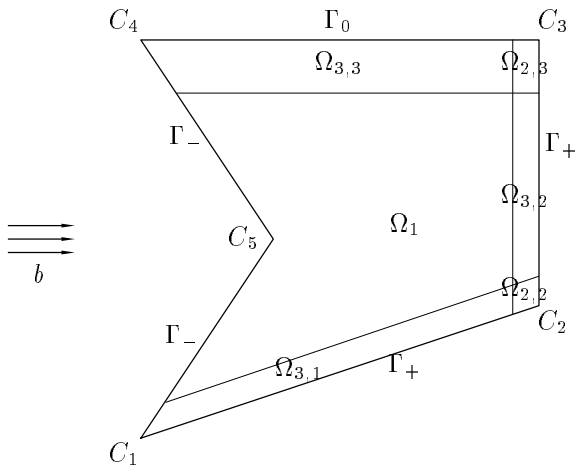

Figure 26.2: Illustration of the partition for a convection dominated problem.

in January 1997 is given in [162]. So we restrict pointers to related literature to a minimum and present only some results for the finite element method on anisotropic meshes. But before we can do that we have to introduce some notation and to discuss assumptions on the analytical solution.

Denote by Γ_-, Γ_+, and Γ_0 the inflow, outflow and characteristic parts of the boundary $\Gamma = \partial\Omega$; the index denotes the sign of $b \cdot n$ where n is the outward unit normal on Γ. Note that corners cannot be classified by this definition, so they do not belong to Γ_-, Γ_+, or Γ_0. For simplicity we assume that the type of the boundary does not change at corners with interior angle greater than or equal to π. We discuss the additional difficulties with concave corners in Remark 26.8 at the end of this section.

The parameter dependent partition of Ω is obtained by introducing lines with a distance a_+ to Γ_+ and a_0 to Γ_0, and eventually (near corners with large angles) some more lines perpendicularly to the parallel lines, see the illustration in Figure 26.2. The parameters a_+ and a_0 will later be chosen as the thickness of the refinement layer ($a_+ \sim \varepsilon|\ln\varepsilon|$, $a_0 \sim \varepsilon^{1/2}|\ln\varepsilon|$, or $a_+ \sim \varepsilon|\ln h|$, $a_0 \sim \varepsilon^{1/2}|\ln h|$). Again, the interior domain is denoted by Ω_1, the union of the small subdomains $\Omega_{2,j}$ near corners C_j by $\Omega_2 := \bigcup_j \Omega_{2,j}$, and the union of all boundary strips $\Omega_{3,j}$ near Γ_+ and Γ_0 by $\Omega_3 := \bigcup_j \Omega_{3,j}$. Note that there are no such subdomains near Γ_-. Moreover, we introduce $\Omega_+ := \bigcup_{i=2}^3 \bigcup_{j\,:\,\partial\Omega_{i,j}\cap\Gamma_+\neq\emptyset} \Omega_{i,j}$ and $\Omega_0 := \bigcup_{i=2}^3 \bigcup_{j\,:\,\partial\Omega_{i,j}\cap\Gamma_0\neq\emptyset} \Omega_{i,j}$.

In Ω_3 we can define a boundary fitted Cartesian coordinate system (x_1, x_2) with $x_2 = \operatorname{dist}(x, \Gamma)$. Particular (in general non-orthogonal) coordinate systems are also considered near ($r \lesssim \varepsilon^{1/2}|\ln\varepsilon|$) corners $C_j \in \overline{\Gamma_+} \cap \overline{\Gamma_0}$. Then C_j is assumed to be the origin, $\Gamma_+ \cap \partial\Omega_{2,j}$ is part of the x_1-axis, and $\Gamma_0 \cap \partial\Omega_{2,j}$ is part of the x_2-axis. Derivatives $(D^\alpha u)(x)$ for x in these subdomains are to be understood with respect to these coordinate systems. Points in the remaining subdomains can be considered in any Cartesian coordinate system. Finally, we define by r the distance to the set of corners $\{C_j\}_{j=1}^J$.

Assumption 26.2 *Let u be the solution of problem (26.1) where b, c, and f are sufficiently smooth functions satisfying (26.2) and certain compatibility conditions. Define index sets*

$$
\begin{aligned}
J_{++} &:= \{j : (\partial\Omega_{2,j} \cap \Gamma) \subset \overline{\Gamma_+}\}, & J_+ &:= \{j : (\partial\Omega_{3,j} \cap \Gamma) \subset \Gamma_+\},\\
J_{00} &:= \{j : (\partial\Omega_{2,j} \cap \Gamma) \subset \overline{\Gamma_0}\}, & J_0 &:= \{j : (\partial\Omega_{3,j} \cap \Gamma) \subset \Gamma_0\},\\
J_{0+} &:= \{j : C_j \in \overline{\Gamma_+} \cap \overline{\Gamma_0})\}.
\end{aligned}
$$

Then the solution u can be split into a smooth term $u_{\rm s}$, boundary layer terms $u_{{\rm b},j}$, $j \in J_+ \cup J_0$, and corner layer terms $u_{{\rm c},j}$, $j \in J_{++} \cup J_{00} \cup J_{0+}$,

$$u = u_{\rm s} + \sum_{j \in J_+ \cup J_0} u_{{\rm b},j} + \sum_{j \in J_{++} \cup J_{00} \cup J_{0+}} u_{{\rm c},j},$$

such that

$$|D^\alpha u_{\rm s}| \lesssim 1 \qquad \text{in } \Omega,$$

$$|D^\alpha u_{{\rm b},j}| \lesssim \begin{cases} \varepsilon^{-\alpha_2} e^{-\gamma_0 x_2/\varepsilon} & \text{in } \Omega_{3,j},\ j \in J_+, \\ \varepsilon^{-|\alpha|} e^{-\gamma_0 \operatorname{dist}(x, \Gamma \cap \overline{\Omega_{3,j}})/\varepsilon} & \text{in } \Omega \setminus \Omega_{3,j},\ j \in J_+, \\ \varepsilon^{-\alpha_2/2} e^{-\gamma_0 x_2/\sqrt{\varepsilon}} & \text{in } \Omega_{3,j},\ j \in J_0, \\ \varepsilon^{-|\alpha|/2} e^{-\gamma_0 \operatorname{dist}(x, \Gamma \cap \overline{\Omega_{3,j}})/\sqrt{\varepsilon}} & \text{in } \Omega \setminus \Omega_{3,j},\ j \in J_0, \end{cases}$$

$$|D^\alpha u_{{\rm c},j}| \lesssim \begin{cases} \varepsilon^{-|\alpha|} e^{-\gamma_0 \operatorname{dist}(x, C_j)/\varepsilon} & \text{if } j \in J_{++}, \\ \varepsilon^{-|\alpha|/2} e^{-\gamma_0 \operatorname{dist}(x, C_j)/\sqrt{\varepsilon}} & \text{if } j \in J_{00}, \\ \varepsilon^{-\alpha_1/2} e^{-\gamma_0 x_1/\sqrt{\varepsilon}} \varepsilon^{-\alpha_2} e^{-\gamma_0 x_2/\varepsilon} & \text{if } j \in J_{0+},\ r \lesssim \varepsilon^{1/2} |\ln \varepsilon|, \\ \varepsilon^{-|\alpha|/2} e^{-\gamma_0 \operatorname{dist}(x, C_j)/\sqrt{\varepsilon}} & \text{if } j \in J_{0+},\ r \gtrsim \varepsilon^{1/2} |\ln \varepsilon|, \end{cases}$$

with some constant $\gamma_0 > 0$.

This assumption covers the typical behaviour of the solution within (ordinary and parabolic) boundary layers, see also Example 26.3. However, problems with corner singularities and interior layers are excluded. The treatment of corner singularities is not completely clear since they may, due to the convection, influence not only a neighbourhood of the corners. The treatment of interior layers was already discussed in Remark 24.6. They do not appear in so-called *problems of channel type* [13, 141] if the right hand side f and the inflow boundary are sufficiently smooth [141, Theorem 2.3]. We admit also that the description of the behaviour near $C_j \in \overline{\Gamma_+} \cup \overline{\Gamma_0}$ is speculative. We did not exclude parabolic layers, as it is done in Example 26.3, because we wanted to stress that there is no approximation problem with the terms $u_{{\rm b},j}$, $j \in J_0$.

Example 26.3 Consider

$$\Omega = (0,1)^2, \quad c \equiv 0, \quad b_1(x) \le -2\gamma_0 < 0, \quad b_2(x) \le -2\gamma_0 < 0. \tag{26.4}$$

Then we have only ordinary boundary layers at the sides $x_1 = 0$ and $x_2 = 0$. It is proved in [73] that the solution u fulfills Assumption 26.2 for $|\alpha| \le 2$ provided that the right hand side satisfies the compatibility conditions

$$f(C_j) = 0,\ j = 1, \ldots, 4, \qquad (D^s f)(1,1) = 0,\ |s| \le 2. \tag{26.5}$$

In particular, condition (26.5) guarantees that no interior layer emanates from the corner $(1,1)$ in the inflow boundary layer. □

Let us discuss now the finite element solution of (26.1). The variational formulation of (26.1) reads:

$$\textit{Find } u \in V_0 : a(u,v) = (f,v)_\Omega \quad \forall v \in V_0, \tag{26.6}$$

where

$$a(u,v) := \varepsilon(\nabla u, \nabla v)_\Omega + \frac{1}{2}\{(b \cdot \nabla u, v)_\Omega - (b \cdot \nabla v, u)_\Omega\} + (cu, v)_\Omega.$$

For a family $\mathcal{T}_h$ of admissible triangulations we can define a finite element space V_h, see Section 3. We consider the following stabilized finite element method of Galerkin/Least-squares type [105].

$$\textit{Find } u_h \in V_{0h} : a_h(u_h, v_h) = \langle f, v_h \rangle_h \quad \forall v_h \in V_{0h}, \tag{26.7}$$

with

$$\begin{aligned} a_h(u,v) &:= a(u,v) + \sum_e \delta_e \, (L_\varepsilon u, L_\varepsilon v)_e, \\ \langle f, v \rangle_h &:= (f,v)_\Omega + \sum_e \delta_e \, (f, L_\varepsilon v)_e, \end{aligned}$$

and a set $\{\delta_e\}$ of non-negative numerical diffusion parameters.

Remark 26.4 Method (26.7) is of Galerkin-Petrov type. This can be seen easily by rewriting $a_h(.,.)$ and $\langle f, . \rangle_h$,

$$\begin{aligned} a_h(u,v) &:= \sum_e (L_\varepsilon u, v + \delta_e \, L_\varepsilon v)_e, \\ \langle f, v \rangle_h &:= \sum_e (f, v + \delta_e \, L_\varepsilon v)_e. \end{aligned}$$

Other methods of stabilization can be obtained, for example, by replacing $+\delta_e \, L_\varepsilon v$ by $-\delta_e \, L_\varepsilon^* v$ in the expressions above, see also the explanation in Remark 24.7, page 134.

26.2 Error estimates for the pure Galerkin method

With $\delta_e = 0 \; \forall e \in \mathcal{T}_h$ we obtain by (26.7) the standard Galerkin method. At least on isotropic meshes the Galerkin solution may suffer from non-physical oscillations (wiggles) unless the elementwise numbers

$$P_e := \varepsilon^{-1} \mathrm{diam}\, e \, \|b; [L^\infty(e)]^d\|, \quad \Gamma_e := \varepsilon^{-1} (\mathrm{diam}\, e)^2 \|c; L^\infty(e)\|, \tag{26.8}$$

are sufficiently small. As a remedy, stabilized variants have been developed, for example (26.7) with $\delta_e > 0$ [105]. Practical calculations on quasi-uniform (isotropic) meshes show that wiggles occur globally in Ω for the standard Galerkin method, but they are restricted to a numerical layer region of width $\mathcal{O}(h^{\kappa_2} |\ln h|)$ for method (26.7) with suitable chosen parameters δ_e. The numerical layers are in general larger than the boundary and interior layers which have a width $\mathcal{O}(\varepsilon^{\kappa_1} |\ln \varepsilon|)$. The size of κ_1 depends on the problem and characterizes the layer, see Example 26.1, whereas κ_2 depends on the discretization and is not known in general.

One can try to resolve the layers by means of anisotropic mesh refinement. For the construction of the finite element mesh we use ideas from Sections 24 and 25. The boundary strips $\Omega_{3,i}$ are subdivided into $\mathcal{O}(h^{-1}) \times \mathcal{O}(h^{-1})$ trapezoids which can be divided further into two triangles. Each of the subdomains Ω_1 and $\Omega_{2,j}$ is split into $\mathcal{O}(h^{-2})$ elements e satisfying the maximal angle condition. In each subdomain the elements shall have comparable size.

The Galerkin finite element method on such meshes is analyzed for bilinear rectangular elements in [186]. The problem is like the one described in Example 26.3, but with $c \geq c_0 > 0$,

$$\Omega = (0,1)^2, \quad c \geq c_0 > 0, \quad b_1(x) \leq -2\gamma_0 < 0, \quad b_2(x) \leq -2\gamma_0 < 0. \tag{26.9}$$

For $a_+ = \min\{1/2; \; (2/\gamma_0)\varepsilon |\ln h|\}$ these authors prove the interpolation error estimates

$$\begin{aligned} \|u - \mathrm{I}_h u; L^\infty(\Omega_1)\| &\lesssim h^2, \\ \|u - \mathrm{I}_h u; L^\infty(\Omega \setminus \Omega_1)\| &\lesssim h^2 |\ln h|^2, \\ |\!|\!| u - \mathrm{I}_h u |\!|\!|_\Omega &\lesssim h |\ln h|, \end{aligned} \tag{26.10}$$

[186, Theorems 4.2 and 4.3] where

$$|||\, v \,|||_\Omega^2 := \varepsilon |v; W^{1,2}(\Omega)|^2 + \|v; L^2(\Omega)\|^2.$$

Theorem 26.5 *Let u be the solution of (26.1) and assume that (26.2), (26.3), (26.5), and (26.9) are valid. Assume that $u_h \in V_{0h}$ is the Galerkin solution ($\delta_e = 0$ for all e in (26.7)) on a Shishkin mesh with bilinear rectangular elements and $a_+ = \min\{1/2;\ (2/\gamma_0)\varepsilon|\ln h|\}$. Then the error estimate*

$$|||\, u - u_h \,|||_\Omega \lesssim h|\ln h| \tag{26.11}$$

holds.

Proof With

$$\begin{aligned}
&|||\, u - u_h \,|||_\Omega \\
&\lesssim |||\, u - \mathrm{I}_h u \,|||_\Omega + \left(\sum_{e \in \mathcal{T}_h} \min\left\{ h_2^{-2} \|u - \mathrm{I}_h u; L^2(e)\|^2;\ \varepsilon^{-1} \mathrm{meas}_2 e\, \|u - \mathrm{I}_h u; L^\infty(e)\|^2 \right\} \right)^{1/2} \\
&\lesssim |||\, u - \mathrm{I}_h u \,|||_\Omega + h^{-1} \|u - \mathrm{I}_h u; L^2(\Omega_1)\| + \varepsilon^{-1/2} (\mathrm{meas}_2 (\Omega \setminus \Omega_1))^{1/2} \|u - \mathrm{I}_h u; L^\infty(\Omega \setminus \Omega_1)\|
\end{aligned}$$

and (26.10) the result (26.11) is obtained [186]. ∎

Moreover, the pointwise error estimate

$$\max_i |(u - u_h)(X^{(i)})| \lesssim h^{1/2} |\ln h|^{3/2}, \qquad X^{(i)} \in \Omega \setminus \Omega_1, \tag{26.12}$$

in the refinement layer is proved in [186] by using the discrete Green function. But this estimate is not optimal.

We remark also that the estimate (26.10) was proved later in a simpler, more specific (term by term) way in [73]: these authors obtained for triangular and rectangular elements with $k = 1$

$$\begin{aligned}
\|u - \mathrm{I}_h u; L^2(\Omega)\| &\lesssim h^2 (1 + \varepsilon^{1/2} |\ln h|^2), && (26.13)\\
\varepsilon^{1/2} |u - \mathrm{I}_h u; W^{1,2}(\Omega_1)| &\lesssim h, && (26.14)\\
\varepsilon^{1/2} |u - \mathrm{I}_h u; W^{1,2}(\Omega \setminus \Omega_1)| &\lesssim h|\ln h|, && (26.15)
\end{aligned}$$

by using the anisotropic interpolation error estimates of Theorems 5.5 and 7.3. Since these local estimates are now available also for trapezoidal elements, see Theorem 7.17, these results extend to more general domains, provided that Assumption 26.2 can be proved.

From the theoretical point of view, estimates (26.11) and (26.12) show that the pure Galerkin method converges uniformly with respect to $\varepsilon \ll 1$. However, as reported in [162], practical calculations with linear and bilinear elements show that these estimates are very sensitive to the choice of the parameter a_+. Such non-robust behaviour reduces the practical importance of the pure Galerkin method.

26.3 Error estimates for a stabilized Galerkin method

Let us consider from now on the stabilized Galerkin method of Galerkin/Least-squares type as given by (26.7) with $\delta_e > 0$. The potential of this method, when combined with anisotropic finite element meshes, was first investigated theoretically in [14] and numerically in [176]. Let us recall some results of [14].

One can prove existence and uniqueness of the solution $u_h \in V_{0h}$ of (26.7) on a general admissible mesh (including anisotropic refinement) [14, Theorem 3.4]. The bilinear form $a_h(.,.)$ induces a norm in V,

$$|||\, v \,|||_{\Omega,\delta}^2 := a_h(v,v) = \varepsilon |v; W^{1,2}(\Omega)|^2 + \|c^{1/2} v; L^2(\Omega)\|^2 + \sum_{e \subset \Omega} \delta_e \|L_\varepsilon v; L^2(e)\|^2. \tag{26.16}$$

The finite element error can be estimated in this norm via interpolation error estimates by [14, estimate (3.28)]

$$|||\, u - u_h \,|||_{\Omega,\delta}^2 \le \inf_{v_h \in V_{0h}} \left(2 |||\, u - v_h \,|||_{\Omega,\delta}^2 + \sum_{e \in \mathcal{T}_h} Z_e^2 \|u - v_h; L^2(e)\|^2 \right) \tag{26.17}$$

with $Z_e := \min\{\varepsilon^{-1} \|b; [L^\infty(e)]^d\|^2;\ 2\delta_e^{-1}\}$. (By using the technique of [186, (5.2)–(5.3)] one can improve Z_e to $Z_e := \min\{\varepsilon^{-1} \|b; [L^\infty(e)]^d\|^2;\ 2\delta_e^{-1},\ h_{2,e}^{-1} B_e (\min_e c(x))^{-1/2}\}$ which is helpful for $c(x) \ge c_0 > 0$ and the treatment of Shishkin meshes.) Inserting the local interpolation error estimates (Theorems 5.5 and 7.3) and the assumptions on the analytical solution u, and equilibrating some terms leads to a suitable choice of δ_e,

$$\delta_e = \varepsilon^{-1} h_{2,e}^2 (1 + P_e^2 + \Gamma_e^2)^{-1/2} \qquad \text{if } P_e^4 \ge 1 + P_e^2 + \Gamma_e^2, \tag{26.18}$$

$$\delta_e = \min\left\{ \frac{\varepsilon}{B_2^2};\ \frac{h_{2,e}^2}{\varepsilon} \frac{1 + P_e^2 + \Gamma_e}{1 + P_e^2 + \Gamma_e^2} \right\} \qquad \text{if } P_e^4 \le 1 + P_e^2 + \Gamma_e^2, \tag{26.19}$$

with $P_e := \varepsilon^{-1} h_{2,e} B_e$, $B_e := \|b; [L^\infty(e)]^2\|$, $\Gamma_e := \varepsilon^{-1} h_{2,e}^2 C_e$, $C_e := \|c; L^\infty(e)\|$, $h_{2,e} \le h_{1,e}$. With this choice we get for a slightly different mesh than introduced above ($h_{2,e} = \varepsilon h$ in the ordinary boundary layer and $h_{2,e} = \varepsilon^{1/2} h$ in the characteristic boundary layer which leads to a number of elements of order $N_{\mathrm{el}} \sim h^{-2} |\ln \varepsilon|^2$) the error estimate

$$|||\, u - u_h \,|||_{\Omega,\delta} \lesssim h^k |\ln \varepsilon|^{1/2} (1 + \|b; [L^\infty(\Omega)]^2\| h + \|c; L^\infty(\Omega)\| h^2)^{1/2} \sim N_{\mathrm{el}}^{-k/2} |\ln \varepsilon|^{k+1/2}. \tag{26.20}$$

We will give now an error estimate for the Shishkin type meshes introduced before in this section ($a_+ \sim \varepsilon |\ln \varepsilon|$, $a_0 \sim \varepsilon^{1/2} |\ln \varepsilon|$). We comment on Shishkin meshes ($a_+ \sim \varepsilon |\ln h|$, $a_0 \sim \varepsilon^{1/2} |\ln h|$) im Remark 26.7 at the end of this section. Since we did not include the dependence of $u(x)$ on $b(x)$ and $c(x)$ in Assumption 26.2 we simplify further by assuming

$$\varepsilon \ll 1, \qquad |b(x)| \sim 1, \qquad |c(x)| \lesssim 1 \quad \text{in } \Omega, \tag{26.21}$$

which results in (26.18) as the proper choice of δ_e,

$$\delta_e = h_{2,e}^2 (\varepsilon^2 + h_{2,e}^2 B_e^2 + h_{2,e}^4 C_e^2)^{-1/2}. \tag{26.22}$$

Theorem 26.6 *Let u satisfy Assumption 26.2 and let $\mathcal{T}_h$ be as described above with $a_+ = a_* \varepsilon |\ln \varepsilon|$, $a_0 = (a_*/2) \varepsilon^{1/2} |\ln \varepsilon|$, $a_* \ge (k+1)/\gamma_0$. Choose δ_e as given by (26.22) and assume (26.21). Then the error estimate*

$$|||\, u - u_h \,|||_{\Omega,\delta} \lesssim h^k |\ln \varepsilon|^{k+1} (|\ln \varepsilon|^{-1} + \|b; [L^\infty(\Omega)]^2\| h + \|c; L^\infty(\Omega)\| h^2)^{1/2} \tag{26.23}$$

$$\lesssim h^k |\ln \varepsilon|^{k+1/2} \sim N_{\mathrm{el}}^{-k/2} |\ln \varepsilon|^{k+1/2} \tag{26.24}$$

is valid.

Proof We follow the steps of the proof of the related result (26.20) in [14]. From (26.17) we obtain by using the anisotropic interpolation error estimates

$$\begin{aligned}
|||\, u-u_h \,|||^2_{\Omega,\delta} &\lesssim \sum_{e\in\mathcal{T}_h} \Big[\varepsilon |u-\mathrm{I}_h u; W^{1,2}(e)|^2 + \|c^{1/2}(u-\mathrm{I}_h u); L^2(e)\|^2 + \\
&\qquad + \delta_e \|\varepsilon\Delta(u-\mathrm{I}_h u) + b\cdot\nabla(u-\mathrm{I}_h u) + c(u-\mathrm{I}_h u); L^2(e)\|^2 + \\
&\qquad + \delta_e^{-1}\|u-\mathrm{I}_h u; L^2(e)\|^2\Big] \qquad (26.25)\\
&\lesssim \sum_{e\in\mathcal{T}_h} \Big[\varepsilon^2\delta_e |u-\mathrm{I}_h u; W^{2,2}(e)|^2 + (\varepsilon+\delta_e B_e^2)|u-\mathrm{I}_h u; W^{1,2}(e)|^2 + \\
&\qquad + (C_e + \delta_e C_e^2 + \delta_e^{-1})\|u-\mathrm{I}_h u; L^2(e)\|^2\Big] \\
&\lesssim \sum_{e\in\mathcal{T}_h}\sum_{|\alpha|=k-1}\sum_{|\beta|=1}\sum_{|\gamma|=1} E_{e,\beta,\gamma} h_e^{2(\alpha+\beta+\gamma)} \|D^{\alpha+\beta+\gamma}u; L^2(e)\|^2 \qquad (26.26)
\end{aligned}$$

with

$$\begin{aligned}
E_{e,\beta,\gamma} &:= \varepsilon^2\delta_e h_e^{-2(\beta+\gamma)} + (\varepsilon+\delta_e B_e^2)h_e^{-2\gamma} + (C_e + \delta_e C_e^2 + \delta_e^{-1}) \\
&\lesssim \varepsilon h_e^{-2\gamma} + C_e + \delta_e(\varepsilon^2 h_e^{-2(\beta+\gamma)} + B_e^2 h_e^{-2\gamma} + C_e^2) + \delta_e^{-1} \\
&\lesssim \varepsilon h_{2,e}^{-2} + B_e h_{2,e}^{-1} + C_e,
\end{aligned}$$

where we have used (26.22), such that

$$\begin{aligned}
|||\, u-u_h \,|||^2_{\Omega,\delta} &\lesssim \sum_{e\in\mathcal{T}_h} (\varepsilon h_{2,e}^{-2} + B_e h_{2,e}^{-1} + C_e) \sum_{|\alpha|=k+1} h_e^{2\alpha}\|D^\alpha u; L^2(e)\|^2 \\
&\lesssim \sum_{e\in\mathcal{T}_h} (\varepsilon h_{2,e}^{-1} h_{1,e} + B_e h_{1,e} + C_e h_{1,e} h_{2,e}) \sum_{|\alpha|=k+1} h_e^{2\alpha}\|D^\alpha u; L^\infty(e)\|^2. \qquad (26.27)
\end{aligned}$$

We show now that

$$\sum_{|\alpha|=k+1} h_e^{2\alpha}\|D^\alpha u; L^\infty(e)\|^2 \lesssim h^{2(k+1)} |\ln\varepsilon|^{2(k+1)} \qquad (26.28)$$

for all $e\in\mathcal{T}_h$ by distinguishing several cases.

First, let $e\subset\Omega_1$. From Assumption 26.2 we obtain for $|\alpha| = k+1$

$$\begin{aligned}
|D^\alpha u_{\mathrm{b},j}| &\lesssim \varepsilon^{-(k+1)} e^{-\gamma_0 a_+/\varepsilon} \lesssim \varepsilon^{-(k+1)} e^{-(k+1)|\ln\varepsilon|} = 1 && \text{for } j\in J_+,\\
|D^\alpha u_{\mathrm{b},j}| &\lesssim \varepsilon^{-(k+1)/2} e^{-\gamma_0 a_0/\sqrt{\varepsilon}} \lesssim \varepsilon^{-(k+1)/2} e^{-(k+1)|\ln\varepsilon|/2} = 1 && \text{for } j\in J_0,\\
|D^\alpha u_{\mathrm{c},j}| &\lesssim \varepsilon^{-\alpha_1/2} e^{-\gamma_0 a_0/\sqrt{\varepsilon}} \varepsilon^{-\alpha_2} e^{-\gamma_0 a_+/\varepsilon} \lesssim \varepsilon^{(k+1)/2} && \text{for } j\in J_{0+}, r\lesssim \varepsilon^{1/2}|\ln\varepsilon|,\\
|D^\alpha u_{\mathrm{c},j}| &\lesssim \varepsilon^{-(k+1)/2} e^{-\gamma_0 a_0/\sqrt{\varepsilon}} \lesssim 1 && \text{for } j\in J_{0+}, r\gtrsim \varepsilon^{1/2}|\ln\varepsilon|.
\end{aligned}$$

We can treat $u_{\mathrm{c},j}$ with $j\in J_{++}$ and $j\in J_{00}$ like $u_{\mathrm{b},j}$ with $j\in J_+$ and $j\in J_0$, respectively. That means $\|D^\alpha u; L^\infty(e)\| \lesssim 1$. With $h_{1,e}\lesssim h$, $h_{2,e}\lesssim h$, we obtain (26.28) where the logarithmic term is even avoided.

The case $e\subset\Omega_{2,j}$ can be treated with equal ideas for $j\in J_{++}$ and $j\in J_{00}$. Therefore we introduce the parameter κ by

$$\kappa = 1 \quad \text{for } j\in J_{++}, \qquad \kappa = \frac{1}{2} \quad \text{for } j\in J_{00}.$$

We have

$$\|D^\alpha (u_{\mathrm{c},j} + u_{\mathrm{b},j-1} + u_{\mathrm{b},j}); L^\infty(e)\| \lesssim e^{-\kappa|\alpha|},$$

all other terms can be treated as in Ω_1. Consequently, we get $\|D^\alpha u; L^\infty(e)\| \lesssim e^{-\kappa|\alpha|}$, and with $h_{1,e} \sim h_{2,e} \sim \varepsilon^\kappa |\ln\varepsilon| h$ we obtain (26.28).

In corner domains $\Omega_{2,j}$ with $j \in J_{0+}$ we have

$$\begin{aligned}
\|D^\alpha u_{\mathrm{c},j}; L^\infty(e)\| &\lesssim e^{-\alpha_1/2-\alpha_2}, \\
\|D^\alpha u_{\mathrm{b},j-1}; L^\infty(e)\| &\lesssim e^{-\alpha_1/2}, \\
\|D^\alpha u_{\mathrm{b},j}; L^\infty(e)\| &\lesssim e^{-\alpha_2}.
\end{aligned}$$

Consequently, it is $\|D^\alpha u; L^\infty(e)\| \lesssim e^{-\alpha_1/2-\alpha_2}$ and with $h_{1,e} \sim \varepsilon^{1/2}|\ln\varepsilon| h$, $h_{2,e} \sim \varepsilon|\ln\varepsilon| h$, we find again that (26.28) is valid. Note that we did not distinguish here between the non-orthogonal coordinate system introduced in the paragraph before Assumption 26.2, and a Cartesian coordinate system $(x_{1,\perp}, x_{2,\perp})$ suited for the anisotropic interpolation error estimates, for example, $x_{1,\perp} = x_1$, $x_{2,\perp} = x_1\cos\omega_j + x_2\sin\omega_j$, where $\omega_j < \pi$ is the interior angle at C_j. The exposition is to be understood that we have transformed between the two systems whenever necessary. Since this transformation is independent of ε and h and since $\partial/\partial x_2 = \partial/\partial x_{2,\perp}$, this approach is admissible.

In the subdomains $\Omega_{3,j}$ we proceed similarly. Set $\kappa = 1$ if $j \in J_+$ and $\kappa = 1/2$ if $j \in J_0$. Then we have

$$\begin{aligned}
\|D^\alpha u_{\mathrm{b},j}; L^\infty(e)\| &\lesssim e^{-\kappa\alpha_2}, \\
\|D^\alpha u_{\mathrm{b},i}; L^\infty(e)\| &\lesssim \begin{cases} \varepsilon^{-|\alpha|} e^{-\gamma_0 a_+/\varepsilon} & \lesssim 1 \quad \forall i \neq j, i \in J_+, \\ \varepsilon^{-|\alpha|/2} e^{-\gamma_0 a_0/\sqrt{\varepsilon}} & \lesssim 1 \quad \forall i \neq j, i \in J_0, \end{cases} \\
\|D^\alpha u_{\mathrm{c},i}; L^\infty(e)\| &\lesssim \begin{cases} \varepsilon^{-|\alpha|} e^{-\gamma_0 a_+/\varepsilon} & \lesssim 1 \quad \forall i \in J_{++} \cap \{j, j+1\}, \\ \varepsilon^{-|\alpha|/2} e^{-\gamma_0 a_0/\sqrt{\varepsilon}} & \lesssim 1 \quad \forall i \in (J_{00} \cup J_{0+}) \cap \{j, j+1\}, \\ \varepsilon^{-|\alpha|} e^{-\gamma_0/\sqrt{\varepsilon}} & \ll 1 \quad \forall i \notin \{j, j+1\}. \end{cases}
\end{aligned}$$

Consequently, it is $\|D^\alpha u; L^\infty(e)\| \lesssim e^{-\kappa\alpha_2}$ and we get (26.28) with $h_{1,e} \lesssim h$, $h_{2,e} \lesssim \varepsilon^\kappa |\ln\varepsilon| h$.

Finally, we have proved (26.28) for all e. By inserting (26.28) into (26.27) we obtain

$$|||\, u - u_h \,|||^2_{\Omega,\delta} \lesssim h^{2(k+1)} |\ln\varepsilon|^{2(k+1)} \sum_{e \in \mathcal{T}_h} (\varepsilon h_{2,e}^{-1} h_{1,e} + B_e h_{1,e} + C_e h_{1,e} h_{2,e})$$

which is the desired result since the number of elements is of order h^{-2} and $\varepsilon h_{2,e}^{-1} h_{1,e} \leq |\ln\varepsilon|^{-1}$, $h_{1,e} \lesssim h$, $h_{2,e} \lesssim h$ for all $e \in \mathcal{T}_h$. ∎

Remark 26.7 Consider now the analysis of the stabilized method for Shishkin meshes ($a_+ \sim \varepsilon|\ln h|$, $a_0 \sim \varepsilon^{1/2}|\ln h|$). Estimate (26.25) indicates that a term $\delta_e |u - \mathrm{I}_h u; W^{1,2}(e)|^2$ has to be treated. From the estimates (26.14), (26.15), we conjecture that δ_e cannot be chosen larger than $\mathcal{O}(\varepsilon)$,

$$\delta_e = \min\{\varepsilon;\ h_{2,e}^2 (\varepsilon^2 + h_{2,e}^2 B_e^2 + h_{2,e}^4 C_e^2)^{-1/2}\}. \tag{26.29}$$

The remaining analysis for proving (26.11) can be done for (bi-)linear elements ($k = 1$) as discussed above for the pure Galerkin method. It is the task of further tests whether a stabilization with $\delta_e \sim \varepsilon$ in Ω_1 and $\Omega_{2,j}$, $j \in J_{00}$, helps. Recall that this is much less than the stabilization suggested in [14], see (26.18), (26.19), or (26.22). It is not clear whether a result like (26.11) can be shown for δ_e larger than that given by (26.29).

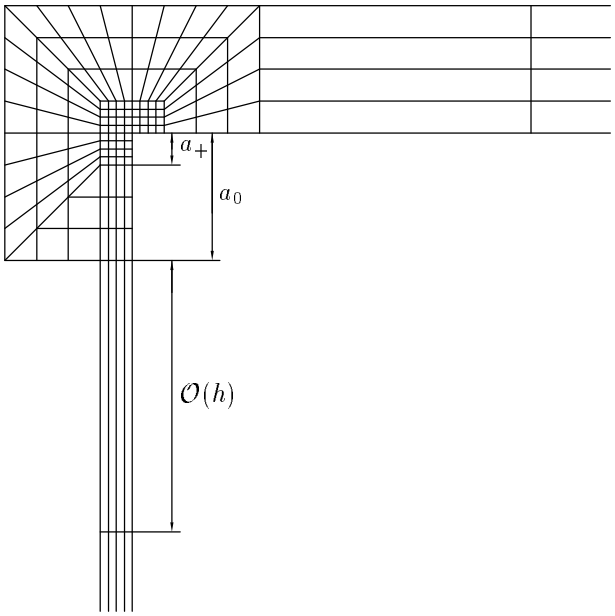

Figure 26.3: Proposed mesh near a concave corner.

For a comparison of Shishkin and Shishkin type meshes we refer to Remark 25.8 which is essentially applicable also for convection-diffusion-reaction problems.

Remark 26.8 In this section we assumed for simplicity that the type of the boundary (inflow, outflow or characteristic) does not change at concave corners. The reason is that near such corners different types of mesh refinement have to overlap in a way which is not clear. In Figure 26.3 we give an example of a corner $C_j \in \overline{\Gamma_+} \cap \overline{\Gamma_0}$ with our proposal how the mesh should be constructed in the refinement layers. One can observe the transition between mesh sizes $a_+ h$ and $a_0 h$. A similar layer has to be added for the transition to elements with mesh size h.

Chapter VI

Open problems

The main part of this chapter (Sections 27–29) is devoted to some topics which are treated unsatisfactorily up to now. They include a-priori and a-posteriori error analysis as well as the solution of the arising system of linear equations.

Finally, with Section 30, a short description of software is appended. The three software packages were used for the numerical examples throughout the whole monograph.

27 A-priori error analysis and further applications

Anisotropic mesh refinement offers a great potential for the effective numerical solution of all kinds of boundary value problems from science and engineering where the solution has different behaviour in different space directions. This includes in particular boundary layers in viscous flow problems and in various plate and shell models, shock phenomena in flow problems, and singularities near edges in Poisson type problems like diffusion and linear elasticity.

We are on the way of the understanding of the finite element method on meshes without a minimal angle condition. The beginning of this development goes back to the fifties and seventies. A large heuristic and experimental contribution has been made in particular by scientists and engineers from the field of computational fluid dynamics. This monograph complements this with an attempt to summarize numerical-analytical results in this field and to contribute to the mathematical foundation.

In Chapters IV and V we studied simple model problems and focused on a careful a-priori error analysis. The strengths of this investigation are the consideration of two- *and three-dimensional* problems in *general* polygonal/polyhedral domains, and the treatment of lower *and higher* order finite elements. We have seen that we needed a large amount of local interpolation error analysis. We have also seen that the problems are difficult to treat since very accurate information on the behaviour of the solution is necessary. This results in open questions even for these simple problems.

1. In Chapters II and III we developed a quite extensive machinery of anisotropic local interpolation error estimates. Remaining tasks include

   - the development of an interpolation theory for non-smooth functions on non-tensor product meshes, and
   - the definition and investigation of an interpolation operator Q_h which is applicable for three-dimensional needle elements ($h_{1,e} \sim h_{2,e} \ll h_{3,e}$) and which has the following

properties:

$$\begin{aligned} |u - Q_h u; W^{1,2}(e)| &\lesssim |u; W^{1,2}(S_e)| \\ \|u - Q_h u; L^2(e)\| &\lesssim \sum_{|\alpha|=1} h_e^\alpha \|D^\alpha u; L^2(S_e)\|. \end{aligned}$$

These estimates are needed for the investigation of reliability and efficiency of a-posteriori error estimates using the ideas of [189].

2. Refinement strategies for the treatment of corner and edge singularities were considered in Chapter IV for diffusion problems. For isotropic mesh refinement it is shown in [23] that the theory extends straightforward to general boundary value problems of second order including systems of differential equations. An important application is the Lamé system of linear elasticity. However, the results of Sections 20 and 21 are not sufficient for this generalization in the case of anisotropic refinement.

   First, we cannot exclude corner singularities as in Section 20 since this was possible only due to the simplicity of the Poisson equation.

   Second, for the proof of Theorem 21.4 we proved the anisotropic regularity in Banach spaces $V^{k,p}_{\beta,\delta}(\Omega)$ with $p > 2$. It is not clear how to do this for the Lamé system. It would be desirable to have an approximation theory for $p = 2$, compare Remark 21.7. This would be a basis for an extension to general problems.

   Finally, we mention that there were some open questions in the treatment of the boundary conditions, see Remark 20.5. Pointwise finite error estimates have also not been considered yet for anisotropically refined meshes.

3. In Chapter V we considered singularly perturbed problems. The main drawback is the lack in the analysis of the solution of such problems, for example, in order to put Assumption 26.2 on a solid mathematical basis. In particular, the influence of corner and edge singularities and their appropriate numerical treatment is far from being satisfactorily solved. For convection-diffusion-reaction problems there is also not much theory for $L^\infty(\Omega)$-estimates of the finite element error [162].

Regardless of these unsolved problems we will mention other challenges:

- the construction of reliable and efficient *a-posteriori error estimators* and automatic *mesh adapting procedures*,
- the investigation of the influence of anisotropic mesh refinement on the linear algebra part of the finite element calculation, in particular the development of *robust and efficient solution techniques*, and
- the application and extension of the results from Chapters II–V to *real application problems*.

In two separate sections, 28 and 29, we review some literature and report on our ongoing research into the first two topics. Concerning the third point we mention in particular flow problems where first results on the resolution (with anisotropic meshes) of all kinds of layers, shock fronts and other anisotropic peculiarities can be found in the literature [42, 41, 97, 114, 134, 140, 152, 205]. (This list is certainly incomplete.) We illustrate the utilization of anisotropic meshes by one example from [134].

Example 27.1 Viscous, compressible flow problems were discretized in [134] by an implicit finite volume method. We reproduce here one of the examples given there which was used to test the efficiency and reliability of this discretization. The example in [134, Subsection 4.2.2] describes a laminar flow where two shock waves and a solid body (a cylinder) interact and produce all types of peculiarities (a contact discontinuity, a shock wave, an expansion wave, and a boundary layer). The reference values of the Reynolds number and the Mach number were given by $\mathrm{Re}_\infty = 193.75$ and $\mathrm{Ma}_\infty = 8.03$ at the inflow boundary. Figure 27.1 shows a triangulation of part of the domain (left hand side) and the isolines of the Mach number (right hand side). In Figure 27.2 we zoom into the mesh in a boundary layer region at the lower side of the cylinder. We see that elements with high aspect ratio were used. □

We will end this section by pointing to a further anisotropic approximation problem.

Example 27.2 Consider the numerical solution of the Euler equations by a finite element method on triangular meshes [77, 94, 98, 103, 107]. In order to obtain values at the nodes of the mesh we use a *dual mesh* and call its elements *cells*. The simplest numerical solution is piecewise constant. This constant value in each cell can be interpreted as an average value. In order to increase accuracy, polynomials of a higher degree (≥ 1) are reconstructed from the cell averages, for example by a TVD (Total Variation Diminishing) or ENO (Essentially Non-Oscillatory) technique, see [179] and the literature cited there. These techniques are well developed for isotropic meshes but they produce non-physical solutions on anisotropic meshes unless heuristic (up to now) modifications are introduced. The mathematical theory for a reconstruction which is robust with respect to anisotropic cells, is still in its infancy. □

28 A-posteriori error estimates and adaptive mesh refinement

A-priori analysis considers only the *asymptotic behaviour* of the finite element solution as the number of degrees of freedom tends to infinity. This is important because it can demonstrate that a certain family of meshes is optimal in this sense. However, for detailed knowledge of the errors in a particular finite element approximation and for assessing its acceptability, an *a-posteriori* error estimator has to be provided.

Usually, the a-posteriori error estimator is calculated locally and can thus serve as an indicator for regions with large and small errors, respectively, as the quality of the finite element approximation in general varies over the computational domain. So-called *automatic mesh adapting finite element strategies* consist in repeating the three steps

1. calculating an approximate solution,

2a. estimating the error locally (and globally),

3. generating an improved mesh,

until the error is within a desired tolerance. If the adaptive procedure takes account of an anisotropic solution, then more information has to be extracted from the approximate solution. This includes at least

2b. determining an appropriate aspect ratio and the stretching direction of the finite elements.

The aim of this section is not to give an overview over error estimators and refinement strategies in general. For this, see, for example, [148, 183, 184, 189]. Rather, we will discuss some aspects and point to difficulties and open problems in the context of anisotropic discretizations.

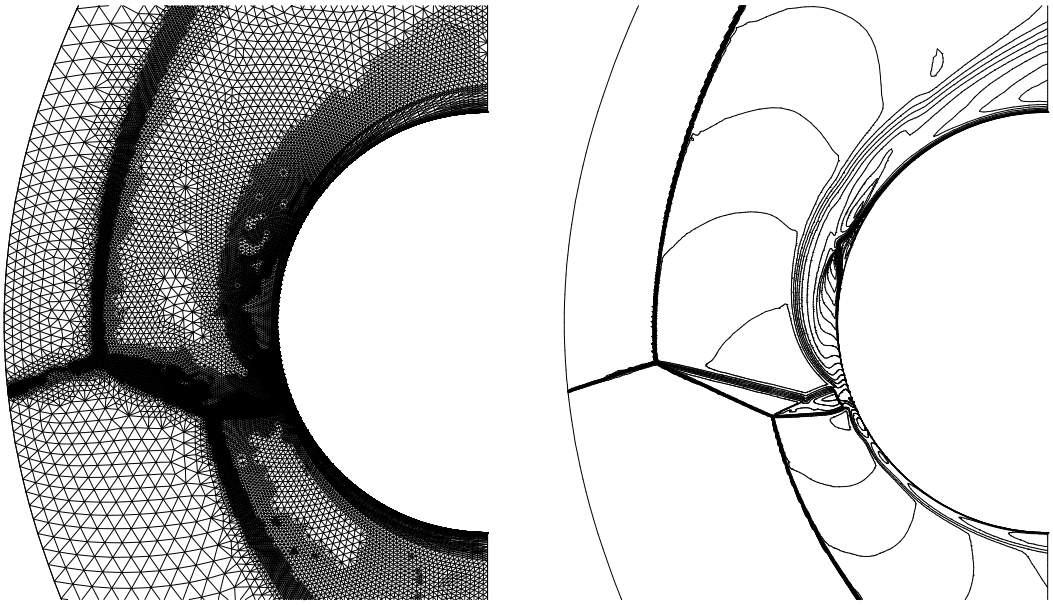

Figure 27.1: Example 27.1: triangulation of part of the domain (left) and isolines of the Mach number (right).

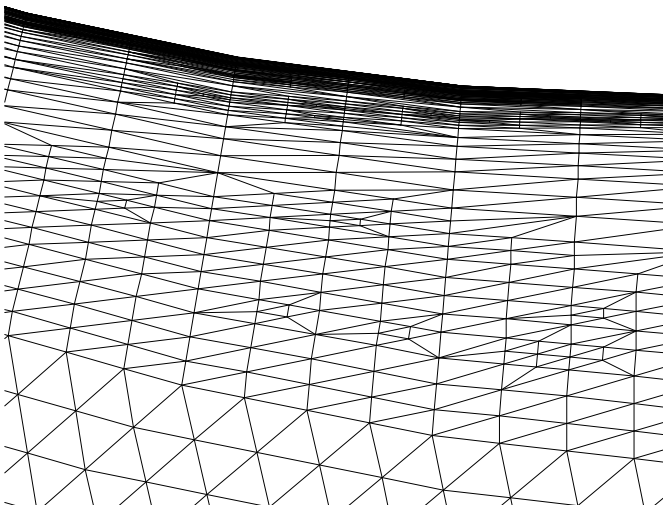

Figure 27.2: Example 27.1: window with a small part of the triangulation.

Let us start with error estimation. The estimator is an expression which can be calculated from the data of the problem and its numerical solution. Usually, the error ist estimated elementwise by some quantity η_e which can then be accumulated to a global error estimate η, for example, $\eta = \left(\sum_e \eta_e^2\right)^{1/2}$. It is desired that the following two properties can be proved.

Reliability. The error estimator should not underestimate the true error in the norm of a space $X(e)$, for example $X = L^2$ or $X = W^{1,2}$,

$$\eta_e \geq \|u - u_h\,; X(e)\|.$$

Often, this property can be ensured only globally and modulo a constant,

$$\eta \geq C_1 \|u - u_h\,; X(\Omega)\|. \tag{28.1}$$

Effectivity. The error estimator should not overestimate the true error,

$$\eta_e \leq \|u - u_h\,; X(e)\|,$$

in order to avoid unnecessary refinement. This property can often be ensured locally, but up to a constant C_2 (in some cases $C_2 = 1$) and with respect to some domain of influence $\omega_e \supset e$ at the right hand side,

$$\eta_e \leq C_2 \|u - u_h\,; X(\omega_e)\|. \tag{28.2}$$

The ratio of estimated error and true error is called *effectivity index*, $\theta := \eta / \|u - u_h\,; X(\Omega)\|$. Clearly, if (28.2) can be proved, then the effectivity index is bounded. In particular, it is desired that the effectivity index approaches one, $\theta \to 1$, as the exact error tends to zero. Then the estimator η is said to be *asymptotically exact*. Note that this property includes reliability, at least for $h \leq h_0$.

In the literature the estimators are often evaluated with respect to these properties: can reliability and efficiency be proved (analytically, sometimes only by numerical evidence), and if yes, how large are the constants? Can asymptotical exactness be proved? Let us add here another point. If we can say nothing about the constants we may have a bad error estimate. However, the estimator can be a good error indicator, this means, an indicator where to refine or coarsen the mesh. For this it is desirable that the error estimator behaves uniformly in the whole domain and for any mesh size. The expression $\eta_e / \|u - u_h\,; X(e)\|$ should not depend on e, and in particular not on h_e. A consequence would be that

$$\eta = \eta(u_h) \sim h^\alpha \quad \text{if } \|u - u_h\,; X(\Omega)\| \sim h^\alpha. \tag{28.3}$$

Example 28.1 Consider the Poisson problem with homogeneous Dirichlet boundary conditions,

$$-\Delta u = f \quad \text{in } \Omega, \qquad u = 0 \quad \text{on } \partial\Omega.$$

The frequently used residual type error estimator [29] for estimating the energy norm of the error reads

$$\eta_{R,e}^2(u_h) := c_1 h_e^2 \|r_e(u_h)\,; L^2(e)\|^2 + c_2 \sum_{E \subset \partial e \setminus \partial\Omega} h_E \|r_E(u_h)\,; L^2(E)\|^2 \tag{28.4}$$

where the element residual r_e and the edge residual r_E (gradient jump) are defined by

$$\begin{aligned} r_e(u_h) &:= f + \Delta u_h \\ r_E(u_h) &:= \lim_{t \to +0} \left[\frac{\partial}{\partial n_E} u_h(x + t n_E) - \frac{\partial}{\partial n_E} u_h(x - t n_E) \right], \quad x \in E. \end{aligned}$$

Here, E denotes a face of e and n_E is any of the two unitary normal vectors to E. For a detailed analysis one has to modify the element residual by replacing f by some projection into a finite-dimensional space [189] but we will not go into these details here. There is not much known about the constants c_1 and c_2 in (28.4); see [60, 61] for latest attempts to compute these constants for isotropic meshes.

While the actual choice of $\hbar_e$ and $\hbar_E$ is of less importance for isotropic meshes this is problematic in the anisotropic case. The elements are no longer characterized by one single size parameter. In particular, we point out that an inappropriate choice may give misleading results. For the tests in [18] we experimented with $\hbar_E := (\mathrm{meas}_2 E)^{1/2}$ and $\hbar_E := (\mathrm{meas}_3 e)^{1/3}$ and obtained inaccurate approximation orders; (28.3) was not satisfied. Later, better choices were proposed in [174]

$$\hbar_e := \min_{i=1,\dots,d} \{h_{i,e}\}, \qquad \hbar_E := \frac{\mathrm{meas}_d e}{\mathrm{meas}_{d-1} E}, \tag{28.5}$$

and in [117]

$$\hbar_e := \min_{i=1,\dots,d} \{h_{i,e}\}, \qquad \hbar_E := \hbar_e^2 \, \frac{\mathrm{meas}_{d-1} E}{\mathrm{meas}_d e}. \tag{28.6}$$

Both authors analyzed their choices and were able to prove results concerning reliability and efficiency.

Efficiency is not critical, but the constant C_2 in (28.2) depends on u_h and $\mathcal{T}_h$ for the estimator (28.4), (28.5), $C_2 = C_2(u_h, \mathcal{T}_h)$ [174]. For adequately refined meshes we get an uniform bound for $C_2(u_h, \mathcal{T}_h)$. The expression $C_2(u_h, \mathcal{T}_h)$ can also be monitored during the finite element calculation. Estimator (28.4), (28.6) is proved to be efficient without this dependence on $C_2(u_h, \mathcal{T}_h)$.

The critical point for both estimators is reliability. The "constant" C_1 in (28.1) depends in both papers on $\nabla(u - u_h)$ and $\mathcal{T}_h$, at least can the assumptions be reformulated in this way, see [118]. It turns out again that we obtain $C_1(\nabla(u - u_h), \mathcal{T}_h) \lesssim 1$ for adequately refined meshes. But what happens in the general case? In [118] it is proposed to approximate

$$C_1(\nabla u - \nabla u_h, \mathcal{T}_h) \approx C_1(\nabla^R u_h - \nabla u_h, \mathcal{T}_h)$$

where $\nabla^R u_h$ is a recovered gradient. First numerical results show that this works well. □

In Example 28.1 we discussed only the simplest model problem. Even for this it is not clear at present time which one of the following two hypotheses is true.

H1. It is possible to define $\hbar_e$ and $\hbar_E$ in a way such that efficiency and reliability can be proved without any assumptions or expressions like $C_1(\nabla u - \nabla u_h, \mathcal{T}_h)$, $C_2(u_h, \mathcal{T}_h)$.

H2. There is no choice of $\hbar_e$ and $\hbar_E$ such that the corresponding error estimator is both reliable and efficient for any u and $\mathcal{T}_h$.

Current insight is supporting the second hypothesis [70]. In [117] and subsequent work of this author the theory of error estimators for discretizations with anisotropic meshes is extended in various directions:

- further error estimators for the Poisson equation (a residual based estimator for the L^2-norm of the error, local Dirichlet problem error estimators for the energy norm and the L^2-norm, a Zienkiewicz-Zhu [206, 207] like error estimator),
- further boundary conditions (Neumann conditions $\partial u/\partial n = g_2$ and Robin conditions $\partial u/\partial n = \sigma(g_2 - u)$),

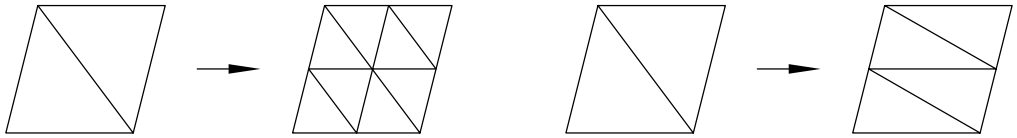

Figure 28.1: Element subdivision strategies: red refinement (left), blue refinement (right).

- a residual error estimator for the reaction-diffusion problem $-\varepsilon^2\Delta u + cu = f$ in Ω, $u = 0$ on $\partial\Omega$.

Care is taken that the error estimator works uniformly well for $\sigma \in (0, \infty)$ in the case of Robin conditions and for $\varepsilon \in (0, 1)$ in the reaction-diffusion problem. In all cases we find that the reliability can only be proved up to the factor $C_1(\nabla(u - u_h), \mathcal{T}_h)$.

Finally, we remark that there are other error estimators/indicators for anisotropic discretizations [42, 152, 155] but the analytical foundation in the above sense is less well developed.

Let us focus now on the generation of an improved mesh. Several authors use the heuristic argument that (in two dimensions) the local aspect ratio should correspond to the ratio of the eigenvalues of the matrix of the (approximated) second order partial derivatives of the solution, and the stretching direction is determined by the eigenvector to the largest eigenvalue of that matrix, see [2, 68, 69, 152, 205] and the literature cited there. (If the solution is vector-valued, either a key variable is chosen [205] or the Hessians of the components are combined [62].) It is not clear whether this choice is also suitable for higher order shape functions, $k \geq 2$.

In other applications the direction can be determined from the data, for example from the streamlines in convection-diffusion problems [176]. One can also try to detect internal layers or shocks by analyzing the gradient (or gradient jump) of some values [205].

With this information one can construct the new mesh. There are three main strategies.

Remeshing. The first one demands a complete remeshing on the basis of some background information (local mesh sizes, stretching direction); see the overview article [175] and the literature cited there. Some authors report on anisotropic meshes which have nearly equilateral elements in a local non-Euclidean metric. In this way standard mesh generating techniques are used to solve the meshing problem [62].

Large angles are either ignored, see the discussion in Remark 5.9 on page 29, or a structured mesh is introduced locally [205].

Remeshing is quite expensive but one can produce meshes with a gradually changing mesh size and arbitrary stretching directions.

Subdivision. The second strategy is based on a subdivision of the existing elements (bisection [34, 127], division into 2^d elements [33, 46] by *red refinement*, see Figure 28.1, left hand side). This approach is inexpensive and fits very well into multi-grid/multi-level strategies for the solution of the corresponding finite element equation system. The subdivision strategy was adapted for anisotropic refinement in [114], called *blue refinement*, see Figure 28.1, right hand side.

The disadvantages are that the mesh size does not change as gradually as in the first approach, and, worse, that the initial mesh determines severely the possible stretching directions of the elements. This can be compensated by node relocation techniques, sometimes also called adaptive grid orientation [114] or node relaxation techniques [157].

Relocation. In the third strategy one concentrates on the relocation of the nodes, it is also called the r-version of the finite element method. But in order to produce a converging

method one has to combine this with node insertion or element splitting. In this way there is a relation to strategy 2. In the recent article [58] such an algorithm is described which allows anisotropic refinement on the basis of a local non-Euclidean metric tensor.

It is hard to judge these strategies. The main point is that all of them have to be programmed carefully, in particular in three dimensions. Preferences in different institutions depend probably strongly on the available software and on the aim of the programs (treatable problems, applied discretization and solution techniques). A common feature of all strategies is that hierarchical meshes in the sense of a classical multi-grid or multi-level method are hardly obtained. The search for a good compromise among the requirements on a family of meshes (see Section 18, page 95) is rarely discussed. Here, we see a strength of a-priori refined meshes as investigated in Chapters IV and V. They are both structured and anisotropic. Of course their applicability is limited. A good compromise could be to use locally structured meshes [176, 205]. A further discussion of the *maximum efficiency mesh problem* can be found in [175].

Remark 28.2 Let us finally review some experiments from [18]. The initial situation was the following.

- We know from a-priori error analysis that anisotropic mesh refinement is suited for compensating the influence of an edge singularity on the approximation order, see also Sections 19, 20, and 21. We know qualitatively how these refined meshes must be constructed. But it is not completely clear how large the refinement neighbourhood has to be.

- A-posteriori error analysis is suited to detect refinement regions. However, it is not straightforward how to realize an adaptive algorithm with anisotropic mesh refinement, see the discussion above.

- The test examples for validating the a-priori error estimates were realized using a coordinate transformation.

- We wanted to use a graded initial mesh for the adaptive procedure in order to exploit a-priori information.

Therefore we tested the following adaptive strategy. Repeat the steps coordinate transformation (grading), calculation of the approximate solution, error estimation (possibly termination of the loop), marking elements for refinement, coordinate transformation ("ungrading"), refinement (2^d elements from each marked element, "green closure"). In this way we combined the advantages of a-priori and a-posteriori refinement. In two test examples, see also Example 28.3, we obtained the desired discretization error with less degrees of freedom and in particular less refinement cycles than in an classical (isotropic) adaptive procedure. The drawback of this strategy is the coordinate transformation which had been programmed especially for the test examples (two- and three-dimensional). It is not clear how to do this in the general case.

Example 28.3 The three-dimensional example was the one from Example 19.2. In Figure 28.2 we illustrate the different behaviour of the algorithms by showing cross-cuts through the final meshes at $x_3 = 1/3$. The development of the finite element error is shown in Figure 28.3 where the aim was to reach a relative error of 3%. For details see [15, 17]. □

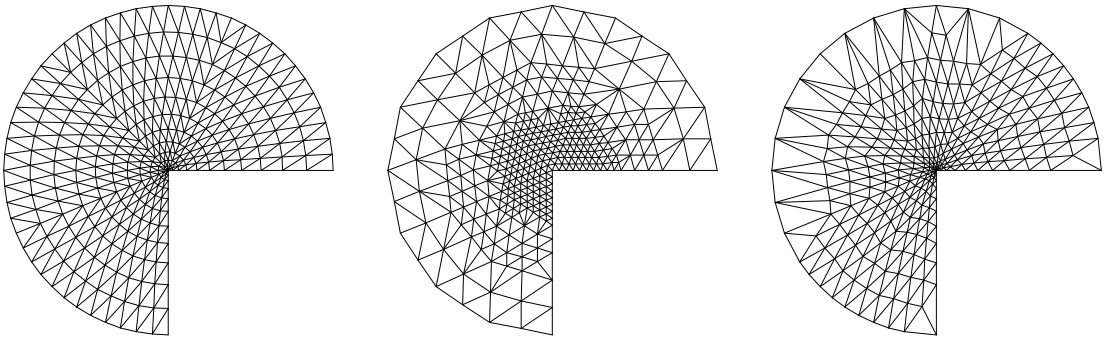

Figure 28.2: Cross-cuts through final meshes at $x_3 = 1/3$: a-priori grading (left), adaptive without grading (middle), adaptive with grading (right).

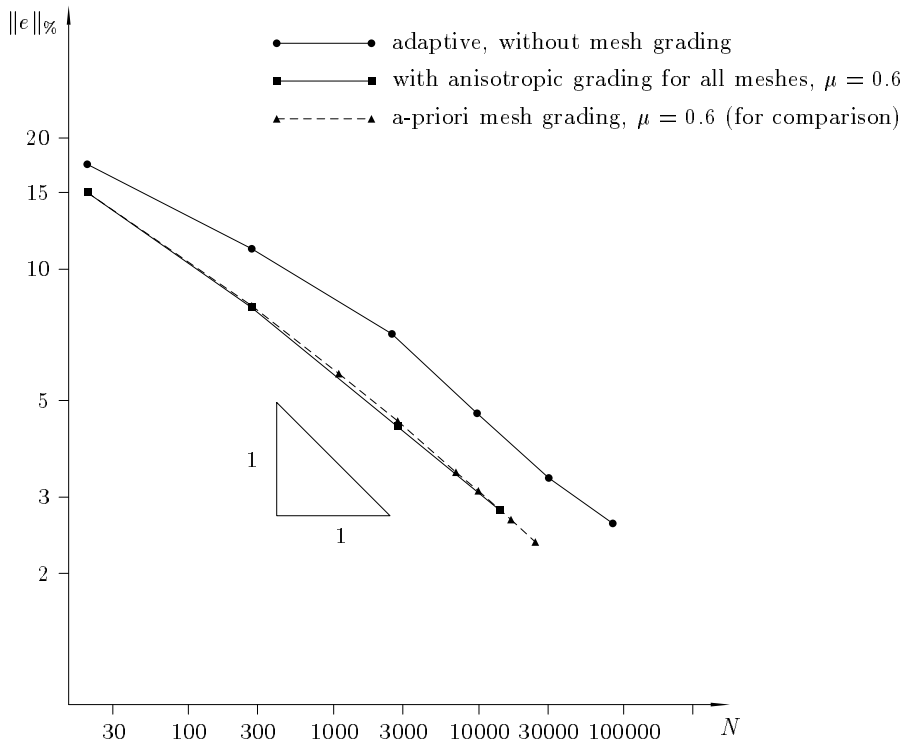

Figure 28.3: Example 19.2: error in the energy norm for adaptive mesh refinement strategies, grading parameter $\mu = 0.6$, final relative error $\varepsilon = 0.03\,\|u_h\|_E$.

N	$\mu = 1.0$	$\mu = 0.8$	$\mu = 0.6$	$\mu = 0.4$
225	21	22	23	26
1377	31	34	40	54
9537	36	41	54	88
70785	40	48	73	140
545025	42	55	97	217

Table 29.1: Numbers of iterations for Example 29.1 with different N and μ.

29 Solution of the arising system of linear equations

Choosing an appropriate discretization is only one part of the numerical solution of a boundary value problem. Additionally, one has to solve a (preconditioned) algebraic system of equations for the coefficients of the representation of u_h in a certain basis. Let us focus here on symmetric, positive definite problems. In modern techniques the number of operations for the solution is proportional to the number of unknowns. Such techniques include multi-grid methods [52, 92, 95, 185], the method of conjugate gradients (CG) [102] with preconditioning (for example multi-level preconditioners [24, 25, 26, 50, 55, 65, 85, 109, 151, 197, 198, 199, 200, 203] and domain decomposition preconditioners [54, 74, 188, 136, 143, 142, 177]) and combinations of these ideas.

Multi-level preconditioners work with a sequence of discretizations which is (in the h-version of the finite element method) based on a sequence of finite element meshes. One of these preconditioners, called BPX, was proposed in [55, 197]. Interestingly, the BPX preconditioner can be analyzed in the additive Schwarz context [203] which gives on the one hand the optimal estimate for the condition number of the preconditioned system. (For other proofs, see [151, 65].) On the other hand, it leads to a variant of this preconditioner, called multi-level diagonal scaling (MDS), which has advantages especially for problems with variable (including piecewise constant) coefficients, see also [50, 151].

Typically, the solution methods are analyzed first for a discretization of the Dirichlet problem for the Poisson equation over the unit square, in general with a five-point finite difference method or a first order finite element discretization on uniform meshes. Later the results are extended to more general differential operators, more general domains, other discretizations, and higher space dimensions. Eventually one finds that the methods cannot be understood as fixed algorithms but they have to be adapted (at least in some components) to the problem under consideration. Of course, methods are preferable which are applicable without change for a fairly large class of problems/discretizations. Then they are called *robust*. Let us consider now the two introductory examples (see Sections 19 and 24) and look at the robustness of the BPX preconditioner with respect to anisotropic discretizations.

Example 29.1 Consider the Poisson problem

$$-\Delta u = 0 \quad \text{in } \Omega, \qquad u = (10 + x_3)\, r^{2/3} \sin \tfrac{2}{3}\phi \quad \text{on } \partial\Omega,$$

see Example 19.2 on page 101. The problem was calculated with the finite element package *SPC-PM Po 3D* (see Comment 30.3 on page 173 for a short description) on sequences of unrefined ($\mu = 1.0$) and anisotropically refined ($\mu = 0.8, 0.6, 0.4$) finite element meshes. The arising systems of linear equations were solved using the CG method with BPX preconditioning and a coarse grid solver [16]. Table 29.1 shows the numbers of iterations for different numbers N of nodal points and different mesh grading parameters μ. We can observe for the non-optimal discretization with $\mu = 1.0$ that the number of iterations becomes constant for $N \to \infty$.

However, this optimal property of the BPX preconditioner gets lost when anisotropic refinement is introduced. A similar behaviour is obtained in other examples, including the Lamé system of elasticity in the same domain. Therefore we omit the tables with these results here. □

Example 29.2 Consider two singularly perturbed reaction diffusion problems as introduced in Section 24. The first test problem is the one from example 24.4 on page 132 which was originally calculated in [168]:

$$-\varepsilon^2 \Delta u + u = 0 \quad \text{in } \Omega = (0,1)^2, \qquad u = e^{-x_1/\varepsilon} + e^{-x_2/\varepsilon} \quad \text{on } \partial\Omega. \tag{29.1}$$

Since the results are sometimes quite different we document also a second test case,

$$-\varepsilon^2 \Delta u + u = 1 \quad \text{in } \Omega = (0,1)^2, \qquad u = 0 \quad \text{on } \Gamma_1, \qquad \frac{\partial u}{\partial n} = 0 \quad \text{on } \Gamma_2, \tag{29.2}$$

$\Gamma_1 := \{x \in \partial\Omega : x_1 = 0 \vee x_2 = 0\}$, $\Gamma_2 := \partial\Omega \setminus \Gamma_1$. In both problems boundary layers appear at $\{x \in \partial\Omega : x_1 = 0 \vee x_2 = 0\}$. So we use the same family of meshes as described in example 24.4 on page 132. In Tables 29.2–29.4 we present the numbers of iterations when the CG method is applied

(a) with diagonal (Jacobi) preconditioning (CG-D),

(b) with the BPX with multi-level diagonal scaling (BPX-MDS).

In all cases we terminated the CG method when a relative error of 10^{-6} was reached. One can draw the following conclusions:

- For large ε the behaviour of the system matrix $A = \varepsilon^2 K + M$ is dominated by the stiffness matrix K. The iteration number behaves as $h^{-1} \sim N^{1/2}$ for CG-D. For uniform meshes BPX-MDS converges with a constant number of iterations, but this behaviour is not robust with respect to a distortion of the mesh towards anisotropic refinement in the layers.

- For small ε (in comparison with h) the system matrix is dominated by the mass matrix M. For uniform meshes the iteration numbers of $BPX - MDS$ remain almost the same as for large ε (robustness with respect to ε). However the system can be solved cheaper by CG-D which has also constant iteration numbers.

  If we use a better discretization method, namely anisotropic mesh refinement in the layers, we find that these good properties of the two solvers get lost. First, we observe a different behaviour in the two quite similar examples, especially with BPX-MDS. For problem (29.1) there is no hint that BPX-MDS has constant iteration numbers. Second, we see in the case CG-D that the small iteration numbers obtained with uniform meshes, are not preserved (CG-D is not robust with respect to a distortion of the mesh).

□

From both examples, 29.1 and 29.2, we find that well-known solution techniques have to be modified in order to cope with anisotropic mesh refinement. Let us now review some results connected with anisotropy and found in the literature.

Some authors investigate the robustness of their methods with respect to the coefficients in the differential operator. A typical example is the anisotropic equation

$$-a\frac{\partial^2 u}{\partial x_1^2} - b\frac{\partial^2 u}{\partial x_2^2} = f \quad \text{in } \Omega = (0,1)^2, \qquad u = 0 \quad \text{on } \partial\Omega. \tag{29.3}$$

	$a = 0.5$ (uniform)				$a = 2\varepsilon\lvert\log_{10}\varepsilon\rvert$ (anisotropic)			
	CG-D		BPX-MDS		CG-D		BPX-MDS	
N	(29.1)	(29.2)	(29.1)	(29.2)	(29.1)	(29.2)	(29.1)	(29.2)
81	13	14	11	11	17	17	16	15
289	26	27	15	15	37	37	29	25
1089	50	55	17	18	71	74	41	34
4225	95	111	19	21	134	147	49	42
16641	182	222	20	23	252	293	57	48

Table 29.2: Numbers of iterations for Example 29.2 with $\varepsilon = 10^{-1}$ and methods CG-D and BPX-MDS.

	$a = 0.5$ (uniform)				$a = 2\varepsilon\lvert\log_{10}\varepsilon\rvert$ (anisotropic)			
	CG-D		BPX-MDS		CG-D		BPX-MDS	
N	(29.1)	(29.2)	(29.1)	(29.2)	(29.1)	(29.2)	(29.1)	(29.2)
81	11	10	13	11	12	8	15	10
289	12	10	18	16	22	15	28	17
1089	12	10	21	19	39	27	55	29
4225	11	9	24	21	69	52	111	46
16641	10	8	25	22	121	101	214	58

Table 29.3: Numbers of iterations for Example 29.2 with $\varepsilon = 10^{-3}$ and methods CG-D and BPX-MDS.

	$a = 0.5$ (uniform)				$a = 2\varepsilon\lvert\log_{10}\varepsilon\rvert$ (anisotropic)			
	CG-D		BPX-MDS		CG-D		BPX-MDS	
N	(29.1)	(29.2)	(29.1)	(29.2)	(29.1)	(29.2)	(29.1)	(29.2)
81	11	10	13	11	12	6	14	6
289	12	10	18	16	18	8	24	8
1089	12	10	22	19	32	12	46	10
4225	12	10	25	21	54	20	101	13
16641	12	9	27	23	86	37	161	16

Table 29.4: Numbers of iterations for Example 29.2 with $\varepsilon = 10^{-5}$ and methods CG-D and BPX-MDS.

In [92, Subsection 10.1] the problem is first considered for $a = \varepsilon \ll 1$, $b = 1$. The discretization with a five-point scheme on a uniform grid gives the matrix entries

$$h^{-2} \begin{bmatrix} 0 & -1 & 0 \\ -\varepsilon & 2+2\varepsilon & -\varepsilon \\ 0 & -1 & 0 \end{bmatrix} \approx h^{-2} \begin{bmatrix} -1 \\ 2 \\ -1 \end{bmatrix}.$$

If a multi-grid method is applied for the solution of the resulting algebraic system of equations one finds that the y-line Gauß-Seidel iteration S^y is an appropriate smoother but not red-black Gauß-Seidel or x-line Gauß-Seidel. What can we learn from this example?

1. In the example, the connection between adjacent nodes is anisotropic, this means, the connection to some neighbours is more tight than to others, the off-diagonal elements in one row are of different order of magnitude. Then it is vital to pay attention to the tight connections. We come back to this later on.

2. The method used above is not really robust with respect to the size of the coefficients. As soon as $a \gg b$, an x-line Gauß-Seidel smoother S^x has to be used. One could think that a smoother $S^y \circ S^x$ based on alternating directions is suited but this is not true any more if a differential operator like

$$-\frac{1}{2}\left(\frac{\partial}{\partial x_1} + \frac{\partial}{\partial x_2}\right)^2 - \frac{\varepsilon}{2}\left(\frac{\partial}{\partial x_1} - \frac{\partial}{\partial x_2}\right)^2$$

   is considered where a diagonal-line Gauß-Seidel smoother has to be applied. The remedy proposed in [92] is to use an ILU (incomplete LU decomposition) or ILLU (incomplete line LU decomposition) smoother. Later, the same author proposes to use the frequency decomposition multi-grid method [93]. In this method, multiple coarse grid corrections are used together with particularly associated prolongations and restrictions.

   Other authors argue that a-priori information can be used in the solver, so the coefficients of the differential operator [86]. These authors investigated the problem

$$-\sum_{i=1}^{d} c_i \frac{\partial^2 u}{\partial x_i^2} + c_0 u = f \quad \text{in } \Omega = (0,1)^d, \qquad u = 0 \quad \text{on } \partial\Omega,$$

   for $c_0 \geq 0$, $c_i > 0$, $i = 1, \ldots, d$, and any space dimension d. Their multi-level iterative method with tensor product subspace splitting shows convergence rates independent of h and the coefficients c_i, $i = 1, \ldots, d$.

3. In [92, Subsection 10.5] it is mentioned that the approximation of the Poisson problem on an anisotropic mesh (like in Example 29.1) results in an anisotropic discrete problem. Using the ideas of Item 1 we conjecture that a multi-grid method with a Gauß-Seidel smoother is appropriate which treats all points with the same x_3-coordinate together. Unfortunately, the subsystems are not tri-diagonal here. A further investigation has still to be done.

The argument of Item 3 is also turned around in [92, Subsection 10.5]: anisotropic problems produce isotropic discrete equations if one succeeds in constructing a suitable grid. This approach is followed in [144]. The basic idea is that the problem

$$-\varepsilon^2 \frac{\partial^2 u}{\partial x_1^2} - \frac{\partial^2 u}{\partial x_2^2} = f(x_1, x_2) \quad \text{in } \Omega = (0,1)^2, \qquad u = 0 \quad \text{on } \partial\Omega, \tag{29.4}$$

is equivalent to the problem

$$-\Delta u = f(\varepsilon^{-1}x_1, x_2) \quad \text{in } \tilde{\Omega} = (0, \varepsilon^{-1}) \times (0,1), \qquad u = 0 \quad \text{on } \partial\tilde{\Omega}.$$

If $\tilde{\Omega}$ is discretized with a family of quasi-uniform meshes then the discrete equations are isotropic. The drawback of this approach is that the number N of nodes grows with ε^{-1}, $N \sim \varepsilon^{-1}h^{-2}$.

We conclude that problem (29.3) has been considered in the literature occasionally in order to investigate robust solver techniques, see also [56, 112] and the references cited there. But the author does not know about a reference where the problem is discretized in an adequate way. Problem (29.4) is of singularly perturbed type. For $\varepsilon = 0$ we obtain a parameter dependent one-dimensional problem where it is possible to satisfy the boundary conditions given for $x_2 = 0$ and $x_2 = 1$ but not for $x_1 = 0$ and $x_1 = 1$. One can expect layers of width $\mathcal{O}(\varepsilon|\ln\varepsilon|)$ at these two sides if $0 \le \varepsilon \ll 1$ is considered [43, 83]. With the ideas of Section 25 it should be possible to prove optimal ε-independent approximation error estimates for a family of meshes which are anisotropically refined in the two layer regions, Ω_1 and Ω_2, and isotropic in the remainder of the domain, Ω_0. For the solution of the resulting algebraic system of equations we have then to combine the ideas cited above. In Ω_0, we have an isotropic, quasi-uniform discretization as investigated in [86, 92, 93], whereas in Ω_1 and Ω_2 we have almost (up to the $|\ln\varepsilon|$-term) isotropic discrete equations as investigated in [144]. A comprehensive analysis has still to be done.

Let us come back to Poisson type problems which are equivalent to

$$-\Delta u = f \quad \text{in } \Omega, \qquad u = 0 \quad \text{on } \partial\Omega.$$

In [155] an adaptive procedure is described which results in anisotropic meshes, see Section 28. This author had in mind examples like such with an exact solution $u = (1-x_1^2)^2(1-x_2^2)^2$ which has a layer near the sides $x_1 = 1$ and $x_2 = 1$. He develops in the subsequent paper [156] an overlapping domain decomposition preconditioner for this type of discretization. Following the idea of [75] it is stated that the ratio H_j/δ_j of the diameter H_j of the subdomain Ω_j and the minimal thickness δ_j of the overlap between Ω_j and $\bigcup_{i\neq j}\Omega_i$, influences the condition number of the preconditioned system. The (probably not astonishing) consequence is that

- isotropic subdomains with an overlap of width of the order of the diameter of the subdomain should be used,
- the local problems in the subdomain should be easily solvable.

Note that this is in agreement with Item 1 above, namely that the nodes with a tight connection should be treated together.

If we combine these conclusions with the idea that the BPX-MDS preconditioner can be viewed as an additive Schwarz method with one-dimensional subspaces [203], we suggest the following preconditioner for the reaction diffusion problem in Example 29.2.

Let $\varphi_{j,i}$, $i = 1, \ldots, N_j$, be the nodal basis functions of level j, $j = 1, \ldots, J$. Define for all j a decomposition $\Omega = \bigcup_{i=1}^{n_j}\Omega_{j,i}$ such that the following conditions are satisfied.

(i) $\Omega_{j,i}$ is a union of finite elements of level j. (Finite elements are considered here as closed sets.)

(ii) Each element of level j is contained in at most N_c subdomains $\Omega_{j,i}$ where N_c is independent of j.

(iii) For all $\Omega_{j,i}$ there is at least one $\varphi_{j,i'}$ such that $\operatorname{supp}\varphi_{j,i'} \subset \Omega_{j,i}$.

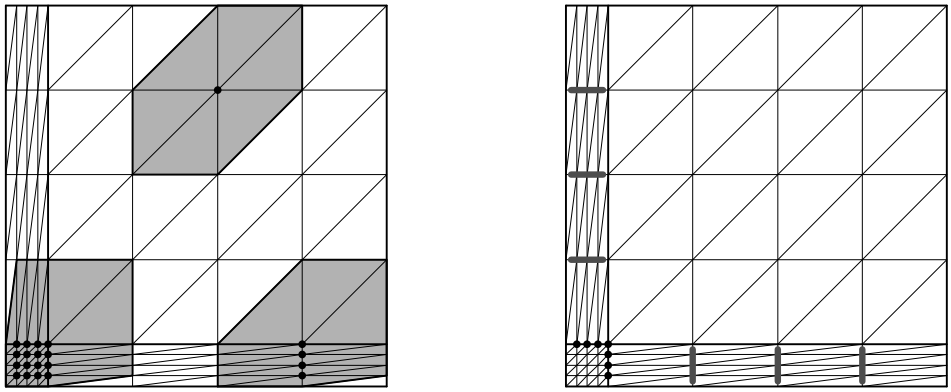

Figure 29.1: Illustration of the subdomains for a modified BPX-like preconditioner (left) and lines of clustered points in the preconditioner BPX-3 (right).

(iv) The subdomains $\Omega_{j,i}$, $i = 1, \ldots, n_j$, $j = 1, \ldots, J$, are isotropic.

(v) The minimal thickness $\delta_{j,i}$ of the overlap between $\Omega_{j,i}$ and $\bigcup_{j' \neq j} \bigcup_{i' \neq i} \Omega_{j',i'}$ is of order $\operatorname{diam} \Omega_{j,i}$.

An example for this domain decomposition is illustrated in Figure 29.1, left hand side. The subdomains with nodes on one line do not introduce difficulties. The corresponding local problems have tridiagonal system matrices which can be solved directly with optimal performance. The only difficulty is the subdomain in the lower left corner. In a first test we avoided this two-dimensional arrangement of nodes and used only one-dimensional subspaces in this corner. Hence the resulting preconditioner BPX-3 (3 for 3-dimensional subsystems) is different from BPX-MDS only in the common consideration of points at the lines illustrated in Figure 29.1, right hand side. It does not satisfy conditions (iv) and (v) for a small number of points.

Example 29.3 We continue example 29.2 by displaying the iteration numbers for the CG with preconditioner BPX-3. Additionally, we used the three-diagonal matrix of the finest level as a simple preconditioner, CG-3. This can be considered as some kind of Jacobi preconditioning. The results are given in Tables 29.5–29.7. We find that BPX-3 is a preconditioner with a very similar behaviour for both test examples and for all ε. In particular, the iteration numbers are nearly the same as for BPX-MDS and uniform mesh refinement. The simpler preconditioner CG-3 has its strength for small ε where it could be used instead of CG-D when a multi-level algorithm is not implemented. □

We remark that a preconditioner corresponding to (i)–(v) above can be defined without difficulty in other model situations. In [170], problems with bad parameters were considered. As a motivation, the Poisson problem was treated in a strip domain $\Omega = (0,1) \times (0,\varepsilon)$. For $h > \varepsilon$ the quadrilateral mesh had only one element in x_2-direction. Every pair of nodes with the same x_1-coordinate was considered together. In this way one can satisfy conditions (i)–(iii) and (v). Condition (iv) can be fulfilled only for $h \lesssim \varepsilon$. In [170], another approach was used: the pairs of nodes defined a block diagonal matrix with 2×2 blocks which was used within the Jacobi smoother of a multi-grid method. As a consequence, the smoother behaved ε-independent (but h-dependent).

From all the literature, tests and remarks in this section we can conclude that it is not satisfactorily clear how to solve the algebraic systems arising from the finite element discretization with (locally) anisotropic finite element meshes, even in the case of a symmetric, positive

	$a = 2\varepsilon\lvert\log_{10}\varepsilon\rvert$ (anisotropic)			
	CG-3		BPX-3	
N	(29.1)	(29.2)	(29.1)	(29.2)
81	10	11	11	11
289	23	23	16	16
1089	44	47	19	20
4225	84	97	21	23
16641	164	198	22	26

Table 29.5: Numbers of iterations for Example 29.2 with $\varepsilon = 10^{-1}$ and methods CG-3 and BPX-3.

	$a = 2\varepsilon\lvert\log_{10}\varepsilon\rvert$ (anisotropic)			
	CG-3		BPX-3	
N	(29.1)	(29.2)	(29.1)	(29.2)
81	11	7	13	8
289	16	12	16	10
1089	28	21	19	14
4225	49	36	22	17
16641	89	64	27	22

Table 29.6: Numbers of iterations for Example 29.2 with $\varepsilon = 10^{-3}$ and methods CG-3 and BPX-3.

	$a = 2\varepsilon\lvert\log_{10}\varepsilon\rvert$ (anisotropic)			
	CG-3		BPX-3	
N	(29.1)	(29.2)	(29.1)	(29.2)
81	–	5	–	5
289	14	6	18	6
1089	24	8	21	7
4225	40	11	23	9
16641	61	8	24	10

Table 29.7: Numbers of iterations for Example 29.2 with $\varepsilon = 10^{-5}$ and methods CG-3 and BPX-3.

definite system matrix. From the material developed in this section we think that it is worth to investigate further the following ideas.

- For the Poisson problem in domains with edges:
  - multi-grid methods with clustering nodes,
  - the CG method with BPX-like preconditioners derived by clustering nodes.

  It is not clear whether one can cluster together all nodes with the same x_3-coordinate (in Example 29.1) where one does not satisfy condition (iv), or if one has to cluster smaller portions in order to satisfy condition (iv). Possibly one can use ideas from the algebraic multi-grid approach to find appropriate subspaces.

- The same ideas could be explored for the singularly perturbed problem of Example 29.2. A promising first test was described in Example 29.3. Open is the treatment of the corner regions. Additional ideas are:
  - using multi-grid methods with an ILU smoother, and
  - using a classical domain decomposition approach with 4 subdomains. The subdomain solvers could be constructed with the ideas above since they are meshed in a uniform way. But it is not clear which Schur complement preconditioner and which basis transformation has to be used.

It is a task of future research to give a mathematical foundation for the algorithms and to extend the class of treatable problems.

30 Short description of utilized software

At several places in this monograph we presented numerical test examples. They were calculated with software which was developed mainly at the *Fakultät für Mathematik* of the *Technische Universität Chemnitz*. In this final section we want to describe these packages. (We remark that this section does not necessarily belong to the topic of this chapter although, of course, any software has its open problems.)

30.1 The sequential finite element package *FEMGPM*. The *Finite Element Multi-Grid Package Mechanics FEMGPM* [180] is a member of the *FEMGP* family which has been implemented by B. Heise, M. Jung, W. Queck, T. Steidten and others since 1985. With *FEMGPM* the user can solve linear elliptic problems (including the heat equation, plane stress and plane strain problems), linear and non-linear parabolic problems and coupled thermo-elasticity problems. In all problems the spatial dimension is two which includes also rotationally symmetric three-dimensional domains (Fourier finite element method [99, 147, 193]).

Main features are the following.

- A user mesh must be provided in a file. *FEMGPM* works with linear or quadratic shape functions on triangles. Coefficients and the right hand side must be programmed and linked.

- After reading the file, the user mesh is hierarchically refined. This refinement can be controlled with several options, for example, to adapt the mesh to material boundaries or to singular points.

- The finite element system of equations can be solved with multi-grid methods or with preconditioned conjugate gradient methods. Preconditioners include multi-grid and methods based on hierarchical bases (Yserentant [199], BPX [55, 197]).

- Various information (including CPU times, error norms, pointwise solutions) can be printed. There is also graphical output for meshes, isolines and deformed domains. Other postprocessing includes the calculation of derivatives (stresses) using superconvergence effects.

30.2 The sequential finite element package *FEMPS3D*. *FEMPS3D* is a finite element code for solving the Poisson equation with (in general inhomogeneous, mixed) boundary conditions of Dirichlet, Neumann or Newton (Robin) type. The first version was developed in 1987-1989 by the author at a VAX workstation. In 1993 it was ported by G. Hanke to the UNIX operating system. The main features are the following:

- The mesh can consist of tetrahedra, hexahedra, and pentahedra. Linear and quadratic shape functions can be used.

- The code does not contain a general mesh generator. It is possible to read mesh data from a file generated by any code, eventually after adapting the data structure. Later, we developed also some special routines to triangulate our test domains.

- The problem data are given in general by function subroutines. For Dirichlet data we developed the additional feature to interpolate some pointwise values over the surface.

- For the assembly of the equation system many different integration rules are programmed. Only the non zero elements of the upper right triangle of the matrix are stored. The system is solved with a conjugate gradient method, preconditioned with different types of incomplete Cholesky factorization (IC(0), IC(1), MIC), see [161].

- The resulting solution can be interpreted with tables of values in subdomains and with a representation of isolines. When the exact solution is known in academic examples, the table of values and the isolines can be given for the error as well. Additionally the error norms in $H^1(\Omega)$, $L_2(\Omega)$ and in a discrete maximum norm are calculated.

In 1993/94 the code was extended by F. Milde and the author, but only for linear tetrahedral elements:

- In Version 2 we included an error estimator of residual type and an adaptive mesh refinement procedure, see details in [17] and in the preprint version of [15].

- For Version 3, parts of the package were reprogrammed. Moreover, the isotropic a-priori mesh grading by dyadic partition (see Section 19) was included.

- In the expectation of an optimization of the meshes two nodal relaxation procedures were included: the standard Laplace smoothing and the improved version introduced in [157] for graded meshes.

- An interface to the visualization package *GRAPE* [195] was developed.

In 1997 the meshing strategies of Section 21 were included with the help of U. Reichel.

30.3 The parallel finite element package *SPC-PM Po 3D*, Version 2. At present time much effort is being spent in both developing and implementing parallel algorithms. The experimental package *SPC-PM Po 3D* is part of the ongoing research of the Chemnitz research group Scientific Parallel Computing (SPC) into finite element methods for problems over three-dimensional domains. Special emphasis is paid to choose finite element meshes which exhibit an optimal order of the discretization error, to develop preconditioners for the arising finite element system based on domain decomposition and multilevel techniques, and to treat problems in complicated domains as they arise in practice.

- In Version 2 [4, 16] the program can solve the Poisson equation and the Lamé system of linear elasticity with in general mixed boundary conditions of Dirichlet and Neumann type. The domain $\Omega \subset \mathbb{R}^3$ can be an arbitrary bounded polyhedron.
- The input is a coarse mesh, a description of the data and some control parameters. The program distributes the elements of the coarse mesh to the processors, refines the elements, generates the system of equations using linear or quadratic shape functions, solves this system and offers graphical tools to display the solution.
- Further, the behavior of the algorithms can be monitored: arithmetic and communication time is measured, the discretization error is measured, different preconditioners can be compared.
- The program has been developed for MIMD computers; it has been tested on Parsytec machines (GCPowerPlus–128 with Motorola Power PC601 processors and GCel–192 on transputer basis) and on workstation clusters using PVM. The special case of only one processor is included, that means the package can be compiled for single processor machines without any change in the source files.

We point out that the implementation is based on a special data structure which allows that all components of the program run with almost optimal performance ($\mathcal{O}(N)$ or $\mathcal{O}(N \ln N)$).

The package *SPC-PM Po 3D* is based on a set of libraries which are still under development. They are documented in the Programmer's Manual [16] and in other separate papers [90, 133, 137, 138]. An overview over the program, its capabilities, its installation, and handling is provided in the User's Manual [4]. Test examples are included in [4, 10, 22, 159].

The historical roots of the program are at one hand in several parallel programs for solving problems over two-dimensional domains using domain decomposition techniques. These codes have been developed since about 1988 by A. Meyer, M. Pester, and other collaborators. On the other hand, the author developed 1987–89 a sequential program for the solution of the Poisson equation over three-dimensional domains which was extended 1993–94 together with F. Milde Comment 30.2 on page 172. *SPC-PM Po 3D*, Version 2 [4, 16], was developed in 1995–1996 under the supervision of A. Meyer and the author. Other main contributors are D. Lohse, M. Meyer, F. Milde, M. Pester, and M. Theß. Meanwhile the package is being extended to include a multi-grid solver (M. Jung), adaptivity (F. Milde), the solution of the Navier-Stokes equations (St. Meinel) and a plasticity model (D. Michael).

The research group SPC (Scientific Parallel Computing) is located at the *Fakultät für Mathematik* of the *Technische Universität Chemnitz*. It is part of the DFG-Sonderforschungsbereich 393 *Numerical simulation on massively parallel computers*.

Bibliography

[1] R. A. Adams. *Sobolev Spaces.* Academic Press, New York, 1975.

[2] D. Ait-Ali-Yahia, W.G. Habashi, A. Tam, M.-G. Vallet, and M. Fortin. A directionally adaptive methodology using an edge-based error estimate on quadrilateral grids. *Int. J. Numer. Methods Fluids*, 23:673–690, 1996.

[3] Th. Apel. *Finite-Elemente-Methoden über lokal verfeinerten Netzen für elliptische Probleme in Gebieten mit Kanten.* PhD thesis, TU Chemnitz, 1991.

[4] Th. Apel. *SPC-PM Po 3D* — User's Manual. Preprint SPC95_33, TU Chemnitz-Zwickau, 1995.

[5] Th. Apel. Anisotropic interpolation error estimates for isoparametric quadrilateral finite elements. *Computing*, 60:157–174, 1998.

[6] Th. Apel. Treatment of boundary layers with anisotropic finite elements. *Z. Angew. Math. Mech.*, 78(S3):S855–S856, 1998.

[7] Th. Apel. Interpolation of non-smooth functions on anisotropic finite element meshes. Preprint SFB393/97-6, TU Chemnitz-Zwickau, 1997. Submitted to Math. Modeling Numer. Anal.

[8] Th. Apel. Anisotropic mesh refinement for the treatment of boundary layers. In M. Bach, C. Constanda, G. C. Hsiao, A.-M. Sändig, and P. Werner, editors, *Analysis, numerics and applications of differential and integral equations*, volume 379 of *Pitman Research Notes in Mathematics*, pages 12–16, Harlow, 1998. Longman.

[9] Th. Apel and M. Dobrowolski. Anisotropic interpolation with applications to the finite element method. *Computing*, 47:277–293, 1992.

[10] Th. Apel, G. Haase, A. Meyer, and M. Pester. Parallel solution of finite element equation systems: efficient inter-processor communication. Preprint SPC95_5, TU Chemnitz-Zwickau, 1995.

[11] Th. Apel and B. Heinrich. Mesh refinement and windowing near edges for some elliptic problem. *SIAM J. Numer. Anal.*, 31:695–708, 1994.

[12] Th. Apel and G. Lube. Local inequalities for anisotropic finite elements and their application to convection-diffusion problems. Preprint SPC94_26, TU Chemnitz-Zwickau, 1994.

[13] Th. Apel and G. Lube. Anisotropic mesh refinement in stabilized Galerkin methods. *Numer. Math.*, 74:261–282, 1996.

[14] Th. Apel and G. Lube. Anisotropic mesh refinement for a singularly perturbed reaction diffusion model problem. *Appl. Numer. Math.*, 26:415–433, 1998.

[15] Th. Apel and F. Milde. Comparison of several mesh refinement strategies near edges. *Comm. Numer. Methods Engrg.*, 12:373–381, 1996.

[16] Th. Apel, F. Milde, and M. Thess. *SPC-PMPo 3D* — Programmer's Manual. Preprint SPC95_34, TU Chemnitz-Zwickau, 1995.

[17] Th. Apel, R. Mücke, and J. R. Whiteman. An adaptive finite element technique with a-priori mesh grading. Technical Report 9, BICOM Institute of Computational Mathematics, 1993.

[18] Th. Apel, R. Mücke, and J. R. Whiteman. Incorporation of a-priori mesh grading into a-posteriori adaptive mesh refinement. In A. Casal, L. Gavete, C. Conde, and J. Herranz, editors, *III Congreso Matemática Aplicada/XIII C.E.D.Y.A. Madrid, 1993*, pages 79–92, Madrid, 1995. Shortened version of Report 93/9, BICOM Institute of Computational Mathematics, 1993.

[19] Th. Apel and S. Nicaise. Elliptic problems in domains with edges: anisotropic regularity and anisotropic finite element meshes. In J. Cea, D. Chenais, G. Geymonat, and J. L. Lions, editors, *Partial Differential Equations and Functional Analysis (In Memory of Pierre Grisvard)*, pages 18–34. Birkhäuser, Boston, 1996. Shortened version of Preprint SPC94_16, TU Chemnitz-Zwickau, 1994.

[20] Th. Apel and S. Nicaise. The finite element method with anisotropic mesh grading for the Poisson problem in domains with edges. Technical report, TU Chemnitz-Zwickau, 1996. Improved version of Preprint SPC94_16, TU Chemnitz-Zwickau, 1994, available only via ftp, server ftp.tu-chemnitz.de, directory pub/Local/mathematik/Apel, file an1.ps.Z.

[21] Th. Apel and S. Nicaise. The finite element method with anisotropic mesh grading for elliptic problems in domains with corners and edges. *Math. Methods Appl. Sci.*, 21:519–549, 1998.

[22] Th. Apel and U. Reichel. Partitioning of finite element meshes for parallel computing: A case study. Preprint SFB393/96-18a, TU Chemnitz-Zwickau, 1997.

[23] Th. Apel, A.-M. Sändig, and J. R. Whiteman. Graded mesh refinement and error estimates for finite element solutions of elliptic boundary value problems in non-smooth domains. *Math. Methods Appl. Sci.*, 19:63–85, 1996.

[24] O. Axelsson and I. Gustafsson. Preconditioning and two-level multigrid methods of arbitrary degree of approximation. *Math. Comp.*, 40:219–242, 1983.

[25] O. Axelsson and P. S. Vassilevski. Algebraic multilevel preconditioning methods I. *Numer. Math.*, 56:157–177, 1989.

[26] O. Axelsson and P. S. Vassilevski. Algebraic multilevel preconditioning methods II. *SIAM J. Numer. Anal.*, 27(6):1569–1590, 1990.

[27] I. Babuška and A. K. Aziz. On the angle condition in the finite element method. *SIAM J. Numer. Anal.*, 13:214–226, 1976.

[28] I. Babuška, R. B. Kellogg, and J. Pitkäranta. Direct and inverse error estimates for finite elements with mesh refinements. *Numer. Math.*, 33:447–471, 1979.

[29] I. Babuška and W. C. Rheinboldt. A-posteriori error estimates for the finite element method. *Internat. J. Numer. Methods Engrg.*, 12:1597–1615, 1978.

[30] I. Babuška, T. von Petersdorff, and B. Andersson. Numerical treatment of vertex singularities and intensity factors for mixed boundary value problems for the Laplace equation in $\mathbb{R}^3$. *SIAM J. Numer. Anal.*, 31:1265–1288, 1994.

[31] C. Baiocchi, F. Brezzi, and L. P. Franca. Virtual bubbles and galerkin-least-squares type methods. *Comput. Methods Appl. Mech. Engrg.*, 105:125–141, 1993.

[32] N. S. Bakhvalov. Optimization of methods for the solution of boundary value problems in the presence a of boundary layer. *Zh. Vychisl. Mat. i Mat. Fiz.*, 9:841–859, 1969. In Russian.

[33] R. E. Bank. The efficient implementation of local mesh refinement algorithms. In *Adaptive computational methods for partial differential equations*, pages 74–81, 1983. Proc. Workshop College Park/Md. 1983.

[34] E. Bänsch. Local mesh refinement in 2 and 3 dimensions. *IMPACT of Computing in Science and Engineering*, 3:181–191, 1991.

[35] E. Bänsch. Anisotropic interpolation estimates. Preprint 373, SFB 256, Rheinische Friedrich-Wilhelms-Universität Bonn, 1994.

[36] R. E. Barnhill and J. A. Gregory. Sard kernel theorems on triangular domains with application to finite element error bounds. *Numer. Math.*, 25:215–229, 1976.

[37] R. E. Barnhill and J. A. Gregory. Interpolation remainder theory from Taylor expansions on triangles. *Numer. Math.*, 25:401–408, 1976.

[38] A. E. Beagles and J. R. Whiteman. Treatment of a re-entrant vertex in a three-dimensional Poisson problem. In P. Grisvard, W. Wendland, and J. R. Whiteman, editors, *Singularities and constructive methods of their treatment*, Lecture Notes in Mathematics, vol. 1121, pages 19–27. Springer, 1985.

[39] A. E. Beagles and J. R. Whiteman. Finite element treatment of boundary singularities by augmentation with non-exact singular functions. *Numer. Methods Partial Differ. Equations*, 2:113–121, 1986.

[40] A. E. Beagles and J. R. Whiteman. General conical singularities in three dimensional Poisson problems. *Mat. Methods Appl. Sci.*, 11:215–235, 1989.

[41] R. Becker. *An adaptive finite element method for the incompressible Navier–Stokes equations on time-dependent domains.* PhD thesis, Ruprecht-Karls-Universität Heidelberg, 1995.

[42] R. Beinert and D. Kröner. Finite volume methods with local mesh alignment in 2–D. In *Adaptive Methods – Algorithms, Theory and Applications*, volume 46 of *Notes on Numerical Fluid Mechanics*, pages 38–53, Braunschweig, 1994. Vieweg.

[43] T. Benkiran. On a singular perturbation problem. *Differ. Equ. Dyn. Syst.*, 3:157–164, 1995.

[44] C. Bernardi. Optimal finite-element interpolation on curved domains. *SIAM J. Numer. Anal.*, 26:1212–1240, 1989.

[45] C. Bernardi, Y. Maday, and A. T. Patera. A new nonconforming approach to domain decomposition: The mortar element method. In H. Brézis and J.-L. Lions, editors, *Collège de France Seminar, XI*, pages 13–51. Pitman, 1994.

[46] J. Bey. Tetrahedral grid refinement. *Computing*, 55:355–378, 1995.

[47] I. A. Blatov. The Galerkin finite-element method for elliptic quasilinear singularly perturbed boundary value problems. III: Problems with corner boundary layers. *Differ. Uravn.*, 30:467–479, 1994. In Russian.

[48] H. Blum. On local coupling and defect correction techniques in the numerical treatment of singularities. Talk given at MAFELAP 1996, the Conference on the Mathematics of Finite Elements and Applications, Brunel University of West London, 1996.

[49] H. Blum and M. Dobrowolski. On finite element methods for elliptic equations on domains with corners. *Computing*, 28:53–63, 1982.

[50] F. A. Bornemann and H. Yserentant. A basic norm equivalence for the theory of multilevel methods. *Numer. Math.*, 64:455–476, 1993.

[51] M. Bourlard, M. Dauge, M. S. Lubuma, and S. Nicaise. Coefficients of the singularities for elliptic boundary value problems on domain with conical points III: Finite elements methods on polygonal domains. *SIAM J. Numer. Anal.*, 29:136–155, 1992.

[52] D. Braess. *Finite Elemente*. Springer, Berlin, 1992.

[53] J. H. Bramble and S. R. Hilbert. Bounds for a class of linear functionals with applications to Hermite interpolation. *Numer. Math.*, 16:362–369, 1971.

[54] J. H. Bramble, J. E. Pasciak, and A. H. Schatz. The construction of preconditioners for elliptic problems by substructuring I–IV. *Math. Comp.*, 1986, 1987, 1988, 1989. 47, 103–134, 49, 1–16, 51, 415–430, 53, 1–24.

[55] J. H. Bramble, J. E. Pasciak, and J. Xu. Parallel multilevel preconditioners. *Math. Comp.*, 55:1–22, 1990.

[56] J. H. Bramble and X. Zhang. Uniform convergence of the multigrid V-cycle for an anisotropic problem. Preprint, Texas A&M University.

[57] S. C. Brenner and L. R. Scott. *The mathematical theory of finite element methods*. Springer, New York, 1994.

[58] G. C. Buscaglia and E. A. Dari. Anisotropic mesh optimization and its application in adaptivity. *Internat. J. Numer. Methods Engrg.*, 40:4119–4136, 1997.

[59] G. F. Carey and J. T. Oden. *Finite Elements: Computational aspects*. The Texas Finite Element Series, vol. III. Prentice–Hall Inc., Englewood Cliffs, 1983.

[60] C. Carstensen and S. A. Funken. Constants in Clément-interpolation error and residual based a-posteriori error estimates in finite element methods. Bericht 97-11, Universität Kiel, Mathematisches Seminar, 1997.

[61] C. Carstensen and S. A. Funken. Fully reliable localized error control in the FEM. Bericht 97-12, Universität Kiel, Mathematisches Seminar, 1997.

[62] M. J. Castro-Diaz, F. Hecht, and B. Mohammadi. New progress in anisotropic grid adaption for inviscid and viscous flow simulations. In *Proceedings of the* 4^{th} *Annual International Meshing Roundtable*, pages 73–85, Albuquerque, NM, 1995. Sandia national Laboratories.

[63] P. G. Ciarlet. *The finite element method for elliptic problems*. North-Holland, Amsterdam, 1978.

[64] P. Clément. Approximation by finite element functions using local regularization. *RAIRO Anal. Numer.*, 2:77–84, 1975.

[65] W. Dahmen and A. Kunoth. Multilevel preconditioning. *Numer. Math.*, 63:315–344, 1992.

[66] M. Dauge. *Elliptic boundary value problems on corner domains*, volume 1341 of *Lecture Notes in Mathematics*. Springer, Berlin, 1988.

[67] M. Dauge. Personal communication, 1997.

[68] E. F. D'Azevedo and R. B. Simpson. On optimal interpolation triangle incidences. *SIAM J. Sci. Stat. Comput.*, 10:1063–1075, 1989.

[69] E. F. D'Azevedo and R. B. Simpson. On optimal triangular meshes for minimizing the gradient error. *Numer. Math.*, 59:321–348, 1991.

[70] M. Dobrowolski. A posteriori error estimates for treating the Poisson equation on anisotropic meshes. Talk given at the workshop "Numerical Methods for Singular Perturbations", Oberwolfach, Germany, 1998.

[71] M. Dobrowolski. Numerical approximation of elliptic interface and corner problems. Habilitationsschrift, Universität Bonn, 1981.

[72] M. Dobrowolski. Personal communication, 1991.

[73] M. Dobrowolski and H.-G. Roos. A priori estimates for the solution of convection-diffusion problems and interpolation on Shishkin meshes. *Z. Anal. Anwend.*, 16:1001–1012, 1997.

[74] M. Dryja and O. B. Widlund. Towards a unified theory of domain decomposition algorithms for elliptic problems. In T. F. Chan, R. Glowinski, J. Periaux, and O. B. Widlund, editors, *Domain decomposition methods for partial differential equations*, pages 3–21, Philadelphia, 1990. SIAM. Proc. of the 3rd International Symposium, Houston, 1989.

[75] M. Dryja and O. B. Widlund. Additive Schwarz methods for elliptic finite element problems in three dimensions. In T. F. Chan, D. E. Keyes, G. A. Meurant, J. S. Scroggs, and R. Voigt, editors, *Domain decomposition methods for partial differential equations*, pages 3–18, Philadelphia, 1992. SIAM. Proc. of the Fifth Conference on Domain Decomposition Methods for Partial Differential Equations, Norfolk, 1991.

[76] T. Dupont and R. Scott. Polynomial approximation of functions in Sobolev spaces. *Math. Comp.*, 34:441–463, 1980.

[77] L. Fezoui and B. Stoufflet. A class of implicit upwind schemes for Euler simulations with unstructured meshes. *J. Comp. Phys.*, 84:174–206, 1989.

[78] L. E. Fraenkel. Formulae for high derivatives of composite functions. *Math. Proc. Camb. Phil. Soc.*, 83:159–165, 1978.

[79] L. P. Franca and C. Farhat. Bubble functions prompt unusual stabilized finite element methods. *Comput. Methods Appl. Mech. Engrg.*, 123:299–308, 1995.

[80] R. Fritzsch. *Optimale Finite-Elemente-Approximationen für Funktionen mit Singularitäten*. PhD thesis, TU Dresden, 1990.

[81] R. Fritzsch and P. Oswald. Zur optimalen Gitterwahl bei Finite-Elemente-Approximationen. *Wissenschaftliche Zeitschrift TU Dresden*, 37(3):155–158, 1988.

[82] V. Girault and P.-A. Raviart. *Finite element methods for Navier-Stokes equations, Theory and algorithms*, volume 5 of *Springer Series in Computational Mathematics*. Springer, Berlin, 1986.

[83] D. Goehde. Personal communication, 1996.

[84] J. A. Gregory. Error bounds for linear interpolation in triangles. In J. R. Whiteman, editor, *The Mathematics of Finite Elements and Applications II*, pages 163–170. Academic Press, London, 1975.

[85] M. Griebel. *Multilevelmethoden als Iterationsverfahren über Erzeugendensystemen*. Teubner, Stuttgart, 1994.

[86] M. Griebel and P. Oswald. Tensor product type subspace splittings and multi-level iterative methods for anisotropic problems. *Adv. Comput. Math.*, 4:171–206, 1995.

[87] P. Grisvard. *Elliptic problems in nonsmooth domains*. Pitman, Boston–London–Melbourne, 1985.

[88] P. Grisvard. Singular behaviour of elliptic problems in non Hilbertian Sobolev spaces. *J. Math. Pures Appl.*, 74:3–33, 1995.

[89] B. Q. Guo. The h-p version of the finite element method for solving boundary value problems in polyhedral domains. In M. Costabel, M. Dauge, and S. Nicaise, editors, *Boundary value problems and integral equations in nonsmooth domains*, volume 167 of *Lecture Notes in Pure and Applied Mathematics*, pages 101–120. Marcel Dekker, New York, 1994.

[90] G. Haase, Th. Hommel, A. Meyer, and M. Pester. Bibliotheken zur Entwicklung paralleler Algorithmen. Preprint SPC95_20, TU Chemnitz–Zwickau, 1995. Updated version of SPC94_4 and SPC93_1.

[91] W. Hackbusch. Local defect correction method and domain decomposition techniques. *Computing*, 5:89–113, 1984.

[92] W. Hackbusch. *Multi-grid methods and applications*. Springer, Heidelberg, 1985.

[93] W. Hackbusch. The frequency decomposition multi-grid method. Part I: Application to anisotropic equations. *Numer. Math.*, 56:229–245, 1989.

[94] W. Hackbusch. On first and second order box schemes. *Computing*, 41:277–296, 1989.

[95] W. Hackbusch. *Iterative Lösung großer schwachbesetzer Gleichungssysteme*. Teubner, Stuttgart, 1991. English translation: Iterative solution of large sparse systems of equations. Springer, New York, 1994.

[96] H. Han and R. B. Kellogg. Differentiability properties of solutions of the equation $-\varepsilon^2\Delta u + ru = f(x,y)$ in a square. *SIAM J. Math. Anal.*, 21:394–408, 1990.

[97] V. Hannemann. *Numerische Simulation von Stoß-Stoß-Wechselwirkungen in Hochenthalpieströmungen unter Berücksichtigung von chemischen und thermischen Nichtgleichgewichtseffekten*. PhD thesis, Universität Göttingen, 1996.

[98] B. Heinrich. *Finite difference methods on irregular networks*, volume 82 of *International Series of Numerical Mathematics*. Birkhäuser, Basel, 1987.

[99] B. Heinrich. Singularity functions at axisymmetric edges and their representation by Fourier series. *Math. Methods Appl. Sci.*, 16:837–854, 1993.

[100] B. Heinrich. The Fourier-finite-element method for Poisson's equation in axisymmetric domains with edges. *SIAM J. Numer. Anal.*, 33:1885–1911, 1996.

[101] B. Heinrich and B. Weber. Fourier–finite-element approximation of elliptic interface problems in axisymmetric domains. *Math. Methods Appl. Sci.*, 19:909–931, 1996.

[102] M. R. Hestenes and E. Stiefel. Methods of conjugate gradients for solving linear systems. *J. Res. Nat. Bur. Standards*, 49:409–436, 1952.

[103] C. Hirsch. *Numerical Computation of Internal and External Flows, Volume 2: Computational Methods for Inviscid and Viscous Flows*. Wiley, 1990.

[104] S. M. Hudson. Polynomial approximation in Sobolev spaces. *Indiana Math. J.*, 39:199–228, 1990.

[105] T. J. R. Hughes, L. P. Franca, and G. M. Hulbert. A new finite element formulation for computational fluid dynamics VIII: The Galerkin/Least squares method for the advective diffusive equation. *Comput. Methods Appl. Mech. Engrg.*, 73:173–189, 1989.

[106] V. P. Il'in. On inequalities between the norms of partial derivatives of functions of several variables. *Tr. Mat. Inst. Steklov*, 84:144–173, 1965. In Russian. Translated in *Trudy Mat. Inst. Steklov*, 84:161–194, 1968.

[107] A. Jameson. Computational transonics. *Comm. Pure Appl. Math.*, XLI:507–549, 1988.

[108] P. Jamet. Estimations d'erreur pour des éléments finis droits presque dégénérés. *R.A.I.R.O. Anal. Numér.*, 10:43–61, 1976.

[109] M. Jung and U. Langer. Applications of multilevel methods to practical problems. *Surv. Math. Ind.*, 1:217–257, 1991.

[110] R. B. Kellogg. Boundary layers and corner singularities for a self-adjoint problem. In M. Costabel, M. Dauge, and S. Nicaise, editors, *Boundary value problems and integral equations in nonsmooth domains*, volume 167 of *Lecture Notes in Pure and Applied Mathematics*, pages 121–149. Marcel Dekker, New York, 1994.

[111] R. B. Kellogg. Boundary layers and corner singularities for a self-adjoint problem. Unpublished manuscript (revised version of [110]), 1997.

[112] B. N. Khoromskij and G. Wittum. Robust interface reduction for highly anisotropic elliptic equations. In W. Hackbusch and G. Wittum, editors, *Proceedings of the Fifth European Multi-Grid Conference*. to appear, 1998.

[113] V. A. Kondrat'ev. Singularities of the solution of the Dirichlet problem for a second order elliptic equation in the neighbourhood of an edge. *Differencial'nye uravnenija*, 13(11):2026–2032, 1977. In Russian.

[114] R. Kornhuber and R. Roitzsch. On adaptive grid refinement in the presence of internal and boundary layers. *IMPACT of Computing in Sci. and Engrg.*, 2:40–72, 1990.

[115] A. Kufner, O. John, and S. Fučík. *Function Spaces.* Academia, Prague, 1977.

[116] A. Kufner and A.-M. Sändig. *Some Applications of Weighted Sobolev Spaces.* Teubner, Leipzig, 1987.

[117] G. Kunert. Error estimation for anisotropic tetrahedral and triangular finite element meshes. Preprint SFB393/97-17, TU Chemnitz, 1997.

[118] G. Kunert. A residual error estimator for the finite element method with anisotropic tetrahedral meshes, 1998. In preparation.

[119] M. Křížek. On semiregular families of triangulations and linear interpolation. *Appl. Math.*, 36:223–232, 1991.

[120] M. Křížek. On the maximum angle condition for linear tetrahedral elements. *SIAM J. Numer. Anal.*, 29:513–520, 1992.

[121] D. Leguillon and E. Sanchez-Palencia. *Computation of singular solutions in elliptic problems and elasticity.* Masson, Paris, 1987.

[122] M. S. Lubuma and S. Nicaise. Singular function method for boundary value problems with edge corners. Preprint 240, FRD/UCD Centre for Research in Computatinal and Applied Mathematics, University of Cape Town, South Africa, 1994.

[123] M. S. Lubuma and S. Nicaise. Dirichlet problems in polyhedral domains II: approximation by FEM and BEM. *J. Comp. Appl. Math.*, 61:13–27, 1995.

[124] M. S. Lubuma and S. Nicaise. Finite element method for elliptic problems with edge corners. *J. Comp. Appl. Math.*, submitted.

[125] N. Madden and M. Stynes. Efficient generation of oriented meshes for solving convection diffusion problems. *Int. J. Numer. Methods Engrg.*, 40:565–576, 1997.

[126] M. Maischak. *hp-Methoden für Randintegralgleichungen bei 3D-Problemen, Theorie und Implementierung.* PhD thesis, Universität Hannover, 1996.

[127] J. M. Maubach. Local bisection refinement for N-simplicial grids generated by reflection. *SIAM J. Sci. Comp.*, 16:210–227, 1995.

[128] V. G. Maz'ya (W. Mazja). *Einbettungssätze für Sobolewsche Räume, Teil 1.* Teubner, Leipzig, 1979.

[129] V. G. Maz'ya and B. A. Plamenevskiĭ. L_p-estimates of solutions of elliptic boundary value problems in domains with edges. *Trudy Moskov. Mat. Obshch.*, 37:49–93, 1978. In Russian. Translated in *Trans. Moskow Math. Soc.*, 1:49–97, 1980.

[130] V. G. Maz'ya and B. A. Plamenevskiĭ. The first boundary value problem for classical equations of mathematical physics in domains with piecewise smooth boundaries, part I. *Z. Anal. Anwend.*, 2:335–359, 1983. In Russian.

[131] V. G. Maz'ya and J. Roßmann. Über die Asymptotik der Lösung elliptischer Randwertaufgaben in der Umgebung von Kanten. *Math. Nachr.*, 138:27–53, 1988.

[132] M. Meisel. *Integralbilanzmethode für Randwertaufgaben mit Lösungen im Sobolevraum* $W_2^{1+\tau}$. PhD thesis, TU Chemnitz, 1990.

[133] M. Meisel and A. Meyer. Implementierung eines parallelen vorkonditionierten Schur-Komplement CG-Verfahrens in das Programmpaket FEAP. Preprint SPC95_2, TU Chemnitz–Zwickau, 1995.

[134] A. Meister. *Zur zeitgenauen numerischen Simulation reibungsbehafteter, kompressibler, turbulenter Strömungsfelder mit einer impliziten Finite-Volumen-Methode vom Box-Typ.* PhD thesis, TH Darmstadt, 1996.

[135] J. M. Melenk and C. Schwab. *hp* fem for reaction-diffusion equations. I: Robust exponential convergence, II: Regularity theory. Research reports 97-03 and 97-04, ETH Zürich, Seminar für Angewandte Mathematik, 1997.

[136] A. Meyer. A parallel preconditioned conjugate gradient method using domain decomposition and inexact solvers on each subdomain. *Computing*, 45:217–234, 1990.

[137] A. Meyer and M. Pester. Verarbeitung von Sparse-Matrizen in Kompaktspeicherform (KLZ/KZU). Preprint SPC94_12, TU Chemnitz–Zwickau, 1994.

[138] M. Meyer. Grafik-Ausgabe vom Parallelrechner für 3D-Gebiete. Preprint SPC95_4, TU Chemnitz–Zwickau, 1995.

[139] J. J. H. Miller, E. O'Riordan, and G. I. Shishkin. *Fitted numerical methods for singular perturbation problems — Error estimates in the maximum norm for linear problems in one and two dimensions.* World Scientific Publishing Co., Singapore, 1996.

[140] B. Müller. *Berechnung abgelöster, laminarer Überschallströmungen um nichtangestellte stumpfe Körper.* PhD thesis, RWTH Aachen, 1995.

[141] U. Nävert. *A finite element method for convection-diffusion problems.* PhD thesis, Chalmers University of Technology, Göteborg, 1982.

[142] S. V. Nepomnyaschikh. Mesh theorems on traces, normalization of function traces and their inversion. *Sov. J. Numer. Anal. Math. Modelling*, 6:1–25, 1991.

[143] S. V. Nepomnyaschikh. Method of splitting into subspaces for solving elliptic boundary value problems in complex–form domains. *Sov. J. Numer. Anal. Math. Modelling*, 6:151–168, 1991.

[144] S. V. Nepomnyaschikh. Decomposition for elliptic problems with disproportional parameters, 1996.

[145] N. Neuß. *Homogenisierung und Mehrgitter.* PhD thesis, Ruprecht-Karls-Universität Heidelberg, 1995.

[146] J. Nečas. *Les méthodes directes en théorie des équations elliptiques.* Academia, Prague, 1967.

[147] B. Nkemzi. *Numerische Analysis der Fourier–Finite–Elemente–Methode für die Gleichungen der Elastizitätstheorie.* PhD thesis, Technische Universität Chemnitz–Zwickau, 1996. Published by Tectum, Marburg, 1997.

[148] J. T. Oden, L. Demkowicz, T. A. Westermann, and W. Rachowicz. Toward a universal h-p adaptive finite element strategy. Part 2. A posteriori error estimates. *Comput. Methods Appl. Mech. Engrg.*, 77:113–180, 1989.

[149] L. A. Oganesyan and L. A. Rukhovets. On variational-difference methods for linear elliptic equations of second order in two-dimensional domains with piecewise smooth boundary. *Zh. Vytcheslit. Math. Fiz.*, 8:97–114, 1968. In Russian.

[150] L. A. Oganesyan and L. A. Rukhovets. *Variational-difference methods for the solution of elliptic equations.* Izd. Akad. Nauk Armyanskoi SSR, Jerevan, 1979. In Russian.

[151] P. Oswald. *Multilevel Finite Element Approximation: Theory and Applications.* Teubner, Stuttgart, 1994.

[152] J. Peraire, M. Vahdati, K. Morgan, and O. C. Zienkiewicz. Adaptive remeshing for compressible flow computation. *J. Comp. Phys.*, 72:449–466, 1987.

[153] T. von Petersdorff. *Randwertprobleme der Elastizitätstheorie für Polyeder — Singularitäten und Approximationen mit Randelementmethoden.* PhD thesis, TH Darmstadt, 1989.

[154] T. von Petersdorff and E. Stephan. Decompositions in edge and corner singularities for the solution if the Dirichlet problem of the Laplacian in a polyhedron. *Math. Nachr.*, 149:71–104, 1990.

[155] W. Rachowicz. An anisotropic h-type mesh refinement strategy. *Comput. Methods Appl. Mech. Engrg.*, 109:169–181, 1993.

[156] W. Rachowicz. An overlappinf domain decomposition preconditioner for an anisotropic h-adaptive finite element method. *Comput. Methods Appl. Mech. Engrg.*, 127:269–292, 1995.

[157] E. Rank, M. Schweingruber, and M. Sommer. Adaptive mesh generation and transformation of triangular to quadrilateral meshes. *Comm. Numer. Methods Engrg.*, 9:121–129, 1993.

[158] G. Raugel. Résolution numérique par une méthode d'éléments finis du problème Dirichlet pour le Laplacien dans un polygone. *C. R. Acad. Sci. Paris, Sér. A*, 286(18):A791–A794, 1978.

[159] U. Reichel. Partitionierung von Finite-Elemente-Netzen. Preprint SFB393/96-18, TU Chemnitz–Zwickau, 1996.

[160] S. Rippa. Long and thin triangles can be good for linear interpolation. *SIAM J. Numer. Anal.*, 29:257–270, 1992.

[161] S. Rjasanow. Dokumentation und theoretische Grundlagen zum Programm SOLKLZ. Preprint 15, TU Karl-Marx-Stadt (Chemnitz), 1986.

[162] H.-G. Roos. Layer-adapted grids for singular perturbation problems. Preprint MATH-NM-03-1997, TU Dresden, 1997.

[163] H.-G. Roos, M. Stynes, and L. Tobiska. *Numerical methods for singularly perturbed differential equations. Convection-diffusion and flow problems.* Springer, Berlin, 1996.

[164] J. Roßmann. Gewichtete Sobolev–Slobodetskiĭ–Räume und Anwendungen auf elliptische Randwertaufgaben in Gebieten mit Kanten. Habilitationsschrift, Universität Rostock, 1988.

[165] J. Roßmann. On two classes of weighted sobolev-slobodetskiĭ spaces in a dihedral angle. In *Partial Differential Equations*, volume 27 of *Banach Center Publications*, pages 399–424. Institute of Mathematics, Polish Academy of Sciences, 1992.

[166] A.-M. Sändig. Error estimates for finite element solutions of elliptic boundary value problems in non-smooth domains. *Z. Anal. Anwend.*, 9(2):133–153, 1990.

[167] A. H. Schatz and L. B. Wahlbin. Maximum norm estimates in the finite element method on plane polygonal domains. Part 2: Refinements. *Math. Comp.*, 33(146):465–492, 1979.

[168] A. H. Schatz and L. B. Wahlbin. On the finite element method for singularly perturbed reaction–diffusion problems in two and one dimensions. *Math. Comp.*, 40:47–89, 1983.

[169] H. Schmitz, K. Volk, and W. L. Wendland. On three-dimensional singularities of elastic fields near vertices. *Numer. Methods Partial Differ. Equations*, 9:323–337, 1993.

[170] J. Schöberl. Robust multigrid preconditioning for parameter-dependent problems I: the Stokes-type case. In W. Hackbusch and G. Wittum, editors, *Multigrid Methods V. Proceedings of the fifth European Multigrid Conference, Stuttgart, 1996.* to appear, 1998.

[171] L. R. Scott and S. Zhang. Finite element interpolation of non-smooth functions satisfying boundary conditions. *Math. Comp.*, 54:483–493, 1990.

[172] G. I. Shishkin. Approximation of solutions of singularly perturbed boundary value problems with a corner boundary layer. *Zh. Vychisl. Mat. i Mat. Fiz.*, 27:1360–1374, 1987.

[173] G. I. Shishkin. *Mesh approximations of singularly perturbed elliptic and parabolic problems.* Russ. Acad. Sci., Ekaterinburg, 1992. In Russian.

[174] K. Siebert. An a posteriori error estimator for anisotropic refinement. *Numer. Math.*, 73:373–398, 1996.

[175] R. B. Simpson. Anisotropic mesh transformation and optimal error control. *Applied Numerical Mathematics*, 14:183–198, 1994.

[176] T. Skalický and H.-G. Roos. Anisotropic mesh refinement for problems with internal and boundary layers. Preprint MATH-NM-09-1997, TU Dresden, 1997.

[177] B. Smith, P. Bjorstad, and W. Gropp. *Domain Decomposition: Parallel Multilevel Methods for Elliptic Partial Differential Equations.* Cambridge University Press, New York, 1996.

[178] K. T. Smith. Inequalities for formally positive integro-differntial forms. *Bull. Amer. Math. Soc.*, 67:368–370, 1961.

[179] Th. Sonar. Multivariate Rekonstruktionsverfahren zur numerischen Lösung hyperbolischer Erhaltungsgleichungen. Habilitationsschrift, TH Darmstadt, 1995. Forschungsbericht FB 95-02, DLR G"ottingen, 1995.

[180] T. Steidten and M. Jung. Das Multigrid-Programmsystem FEMGPM zur Lösung elliptischer und parabolischer Differentialgleichungen einschließlich mechanisch–thermisch gekoppelter Probleme (Version 06.90). Manual, Technische Universität Karl-Marx-Stadt, Sektion Mathematik, 1990.

[181] E. P. Stephan and J. R. Whiteman. Singularities of the Laplacian at corners and edges of three-dimensional domains and their treatment with finite element methods. *Math. Methods Appl. Sci.*, 10(3):339–350, 1988.

[182] G. Strang and G. Fix. *An analysis of the finite element method.* Prentice–Hall Inc., Englewood Cliffs, 1973.

[183] T. Strouboulis and K. A. Haque. Recent experiences with error estimation and adaptivity. Part 1: Review of error estimators for scalar elliptic problems. *Comput. Methods Appl. Mech. Engrg.*, 97:399–436, 1992.

[184] T. Strouboulis and K. A. Haque. Recent experiences with error estimation and adaptivity. Part 2: Error estimation for h-adaptive approximations on grids of triangles and quadrilaterals. *Comput. Methods Appl. Mech. Engrg.*, 100:359–430, 1992.

[185] K. Stüben and U. Trottenberg. Multigrid methods: Fundamental algorithms, model problem analysis and applications. In W. Hackbusch and U. Trottenberg, editors, *Multigrid Methods, Proceedings of the Conference held at Köln–Porz, November 23–27, 1981*, volume 960 of *Lecture Notes in Mathematics*, pages 1–176, Berlin, 1982. Springer.

[186] M. Stynes and E. O'Riordan. A uniformly convergent Galerkin method on a Shishkin mesh for a convection-diffusion problem. *J. Math. Anal. and Appl.*, 214:36–54, 1997.

[187] J. L. Synge. *The hypercircle in mathematical physics.* Cambridge University Press, Cambridge, 1957.

[188] P. Le Tallec. Domain Decomposition Methods In Compututional Mechanics. *Computational Mechanics Advances (North Holland)*, 1:121–220, 1994.

[189] R. Verfürth. *A review of a posteriori error estimation and adaptive mesh–refinement techniques.* Wiley, Chichester, 1996.

[190] L. B. Wahlbin. Local behaviour in finite element methods. In P. G. Ciarlet and J. L. Lions, editors, *Handbook of Numerical Analysis, Vol. II: Finite element methods (Part 1)*, pages 353–522. Elsevier, North-Holland, 1991.

[191] H. Walden and R. B. Kellogg. Numerical determination of the fundamental eigenvalue for the Laplace operator on a spherical domain. *J. Eng. Math.*, 11:299–318, 1977.

[192] D. S. Watkins. A generalization of the Bramble-Hilbert lemma and applications to multivariate interpolation. *J. Approx. Theory*, 26:219–231, 1979.

[193] B. Weber. *Die Fourier–Finite–Elemente–Methode für elliptische Interfaceprobleme in axialsymmetrischen Gebieten.* PhD thesis, TU Chemnitz–Zwickau, 1994.

[194] J. R. Whiteman. Finite element methods for treating problems involving singularities, with applications to linear elastic fracture. In E. L. Ortiz, editor, *Numerical approximation of partial differential equations*, pages 109–120. Elsevier Science Publishers B.V. (North Holland), Amsterdam–New York, 1987.

[195] A. Wierse and M. Rumpf. GRAPE – Eine objektorientierte Visualisierungs- und Numerikplattform. *Informatik Forsch. Entw.*, 7:145–151, 1992.

[196] Chr. Xenophontos. *The hp finite element method for singularly perturbed problems*. PhD thesis, University of Maryland, 1996.

[197] J. Xu. *Theory of Multilevel Methods*. PhD thesis, Cornell University, 1989.

[198] J. Xu. Iterative methods by space decomposition and subspace correction. *SIAM Review*, 34:581–613, 1992.

[199] H. Yserentant. On the multi–level splitting of finite element spaces. *Numer. Math.*, 49:379–412, 1986.

[200] H. Yserentant. Two preconditioners based on the multi–level splitting of finite element spaces. *Numer. Math.*, 58:163–184, 1990.

[201] A. Ženíšek. Maximum-angle condition and triangular finite elements of Hermite type. *Math. Comp.*, 64:929–941, 1995.

[202] A. Ženíšek and M. Vanmaele. The interpolation theorem for narrow quadrilateral isoparametric finite elements. *Numer. Math.*, 72:123–141, 1995.

[203] X. Zhang. Multilevel Schwarz methods. *Numer. Math.*, 63:521–539, 1992.

[204] G. Zhou and R. Rannacher. Mesh orientation and anisotropic refinement in the streamline diffusion method. In M. Křížek, P. Neitaanmäki, and R. Stenberg, editors, *Finite Element Methods: Fifty Years of the Courant Element*, volume 164 of *Lecture Notes in Pure and Applied Mathematics*, pages 491–500. Marcel Dekker, Inc., New York, 1993. Also published as Preprint 93-57, Universität Heidelberg, IWR, SFB 359, 1993.

[205] O. C. Zienkiewicz and J. Wu. Automatic directional refinement in adaptive analysis of compressible flows. *Internat. J. Numer. Methods Engrg.*, 37:2189–2210, 1994.

[206] O. C. Zienkiewicz and J. Z. Zhu. The superconvergent patch recovery and a-posteriori error estimates. Part 1: The recovery technique. *Internat. J. Numer. Methods Engrg.*, 33:1331–1364, 1992.

[207] O. C. Zienkiewicz and J. Z. Zhu. The superconvergent patch recovery and a-posteriori error estimates. Part 2: Error estimates and adaptivity. *Internat. J. Numer. Methods Engrg.*, 33:1365–1382, 1992.

[208] M. Zlámal. On the finite element method. *Numer. Math.*, 12:394–409, 1968.

Other titles in the SFB393 series:

97-01 P. Benner, V. Mehrmann, H. Xu. A new method for computing the stable invariant subspace of a real Hamiltonian matrix or Breaking Van Loan's curse? January 1997.

97-02 B. Benhammouda. Rank-revealing 'top-down' ULV factorizations. January 1997.

97-03 U. Schrader. Convergence of Asynchronous Jacobi-Newton-Iterations. January 1997.

97-04 U.-J. Görke, R. Kreißig. Einflußfaktoren bei der Identifikation von Materialparametern elastisch-plastischer Deformationsgesetze aus inhomogenen Verschiebungsfeldern. March 1997.

97-05 U. Groh. FEM auf irregulären hierarchischen Dreiecksnetzen. March 1997.

97-06 Th. Apel. Interpolation of non-smooth functions on anisotropic finite element meshes. March 1997

97-07 Th. Apel, S. Nicaise. The finite element method with anisotropic mesh grading for elliptic problems in domains with corners and edges.

97-08 L. Grabowsky, Th. Ermer, J. Werner. Nutzung von MPI für parallele FEM-Systeme. March 1997.

97-09 T. Wappler, Th. Vojta, M. Schreiber. Monte-Carlo simulations of the dynamical behavior of the Coulomb glass. March 1997.

97-10 M. Pester. Behandlung gekrümmter Oberflächen in einem 3D-FEM-Programm für Parallelrechner. April 1997.

97-11 G. Globisch, S. V. Nepomnyaschikh. The hierarchical preconditioning having unstructured grids. April 1997.

97-12 R. V. Pai, A. Punnoose, R. A. Römer. The Mott-Anderson transition in the disordered one-dimensional Hubbard model. April 1997.

97-13 M. Thess. Parallel Multilevel Preconditioners for Problems of Thin Smooth Shells. May 1997.

97-14 A. Eilmes, R. A. Römer, M. Schreiber. The two-dimensional Anderson model of localization with random hopping. June 1997.

97-15 M. Jung, J. F. Maitre. Some remarks on the constant in the strengthened C.B.S. inequality: Application to h- and p-hierarchical finite element discretizations of elasticity problems. July 1997.

97-16 G. Kunert. Error estimation for anisotropic tetrahedral and triangular finite element meshes. August 1997.

97-17 L. Grabowsky. MPI-basierte Koppelrandkommunikation und Einfluß der Partitionierung im 3D-Fall. August 1997.

97-18 R. A. Römer, M. Schreiber. Weak delocalization dueto long-range interaction for two electrons in a random potential chain. August 1997.

97-19 A. Eilmes, R. A. Römer, M. Schreiber. Critical behavior in the two-dimensional Anderson model of localization with random hopping. August 1997.

97-20 M. Meisel, A. Meyer. Hierarchically preconditioned parallel CG-solvers with and without coarse-matrix-solvers inside FEAP. September 1997.

97-21 J. X. Zhong, U. Grimm, R. A. Römer, M. Schreiber. Level-Spacing Distributions of Planar Quasiperiodic Tight-Binding Models. October 1997.

97-22 W. Rehm (Ed.). Ausgewählte Beiträge zum 1. Workshop Cluster-Computing. TU Chemnitz, 6./7. November 1997.

97-23 P. Benner, Enrique S. Quintana-Ortí. Solving stable generalized Lyapunov equations with the matrix sign function. October 1997

97-24 T. Penzl. A Multi-Grid Method for Generalized Lyapunow Equations. October 1997

97-25 G. Globisch. The hierarchical preconditioning having unstructured threedimensional grids. December 1997

97-26 G. Ammar, C. Mehl, V. Mehrmann. Schur-like forms for matrix Lie groups, Lie algebras and Jordan algebras. November 1997

97-27 U. Elsner. Graph partitioning - a survey. December 1997.

97-28 W. Dahmen, R. Schneider. Composite Wavelet Bases for Operator Equations. December 1997.

97-29 P. L. Levin, M. Spasojević, R. Schneider. Creation of Sparse Boundary Element Matrices for 2-D and Axi-symmetric Electrostatics Problems Using the Bi-orthogonal Haar Wavelet. December 1997.

97-30 W. Dahmen, R. Schneider. Wavelets on Manifolds I: Construction and Domain Decomposition. December 1997.

97-31 U. Elsner, V. Mehrmann, F. Milde, R. A. Römer, M. Schreiber. The Anderson Model of Localization: A Challenge for Modern Eigenvalue Methods. December 1997.

98-01 B. Heinrich, S. Nicaise, B. Weber. Elliptic interface problems in axisymmetric domains. Part II: The Fourier-finite-element approximation of non-tensorial singularities. January 1998.

98-02 T. Vojta, R. A. Römer, M. Schreiber. Two interfacing particles in a random potential: The random model revisited. February 1998.

98-03 B. Mehlig, K. Müller. Non-universal properties of a complex quantum spectrum. February 1998.

98-04 B. Mehlig, K. Müller, B. Eckhardt. Phase-space localization and matrix element distributions in systems with mixed classical phase space. February 1998.

98-05 M. Bollhöfer, V. Mehrmann. Nested divide and conquer concepts for the solution of large sparse linear systems. March 1998.

98-06 T. Penzl. A cyclic low rank Smith method for large, sparse Lyapunov equations with applications in model reduction and optimal control. March 1998.

98-07 V. Mehrmann, H. Xu. Canonical forms for Hamiltonian and symplectic matrices and pencils. March 1998.

98-08 C. Mehl. Condensed forms for skew-Hamiltonian/Hamiltonian pencils. March 1998.

98-09 M. Meyer. Der objektorientierte hierarchische Netzgenerator Netgen69-C++. April 1998.

98-10 T. Ermer. Mappingstrategien für Kommunikatoren. April 1998.

98-11 D. Lohse. Ein Standard-File für 3D-Gebietsbeschreibungen. – Definition des Fileformats V 2.1 –. April 1998.

98-13 L. Grabowsky, T. Ermer. Objektorientierte Implementation eines PPCG-Verfahrens. April 1998.

98-14 M. Konik, R. Schneider. Object-oriented implementation of multiscale methods for boundary integral equations. May 1998.

98-15 W. Dahmen, R. Schneider. Wavelets with complementary boundary conditions - Function spaces on the cube. May 1998.

98-16 P. Hr. Petkov, M. M. Konstantinov, V. Mehrmann. DGRSVX and DMSRIC: Fortran 77 subroutines for solving continuous-time matrix algebraic Riccati equations with condition and accuracy estimates. May 1998.

98-17 D. Lohse. Ein Standard-File für 3D-Gebietsbeschreibungen. - Datenbasis und Programmschnittstelle `data_read`. April 1998.

98-18 A. Fachat, K. H. Hoffmann. Blocking vs. Non-blocking Communication under MPI on a Master-Worker Problem. June 1998.

98-19 W. Dahmen, R. Schneider, Y. Xu. Nonlinear Functionals of Wavelet Expansions - Adaptive Reconstruction and Fast Evaluation. June 1998.

98-20 M. Leadbeater, R. A. Römer, M. Schreiber. Interaction-dependent enhancement of the localisation length for two interacting particles in a one-dimensional random potential. June 1998.

98-21 M. Leadbeater, R. A. Römer, M. Schreiber. Formation of electron-hole pairs in a one-dimensional random environment. June 1998.

98-22 A. Eilmes, U. Grimm, R. A. Römer, M. Schreiber. Two interacting particles at the metal-insulator transition. August 1998.

98-23 M. Leadbeater, R. A. Römer, M. Schreiber. Scaling the localisation lengths for two interacting particles in one-dimensional random potentials. July 1998.

98-24 M. Schreiber, U. Grimm, R. A. Römer, J. X. Zhong. Application of random matrix theory to quasiperiodic systems. July 1998.

98-25 V. Mehrmann, H. Xu. Lagrangian invariant subspaces of Hamiltonian matrices. August 1998.

98-26 B. Nkemzi, B. Heinrich. Partial Fourier approximation of the Lamé equations in axisymmetric domains. September 1998.

98-27 V. Uski, B. Mehlig, R. A. Römer, M. Schreiber. Smoothed universal correlations in the two-dimensional Anderson model. September 1998.

98-28 D. Michael, M. Meisel. Some remarks to large deformation elasto-plasticity (continuum formulation). September 1998.

98-29 V. Mehrmann, H. Xu. Structured Jordan Canonical Forms for Structured Matrices that are Hermitian, skew Hermitian or unitary with respect to indefinite inner products. October 1998.

98-30 G. Globisch. The hierarchical preconditioning on locally refined unstructured grids. October 1998.

98-31 M. Bollhöfer. Algebraic domain decomposition. (PhD thesis) March 1998.

98-32 X. Guan, U. Grimm, R. A. Römer. Lax pair formulation for a small-polaron chain. (Proceedings PILS'98, in: Ann. Physik, Leipzig 1998). November 1998.

98-33 U. Grimm, R. A. Römer, G. Schliecker. Electronic states in topologically disordered systems. (Proceedings PILS'98, in: Ann. Physik, Leipzig 1998). November 1998.

98-34 C. Villagonzalo, R. A. Römer. Low temperature behavior of the thermopower in disordered systems near the Anderson transition. (Proceedings PILS'98, in: Ann. Physik, Leipzig 1998). November 1998.

98-35 V. Uski, B. Mehlig, R. A. Römer. A numerical study of wave-function and matrix-element statistics in the Anderson model of localization. (Proceedings of PILS'98, in: Ann. Physik, Leipzig 1998) November 1998.

98-36 F. Milde, R. A. Römer. Energy level statistics at the metal-insulator transition in the Anderson model of localization with anisotropic hopping. (Proceedings of PILS'98, in: Ann. Physik, Leipzig 1998). November 1998.

98-37 M. Schreiber, U. Grimm, R. A. Römer, J. X. Zhong. Energy Levels of Quasiperiodic Hamiltonians, Spectral Unfolding and Random Matrix Theory. November 1998.

The complete list of current and former preprints is available via
`http://www.tu-chemnitz.de/sfb393/preprints.html`.